

The Effects of Low-Dose Nitrite upon Normal, Hypoxic and Ischaemic Vessels

A Thesis submitted for the Degree of Doctor of Philosophy

by

Dr Thomas E Ingram

MB ChB, MRCP (UK)

Department of Cardiology

Wales Heart Research Institute

Cardiff University

UK

February 2010

UMI Number: U585358

All rights reserved

INFORMATION TO ALL USERS

The quality of this reproduction is dependent upon the quality of the copy submitted.

In the unlikely event that the author did not send a complete manuscript and there are missing pages, these will be noted. Also, if material had to be removed, a note will indicate the deletion.



UMI U585358

Published by ProQuest LLC 2013. Copyright in the Dissertation held by the Author.
Microform Edition © ProQuest LLC.

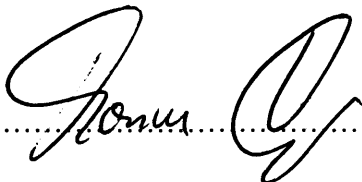
All rights reserved. This work is protected against
unauthorized copying under Title 17, United States Code.



ProQuest LLC
789 East Eisenhower Parkway
P.O. Box 1346
Ann Arbor, MI 48106-1346

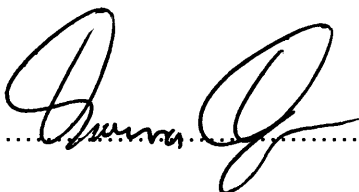
Declaration

This work has not previously been accepted in substance for any degree and is not concurrently submitted in candidature for any degree.

Signed  (candidate) Date... 21/5/10.....

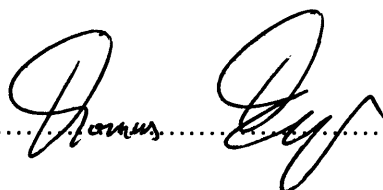
STATEMENT 1

This thesis is being submitted in partial fulfilment of the requirements for the degree of PhD.

Signed  (candidate) Date... 21/5/10.....

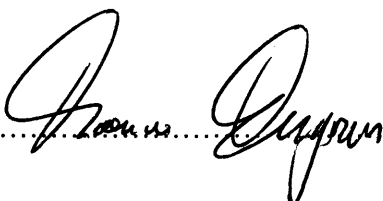
STATEMENT 2

This thesis is the result of my own independent work/investigation, except where otherwise stated. Other sources are acknowledged by explicit references.

Signed  (candidate) Date... 21/5/10.....

STATEMENT 3

I hereby give consent for my thesis, if accepted, to be available for photocopying and for interlibrary loan, and for the title and summary to be made available to outside organisations.

Signed  (candidate) Date... 21/5/10.....

Dedication

To Carla,

the only person who understands the true meaning of this body of work

and

In memory of our daughter, Lucy Annabelle Ingram

Acknowledgements

The large body of work contained in this thesis would not have been possible without the help of several people. First and foremost I am eternally grateful to my supervisor Philip James. Many of the ideas contained within this thesis are a composite of several hours of thought provoking exchanges. The most frustrating feature of these was that Phil was never happy with the answers provided, instead always asking the next question! It is, however, because of the willingness of Phil to investigate basic scientific ideas in complex, systems-based, environments that I have been able to complete this thesis. I am also indebted to my clinical supervisor, Alan Fraser, for his assistance with all things echo.

Andrew Pinder and Damian Bailey deserve special commendation for the instrumental roles which they both played in the hypoxic chamber chapter of this thesis. I am also grateful to Catherine Templeton for her technical assistance in obtaining stress-echocardiography images and Robert Bleasdale for his help with the practicalities of realising that chapter. I thank Elizabeth Ellins and Julian Halcox for sharing their expertise in endothelial function assessment; key to the ischaemia/reperfusion chapter. I am grateful for the faith which the British Heart Foundation placed in me by the award of the Clinical Research Training Fellowship which supported me throughout this PhD.

Lastly, I am forever grateful to my wife Carla and our twin girls Daisy and Jessica, for making me happy.



Abstract

The simple anion inorganic nitrite (NO_2^-) has previously been considered a relatively inert nitric oxide (NO) metabolite. However, recent evidence shows that NO_2^- exhibits an enhanced vasodilator effect in hypoxia. It has been suggested that this effect is mediated by intra-vascular reduction of NO_2^- to NO by deoxygenated-haemoglobin.

This thesis investigated the effects of low-dose NO_2^- supplementation in man, in three different environments where the actions of NO_2^- may be potentiated. Firstly, the effect of systemic sodium nitrite (NaNO_2) administration upon forearm and pulmonary haemodynamics were assessed in healthy volunteers in both hypoxia and normoxia; conditions created by a controlled environmental chamber. The study-infusion resulted in an approximate doubling of plasma $[\text{NO}_2^-]$, with similar pharmacokinetics observed in both hypoxia and normoxia. Forearm vasodilation occurred in hypoxia but not normoxia. In addition a pulmonary vasodilator effect was present in hypoxia only, and was not dependent upon simultaneous elevation of plasma $[\text{NO}_2^-]$.

The same dose of NaNO_2 was given to patients with proven inducible myocardial ischaemia in the second study: a double-blind placebo-controlled clinical trial. Objective markers of myocardial ischaemia were measured by tissue velocity imaging performed during dobutamine stress echocardiography. The results showed that low-dose NaNO_2 acts as an anti-ischaemic agent; despite no vasodilator effect being present in normoxia.

A third set of experiments were performed to assess the potential role of NaNO_2 as an ischaemic conditioning agent in a forearm model of ischaemia/reperfusion injury. Here NaNO_2 was able to act as a pre-conditioning but not a post-conditioning agent.

Two key results subtend this thesis. Firstly, tissue levels of NO_2^- are more important than intra-vascular levels, as its hypoxia-enhanced actions appear to be modulated from this site. Secondly, NaNO_2 may find clinically relevance in the future as a targeted vasodilator, providing a therapeutic effect to tissues in need only.

Commonly used abbreviations

ACh	acetylcholine
ANOVA	analysis of variance
ATP	adenosine tri-phosphate
AUC	area under curve
BA	basal anterior
BAS	basal antero-septal
BI	basal inferior
BL	basal lateral
BP	blood pressure
BPost	basal posterior
BS	basal septal
Ca ²⁺	calcium ion
CAD	coronary artery disease
cGMP	cyclic guanosine monophosphate
CI	confidence interval
CO ₂	carbon dioxide
CWD	continuous-wave Doppler
Cx	circumflex (coronary artery)
deoxy-Hb	deoxygenated haemoglobin
DM	diabetes mellitus
DSE	dobutamine stress echocardiogram
EDRF	endothelium derived relaxing factor
eNOS	endothelial nitric oxide synthase
ETC	electron transport chain
FBF	forearm blood flow
FiO ₂	fraction of inspired oxygen
FMD	flow mediated dilatation

GTN	glyceryl trinitrate
H ⁺	hydrogen ion
Hb	haemoglobin
HbNO	Iron nitrosyl haemoglobin
HbSNO	S-nitrosohaemoglobin
HR	heart rate
iNOS	inducible nitric oxide synthase
IPC	ischaemic pre-conditioning
IPostC	ischaemic post-conditioning
IR	ischaemia/reperfusion
IVRT	isovolumic relaxation time
K ⁺	potassium ion
LAD	left anterior descending (coronary artery)
L-NAME	L-Nitro-Arginine Methyl Ester
L-NMMA	N ^G -monomethyl-L-arginine
LVOT	left ventricular outflow tract
Met-Hb	methaemoglobin
MPT	mitochondrial permeability transition pore
N ₂	nitrogen
Na ⁺	sodium ion
NADPH	nicotinamide adenine dinucleotide phosphate
NaNO ₂	sodium nitrite
nNOS	neuronal nitric oxide synthase
NO	nitric oxide
NO ₂ ⁻	nitrite anion
NO ₃ ⁻	nitrate anion
NOA	nitric oxide analyser
NOx	plasma NO ₂ ⁻ & plasma protein bound NO
O ₂	oxygen
O ₂ ⁻	superoxide

OBC	ozone based chemiluminescence
ONOO ⁻	peroxynitrite
oxy-Hb	oxygenated haemoglobin
PAP	pulmonary arterial pressure
PASP	pulmonary arterial systolic pressure
PAT	pulmonary acceleration time
PSV	peak systolic velocity
PWD	pulsed-wave Doppler
RCA	right coronary artery
RIPC	remote ischaemic pre-conditioning
ROS	reactive oxygen species
RSNO	protein nitrosothiol species
SaO ₂	oxygen saturation
SCD	sickle cell disease
SD	standard deviation
SEM	standard error of the mean
sGC	soluble guanylate cyclase
SGP	strain gauge plethysmography
SNO	nitrosothiol species
TR	tricuspid regurgitation
VTI	velocity time integral
XO	xanthine oxidase

Contents

Declaration	i
Dedication	ii
Acknowledgements	iii
Abstract.....	iv
Commonly used abbreviations	v
Chapter 1: General Introduction.....	1
1.1. The endothelium & nitric oxide	1
1.2. The vasodilator mechanism of action of NO	2
1.3. The alternative biological actions of NO.....	3
1.3.1. Vascular	3
1.3.2. Nervous system	4
1.3.3. Inflammation	4
1.3.3.1. NO as a host defence agent.....	5
1.3.3.2. NO and septic shock	6
1.3.4. Summary of the biological actions of NO	7
1.4. The metabolism of NO in blood	8
1.4.1. Oxidative metabolites of NO	10
1.4.1.1. Inorganic nitrite (NO_2^-)	10
1.4.1.2. Inorganic nitrate (NO_3^-)	11
1.4.1.2.1. NO passage into the erythrocyte.....	11
1.4.1.3. Peroxynitrite (ONOO^-)	13
1.4.1.3.1. Superoxide (O_2^-).....	13
1.4.1.3.2. The biological significance of ONOO^-	14
1.4.2. Thiol bound NO metabolites	15
1.4.3. Intra-erythrocyte NO metabolites	16
1.4.3.1. The molecular structure of Hb	16
1.4.3.2. The allosteric regulation of Hb structure	17
1.4.3.3. Hb bound NO	17
1.4.4. The relative distribution of blood NO metabolites	18
1.4.4.1. NO metabolite distribution as a function of Hb- O_2 saturation	19
1.4.5. Dietary NO_3^- as a source of plasma NO_2^-	20
1.5. The physiological importance of blood NO metabolites	21
1.5.1. The endocrine properties of NO.....	21
1.5.2. HbSNO as a modulator of endocrine NO function	22
1.5.2.1. Theory	22
1.5.2.2. Criticisms of the HbSNO theory.....	24
1.5.3. NO_2^- & deoxy-Hb as modulators of endocrine NO function.....	26

1.5.3.1. Theory.....	26
1.5.3.1.1. Deoxy-Hb as a NO ₂ ⁻ reductase.....	26
1.5.3.2. Criticisms of the deoxy-Hb/NO ₂ ⁻ reductase theory.....	28
1.5.4. Previous human studies of exogenous NO ₂ ⁻ administration.....	30
1.5.4.1. Lauer et al	30
1.5.4.2. Cosby et al	30
1.5.4.3. Dejam et al.....	31
1.5.4.4. Maher et al	31
1.5.4.5. Mack et al	32
1.5.4.6. Criticisms of the above studies.....	32
1.5.5. NO ₂ ⁻ administration to the hypoxia pulmonary vasculature.....	37
1.5.6. Summary of the two theories of endocrine NO function.....	39
1.6. The role of NO ₂ ⁻ in ischaemia/reperfusion (IR) injury	40
1.6.1. IR injury background: the mitochondrion	40
1.6.1.1. Mitochondrion structure	40
1.6.1.2. Mitochondrion function: the electron transport chain.....	41
1.6.2. The pathophysiology of IR Injury.....	43
1.6.2.1. The biochemical cascade of I/R injury	43
1.6.3. The phenomenon of ischaemic conditioning	45
1.6.3.1. The mechanisms responsible for ischaemic conditioning.....	45
1.6.4. The specific role of NO in ischaemic conditioning.....	47
1.6.5. The evidence for NO ₂ ⁻ as an ischaemic conditioning agent	49
1.7. The key ideas contained within this chapter	50
1.8. Aims of this thesis	51
Chapter 2: General Methodology	52
2.1. Controlled environment chamber	52
2.2. Subject recruitment	53
2.2.1. Healthy volunteers	53
2.2.2. Coronary artery disease patients	53
2.3. Forearm blood flow (FBF)	53
2.3.1. Near Infrared spectroscopy (NIRS) plethysmography.....	55
2.3.2. Strain gauge plethysmography (SGP)	55
2.3.3. Comparison between the above two measures of FBF	56
2.4. Pulmonary arterial pressure	57
2.4.1. Pulmonary acceleration time	57
2.4.2. Iso-volumic relaxation time	57
2.4.3. Tricuspid regurgitation velocity.....	58
2.5. Cardiac output.....	59
2.6. Basic haemodynamic & blood measurements	60

2.7. Statistical analyses	60
2.8. Blood NO metabolite measurement.....	61
2.8.1. Blood preparation.....	61
2.8.2. Ozone-based chemiluminescence	62
2.8.3. Sample pre-treatment	63
2.8.3.1. Plasma NO _x	63
2.8.3.2. Erythrocyte associated NO	64
2.8.3.3. Plasma NO ₃ ⁻	65
2.9. Interpretation of data produced by the NOA.....	66
2.10. Calibration of OBC.....	67
2.11. Assessment of endothelial function: Flow mediated dilatation.....	68
2.11.1. Analysis of FMD images	70
2.12. Forearm IR injury protocol.....	70
2.13. Dobutamine stress echocardiography.....	71
2.13.1. Myocardial velocity imaging parameters	73
2.14. Isolated vessel preparation.....	74
Chapter 3: Nitrite and Hypoxia	76
3.1. Introduction	76
3.1.1. The physiological effect of hypoxia upon the cardiovascular system.....	76
3.1.2. Aims of this chapter	78
3.1.3. Original hypotheses	78
3.2. Study design (specific protocols)	79
3.2.1. Protocol 1: Hypoxia/NO ₂ ⁻	79
3.2.2. Protocol 2: Hypoxia/saline.....	81
3.2.3. Protocol 3: Normoxia/NO ₂ ⁻	81
3.3. Results.....	82
3.3.1. Demographics.....	82
3.3.2. The environmental chamber & subject oxygenation	83
3.3.3. Basic haemodynamic variables.....	85
3.3.4. Plasma NO metabolites	86
3.3.4.1. The effect of acute hypoxia upon plasma [NO ₂ ⁻]	88
3.3.4.2. The pharmacokinetics of NaNO ₂	89
3.3.5. Erythrocyte NO metabolites.....	91
3.3.5.1. The effect of acute hypoxia exposure upon [HbNO].....	91
3.3.5.2. The response of [HbNO] to the NaNO ₂ infusion	92
3.3.6. Forearm blood flow	94
3.3.6.1. Changes in FBF compared to key NO metabolites	94
3.3.7. Pulmonary arterial pressure (PAP)	97
3.3.7.1. The effect of acute hypoxia exposure upon PAP	97

3.3.7.2. The effects of NaNO ₂ upon the hypoxic pulmonary vasculature.....	98
3.3.8. Cardiac output	101
3.3.9. Analysis of variance of physiological measures.....	101
3.3.10. Organ chamber bioassay	105
3.4. Discussion.....	106
3.4.1. The effective utilisation of hypoxia in a physiological study	106
3.4.2. Limitations of the physiological measures employed	107
3.4.3. Limitations of the biochemical measures employed	108
3.4.4. The effect of hypoxia upon blood NO metabolites	110
3.4.5. The enhanced vasodilator effects of NaNO ₂ in hypoxia.....	110
3.4.6. Potential mechanisms for the biological activity of NaNO ₂	113
3.4.6.1. Tissue-based reductase activity.....	113
3.4.6.2. An intermediate molecule.....	114
3.5. Chapter summary.....	116
Chapter 4: Nitrite and Ischaemia	117
4.1. Introduction	117
4.1.1. A historical perspective of NO ₂ as an anti-anginal agent	117
4.1.2. Quantification of ischaemia by myocardial tissue Doppler imaging	118
4.1.3. Aims of this chapter	119
4.1.4. Original Hypothesis.....	119
4.2. Study design	120
4.2.1. Data analysis	121
4.2.1.1. Whole myocardial analysis	122
4.2.1.2. Angiography-directed analysis	123
4.2.1.3. Top and bottom halves analysis	123
4.2.1.4. Upper and lower tertile analysis	124
4.3. Results	125
4.3.1. Demographic data and clinical characteristics	125
4.3.2. Anatomical details of subject coronary vasculature	126
4.3.3. Example individual data-set	127
4.3.4. Study haemodynamics.....	131
4.3.5. The effect of NaNO ₂ upon PSV in ischaemic and control myocardium	133
4.3.5.1. Whole myocardial analysis	134
4.3.5.2. Angiography-directed analysis	137
4.3.5.3. Top and bottom halves analysis	140
4.3.5.4. Upper and lower tertiles analysis.....	143
4.3.6. Retrospective analysis of the ΔPSV vs ΔHR data	147
4.3.7. Analysis of variance of the results	149
4.3.7.1. Variability between days	149

4.3.7.2. Intra-observer variability	150
4.4. Discussion.....	151
4.4.1. Limitations of this study	151
4.4.2. Targeted therapeutic delivery by NaNO ₂	153
4.5. Chapter summary.....	155
Chapter 5: Nitrite and Ischaemia/Reperfusion Injury	156
5.1. Introduction	156
5.1.1. Aims of this chapter.....	157
5.1.2. Original Hypotheses.....	157
5.2. Study protocols	158
5.2.1. RIPC protocol	158
5.2.2. Stage of damage protocol	159
5.2.3. NaNO ₂ pre-conditioning protocol.....	159
5.2.4. NaNO ₂ post-conditioning protocol	160
5.2.5. Analysis of pH/SaO ₂ peri-ischaemia	161
5.3. Results	162
5.3.1. RIPC protocol	162
5.3.1.1. Subject demographics	162
5.3.1.2. Plasma NO metabolite profile following RIPC	163
5.3.2. Stage of damage protocol	165
5.3.2.1. Subject demographics	165
5.3.2.2. FMD measurement variability	166
5.3.2.3. Endothelial function	167
5.3.3. NaNO ₂ pre-conditioning protocol.....	168
5.3.3.1. Subject demographics	168
5.3.3.2. FMD measurement variability	168
5.3.3.3. IR injury.....	170
5.3.3.4. The haemodynamic response to the study infusion	171
5.3.4. NaNO ₂ post-conditioning protocol	172
5.3.4.1. Subject demographics	172
5.3.4.2. FMD measurement variability	172
5.3.4.3. IR injury.....	174
5.3.5. Summary of the ischaemic conditioning effects of NaNO ₂	175
5.3.5.1. Analysis of pH / SaO ₂ peri-ischaemia	176
5.3.6. Subsequent analysis: Does NaNO ₂ vasodilate during early reperfusion?	177
5.3.6.1. Results.....	178
5.3.7. Variability of measures employed	180
5.4. Discussion.....	182
5.4.1. Plasma [NO ₂ ⁻] increases in response to RIPC.....	182

5.4.2. Limitations of the forearm model of IR injury	184
5.4.3. NaNO ₂ is a pre-conditioning but not a post-conditioning agent.....	185
5.4.4. A clinical appreciation of the results	188
5.5. Chapter summary.....	190
Chapter 6: Pilot study.....	191
6.1. NO ₂ ⁻ associated myocardial protection in CABG patients	191
6.1.1. Study design.....	191
6.1.2. Results.....	192
6.2. Additional laboratory based pilot work	193
6.2.1. Results.....	194
6.3. Discussion.....	195
6.3.1. The redistribution of NO metabolites	195
6.3.2. The beneficial effects of blood/crystalloid cardioplegia	196
Chapter 7: General Discussion and Future Directions.....	197
7.1. The key findings of this thesis.....	198
7.2. The pharmacokinetics of NaNO ₂ – the forgotten element.....	199
7.3. The clinical implications of NaNO ₂	202
7.3.1. Pulmonary hypertension	202
7.3.2. The modulation of ischaemic environments.....	202
7.3.3. Dietary supplementation of NO ₂ ⁻	203
Publications related to this thesis.....	205
References.....	207

Chapter 1: General Introduction

1.1. The endothelium & nitric oxide

The discovery that the endothelium was more than simply an inert layer of cells lining the inner surface of blood vessels marked a paradigm shift in the field of vascular biology. In his seminal paper in 1980 Furchgott demonstrated, using isolated strips of rabbit aorta, that a transferable factor (which he coined Endothelium Derived Relaxing Factor - EDRF) was released from the endothelium in response to the administration of the known vasodilator acetylcholine (ACh)¹. That this process was endothelium dependent was demonstrated by mechanical removal of the endothelium, which resulted in loss of the ACh effect. Subsequently it was realised that EDRF was in fact the already known exogenous vasodilator nitric oxide (NO)^{2,3}. The mechanism of action by which NO elicits vasodilation is outlined in the next section and summarised in Figure 1-1 (below).

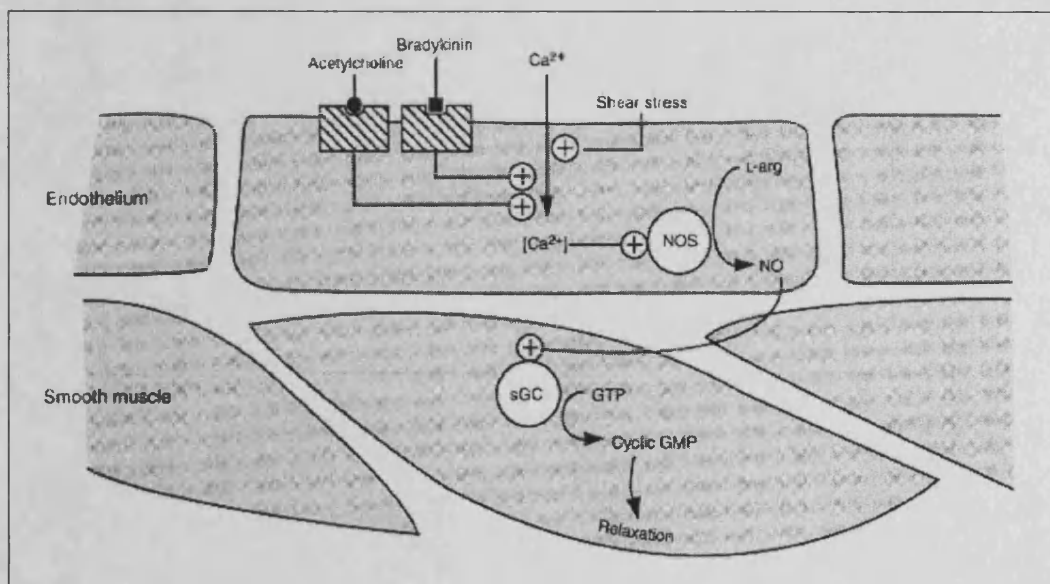


Figure 1-1: The vasodilator mechanism of action of NO. Adapted from Moncada et al⁴.

1.2. The vasodilator mechanism of action of NO

NO is produced by endothelial cells in response to an increase in the radial shear stress placed upon them, or as a result of exposure to different autacoids (e.g. bradykinin or ACh). These stimulating forces increase intracellular calcium (Ca^{2+}) levels which in turn activates the NO producing enzyme endothelial nitric oxide synthase (eNOS). Next eNOS catalyses the synthesis of NO and L-citrulline from the reaction between the amino acid L-arginine, oxygen (O_2) and nicotinamide adenine dinucleotide phosphate (NADPH)⁴. L-arginine is a non-essential amino acid. However, the bodies requirement for NO production is so great and the endogenous production of L-arginine comes at such a high energy cost that some is required to be ingested in the diet in order to remain healthy⁵. NO produced by eNOS next diffuses into vascular smooth muscle cells where it reacts with the enzyme soluble guanylate cyclase (sGC) which in turn forms cyclic guanosine monophosphate (cGMP) from guanosine-5'-triphosphate (GTP). cGMP then activates different protein kinases which in turn leads to smooth muscle cell relaxation.

A basal tone of NO production is present in man. This is demonstrated by the increase in blood pressure observed following the administration of N^G -Monomethyl-L-Arginine (L-NMMA), a competitive NOS inhibitor⁶. However, the changes seen are modest. This is due to a compensatory increase in other endothelial derived vasodilator mechanisms to ensure that adequate tissue perfusion is maintained. These alternative vasodilators include prostacyclin, which is produced via the arachadonic acid pathway⁷ and endothelium derived hyperpolarising factor⁸.

1.3. The alternative biological actions of NO

The realisation that NO was a cellular signalling molecule provided an alternative angle from which many puzzling discoveries previously reported in the bio-medical literature could be reviewed afresh. It soon became apparent that NO is capable of a myriad of different actions throughout the body. Its effects can be broadly divided into three groups, each category being associated with one of the three different sub-types of NOS enzyme.

1.3.1. Vascular

As well as producing smooth muscle cell relaxation, as described in section 1.2 (page 2), NO has other distinct functions upon the circulation. It is an antiplatelet agent⁹, reducing both platelet adhesion and aggregability. NO is also capable of controlling mitochondrial O₂ consumption by inhibiting the enzyme cytochrome c-oxidase (complex 4) on the electron transport chain (ETC)¹⁰ (see section 1.6.1.; page 40). The inhibitory action of NO upon mitochondria was known several years before the biological significance of NO was discovered. This is because the diatomic structure of NO closely resembles that of O₂ and it was therefore used as a competitive inhibitor in early studies of mitochondrial function¹¹.

In summary, the different effects of NO within the vasculature and surrounding tissue act in concert to ensure the adequate local delivery of O₂. Blood flow is promoted through antiplatelet and vasodilator activity. NO also facilitates the distribution of O₂ throughout tissue by decreasing O₂ utilisation at mitochondria proximal to blood vessels and thus promoting O₂ diffusion to more remote tissue¹².

However, the presence of NO is not just intricate to acute O₂ delivery to tissue; it also ensures an adequate supply of blood in the long term via an angiogenic

effect. This property is well demonstrated in the treatment of broncho-pulmonary dysplasia of the premature newborn¹³. Broncho-pulmonary dysplasia is characterised by a lack of pulmonary alveolar and arterial development, resulting in a pruned appearance to the pulmonary arterial vascular tree on angiography as the normal structural complexity of the lung is lost¹⁴. Inhaled NO therapy helps to protect against the development of this condition through the promotion of local angiogenesis.

1.3.2. Nervous system

It was first identified that NO was a neurotransmitter in the intestine; as L-NMMA inhibited the effect of NANC (non-adrenergic non-cholinergic) nerve stimulation¹⁵. Neuronal NOS (nNOS) was subsequently isolated as the discrete source of NO released from these nerves¹⁶. It has since been recognised that NO plays a key role in the modulation of neural tissue function throughout the central and peripheral nervous system¹⁷. It has an expected influence upon cerebral blood flow¹⁸ but also is important in the long term potentiation of nerves; a critical component in the process of memory development^{19, 20} and social-behaviour learning²¹.

It has recently been suggested, in a study using a selective nNOS inhibitor, that the basal tone of NO in blood vessels is released by nNOS from vessel associated nerves rather than from eNOS²².

1.3.3. Inflammation

Whilst both eNOS and nNOS are Ca^{2+} dependent constituent enzymes a third type of NOS, inducible Nitric Oxide Synthase (iNOS), is Ca^{2+} independent and only expressed in response to inflammatory agent stimulation (e.g. pro-inflammatory cytokines or bacterial membrane lipopolysaccharide). Consequently this type of NOS does not produce pulsed bursts of NO but more a sustained high-level release after a

period of cellular up-regulation²³. Production of NO in this manner forms part of the body's host defence mechanism.

1.3.3.1. NO as a host defence agent

The role of NO as a cytotoxic agent was suggested by two experimental observations. Firstly nitrite (NO_2^-) and nitrate (NO_3^-), both metabolites of NO (see section 1.4.1; page 10) were found in the urine of mice that had a concomitant bacterial infection²⁴. Secondly, it was discovered that macrophages require a supply of L-arginine in order to destroy tumour cells²⁵. In the second study it was also noted that tumour cells were not killed when exposed to NO_2^- alone. As a result it was suggested that a '*reactive nitrogen intermediary*' was responsible for the immunological effect of macrophages; an agent which was subsequently recognised as iNOS originating NO ²⁶.

Macrophages are able to utilise the cytotoxic effect of NO by first enveloping their target. Next NO is released into the enclosed space created around the pathogen. NO then diffuses inside the pathogen and disrupts their iron-containing enzymes; a critical component of cellular respiration⁴. Importantly, this process relies upon the concomitant production of superoxide (O_2^-) by the macrophage and therefore the cytotoxic action of NO may require the additional step of conversion to peroxynitrite (ONOO^-) first (see section 1.4.1.3, page 13)²⁷. Evidence supporting this mechanism of action can be found in an electro-paramagnetic resonance spectroscopy image reported in 1983; which displays NO bound to a ferrous component of *c. botulinum*²⁸. The cytotoxic nature of NO displayed in this paper explains the rationale behind the common manufacturing practice of adding sodium nitrite (NaNO_2) to cured meat in order to reduce the incidence of *c. botulinum* food poisoning.

1.3.3.2. NO and septic shock

As the body mounts a response to an infection its rate of NO manufacture is in balance between sufficient production to exhibit an antibacterial effect and an overproduction which will result in systemic vasodilation. If the latter situation occurs it is called septic shock²⁹. Unsurprisingly, there has been substantial interest in the use of NOS inhibitors in septic shock. However, the result of a large scale randomised controlled trial where L-NMMA was given to patients in septic shock was disappointing³⁰. The increased mortality rates observed in the study arm of this trial were attributed to the inability of L-NMMA to isolate the effects of down-regulation of NO production to one specific body compartment³¹. Therefore, despite beneficial haemodynamic effects being observed, organ dysfunction was amplified. The use of iNOS selective inhibitors may be able to overcome these problems, although the results of animal studies have been unconvincing³². The disappointing outcomes from these trials could have perhaps been predicted from the inconclusive results of numerous previous studies of steroid use in sepsis³³; as one of the actions of glucocorticoids therapy is to temper iNOS upregulation³⁴.

1.3.4. Summary of the biological actions of NO

The varied effects of NO arise from its unique biochemistry and are summarised in Figure 1-2 (below). It is a small gaseous molecule which easily diffuses to neighbouring tissue and can readily react with a number of different targets; due to the unpaired electron it possesses, (hence NO is often written as NO \cdot). Consequently, NO is highly unstable and as a discrete molecule in biological systems difficult to identify. Therefore it is often the metabolites of NO which are detected in the circulation, as shadows of previous NO production.

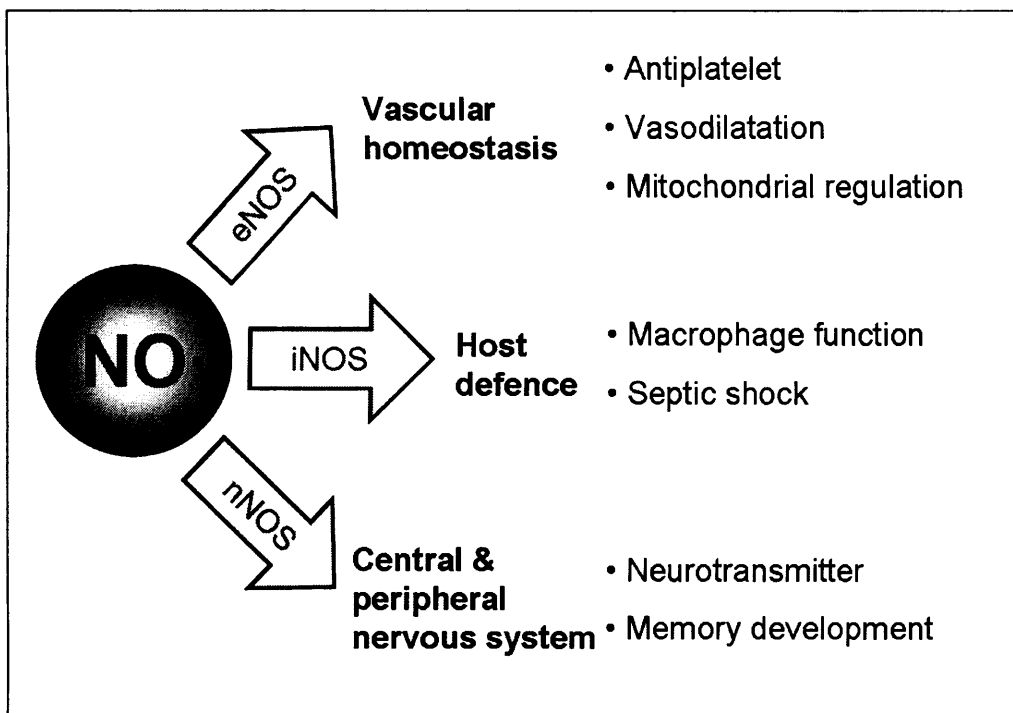


Figure 1-2: Summary of the different actions of NO throughout the body.

1.4. The metabolism of NO in blood

In 1916 HH Mitchell, an American physician, noted that a greater concentration of NO_3^- was excreted in the urine than could be accounted for by diet alone³⁵. This was the first suggestion that the body endogenously produced NO_3^- as what would subsequently be discovered to be the major vascular metabolite of NO production.

It is not possible for NO to be stored in the endothelium and therefore all NO produced from eNOS immediately diffuses away from its source. Some of this NO is responsible for the end organ effects outlined in section 1.3 (page 3), however a significant proportion enters the vessel lumen where it readily reacts with a variety of the different constituents found in blood. Three main groups of reactions occur: that with either dissolved plasma O_2 to form NO_2^- or to a lesser extent O_2^- to form ONOO^- ; erythrocyte metabolism to form methaemoglobin (Met-Hb) & NO_3^- if oxygenated haemoglobin (oxy-Hb) is present or HbNO if deoxygenated haemoglobin (deoxy-Hb) is present; and nitrosylation of thiol-groups on certain proteins to form RSNO species, (see Figure 1-3; page 9). These products of blood metabolism of NO will each be discussed in turn in the next section.

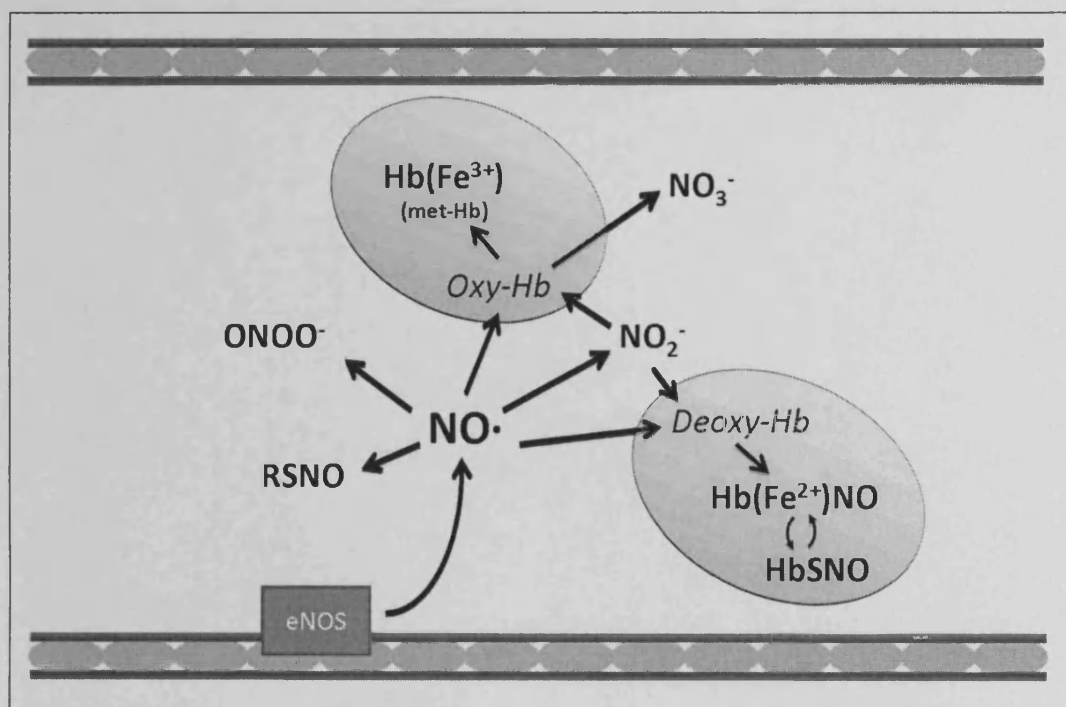


Figure 1-3: Summary diagram of the products of blood metabolism of NO. The reactions of NO within both an oxygenated and a deoxygenated erythrocyte are illustrated, together with the reaction products of NO with O₂, O₂⁻ and plasma proteins.

1.4.1. Oxidative metabolites of NO

1.4.1.1. Inorganic nitrite (NO_2^-)

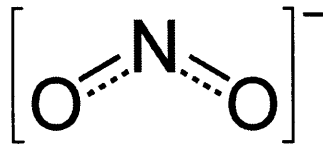


Figure 1-4: *The chemical structure of NO_2^- . An electron is shared between the two oxygen molecules and the nitrogen molecule (dashed line) resulting in anion formation. In turn a nitrite-salt will be formed when NO_2^- binds to a positive ion (e.g. sodium nitrite, NaNO_2).*

The foremost reaction of NO in plasma is with $\frac{1}{2} \text{O}_2$ to form the anion inorganic NO_2^- . The NO_2^- created then forms a salt, predominantly with sodium (Na^+), to give NaNO_2 . NO_2^- is a biochemically stable molecule in normoxic plasma and further oxidation of NO_2^- to NO_3^- is not favoured without the catalytic effect of Hb³⁶.

NO_2^- itself is a vasodilator³⁷. However this effect is relatively weak when compared to specific NO donor agents such as organic nitrates, e.g. glyceryl trinitrate (GTN)³⁸.

1.4.1.2. Inorganic nitrate (NO_3^-)

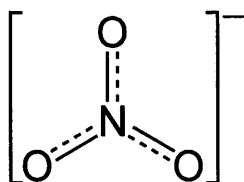


Figure 1-5: *The chemical structure of inorganic NO_3^- . An electron is shared between the three oxygen molecules and the nitrogen molecule (dashed line) resulting in anion formation. Therefore, in turn, a nitrate salt will be formed when NO_3^- binds to a positive ion (e.g. sodium nitrate, NaNO_3).*

The principle reaction of NO in blood is with oxy-Hb³⁹ to form the anion inorganic NO_3^- and met-Hb. The NO_3^- formed is subsequently removed from the erythrocyte into plasma and then excreted by the kidneys.

NO_3^- is a highly stable molecule which has no intrinsic vasodilator properties. However, when ingested orally NO_3^- can be converted into NO_2^- ; a process which can result in a measurable vasodilator effect⁴⁰ (see section 1.4.5; page 20).

1.4.1.2.1. NO passage into the erythrocyte

There is no consensus opinion of the precise mechanism by which NO enters the erythrocyte to participate in the reaction outlined above. NO gas can freely diffuse across the bilayer phospholipid structure of the erythrocyte membrane. However the presence of an erythrocyte free zone adjacent to the endothelium⁴¹, a state favoured by laminar blood flow, will divert free NO as it leaves the endothelium towards the non-erythrocytic metabolic routes outlined in this section. It is therefore more probable that the majority of NO_3^- substrate enters the erythrocyte in the form of NO_2^- ⁴². However, unlike other cellular membranes which allow a free flux of small ions⁴³

(including NO_2^-), the erythrocyte membrane has a high cholesterol composition that renders it relatively impermeable to small ion transit⁴⁴, (see Figure 1-6, below). Consequently, erythrocyte membrane ion transport is controlled by specific channels; anion exchange principally occurring via anion exchange channel 1 (AE1). The primary function of this channel is to allow a smooth flux of bicarbonate (HCO_3^-) across the erythrocyte membrane to aid circulatory carbon dioxide (CO_2) transport and pH buffering. AE1 therefore forms a critical component of erythrocyte function. However, it is not specific to HCO_3^- and the structurally similar NO_2^- can also be ported by it, albeit at a slower rate than NO_2^- is transported into other compartments of the body⁴².

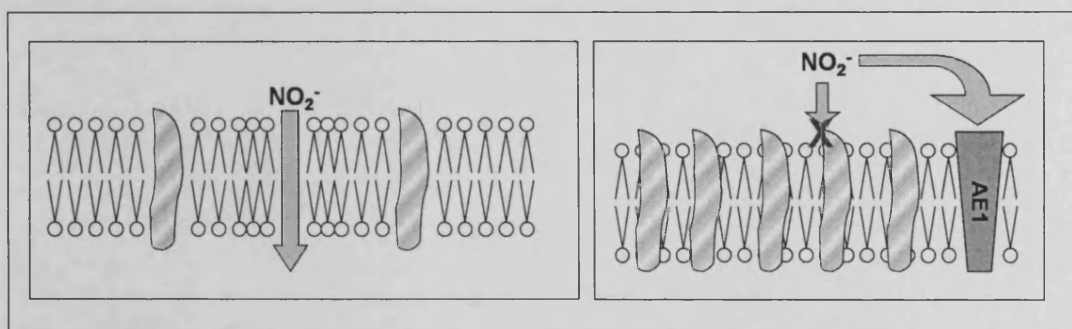


Figure 1-6: *The transit of NO_2^- across different cellular membranes. Left panel = a standard bilayer phospholipid membrane. The fluidity inherent to this structure allows for relatively free ion transit (NO_2^- illustrated). Right panel = the erythrocyte membrane contains a much greater proportion of cholesterol. Correspondingly, anion transit is only possible through the specific ion exchange proteins (AE1 illustrated).*

In summary, NO produced by the endothelium that enters the circulation is predominantly metabolised to NO_3^- in a process which requires Hb. NO_2^- is a potential intermediate of this process, which is formed by the reaction of NO and O_2 in plasma before entering the erythrocyte.

1.4.1.3. Peroxynitrite (ONOO⁻)

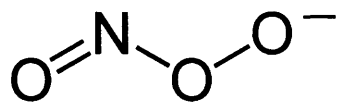


Figure 1-7: *The chemical structure of peroxynitrite*

Peroxynitrite (ONOO⁻) is the product of the reaction between NO and superoxide (O₂⁻)⁴⁵, a form of reactive oxygen species (ROS). This reaction does not require an enzymatic catalyst. It occurs at a near diffusion-limited rate whenever the two substrates are produced in proximity to one another; a situation which arises when the body is placed under any pro-inflammatory stimulus. In the instance of an acute bacterial infection this is beneficial (see section 1.3.3.1; page 5). However, certain chronic diseases are characterised by a constant exposure to a low grade inflammatory stimulus and in these situations the production of ONOO⁻ can be detrimental (see section 1.4.1.3.2; page 14).

1.4.1.3.1. Superoxide (O₂⁻)

There are three main in-vivo sources of O₂⁻. The majority arises as a product of white blood cell NADPH oxidase activity, an important part of the host defence mechanism (see section 1.3.3.1; page 5). In addition, O₂⁻ is produced when incomplete reduction of O₂ takes place along the mitochondrial ETC. This event is known as mitochondrial uncoupling or ‘electron leakage’ and is enhanced by an ischaemic environment (see section 1.6.1.2; page 41). Thirdly, O₂⁻ is generated when an activated NOS enzyme lacks either the substrate L-arginine or the essential co-factor tetrahydrobiopterin; the latter situation is often referred to as ‘NOS uncoupling’⁴⁶. Indeed the presence of O₂⁻ will deplete tetrahydrobiopterin, thus

uncoupling NOS and forming a positive feedback cycle which will exaggerate its own production.

O_2^- will react with and damage any protein or other biological structure which it comes into contact with. To counter this, the enzyme super-oxide dismutase (SOD) is present throughout the body to rapidly remove O_2^- as soon as it is formed. However, the rate-constant for the reaction of NO with O_2^- is greater than that of O_2^- with SOD, thus permitting ONOO⁻ formation⁴⁷.

1.4.1.3.2. The biological significance of ONOO⁻

Unlike NO, ONOO⁻ has little role as a signalling molecule. It is a strong oxidant⁴⁸ and through its production the body is able to convert NO from an integral component of vascular homeostasis to part of the immune system. However, pathologies which chronically up-regulate these processes and favour NO metabolism to ONOO⁻ will detrimentally deter NO from its more usual biological functions. This occurs, for example, in hyperlipidaemia, metabolic syndrome, diabetes mellitus (DM) and rheumatoid arthritis⁴⁹. This specific pathological feature of these diseases is often referred to as 'endothelial dysfunction'. Significantly there is a strong correlation between endothelial dysfunction, as measured by physiological 'stressing' of the endothelium, and cardiovascular mortality⁵⁰.

1.4.2. Thiol bound NO metabolites

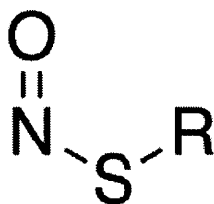


Figure 1-8: *The chemical structure of an S-nitrosylated protein. The 'R' represents the body of the protein chain and the 'S' the thiol group which binds to NO.*

Sulfhydryl groups (-SH, also known as thiol-groups) are frequently found in proteins and play a key role in the post-translational modification of their quaternary structure. This is due to the ability of the labile S-H bond to react with a number of different substrates, and in doing so alter the conformational state of the protein. This process acts as a molecular regulator of protein function, as the resulting shape of the protein either enhances or inhibits the intended action⁵¹. One such substrate is NO, the reaction with this molecule resulting in a semi-stable group of compounds called nitrosothiol (SNO) species³⁸. In plasma, protein thiol bound NO groups are called RSNO groups; the R relating to the associated protein structure on which the thiol-group is found.

The most abundant source of RSNO in plasma is albumin bound SNO⁵². In-vitro experiments show that RSNOs exhibit a NO-type effect upon platelets and vascular smooth muscle, but are more stable than NO gas⁵³. When assessed in equimolar concentrations they are a more potent vasodilator than NO₂⁻³⁸.

1.4.3. Intra-erythrocyte NO metabolites

NO will enter the erythrocyte as either NO gas or NO_2^- and is then primarily metabolised to NO_3^- by oxy-Hb (see section 1.4.1.2; page 11). Although there are reports of a 2:1 intra:extra erythrocyte NO_2^- gradient⁵⁴, other groups report that a much smaller amount of NO_2^- is found inside the erythrocyte⁵⁵. Furthermore, the complex structure of Hb and how this alters with variation in O_2 result in additional metabolites of NO forming within the erythrocyte.

1.4.3.1. The molecular structure of Hb

The most common type of Hb in adults is HbA; a tetrameric molecule consisting of four subunits⁵⁶. Each subunit contains a large globular protein chain called a globin (two of both α and β types) which is tightly associated with a haem group. The haem group consists of an iron molecule held in position by a porphyrin ring. This iron molecule is capable of reversibly binding O_2 (or other diatomic gases, e.g. carbon dioxide (CO_2) or NO) when it is in a ferrous (Fe^{2+}) configuration. In this state an electron is temporarily donated to the bond. However, if the bound diatomic gas extracts itself from the haem group in an oxidised state (i.e. by absorbing this electron into its own structure) then the iron molecule is altered to a Fe^{3+} state. This redox arrangement of haemoglobin is known as methaemoglobin (met-Hb). $\text{Hb}(\text{Fe}^{3+})$ is not capable of binding O_2 . Consequently the erythrocyte contains an enzyme, called methaemoglobin reductase⁵⁷, which reactivates Hb by reducing $\text{Hb}(\text{Fe}^{3+})$ back to $\text{Hb}(\text{Fe}^{2+})$. O_2 transport by Hb in itself does not result in the formation of met-Hb.

1.4.3.2. The allosteric regulation of Hb structure

The four globin molecules of Hb adopt a different allosteric structure as they switch from an oxygenated (relaxed or R state structure) to a deoxygenated form (tense or T state structure). Hb therefore adopts a different conformational structure as each of these four globin groups either gains or loses an O₂ molecule. This in turn results in the sigmoid-shaped binding curve of Hb for O₂ and the regulation of O₂ delivery to tissue.

1.4.3.3. Hb bound NO

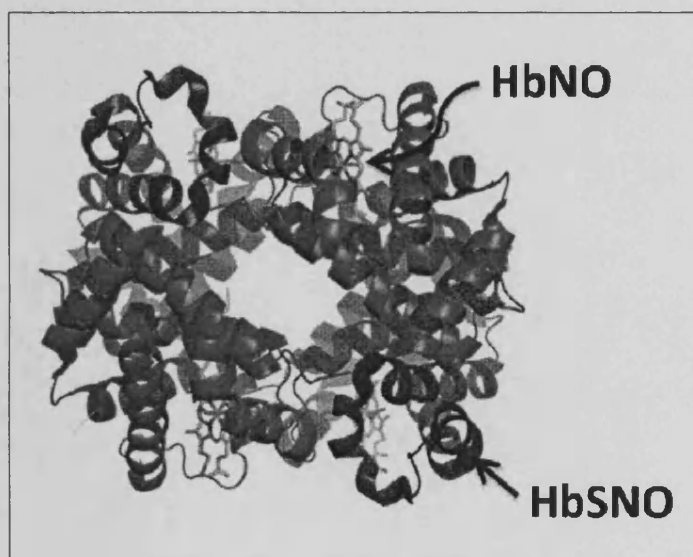


Figure 1-9: Diagram of the four globin units of Hb (red (α) and blue (β)) and their four associated haem units (green rings held within each globin unit). NO will attach at each haem binding site to form HbNO and in addition can bind to a free thiol site on each β -globin unit to form HbSNO. Adapted from www.mcat45.com.

NO will react with Hb at any available empty haem-binding site to form $\text{Hb(Fe}^{2+}\text{)NO}^{58}$. This reaction is favoured more with the T state configuration of deoxy-Hb. Hb can also bind NO on a thiol site of the β -globin subunit at the β -93

cysteine codon; to form HbSNO⁵⁹. This occurs when HbNO is re-oxygenated, as the presence of O₂ displaces NO from the haem-binding site to the β -93 cysteine position. This reaction is therefore favoured when Hb is in the R state⁶⁰. Crucially, when this reaction occurs the haem group retains the Fe²⁺ configuration and therefore remains able to bind O₂. Figure 1-9 (page 17) is a figure illustrating these two forms of Hb bound NO.

1.4.4. The relative distribution of blood NO metabolites

In summary, NO produced at the endothelium is highly reactive and rapidly forms a variety of secondary molecules. Some of these products result in signal transduction and the biological effects of NO. Others occur within the vasculature; the predominant reaction being NO₃⁻ formation by oxy-Hb. Figure 1-10 (below) displays the distribution of the different metabolites of NO typically found in venous blood.

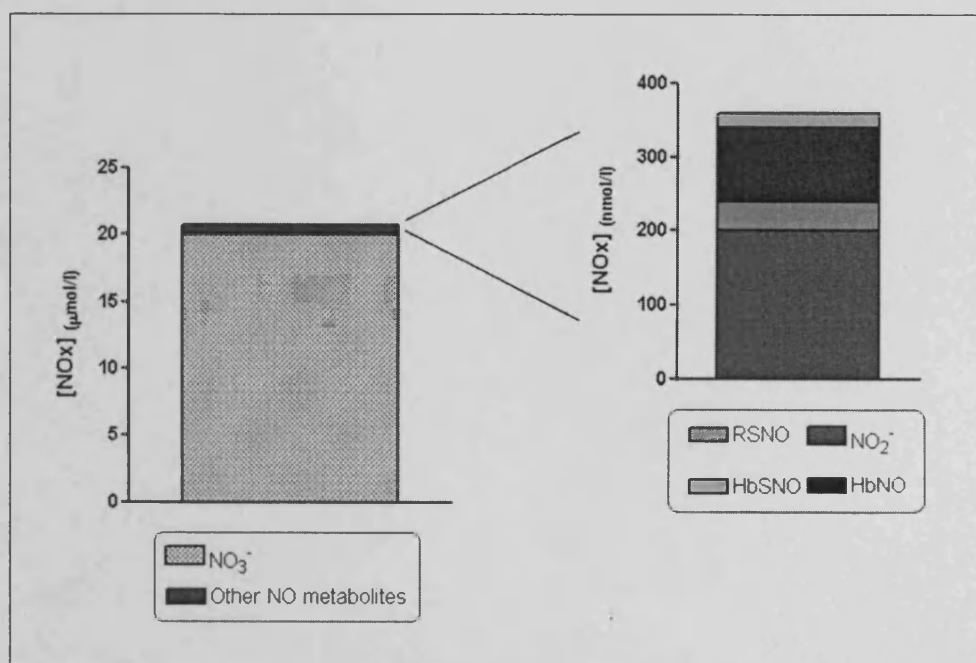


Figure 1-10: The relative distribution of NO metabolites in venous blood. Data taken from chapter 3 of this thesis.

1.4.4.1. NO metabolite distribution as a function of Hb-O₂ saturation

A decrease in Hb-O₂ saturation will cause a decrease in plasma [NO₂⁻] and an increase in [HbNO]⁵⁵, a correlation shown in Figure 1-11 (below). This observation, that the local concentration of O₂ is responsible for the different apportionment of NO metabolites in blood, has been the focus of a large body of research which will be discussed in the next section. The drive behind this work has been the central tenet that the biochemical shifts observed with a decrease in O₂ are responsible for the physiological changes of hypoxia.

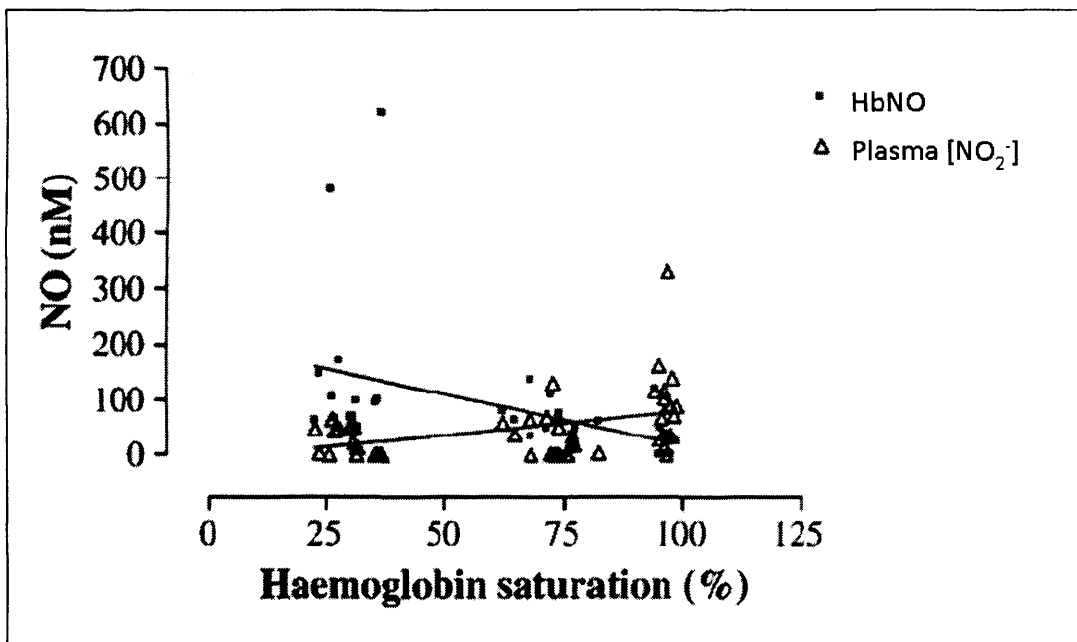


Figure 1-11: The relationship between HbNO and plasma NO₂⁻ levels with altering Hb saturation. Adapted from Rogers et al⁵⁵.

1.4.5. Dietary NO_3^- as a source of plasma NO_2^-

30% of plasma $[\text{NO}_2^-]$ is obtained from the diet, with the balance arising from intravascular metabolism of NO produced by the endothelium⁶¹. The major dietary sources of plasma $[\text{NO}_2^-]$ are foods rich in $\text{NO}_3^-/\text{NO}_2^-$, e.g. vegetables and red meat⁶². After ingestion, commensal bacteria in the upper gastro-intestinal tract reduce NO_3^- to NO_2^- , which is then further reduced to NO by the acidic environment of the stomach. NO gas is then absorbed into the circulation, where it is oxidized to NO_2^- in plasma⁶³.

1.5. The physiological importance of blood NO metabolites

1.5.1. The endocrine properties of NO

The reaction of NO with pure Hb occurs at a near diffusion-limited rate (10^7 m.s^{-1})⁶⁴. Therefore, and despite the presence of the erythrocyte-membrane which retards the diffusion of NO to Hb, the half life of NO in blood is very short (<2ms) and in normoxic tissue it has been estimated to be only marginally longer at approximately 0.1s⁶⁵. Correspondingly NO itself has a limited diffusion distance over which it is capable of exhibiting an effect⁶⁶; a finding which concurs with the observation that NOS enzymes are intricately regulated at a local level and are highly compartmentalised²³. This led to the field of NO research asserting that the metabolism of NO in blood was a one-way process. In addition it was stated that NO had a sphere of influence that was strictly limited to the area immediately adjacent to where it was produced⁶⁷.

This opinion was challenged when a detailed analysis of the physiological effects of inhaled NO gas (at higher doses of 80 parts per million) was performed. Cannon showed that during administration of inhaled NO the expected vasoconstriction that would result from regional L-NMMA infusion into the forearm was prevented⁶⁸. The concentrations of several blood NO metabolites were raised in this experiment, suggesting that one or more of these could be a stable intermediate by which blood was capable of transporting a NO-type effect to a site remote to its production or administration. This observation led to the formation of two different theories; each an attempt to explain the biochemistry responsible for the endocrine properties of NO. These theories will be critiqued in turn in the following sections.

1.5.2. HbSNO as a modulator of endocrine NO function

1.5.2.1. Theory

Stamler demonstrated in 1992 that plasma protein-nitrosothiols vasodilate isolated rings of aorta and inhibit platelets⁵³. The same author also reported, using photolysis-chemiluminescence to measure SNO levels, that the concentration of HbSNO was greater in arteries ($311 \pm 55\text{nM}$) than in veins ($32 \pm 14\text{nM}$)⁶⁰. These observations prompted the formation of the following theory of how HbSNO is involved in the regulation of blood vessel tone⁶⁹.

Hb(Fe^{2+})NO, is formed in the venous circulation as the product of the reaction between NO and deoxy-Hb (i.e. Hb in the T state). Upon reaching the lungs this molecule of ferrous bound NO is transferred to the $\beta 93\text{-cys}$ residue of Hb as the haem-binding site becomes occupied by O_2 and the allosteric conformation of Hb switches to the R state. HbSNO has a less avid binding capacity for NO than ferrous bound NO and, in addition, the thiol bond of HbSNO is stronger in the R state than the T state. These two biochemical features combine to promote the release of NO from HbSNO as the erythrocyte subsequently arrives in the peripheral vasculature. Consequently local ('hypoxic') vasodilatation occurs⁷⁰. This theory is summarised in Figure 1-12 (page 23).

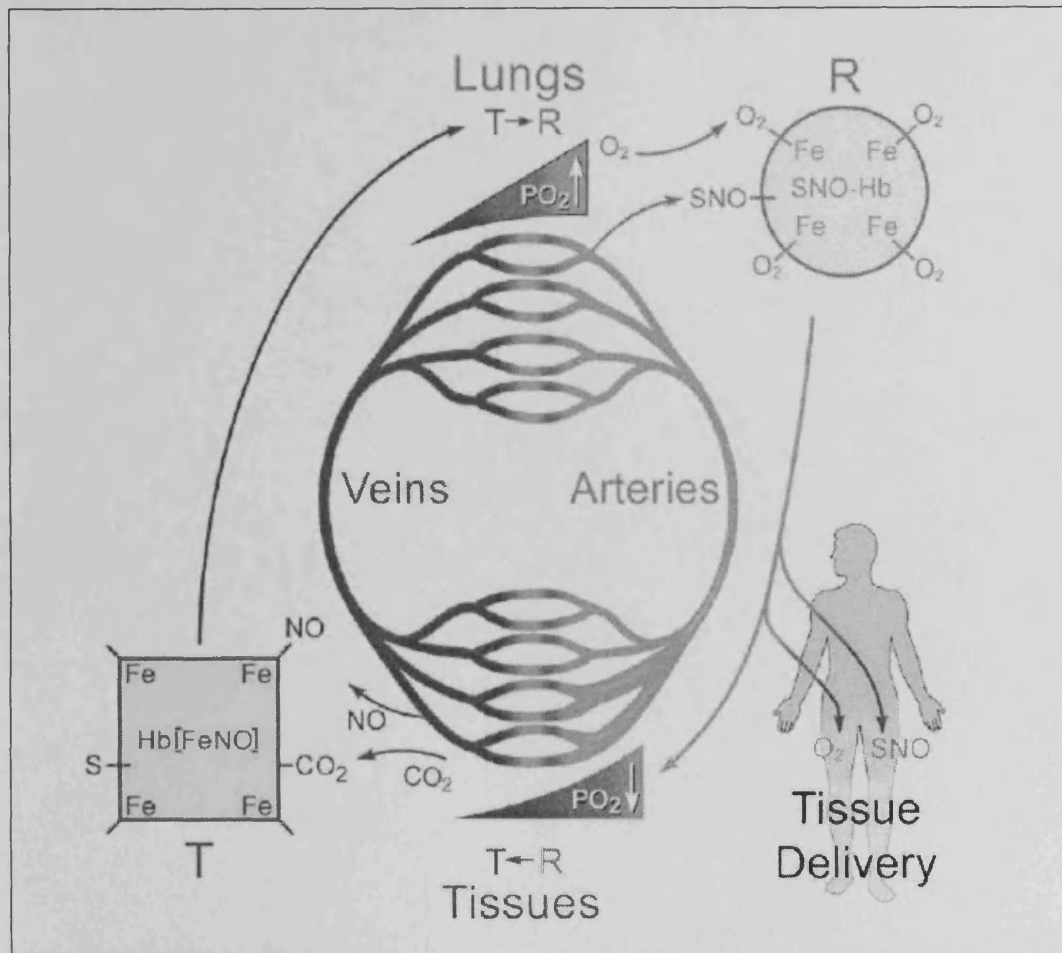


Figure 1-12: The Stamler model of HbSNO delivery of NO to the hypoxic peripheral vasculature. Adapted from McMahon et al⁶⁹

1.5.2.2. Criticisms of the HbSNO theory

The HbSNO model as a means to explain the endocrine properties of NO is intuitively appealing. It offers a simplistic and elegant means by which both biochemical and physical forces are balanced as the environment switches from high to low O₂. However, many groups have queried its validity.

Joshi⁷¹ questioned the biochemical relevance of the supporting experiments performed by Stamler and colleagues. In the original work performed by Gow⁷² it was reported that HbSNO was produced when NO was mixed with Hb. Joshi repeated this experiment but, rather than giving a large bolus of pure NO, instead used an equivalent concentration of an NO-donor agent (*MAHMA-NO*) to provide a slow and steady supply of NO. Under these revised conditions, claimed by the authors to be a closer mimic of physiology, NO₃⁻ was formed to a far greater extent than HbSNO.

Gladwin reported that HbSNO is highly unstable when in the intracellular environment of the erythrocyte⁷³, as opposed to the more stable purified conditions used by Stamler in his original supportive work. In a separate paper⁷⁴ Gladwin also failed to replicate the gradient of HbSNO between artery ($45 \pm 14\text{nM}$) and vein ($63 \pm 13\text{nM}$) previously reported by Stamler⁶⁰. However, a different analytical technique was used in this experiment to detect HbSNO (i.e. tri-iodide chemiluminescence).

Theoretical concerns of the HbSNO theory have also been raised. Schechter suggested that the levels of HbSNO measured in vivo (i.e. less than 70nM) were too low to justify the status of HbSNO as an important agent of vascular reactivity⁷⁵. The quantitative nature of this observation has been disputed due to the methodological differences between groups in how HbSNO is measured⁷⁶. However, irrespective of this point it was countered by Stamler that the absolute level of NO signal produced by a compound when it is measured does not equate to the associated bioactivity of

that molecule⁷⁷. Indeed, Stamler also commented that NO gas is present at just picomolar concentrations in tissue but is still an important vasodilator.

Lastly, studies have been performed using mice where an alanine molecule has been substituted for the cysteine group at the $\beta 93$ position of Hb⁷⁸. Hb from these mice is therefore unable to form HbSNO. Upon testing $\beta 93$ -cys knockout mouse erythrocytes in an isolated vessel preparation it was found that they exhibited a similar hypoxia-dependent vasodilator effect to erythrocytes containing wild type Hb. It is important to clarify that whilst this negative data is significant it does not discount the HbSNO theory altogether. Merely it confirms that in the absence of HbSNO the erythrocyte contains alternative vasodilator mechanisms which can assume equal importance.

In summary, the inability of the proponents of the HbSNO theory to perform any in-vivo experiments, other than simple observational studies, has rendered it difficult for this theory to be convincingly confirmed or refuted. Consequently much of the supporting work has been in the form of laboratory experiments which have been criticised for the methods used and the conclusions drawn from their results.

1.5.3. NO_2^- & deoxy-Hb as modulators of endocrine NO function

1.5.3.1. Theory

NO_2^- is the second most abundant metabolite of NO in blood (after NO_3^-) and is therefore theoretically appealing as the major intra-vascular source of bioactive NO. In a human forearm experiment, performed by Gladwin in 2000, a negative gradient of plasma $[\text{NO}_2^-]$ from artery ($540 \pm 74\text{nM}$) to vein ($466 \pm 79\text{nM}$) was reported⁷⁴. In addition, it had previously shown by another group that a positive gradient of $[\text{HbNO}]$ between artery ($536 \pm 99\text{nM}$) and vein ($894 \pm 126\text{nM}$) exists⁶⁰. In the same paper Gladwin also reported that the cross-vascular gradient of plasma $[\text{NO}_2^-]$ was more pronounced in the presence of (maximal) exercise and L-NMMA; interventions which both act to decrease venous O_2 levels. Therefore it was suggested that consumption of NO_2^- , to form bioactive NO, was occurring with the transit of blood from artery to vein, in response to a decrease in O_2 level. Although no mechanism was investigated in this observational study, it was proposed that NO_2^- was being reduced to NO across the vascular bed and as a result contributing to arterial tone.

1.5.3.1.1. Deoxy-Hb as a NO_2^- reductase

The observations detailed above are consistent with the reaction kinetics of NO_2^- and deoxy-Hb first described by Doyle in 1981⁵⁸:



Equation 1-1: NO_2^- reacts with deoxy-Hb to give met-Hb and NO, this NO is subsequently captured by an adjacent free haem group to produce HbNO.

However, this simplified equation does not explain the complexity of the different reactions between NO_2^- and Hb which occur at different O_2 levels. The bimolecular rate-constant of NO_2^- with R state (oxy-)Hb is ten-times greater than with T state (deoxy-)Hb⁷⁹, but the T state conformation of Hb offers a greater number of unoccupied haem-groups for binding NO_2^- . Furthermore, a study by Cosby (and Gladwin) showed that, using isolated rings of aorta, the vasodilator effect of NO_2^- in the presence of erythrocytes is enhanced when O_2 levels are reduced⁸⁰. However, this result was not replicated when the same experiment was repeated by a different group⁸¹. Cosby also reported that this NO_2^- -erythrocyte dependent vasodilatation initially occurred at an O_2 tension of 50 mmHg, which was calculated to correspond to a Hb saturation of approximately 50%. These findings led Gladwin to suggest that the most efficient conformational state of Hb to allow NO_2^- reduction to NO was at an O_2 saturation of 50%⁸².

As a result of these observations Gladwin proposed that NO_2^- reduction to NO occurs as the environment becomes increasingly hypoxic, and that this process takes place within the erythrocyte. Deoxy-Hb was identified as the reductase responsible for this reaction, with a maximal reaction rate occurring at 50% O_2 saturation, (see Figure 1-13; page 28). Furthermore, it was contended that this process was responsible for both the maintenance of normal blood vessel tone and the phenomenon of hypoxic vasodilation⁸³.

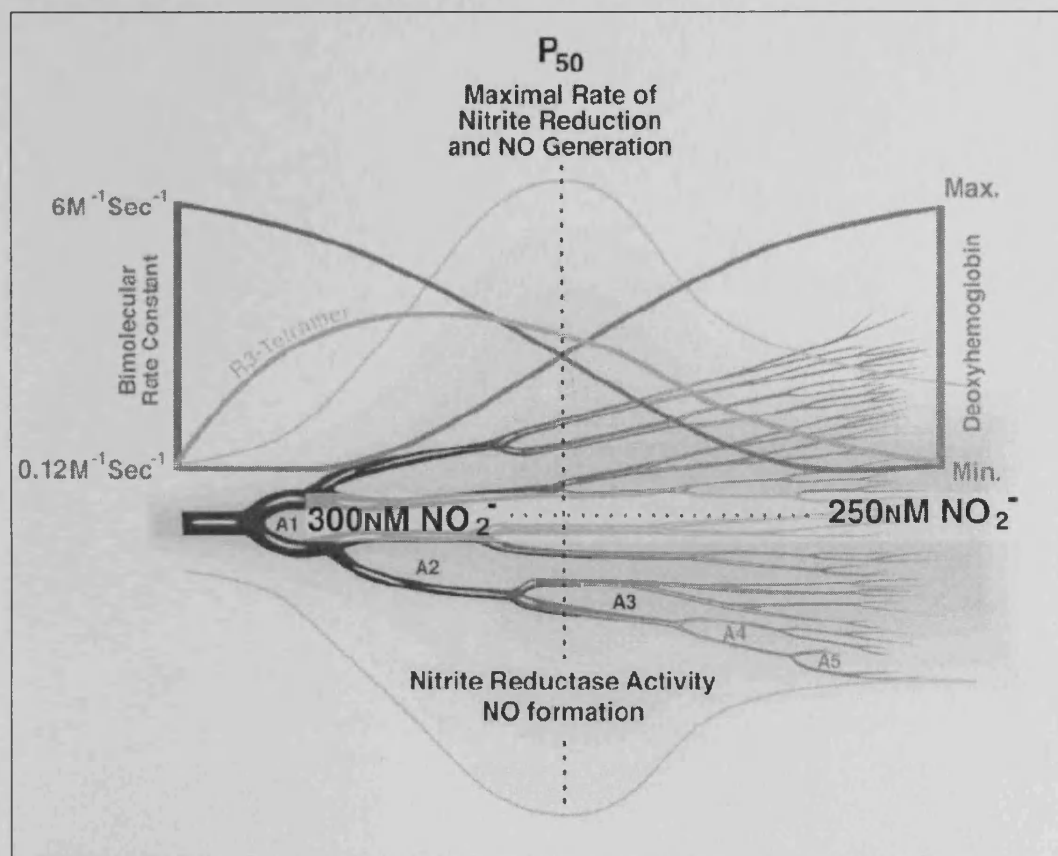


Figure 1-13: Schematic diagram of the deoxy-Hb theory of NO_2^- reduction during transit from artery to vein. Adapted from Gladwin et al⁸³.

1.5.3.2. Criticisms of the deoxy-Hb/ NO_2^- reductase theory

As with the HbSNO theory, there have been many criticisms of the deoxy-Hb theory of NO_2^- reduction as the means to explain the endocrine properties of NO.

The principle concern raised by several groups is the lack of an obvious mechanism by which the NO produced either extracts itself from Hb (which will bind it more avidly the lower O_2 levels become) or once it has extracted itself is able to leave the erythrocyte⁷². The formation of an intermediate molecule has been suggested as a means of bridging this conceptual gap⁵⁴. However no clear

intermediate has been identified and the inclusion of this concept adds an unsatisfactory extra layer of complexity to the theory.

Secondly, other groups have reported that whilst a change in oxygenation will result in a re-apportionment of NO within the vasculature no overall consumption of NO metabolites is present over a single arterial to venous transit cycle⁵⁵.

Thirdly, the vasodilator activity of NO_2^- is enhanced by hypoxia in an isolated vessel model; an environment which is erythrocyte independent⁸⁴. Indeed, there are several haem-containing enzymes found within the blood vessel wall and associated tissue, which are all capable of NO_2^- reductase activity. Xanthine oxidase (XO) is one such enzyme which has been shown to have an enhanced capacity as a NO_2^- reductase in hypoxia⁸⁵. Simple acid disproportionation of NO_2^- will also result in NO formation⁸⁶, although it should be acknowledged that this mechanism is more appropriate to an ischaemic environment rather than a purely hypoxic one.

In summary, the deoxy-Hb/ NO_2^- reductase theory has received a number of criticisms relating to the conceptual gaps it contains and inconsistencies which have been exposed when it has been explored in different models. However, one of the enduring strengths of this theory has been the ability of others to continually support or challenge it by the performance of studies which involve the administration of NO_2^- to humans.

1.5.4. Previous human studies of exogenous NO_2^- administration

There have been five previous studies where the effects of intravenous NO_2^- administration upon humans have been examined. These are addressed individually below and are summarised in Table 1-1 and Table 1-2 (pages 35 & 36).

1.5.4.1. Lauer et al

In 2001, before the publication of the deoxy-Hb/ NO_2^- reductase theory, Lauer reported an experiment where a brachial artery infusion of NaNO_2 was given to three healthy human subjects⁸⁷. No difference in forearm blood flow (FBF) was observed in this study despite a one hundred-fold increase in plasma $[\text{NO}_2^-]$ to $>130\mu\text{M}$. In their discussion the authors discounted the notion that NO_2^- possessed any significant vasodilator action. Instead they proposed that it was simply a marker of regional NO production by the endothelium.

1.5.4.2. Cosby et al

The very small sample size used by Lauer together with the negative result prompted Cosby to perform a similar study in 2003⁸⁰. An infusion of NaNO_2 was given into the brachial artery of healthy human subjects at doses ascribed to be either pharmacological (i.e. associated with an increase in ipsilateral venous plasma $[\text{NO}_2^-]$ from 200nM at baseline to $221\mu\text{M}$ at peak) or physiological (i.e. an increase from 200nM to $2.56\mu\text{M}$). FBF was measured using strain gauge plethysmography (SGP) in the ipsilateral arm to that infused and found to increase in both groups by 175% and 25% respectively. It was further observed that during exercise (which was associated with a reduction in venous O_2 levels) there was an additional increase in FBF and decrease in venous plasma $[\text{NO}_2^-]$. This study forms an important part of the supporting evidence that underpins the deoxy-Hb/ NO_2^- reductase theory.

1.5.4.3. Dejam et al

In 2007 Dejam conducted a series of experiments to explore in-vivo the potential mechanisms responsible for NO_2^- associated vasodilation⁸⁸. The influence of NaNO_2 (delivered via the brachial artery) upon FBF was measured in healthy human subjects. Co-administration of either allopurinol (to block XO) or ascorbic acid (to promote acid disproportionation) accompanied the NO_2^- infusion. Neither of these additional agents had a significant effect upon NO_2^- bioactivity. In addition, a dose escalation regime of NO_2^- was infused and the subsequent decay profiles of both venous [HbNO] and plasma [NO_2^-] were recorded. The profiles of these two NO metabolites followed both each other and the simultaneously recorded profile of ipsilateral FBF. This observational evidence was used by the authors in support of the deoxy-Hb/nitrite reductase theory.

1.5.4.4. Maher et al

In 2008, after this thesis was started, Maher performed an experiment examining the physiological effects of NO_2^- infusion upon the human forearm⁸⁹. Forearm venous volume was measured in addition to FBF. It was reported that veins respond to NO_2^- at a lower dose than arteries do in normoxia. As an additional experiment subjects inhaled a hypoxic gas mixture to reduce their capillary O_2 saturation level from 97% to 83-88%. Equivalent quantities of NO_2^- infused in this environment had an enhanced effect upon FBF than when they had been delivered under normoxia conditions. In addition, an isolated vessel model was used to confirm the relative sensitivity of veins to NO_2^- , when compared to arteries. This model also emphasized an observation reported by other groups^{81, 84} that hypoxia-mediated

changes in vascular sensitivity to NO_2^- can occur in an erythrocyte-independent environment.

1.5.4.5. Mack et al

This phase 1 clinical trial was designed to investigate the physiological effects and safety of a similar infusion regime of NaNO_2 given intra-arterially to either homozygous sickle cell disease (SCD) patients or healthy volunteers⁹⁰. The control group data was taken from the Cosby study, performed 5 years earlier⁸⁰. Mack reported that venous plasma $[\text{NO}_2^-]$ levels measured in the patient group were lower than that recorded in matched controls, despite a slightly greater concentration of NaNO_2 having been infused. Unfortunately the O_2 saturation levels of the two groups were not reported. Unsurprisingly, the lower concentration of plasma NO_2^- achieved in the patient group corresponded with a less pronounced change in ipsilateral FBF compared to the controls. The authors suggested that this was due to a decrease in NO_2^- bioavailability in sickle cell disease patients. It was also proposed that this observation could explain the mechanism behind some of the vascular complications of sickle cell disease.

1.5.4.6. Criticisms of the above studies

Many criticisms can be made of the conclusions derived from these in-vivo studies investigating the effects of NO_2^- supplementation upon vascular function.

Firstly, although Cosby asserted that the infusion of NaNO_2 given in their study was 'physiological' it resulted in a ten-fold increase in plasma $[\text{NO}_2^-]$. The authors claimed that this level was still close to the normal range of human plasma $[\text{NO}_2^-]$. Whilst it should be acknowledged that any infusion is by definition pharmacological and therefore the point at which an infusion becomes

'pharmacological' as opposed to 'physiological' is a somewhat nebulous concept; there is clearly a need to investigate the effect of NO_2^- supplementation at lower doses to those previously employed. An infusion of NaNO_2 which results in a measurable physiological effect at the lowest concentration of plasma $[\text{NO}_2^-]$ possible would be optimal.

A general criticism of the previous studies performed is that high doses of NaNO_2 have tended to be used. This will have had the effect of swamping some of the pathways of NO metabolism and in the process potentially missing subtle physiological and biochemical changes. This defect is well illustrated by Dejam, where a dose escalation regime of NaNO_2 is used to calculate the pharmacokinetic properties of NO_2^- . The standard pharmacological method in this situation would be to use a single infusion dose of NaNO_2 and to observe the decay profile following its cessation.

Secondly, most of the previous investigations have been confined to a single vascular bed; the forearm. By limiting observations in this manner the differential effect of NaNO_2 upon other vascular compartments could have been missed along with important mechanistic insights. In particular the pulmonary vasculature frequently behaves differently to the systemic circulation and as such would provide a potentially insightful environment in which to examine the effects of NaNO_2 .

Thirdly, Maher produced hypoxia through the use of an inhaled low- O_2 mixture delivered via a face mask for approximately 30 minutes. Exposure to hypoxia alone will result in systemic vasodilation which does not plateau until after more than two hours of continuous exposure⁹¹. It is therefore important to allow an adequate hypoxia equilibration period when performing studies in hypoxia, to ensure that a

steady baseline is present on which the effects of the study intervention can be measured.

Lastly, all bar one of the previous studies performed have been in healthy volunteers. Whilst these studies are vital to ensure the safety and efficacy of NO_2^- there is an urgent need to explore the effect of NaNO_2 in patient groups. In particular the effect of NaNO_2 upon patients with cardiovascular disease requires further investigation as this group is the most likely to benefit from NO_2^- -based therapies in the future.

Table 1-1: Previous studies of NO₂⁻ administration to man (part 1).

Author	Year	Number & type of subjects	Physiological measure	NaNO ₂ delivery regime	Results	Conclusions drawn
<i>Lauer et al</i> ⁸⁷	2001	3 (healthy subjects)	SGP measurement of FBF	Brachial artery infusion: • 0.01 - 36µmol/min	<ul style="list-style-type: none"> • Peak venous plasma [NO₂⁻] >130µM. • No change in FBF noted at any dose. 	<ul style="list-style-type: none"> • NO₂⁻ possesses no intrinsic vasodilator properties.
<i>Cosby et al</i> ⁸⁰	2003	18 (healthy subjects)	SGP measurement of FBF	Brachial artery infusion: • 36µmol/min (5 min) • 400nmol/min (5 min)	<ul style="list-style-type: none"> • Peak venous plasma [NO₂⁻] = 221.82µM. 175% increase in ipsilateral FBF & systemic BP ↓ 7mmHg. [HbNO] increase observed. Associated with both NaNO₂ infusion & decreasing SaO₂. • Peak venous plasma [NO₂⁻] = 2.56µM. 28% increase in ipsilateral FBF. 	<ul style="list-style-type: none"> • NO₂⁻ has vasodilator properties at both 'pharmacological' & 'physiological' doses; due to its conversion to NO. • The mechanism of NO₂⁻ reduction to NO is catalysed by deoxy-Hb.
<i>Dejam et al</i> ⁸⁸	2007	<ul style="list-style-type: none"> • Part A = 10 (healthy subjects) • Part B = 15 (healthy subjects) 	SGP measurement of FBF	Brachial artery infusion: • Part A: 7, 14, 28, 55, 110 µmol/min (5 min/dose) • Part B: 0.07, 0.14, 0.35, 1.4, 3.5, 7, 14, 28 µmol/min (5 min/dose) +/- co-infusion: - saline (n=5) - oxypurinol (n=5) - ascorbic acid (n=5)	<ul style="list-style-type: none"> • Ipsilateral & contralateral increase in FBF with each dose given. Venous profile of [HbNO] and plasma [NO₂⁻] identical. • Co-administered agents increased FBF across all doses of NaNO₂ but not significantly at any individual dose. • FBF increased with the lowest dose infusion (i.e. 0.07µmol/min), which was associated with an estimated venous plasma [NO₂⁻] of 350nmol. 	<ul style="list-style-type: none"> • NO₂⁻ is a regional and systemic vasodilator • NO₂⁻ infusion is associated with an increase in [HbNO]; suggesting that deoxy-Hb is the responsible reductase for its vascular function. • Co-infusion with an inhibitor of XO (oxypurinol) or a promoter of acidic disproportionation of NO₂⁻ (ascorbic acid) does not affect NO₂⁻ potency.

Table 1-2: Previous studies of NO_2^- administration to man (part 2).

Author	Year	Number & type of subjects	Physiological measure	NaNO_2 delivery regime	Results	Conclusions drawn
<i>Maher et al</i> ⁸⁹	2008	<ul style="list-style-type: none"> Part A = 26 (healthy subjects) Part B = 14 (healthy subjects) 	SGP measurement of FBF Radionuclide measurement of FVV	Brachial artery infusion: <ul style="list-style-type: none"> Part A: 0.04, 0.1, 0.314, 0.748, 3.14, 7.84 $\mu\text{mol/min}$ (30 min/dose) Part B: Repeat study in hypoxia ($\text{SaO}_2 = 83\text{-}88\%$) with: 0.314 $\mu\text{mol/min}$ (n=7) & 7.48 $\mu\text{mol/min}$ (n=7) 	<ul style="list-style-type: none"> FBF increased at the 3.14 $\mu\text{mol/min}$ dose and above only, in normoxia (venous plasma $[\text{NO}_2^-] = 35\mu\text{M}$) FVV increased at 0.748 $\mu\text{mol/min}$ dose and above in normoxia (venous plasma $[\text{NO}_2^-] = 10\mu\text{M}$) FVV similar in hypoxia to normoxia. FBF increased at 0.314 $\mu\text{mol/min}$ dose and above in hypoxia (venous plasma $[\text{NO}_2^-] = 5\mu\text{M}$). 	<ul style="list-style-type: none"> Veins are more responsive than arteries to NaNO_2. Hypoxic arteries exhibit a greater vasodilator response to NaNO_2 than normoxic arteries. The response of veins is unaffected by hypoxia.
<i>Mack et al</i> ⁹⁰	2008	<ul style="list-style-type: none"> 14 (homozygous SCD patients) Control group taken from study by <i>Cosby et al</i>⁸⁰. 	SGP measurement of FBF	Brachial artery infusion: <ul style="list-style-type: none"> 0.4, 4, 40 $\mu\text{mol/min}$ (8 min each dose) 	<ul style="list-style-type: none"> Ipsilateral venous plasma $[\text{NO}_2^-]$ & FBF increased in response to each dose of NaNO_2 infused. The venous plasma $[\text{NO}_2^-]$ levels achieved were lower in the SCD group compared to the control group. Consequently the SCD-FBF response to NaNO_2 was decreased compared to the control group. 	<ul style="list-style-type: none"> NaNO_2 produces regional vasodilatation in patients with SCD. NaNO_2 does not exhibit any signs of toxicity at the doses administered. The bioavailability of NaNO_2 is lower in patients with SCD compared to control subjects.

1.5.5. NO_2^- administration to the hypoxia pulmonary vasculature

The effect of exogenous NO_2^- administration upon the pulmonary vasculature has not previously been assessed in man. However, three studies have been performed in animals.

Hunter⁹² induced pulmonary hypertension in anaesthetised newborn lambs and treated them with nebulized NO_2^- . Two groups were assessed with invasive haemodynamic monitoring. The first group received a thirty minute exposure to an inhaled hypoxic gas mixture (FiO_2 12%), maintaining their SaO_2 at 55%. Pulmonary arterial pressure increased from 21 to 34mmHg and was subsequently reduced by the administration of nebulized NO_2^- (a 6mM dose was given over twenty minutes) to 25mmHg; a fall of 60%. This effect was associated with an increase in [HbNO] and exhaled NO. In the second group a greater degree of pulmonary hypertension was induced by a thromboxane-analog (24 to 51mmHg) and then reduced to 44mmHg by the same regime of nebulized NO_2^- . Exhaled NO levels increased in this group but interestingly [HbNO] levels did not change.

The second group showed a similar absolute reduction in pulmonary arterial pressure to the first. However, due to the enhanced degree of vasoconstriction present initially only a 25% reduction in pulmonary arterial pressure occurred. The authors capitalised on this baseline discrepancy to propose that NO_2^- is a more potent vasodilator in hypoxia and that this increased efficacy is due to its reduction by deoxy-Hb, inferred by the presence of HbNO.

Following this publication, Casey⁹³ employed a rat model to assess whether NO_2^- exhibits enhanced potency as a pulmonary vasodilator in hypoxia. He showed that in rats treated with a thromboxane-analog, to achieve a pulmonary pressure of 30mmHg, iv NaNO_2 reduced pulmonary arterial pressure by 8mmHg whilst either a

hypoxic gas mixture (FiO_2 10%) or room air was inhaled. This suggested that hypoxia was not the responsible mechanism behind the enhanced vasodilator activity of NO_2^- in hypoxia-driven pulmonary hypertension. However a very short period of exposure to hypoxia was used; long enough to reduce SaO_2 levels but perhaps not long enough to affect other physiological & biochemical changes of hypoxia.

In addition Casey demonstrated that the pulmonary vasodilator action of NO_2^- could be partly attenuated by the addition of allopurinol, in the normoxic, thromboxane-analog model of pulmonary hypertension. This suggests that, in normoxia, deoxy-Hb is not a significant reducer of NO_2^- to NO; as would be expected.

Lastly Diaz-Junior⁹⁴ examined the effect of NO_2^- in a canine model of acute pulmonary embolism. He showed that low-dose NO_2^- (achieving plasma levels of approximately 500nM) reduced indices of pulmonary vascular resistance in this model of pulmonary hypertension. However, it should be noted that this pathological model of acute pulmonary embolism will have resulted in both local hypoxia and ischaemia; both environmental modifications capable of enhancing the vasodilator effect of NO_2^- .

In summary these three studies have demonstrated that NO_2^- is a pulmonary vasodilator in animals whose effect is enhanced when a greater degree of pulmonary vasoconstriction is present; this may be due to hypoxia alone or in combination with other factors. It is uncertain whether deoxygenated Hb is an important catalyst to this process.

1.5.6. Summary of the two theories of endocrine NO function

Each of the two theories outlined in section 1.5.2 (page 22) and section 1.5.3 (page 26) propose that the erythrocyte plays a key role in the regulation of vascular tone and delivery of O₂ to tissue. However, the theories differ in that each one attributes this effect to an alternative intravascular metabolite of NO. Crucially, one theory chooses a more potent but less abundant mediator (i.e. HbSNO) compared to the other theory (i.e. NO₂⁻). It is important to emphasize that donation of NO by any vehicle will increase the pool of circulating NO metabolites, as the reactions outlined in this chapter experience a shift in their kinetic equilibrium. Consequently, the addition of NO₂⁻ to blood will result in an increase in HbSNO levels and vice-versa, regardless of physiological function per-se⁹⁵. It has therefore proved extremely difficult to definitively prove or disprove either theory, as by their very essence they are interconnected.

Advances in the field of NO metabolite research have therefore been curtailed by the complexity inherent to the system being examined. Many of the issues raised are technical relating to the analytical tools being employed, but also it may equally hold true that the whole system is too demanding to allow a systems biologist approach⁹⁶. As a result of this impasse the literature has shifted focus in recent years away from attempts to explain baseline physiology to the pharmacological effect of NO donation in other, pathological, models. A major area of interest has been the effect that NO₂⁻ has upon ischaemia/reperfusion (IR) injury. This will be discussed in the next section.

1.6. The role of NO₂⁻ in ischaemia/reperfusion (IR) injury

One aspect of NO metabolite research in which advances have been forthcoming is that of IR injury and the mitigating effect which NO and certain NO metabolites have upon this process⁹⁷. This represents an important facet of NO bioactivity, one which combines a number of the different biological effects of NO. Central to an understanding of the role of NO in the pathophysiological process of IR injury is the structure and function of the mitochondrion. This will be detailed in the next section.

1.6.1. IR injury background: the mitochondrion

Mitochondria are membrane enclosed organelles found within virtually all human cells. They are responsible for aerobic respiration and are consequently present at different densities in different cell types dependent upon the local tissue energy requirement⁹⁸.

1.6.1.1. Mitochondrion structure

Each mitochondrion comprises of four separate compartments or layers which are shown in Figure 1-14 (page 41). Outermost is the outer membrane, a semi-porous structure which allows relatively free diffusion of most small particles (i.e. < 5000 Daltons). Inside this is found the intermembrane space (IMS). This space contains a similar concentration of simple ions and small molecules to the cytosol surrounding the mitochondria, but also has a number of specific proteins at higher concentration which are intrinsically involved in mitochondrial respiratory function. The inner mitochondrial membrane is beneath the IMS and separates this from the matrix, which is found at the centre of the mitochondrion. Unlike the outer membrane the inner membrane is a highly impermeable structure; thus creating a barrier between the

IMS and the matrix. Within the inner membrane are a number of specific ion channels which span it's structure and operate in unison to effect the aerobic production of energy by the mitochondria; these are collectively known as the electron transport chain (ETC). In order to enhance ETC function the inner membrane has numerous folds to maximise the surface area available between the IMS and the matrix; these are known as cristae.

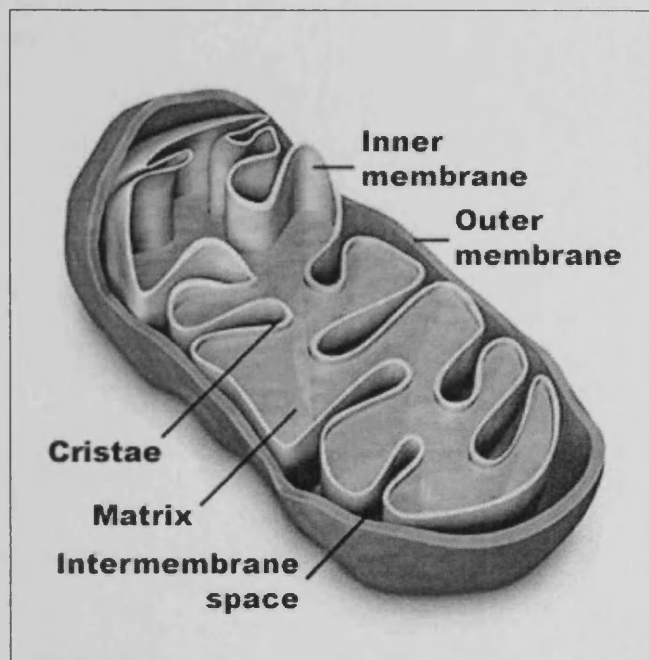


Figure 1-14: *The structure of a mitochondrion. Adapted from www.cartage.org*

1.6.1.2. Mitochondrion function: the electron transport chain

At the core of the ETC are four transmembrane proteins which span the inner mitochondrial membrane. These are called complexes I, II, III & IV and work in series to transport electrons provided by the citric acid cycle (part of the Krebb's cycle) to O_2 and H^+ to make H_2O . The process of this shuttling of electrons causes H^+ ions to be preferentially stored in the IMS; resulting in a pH gradient between the IMS and the matrix which is then used to drive the production of adenosine tri-phosphate

(ATP) by a transmembrane ATPase (also known as complex 5). Figure 1-15 (below) is a schematic diagram of the ETC.

For the purpose of this chapter it is important to emphasize three key features of the ETC. Firstly complex 4 (also known as cytochrome-c) is an integral link of the ETC but is not membrane bound, instead being mobile within the IMS. Secondly, in addition to being able to bind O_2 cytochrome-c can also bind NO. When this occurs the ETC is halted and thus mitochondrion respiration inhibited. Thirdly, complexes I & III are capable of 'electron leakage' under certain conditions. This results in the acceptance of an extra electron by O_2 , producing O_2^- (a form of ROS; see section 1.4.1.3.1, page 13).

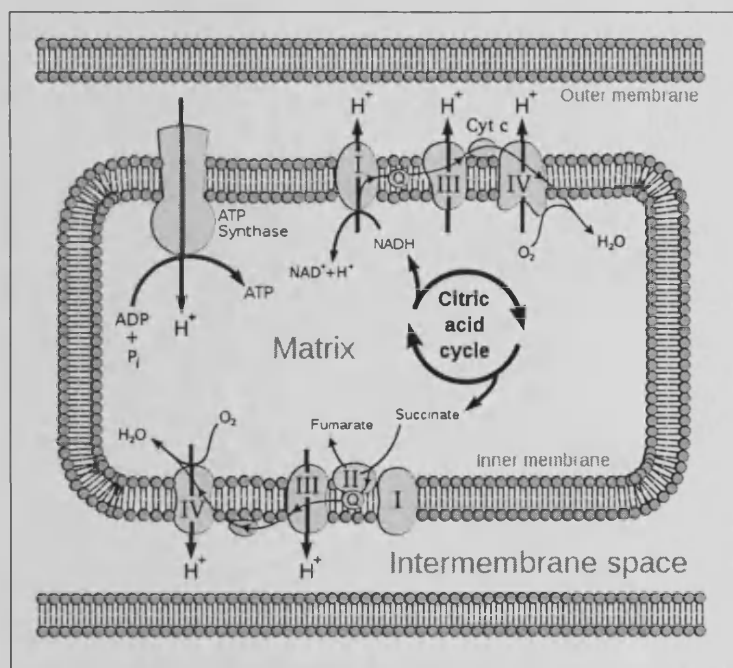


Figure 1-15: Schematic diagram of the electron transport chain (ETC). Adapted from:

www.commonswikimedia.org.

1.6.2. The pathophysiology of IR Injury

The relief of an acute coronary arterial occlusion was discovered to reduce the degree of associated myocardial necrosis by Gink in 1972⁹⁹. However the author noted that a degree of damage persisted despite a re-canalized artery. In 1985 Braunwald¹⁰⁰ recognised that this damage was due to a deleterious effect inherent to the early reperfusion phase following ischaemia, a process which became known as IR injury. He suggested, amongst other mechanisms, a key role for ROS generated by damaged mitochondria in the mediation of this damage. Whilst the currently accepted mechanisms responsible for IR injury are more complex, this insightful observation of the pivotal role that mitochondria play in its development remains at the centre of several explanatory theories.

1.6.2.1. The biochemical cascade of I/R injury

The energy depleted state of ischaemia causes a rise in cytosolic Ca^{2+} via a decrease in ATP-membrane pump activity¹⁰¹ (see Figure 1-16; page 44). A subsequent redistribution of ions in response to osmotic forces results in the mitochondrial matrix becoming overloaded with Ca^{2+} . At reperfusion this leads to the formation of a large indiscriminate conductance megachannel across the mitochondrial membranes called the mitochondrial permeability transition pore (MPT)¹⁰². The exact constituents of the MPT are unknown, though it is thought that several proteins organise at the meeting point of the outer and inner mitochondrial membranes in order to produce it. It is perhaps easier to view the MPT not as a specific protein channel which is turned on at reperfusion, but more a transient state which is favoured during the development of IR injury and characterised by disruption of the usually highly stable mitochondrial membranes. It is probable that the MPT has evolved as part of the apoptotic process; whereby a cell sacrifices itself

when it has been damaged in order that efficient harmony of the remaining tissue continues¹⁰³.

In response to the presence of the MPT, swelling of the mitochondria and leakage of proteins from within it (including cytochrome-c) follows. Consequently the ETC becomes uncoupled and this leads to an abundance of ROS generation. This in turn has a positive feedback effect on the MPT to increase its permeability and a viscous cycle ensues. As a result of this disruption to the energetic powerhouse of the heart myocardial stunning (due to contractile apparatus dysfunction), cellular necrosis and apoptosis all ensue¹⁰³.

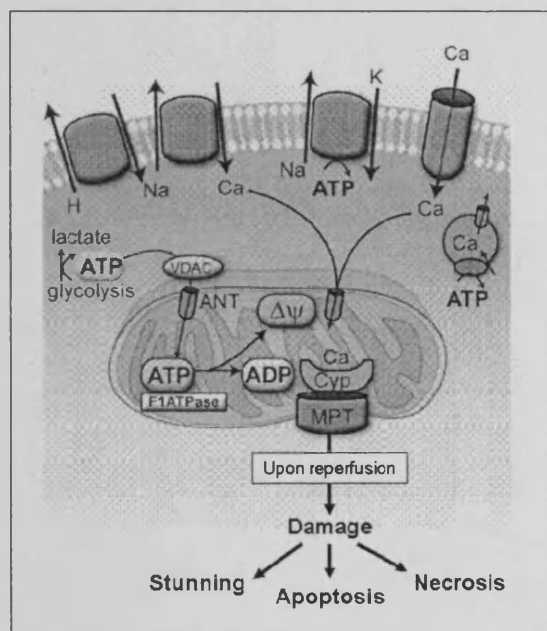


Figure 1-16: Diagram of ischaemia/ion balance. The anaerobic metabolism of ischaemia leads to an increase in intracellular lactate and reduction in pH. The cell attempts to remove these H⁺ ions via the Na⁺/H⁺ exchange channel, which in turn exacerbates ATP demand via the Na⁺/K⁺ port. This results in an increase in intracellular [Ca²⁺] which consequently enters the mitochondria. Once a normal pH is resumed during reperfusion the MPT channel is activated by the increased levels of mitochondrial [Ca²⁺]. Adapted from Murphy et al¹⁰³.

1.6.3. The phenomenon of ischaemic conditioning

In 1986 Murry demonstrated that exposure of a myocardial tissue bed to four cycles of 5 min of ischaemia and 5 min of reperfusion immediately prior to a subsequent sustained ischaemic insult protected against IR injury¹⁰⁴. This phenomenon was termed ischaemic pre-conditioning (IPC).

IPC confers two windows of protection upon the recipient. The first, known as the classic or early window, has an effect which lasts for 3-4 hours. The second, known as the delayed or late window, is not present until 24 hours after the IPC stimulus and lasts for between 24 & 48 hours¹⁰⁵. In addition it is possible in-vivo to provide a similar beneficial window upon ischaemic tissue as with early phase IPC through the application of short bursts of ischaemia in the immediate phase after reperfusion. This phenomenon is known as ischaemic post-conditioning (IPostC)¹⁰⁶.

1.6.3.1. The mechanisms responsible for ischaemic conditioning

IPC & IPostC exhibit their effect via a series of complex biochemical pathways which, although recognised, are incompletely understood. Importantly the common end point is inhibition of the formation of the MPT, by a reduction in mitochondrial ATP depletion and Ca^{2+} uptake¹⁰⁷.

The process of IPC begins by activation of the pro-survival kinases of the Reperfusion Injury Salvage Kinase (RISK) pathway¹⁰⁸. This cascade has both a direct effect upon mitochondria and results in eNOS expression of NO; which in turn leads to sGC/protein kinase activation (as outlined previously in section 1.2; page 2). This causes activation of mitochondrial K_{ATP} channels which act to limit ATP depletion and mitochondrial calcium uptake¹⁰⁹. A summary diagram of the cellular pathways involved in ischaemic conditioning is in Figure 1-17; page 47. Importantly, the process of IPostC follows a similar, though less diverse pathway to IPC.

In animal models of IR injury it has been shown that the beneficial effects of IPC can be mimicked by interventions to promote different stages of this pathway. The RISK pathway is activated by insulin¹¹⁰ and atorvastatin¹¹¹. Agents which limit intracellular Ca^{2+} accumulation during ischaemia such as Ca^{2+} channel blockers¹¹² or Na^+/H^+ exchange inhibitors¹¹³ are also effective. Furthermore drugs which reduce the sensitivity of the MPT to Ca^{2+} (e.g. cyclosporine)⁹⁷ have been shown to reduce subsequent IR injury. Finally, given the key roles that eNOS and NO have in the pathway of IPC it is not surprising their modulation has an influence upon IR injury. Exogenous administration of NO prior to ischaemia is capable of mimicking the benefits of early phase IPC. However, blockade of eNOS with L-NAME does not abolish the effects of IPC¹⁰⁵. These two observations suggest that endogenous eNOS derived NO is a part of, but not integral to, the metabolic mediation of IPC. However, inhibition of either eNOS¹¹⁴ or sGC¹¹⁵ will block the beneficial effects of IPostC, suggesting an integral role of NO in this process.

The effect of different forms of NO donation upon IR injury will be discussed in the next section.

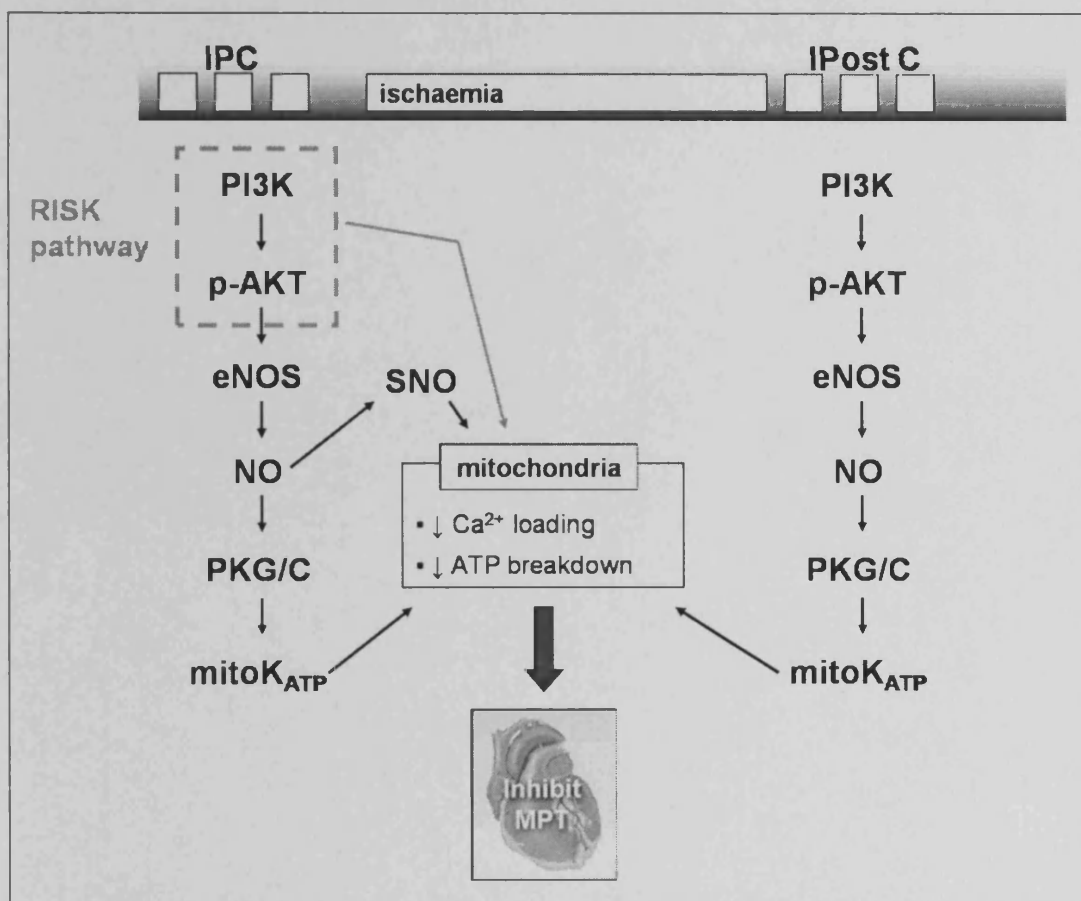


Figure 1-17: Cellular pathways involved in the process of IPC (left hand pathway) and IPostC (right hand pathway). Adapted from Murphy et al¹⁰³.

1.6.4. The specific role of NO in ischaemic conditioning

A variety of different means of NO supplementation have been shown in rodent heart models to be capable of mimicking early phase IPC; these include exogenous NO donation by GSNO¹¹⁶ and sodium nitroprusside¹¹⁷ as well as agents which enhance endogenous NO release, e.g. bradykinin¹¹⁸.

A number of different mechanisms by which NO supplementation is capable of reducing the effects of IR injury have been proposed, (see Figure 1-18; page 48). Firstly, sGC dependent activation of protein kinases reduces MPT opening directly as outlined in the previous section. In addition, the presence of NO will result in S-nitrosylation of key intracellular proteins. For instance, the mitochondrial membrane

L-type Ca^{2+} channel can be S-nitrosylated by NO^{119} ; with an associated reduction in its function. Also complex I of the ETC, which is responsible for 'electron leakage' and an abundance of ROS formation during reperfusion, can be inhibited by S-nitrosylation¹²⁰.

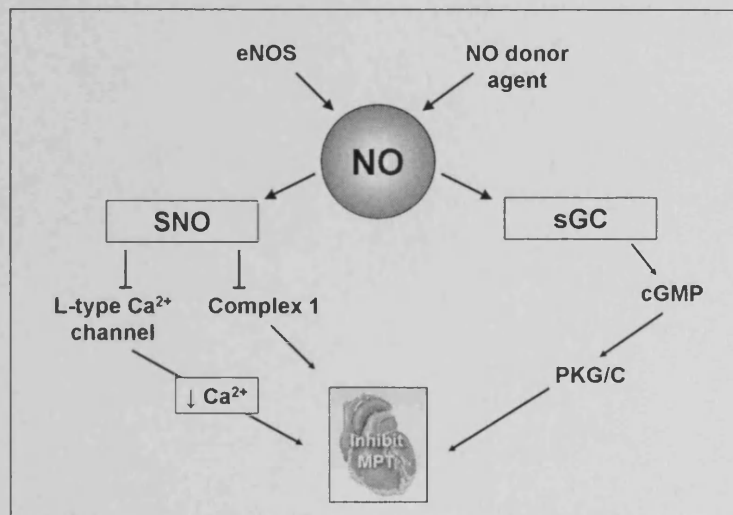


Figure 1-18: The pathways by which NO may act to reduce IR injury. Adapted from Murphy *et al*¹⁰³.

In summary NO is capable of reducing the damage caused by IR injury via a number of different cellular pathways. It is, however, essential for there to be sufficient NO present within the mitochondria at the time of reperfusion to produce these benefits; an observation supported by the existence of mitochondrial NOS¹²¹. eNOS derived NO may not alone be sufficient to achieve high enough levels of NO during early phase IPC; an observation supported by the presence of a threshold effect to the stimuli which provide IPC¹²². However exogenous NO donation is capable of providing sufficient substrate to exhibit an IPC-type effect. In addition significant amounts of NO may potentially be made from NO_2^- during ischaemia, as a low pH environment favours enzymes which convert NO_2^- to NO as well as direct acid disproportionation of NO_2^- .

1.6.5. The evidence for NO_2^- as an ischaemic conditioning agent

NO_2^- reduction to NO is favoured in an ischaemic environment. Zwier demonstrated that this phenomenon was attributable to non-enzymatic acidic disproportionation of NO_2^- ¹²³. However tissue-based haem enzymes, such as myoglobin¹²⁴ and XO¹⁰⁸, have also been implicated as a potential mechanism.

Webb demonstrated in 2004, using a Langendorff model, that NO_2^- administered pre-ischaemia was capable of reducing myocardial infarction (MI) size. This effect was abolished by the co-administration of CPTIO (a NO scavenger) and was also associated with increased XO activity¹²⁵. High (mM) concentrations of NO_2^- were used in this model, but a protective effect of NO_2^- upon liver IR injury has been reported with an increase in plasma $[\text{NO}_2^-]$ of just +200nM¹²⁶.

It has also been proposed in animal models that NO_2^- could act as a post-conditioning agent. Gonzalez used a canine model of a two hour simulated MI to demonstrate that NO_2^- administered during the last sixty minutes or five minutes of ischaemia reduced subsequent infarct size¹¹⁰.

In summary it has been established in both in-vitro and animal in-vivo models that NO_2^- is capable of acting as an IPC and an IPostC agent. It is currently unknown whether NO_2^- will be able to confer a similar degree of benefit in humans. This form of study urgently needs to be performed in order to ascertain whether a large multi-centre study of the effect of NO_2^- upon acute MI would be feasible.

1.7. The key ideas contained within this chapter

- 1. NO has a myriad of effects across the various systems of the body. Two important actions are vasodilation and ischaemic conditioning.**
- 2. Metabolism of NO in blood is predominantly to NO_3^- , an inert product. However a number of other NO metabolites are present in blood, each possessing different degrees of vascular activity.**
- 3. NO_2^- is the second most abundant NO metabolite in blood. As a small anion NO_2^- rapidly equilibrates across all fluid spaces (apart from the erythrocyte).**
- 4. NO_2^- is a weak vasodilator in normoxia. However, its vasoactivity is enhanced in a hypoxic environment. In addition NO_2^- can act as an ischaemic conditioning agent.**

1.8. Aims of this thesis

Overall this thesis has been designed to investigate the effects of NO_2^- supplementation in man, delivered via systemic NaNO_2 infusion. There are two key features which pervade each set of experiments performed that make this body of work novel. Firstly, the dose of NaNO_2 should be as low as possible to observe a physiological effect; and secondly environmental modifications known to enhance the effects of NO_2^- (i.e. hypoxia and ischaemia) will be used in tandem with NaNO_2 administration. There are three specific aims to this thesis.

1. To examine in hypoxia and normoxia the vasodilator effects of a low-dose NaNO_2 infusion upon the systemic and pulmonary vasculature in healthy human subjects.
2. To examine whether a low-dose NaNO_2 infusion, given to patients with established coronary artery disease, reduces objective markers of inducible myocardial ischaemia during a dobutamine stress echocardiogram.
3. To examine whether NaNO_2 is an ischaemic conditioning agent in healthy human subjects in a forearm model of IR injury.

Chapter 2: General Methodology

2.1. Controlled environment chamber

A controlled environmental chamber (Design Environmental Ltd, Ebbw Vale, UK) was used at the University of Glamorgan, Pontypridd, UK. This was a room able to accommodate comfortably both the subject and the investigator, measuring approximately 6m x 5m x 4m. The temperature, humidity and FiO_2 inside the chamber could be adjusted and maintained for several hours. A nitrogen (N_2) rich hypoxic gas mixture was delivered to the room at a high flow rate to create a normobaric/hypoxic environment. Due to this continuous gas exchange CO_2 levels did not alter from those found in normoxia. Figure 2-1, below, is an illustration of the chamber.

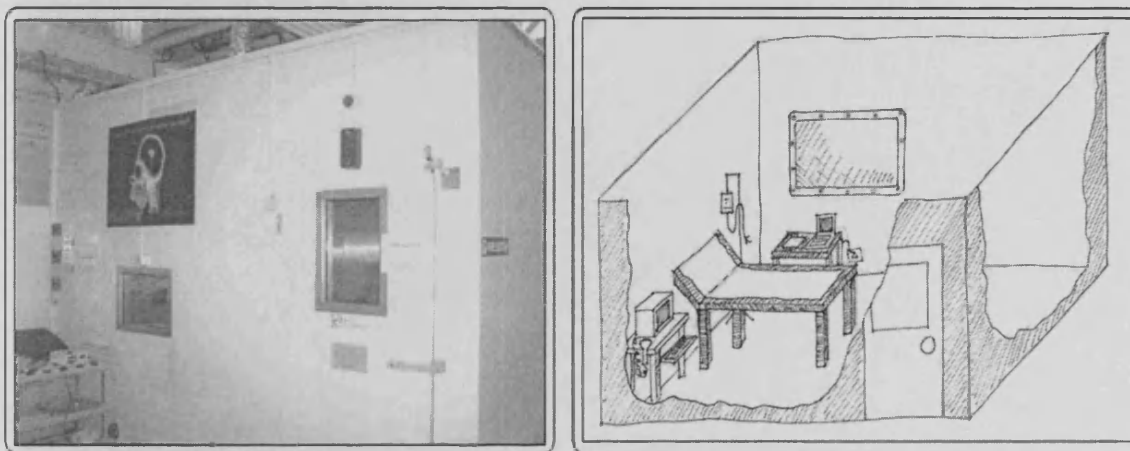


Figure 2-1: Outside (left) and inside (right) the controlled environment chamber.

2.2. Subject recruitment

All studies performed were approved by the South East Wales Regional Ethical Committee – Panel D and each subject gave informed consent prior to participation.

2.2.1. Healthy volunteers

For chapters 3 & 5 healthy volunteers were recruited from the local staff and student population of the Universities of Cardiff & Glamorgan. Exclusion criteria were: hypertension, hypercholesterolaemia, DM, a family history of premature coronary artery disease, being a current smoker and taking regular prescription medication.

Additional criteria were used for studies in chapter 3. Firstly, an echocardiogram was performed prior to inclusion to ensure a structurally normal heart. Secondly, only men were recruited as women have cyclical variability in basal NO metabolite levels¹²⁷ and pulmonary arterial vasoreactivity¹²⁸ which could have interfered with study interpretation.

2.2.2. Coronary artery disease patients

Patients with proven angina, documented by a positive exercise tolerance test and the presence of significant coronary artery disease (CAD) at coronary angiography, were invited to participate in the study in chapter 4. Exclusion criteria were the presence of unstable symptoms requiring urgent treatment or angina upon minimal exertion. The latter was defined as a positive exercise tolerance test at early stage two or sooner of a standard Bruce protocol. Subjects were required to stop all anti-anginal medication for 48 hours prior to each study.

2.3. Forearm blood flow (FBF)

Non-invasive measurement of changes in forearm blood flow (FBF) was performed using forearm plethysmography. Initially, two different techniques were considered to

ascertain the best measure for this thesis. Common to both methods was a plethysmographic means by which arterial inflow to the forearm vascular bed was isolated and measured; expanded on in the next paragraph.

The non-dominant arm was held in a fixed position with the subject sitting and the arm at the level of the right atrium. A wrist cuff was attached to the same arm and inflated to a pressure 50 mmHg above arterial systolic pressure to exclude hand circulation. A cuff was then placed around the upper arm and a rapid cuff inflator (EC-20, Hokanson) used to inflate it to 50mmHg for seven seconds to exclude venous outflow from the arm. Two methods were used to measure the increase in forearm volume resulting from temporary inflation of the proximal cuff; these are illustrated in Figure 2-2 (below).

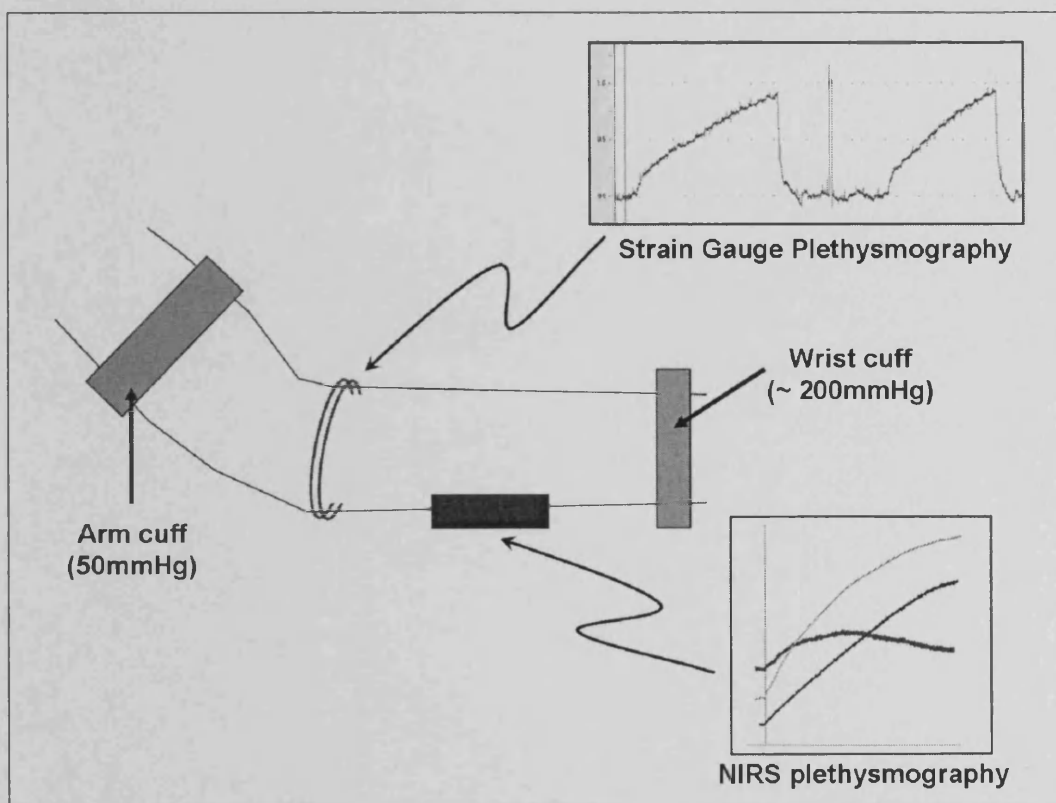


Figure 2-2: Setup of the two different techniques used to measure forearm (arterial) blood flow. SGP records a relative increase in the diameter of the forearm (y-axis) over time (x-axis). NIRS-plethysmography demonstrates an increase in the deoxy-Hb (blue line) oxy-Hb (red line) and total-Hb (green line) signals (y-axis) over time (x-axis).

2.3.1. Near Infrared spectroscopy (NIRS) plethysmography

Light in the near infrared range (wavelength: 700 – 1,000nm) penetrates through skin and soft tissue but is absorbed by Hb. Specifically, light emitted at either 780nm or 830nm will be absorbed by oxy-Hb or deoxy-Hb respectively¹²⁹. Near Infra-Red Spectroscopy (NIRS) plethysmography utilises this phenomenon to provide a measure of the change in the concentration of Hb over time¹³⁰.

A continuous-wave near-infrared spectrophotometer (OXYMON, University of Nijmegen, Nijmegen, The Netherlands), consisting of an emitted and a receiving probe, was placed on the subject's skin. The first probe irradiated the local tissue bed with laser beams at the above discrete wavelengths. An adjacent probe detected the residual light signal present following its passage through the intervening tissue. Both probes were separated by just a few cm and fixed to the forearm by tape. An attached personal computer converted the absorption difference between the two probes into a relative concentration of oxy-Hb and deoxy-Hb, which was combined to give the relative concentration of total-Hb. The increase in total-Hb concentration that occurred during inflation of the proximal forearm cuff was then used to calculate the percentage change in total-Hb concentration per minute (i.e. % change [total-Hb]/min).

2.3.2. Strain gauge plethysmography (SGP)

A mercury-filled silastic strain gauge (EC-6, Hokanson; Bellevue Washington, USA) was attached to the widest part of the forearm and connected to the plethysmography reading device. The change in forearm diameter measured by the strain gauge was transmitted via a Powerlab/4SP system (ADInstruments) and recorded on a personal computer using the software package *Chart* (ADInstruments). The percentage change in FBF was expressed as mL per 100mL of forearm tissue per minute (i.e. ml/100ml/min)¹³¹.

2.3.3. Comparison between the above two measures of FBF

A temperature controlled clinical research laboratory at the Wales Heart Research Institute, Cardiff University, was used for a study of four healthy subjects. Each underwent repeated single-measure assessment of FBF performed using both NIRS-plethysmography and SGP. Figure 2-3 (page 56) contains two graphs illustrating the correlation between the readings taken using each technique.

Agreement was better with SGP (Pearson r 0.81; $p=0.02$) compared to NIRS plethysmography (Pearson r 0.29; $p=0.49$). Therefore it was decided that SGP would be the preferred method for the assessment of FBF used in this thesis. Furthermore, when SGP was used in this thesis, FBF was taken as the average of five consecutive readings with analysis being performed by an interpreter who was blinded to the study performed.

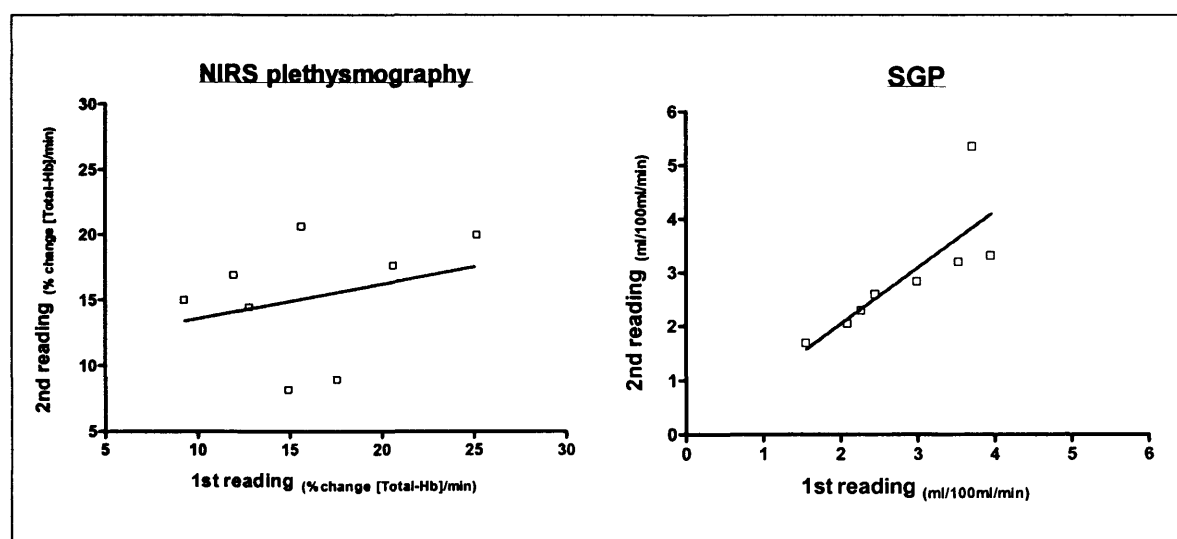


Figure 2-3: Correlation between two consecutive readings of FBF taken using either NIRS plethysmography (left) or SGP (right). The red line in each graph is the mean linear regression line of the values plotted.

2.4. Pulmonary arterial pressure

A commercially available echocardiography system (GE-Vingmed System 5; General Electric, Fairfield, Connecticut, USA) with a 2.5 MHz phased array transducer was used to obtain cross-sectional images, blood pool Doppler profiles, and tissue Doppler images, with the subject in a left lateral decubitus position. Loops, recorded during passive held expiration, were stored digitally for post-processing using an Echopac workstation. Three different validated surrogate markers of pulmonary arterial pressure were used.

2.4.1. Pulmonary acceleration time

Pulmonary arterial flow was sampled using pulsed-wave Doppler (PWD) between the cusps of the pulmonary valve. The pulmonary acceleration time (PAT) was measured as the time (in ms) between the onset and the peak velocity of pulmonary arterial forwards flow¹³². As all readings were taken with a HR <100 bpm PAT was not normalized for the pulmonary ejection time¹³³. Figure 2-4 (page 58) contains an example PWD trace used in the measurement of the PAT.

2.4.2. Iso-volumic relaxation time

In the normal heart, early diastolic pressure in the right ventricle is lower than right atrial pressure and the tricuspid valve opens as systole ends. A normal right ventricle therefore experiences no isovolumic relaxation time (IVRT) period whereas this develops when afterload is increased, for example in pulmonary hypertension¹³⁴. The IVRT was measured from pulsed tissue Doppler traces of lateral tricuspid annular velocity recorded in an apical four chamber view. Figure 2-4 (page 58) contains an example PWD trace used in the measurement of the IVRT period.

2.4.3. Tricuspid regurgitation velocity

The systolic pressure gradient between the right ventricle and the right atrium in mmHg was calculated from the peak velocity of tricuspid regurgitation (TR) using the modified Bernoulli equation¹³⁵. The TR jet was captured in the apical four chamber window and measured using continuous-wave Doppler (CWD). Right atrial pressure was estimated from the change in diameter of the inferior vena cava during respiration and added to the right ventricular systolic pressure to give the pulmonary arterial systolic pressure (PASP)¹³⁶. Figure 2-4, below, contains an example CWD trace used in the measurement of this parameter.

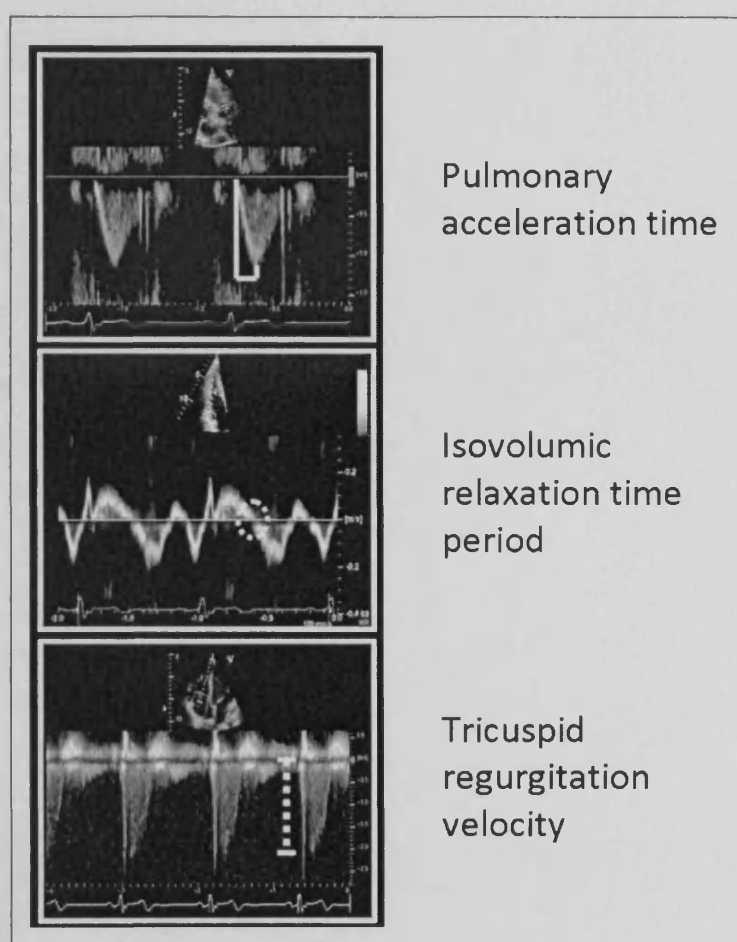


Figure 2-4: Annotated examples of the three echo indices of pulmonary arterial pressure measured.

2.5. Cardiac output

Cardiac output was calculated using echocardiography and haemodynamic variables. PWD at the left ventricular outflow tract (LVOT) was used to measure the velocity time integral of the LVOT (VTI_{LVOT}); also known as the left ventricular stroke distance, (see Figure 2-5, below). The mean of three traces was used. This value, together with the LVOT diameter (in cm) obtained from a parasternal long-axis window and the heart rate (HR), was used to calculate cardiac output (see Equation 2-1, below)¹³⁷. The assumption was made that the LVOT is of circular cross section.

$$((\frac{1}{2} \times \text{LVOT diameter})^2 \times \pi) \times VTI_{LVOT} \times \text{heart rate} / 1000 = \text{cardiac output (L/min)}$$

Equation 2-1: *The calculation of cardiac output.*

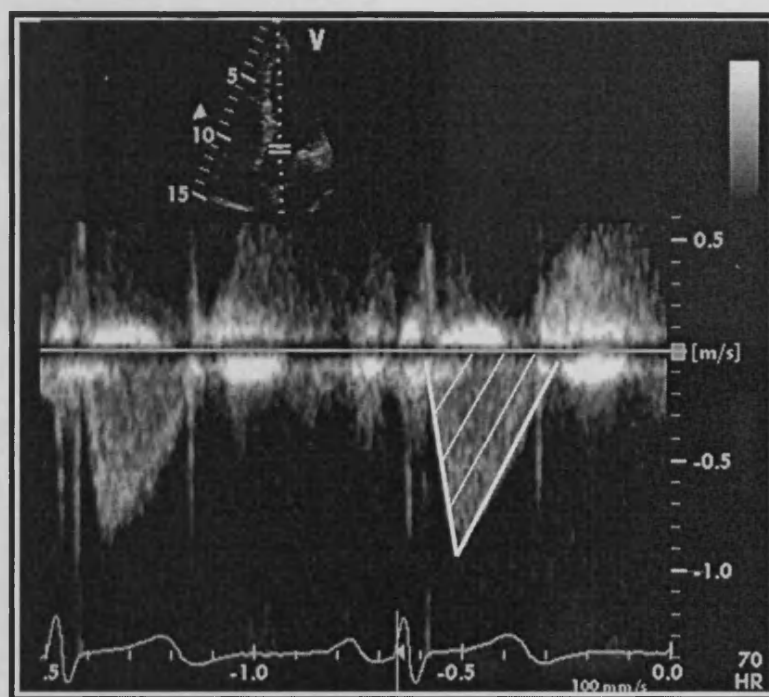


Figure 2-5: *Example PWD trace use in the measurement of the VTI_{LVOT} . The right hand side cardiac cycle has been annotated to illustrate the envelope of forwards blood flow through the LVOT used in the calculation of the VTI_{LVOT} .*

2.6. Basic haemodynamic & blood measurements

Peripheral blood pressure was measured with the subject reclined using a cuff placed around the non-dominant upper arm which was attached to an Omron 705CP automated blood pressure monitor (Omron Corporation, Kyoto, Japan). Capillary oxygen saturation (SaO_2) was measured using a Nellcor N-200 pulse oximeter (Covidien-Nellcor, Boulder, Colorado, USA). Venous blood pH & $[\text{O}_2]$ were measured using a RapidLab 248 blood gas analyzer (Siemens Healthcare Diagnostics, Deerfield, Illinois, USA).

2.7. Statistical analyses

Statistical analysis of data was performed using the software package *GraphPad Prism 4.0* (La Jolla, California, USA). The individual tests performed are identified within the text of each results chapter.

2.8. Blood NO metabolite measurement

Figure 2-6, below, is a summary diagram of the methods employed in the measurement of blood NO metabolites. All chemical were purchased from Sigma (Poole, UK) unless stated otherwise in the text.

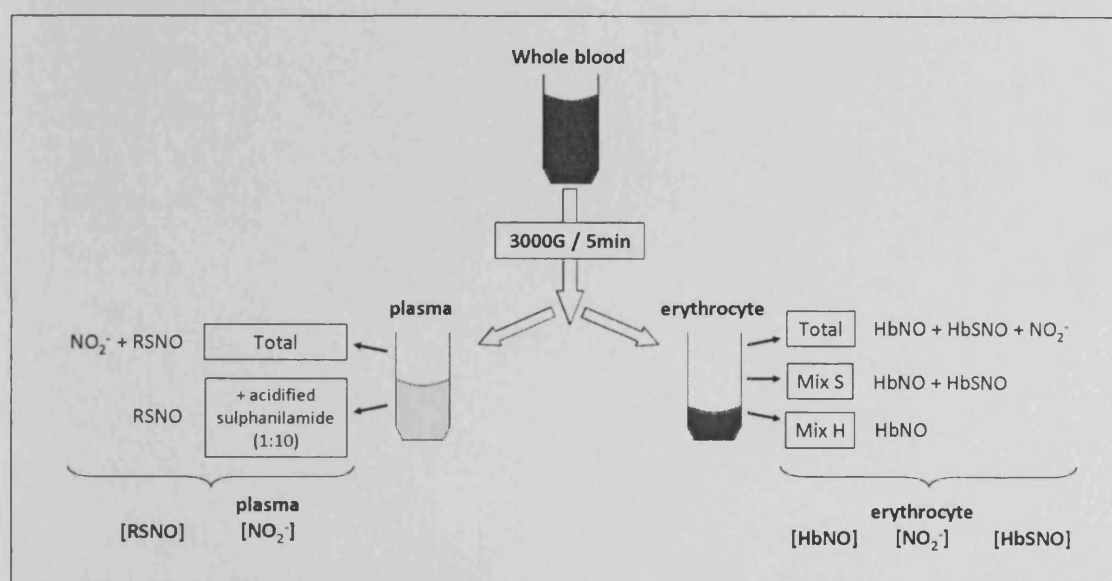


Figure 2-6: Flow diagram of the processes used in the separation and analysis of blood to calculate the constituent NO metabolites. The concentrations of individual NO metabolites are deduced from the results of different pre-treatments performed on plasma or erythrocyte samples.

2.8.1. Blood preparation

Venous samples were injected into 4ml EDTA collection tubes (Greiner Bio-One, Frickenhausen, Germany) and immediately centrifuged (3000G for 5 minutes at 4°C). The plasma and erythrocyte fractions were separated (the intervening buffy coat was discarded), snap frozen in liquid nitrogen and stored at minus 80°C. All samples were analysed within seven days of collection. Immediately prior to analysis aliquots were rapidly thawed by placement in a warm water bath (set at 37°C) for three minutes.

2.8.2. Ozone-based chemiluminescence

Ozone-based chemiluminescence (OBC) was used to detect NO liberated from samples by chemical reagent cleavage⁹⁶; Figure 2-7, below, is a diagram of its components. A chemical reagent (explained in detail in the next three sections) was placed into a glass purge vessel. This vessel was held in a water bath which was kept at a fixed temperature (50°C unless stated otherwise) by a thermostatically controlled hot plate. A constant flow of inert gas (N₂) was bubbled through the reagent to collect NO gas liberated by the assay. The purge vessel was connected to a trap of 25ml sodium hydroxide (NaOH), which removed any acid vapours. The trap was then connected to the NO analyser (NOA) (NOA280i, Sievers, Boulder, USA). The reaction of NO with ozone (O₃) is associated with the production of a photon ($h\nu$). The NOA enables this reaction to occur in a controlled environment and then, via a photo-multiplier tube (PMT), converts this luminescent energy into a potential difference. The output produced by the NOA in response to a supply of NO gas is therefore measured in mV.

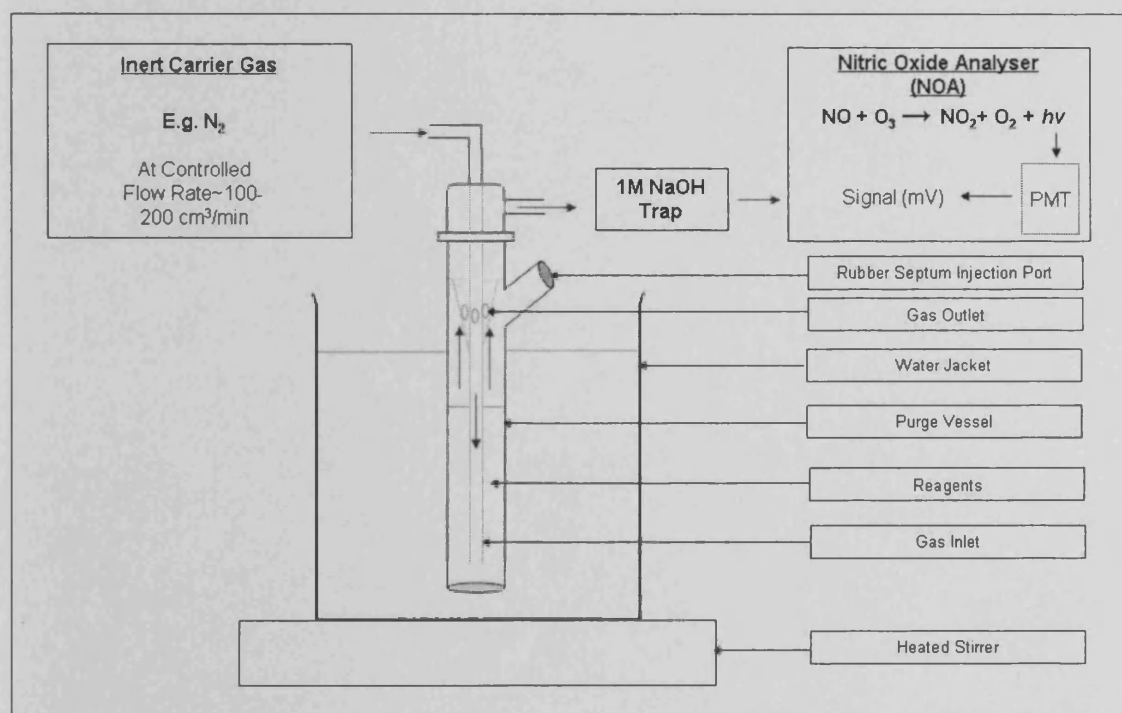


Figure 2-7: Diagram of OBC setup for the measurement of blood NO metabolites.

2.8.3. Sample pre-treatment

Table 2-1, below, contains a summary of the different pre-treatments performed on a sample prior to its injection into the OBC system.

Sample	Reagent	Pre-treatment	NO metabolite(s) measured
Plasma	Acidified tri-iodide solution	Nil	NOx (NO ₂ ⁻ & protein bound NO)
		270µl plasma sample + 30µl 5% acidified sulphanilamide solution	Protein bound NO
	Acidified VCl ₃	Nil	NO ₃ ⁻ & NOx
Erythrocyte	Modified acidified tri-iodide solution	nil	HbNO, HbSNO & erythrocyte-associated NO ₂ ⁻
		200µl erythrocyte sample + 800µl dilute acidified sulphanilamide solution (= Mix S)	HbNO & HbSNO
		270µl Mix S + 30µl HgCl ₂ (= Mix H)	HbNO

Table 2-1: Summary of the pre-treatments performed on and metabolites measured in both plasma and erythrocyte samples.

2.8.3.1. Plasma NOx

An acidified tri-iodide solution was mixed on the day of analysis. This reagent has previously been validated as an efficient reductive agent that provides a good signal for the measurement of blood NO metabolites¹³⁸. To prepare the solution 70ml of glacial acetic acid was mixed with 650mg iodine (I₂) crystals. To this 1g of potassium iodide (KI), dissolved in 20ml HPLC (high performance liquid chromatography) grade water, was added¹³⁹. 5ml of tri-iodide reagent, together with 30µl antifoam 204, was placed into the purge vessel. A fresh purge vessel of tri-iodide reagent was prepared for the analysis

of each sample. 200µl of freshly thawed plasma was injected into the side port of the purge vessel, to generate a plasma total signal (comprising NO_2^- and protein bound NO groups). This group is also known as plasma NOx.

270µl of the same plasma sample was then added to 30µl of 5% acidified sulphanilamide solution (500mg sulphanilamide dissolved in 10ml 1M hydrochloric (HCl) acid) and incubated in the dark for fifteen minutes. Acidified sulphanilamide reacts with NO_2^- to create a highly stable compound from which NO cannot be cleaved by tri-iodide reagent. 200µl of this solution was then injected into the purge vessel to provide a protein bound NO signal. The concentration calculated from this signal was then subtracted from the plasma [NOx] concentration to give the plasma [NO_2^-] concentration.

2.8.3.2. Erythrocyte associated NO

The original tri-iodide solution was modified by the addition of potassium hexacyanoferrate ($\text{K}_3\text{Fe}^{3+}(\text{CN})_6$) immediately prior to sample analysis, (1:10 to tri-iodide). This agent prevents auto-capture of liberated NO by Hb whilst in the assay¹⁴⁰. 8ml modified tri-iodide reagent, together with 30µl antifoam 204, was placed into a purge vessel. 200µl of freshly thawed erythrocyte sample was injected into the purge vessel to generate an erythrocyte-total signal (HbNO, HbSNO and erythrocyte-associated NO_2^-).

200µl of the same erythrocyte sample was then added to 800µl of dilute acidified sulphanilamide solution (1:10 dilution with HPLC grade water) to remove erythrocyte-associated NO_2^- . This solution was known as 'mix S'. 270µl of mix S was then added to 30µl of mercuric chloride (HgCl_2) to give 'mix H'. Both mix S & mix H were incubated in the dark for fifteen minutes. Incubation of the erythrocyte sample with HgCl_2 removed thiol bound NO from Hb; and the resulting free NO is then stabilised by the dilute acidified sulphanilamide present. 200µl of mix S was injected into a fresh purge vessel of modified tri-iodide reagent, to provide a Hb-bound NO signal (HbNO & HbSNO). 200µl

of mix H was then injected to give a HbNO signal. The calculated [HbNO] concentration was subtracted from the [Hb-bound NO] concentration to give the [HbSNO] concentration. To calculate the erythrocyte-associated $[\text{NO}_2^-]$ concentration the [Hb-bound NO] concentration was subtracted from the erythrocyte-total concentration.

2.8.3.3. Plasma NO_3^-

Acidified vanadium III chloride (VCl_3) was used as the chemical reagent in the measurement of plasma NO_3^- by OBC¹⁴¹. VCl_3 is a powerful reducing species, more potent than tri-iodide, and when used at higher temperatures (85°C) is able to liberate NO from all plasma sources, including NO_3^- . A 50mM reagent solution was prepared by the addition of 0.785g VCl_3 (dissolved in 20ml HPLC grade water) to 80ml 1M HCl acid. 30ml of acidified VCl_3 was added to a larger-sized purge vessel. A Liebig condenser was connected between the purge vessel and the NaOH trap but otherwise the setup was unaltered from that previously stated. 20 μl of freshly thawed plasma was injected into the purge vessel to generate a plasma NO_3^- & NO_x signal. From this concentration the plasma [NO_x] concentration was subtracted to give the plasma $[\text{NO}_3^-]$ concentration.

2.9. Interpretation of data produced by the NOA

The software package *Origin 7.0* (OriginLab Corps, Massachusetts, USA) was used to analyse the signal output of the NOA. This signal (in mV) was plotted vs time (in seconds) to give a raw trace and then a fifty-point adjacent averaging algorithm was used to smooth this trace. The *peak analysis package* for *Origin* was then used to calculate the area under curve (AUC) of each peak (mV.s) which was converted to a concentration of NO using a standard curve, expanded on in the next section. Figure 2-8, below, illustrates this analytical process.

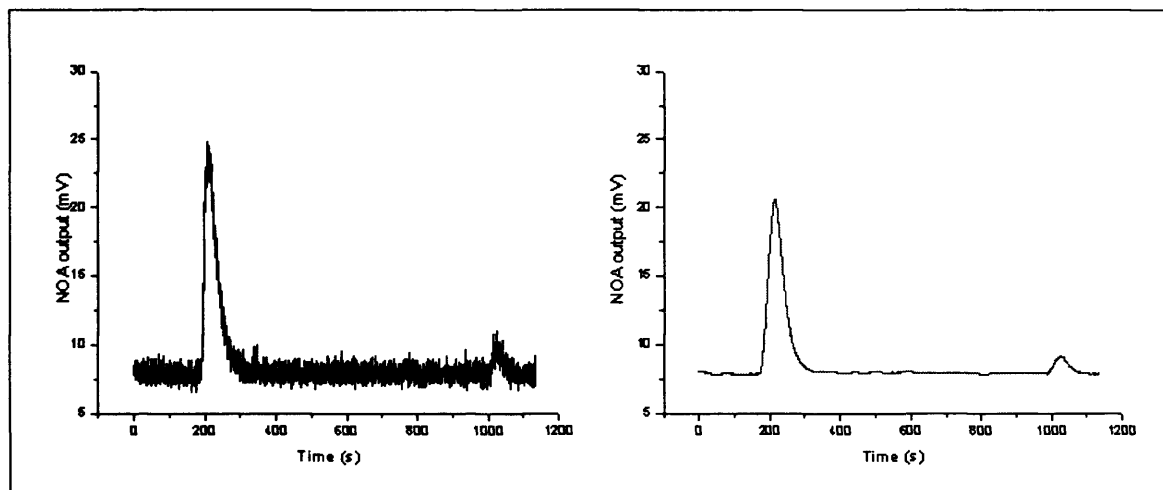


Figure 2-8: Analysis of NOA output using *Origin 7.0*. The left graph contains the raw output and the right graph the smoothed data. The first peak in each represents a plasma-total injection (i.e. plasma NO_x) and the second, smaller, peak a plasma + sulphanilamide injection (i.e. plasma protein bound NO).

2.10. Calibration of OBC

A 200 μ l standard curve, using freshly prepared standards of either NaNO₂ or NaNO₃, was performed each day for each separate chemical reagent used. The AUC measured from increasing concentration of known standards was plotted and linear regression analysis of this data provided a multiplication factor by which an NOA reading (in mV.s) could be converted into a concentration (in nmol/l). Figure 2-9, below, is an example standard plot.

Our laboratory has previously reported a co-efficient of variability of 7% & 10% respectively for intra-assay and inter-assay repeated analysis of blood NO metabolite measurement¹⁴².

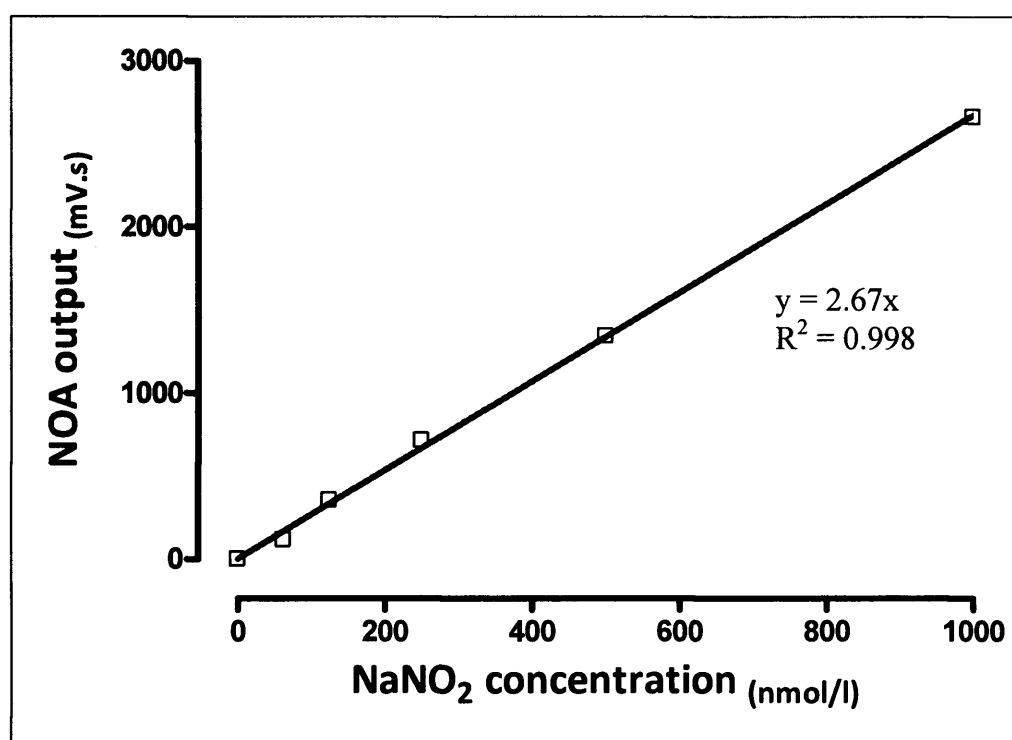


Figure 2-9: Example of a standard curve plot of the NOA output measured against increasing concentrations of NaNO₂ analysed using tri-iodide reagent based OBC. In this case the NOA output of subsequent samples would need to be divided by 2.67 to be interpreted as a concentration of NO₂⁻.

2.11. Assessment of endothelial function: Flow mediated dilatation

Endothelial function was assessed by flow mediated dilatation (FMD) of the brachial artery in the non-dominant arm¹⁴³. Subjects were reclined horizontally on a bed in a temperature-controlled dedicated clinical research room at the Wales Heart Research Institute, Cardiff University. A B-mode scan in the longitudinal axis of the brachial artery at a point 5-10cm above the antecubital fossa was obtained using a high-resolution vascular ultrasound machine; Aloka ProSound SSD-5500 (Aloka, Tokyo, Japan). Electrocardiogram (ECG)-gated end-diastolic images were acquired in this window every three seconds for offline analysis. A 1-2cm segment of artery was highlighted for processing using the automated edge detection software package *Brachial Analyser for Research 5* (Medical Imaging Applications LLC, Coralville, Iowa, USA). This gave a profile of the diameter of the brachial artery for each image taken during the protocol. In addition PWD blood flow velocity at the centre of the brachial artery was recorded continuously and analysed using the same software.

Arterial flow was manipulated by means of a blood pressure cuff placed around the forearm immediately below the antecubital fossa. After one minute of baseline recording the cuff was inflated to 200mmHg using a rapid cuff inflator. The cuff remained inflated for five minutes and was then released, resulting in a period of reactive hyperaemia during which time the brachial arterial diameter increased. This change in diameter was recorded for five minutes. Each FMD protocol therefore lasted eleven minutes and was recorded by a total of 220 images. Figure 2-10 (page 69) is a summary illustration of this method.

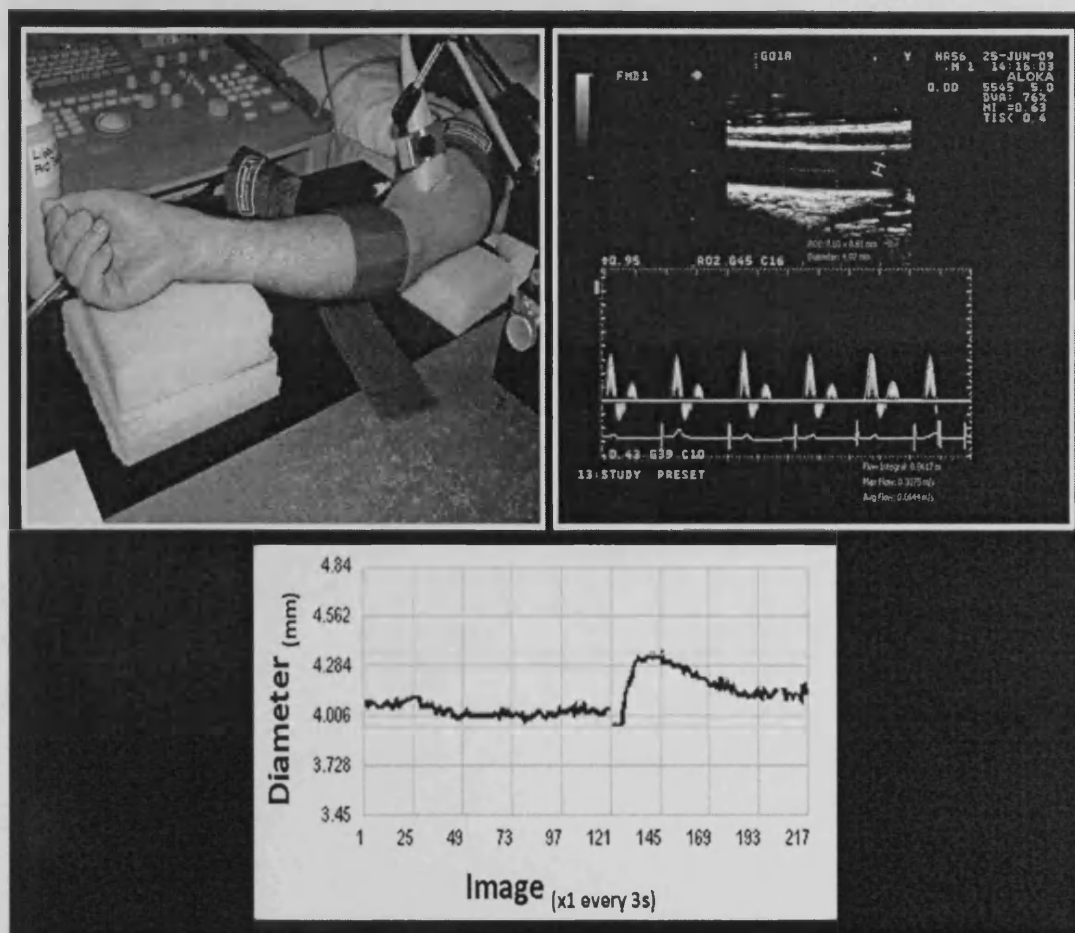


Figure 2-10: FMD analysis. Clockwise from top left. 1. Picture of the setup for brachial arterial FMD analysis. 2. Ultrasound imaging of the brachial artery (top = longitudinal image of the artery with the region for analysis highlighted, bottom = PWD flow velocity trace from the centre of the artery). 3. Brachial arterial diameter profile during the FMD protocol. Note the steady baseline in the first minute (images 0-20), followed by an increase in arterial diameter after cuff deflation at six minutes (image 120).

2.11.1. Analysis of FMD images

The baseline diameter of the brachial artery was the mean of the first twenty images recorded. Peak arterial diameter was the mean of the three largest diameters obtained following cuff deflation. FMD was expressed as the percentage increase in arterial diameter at peak compared to baseline.

The brachial arterial PWD flow velocity of a single cardiac cycle was measured on each image. A baseline value was the mean of three cardiac cycles recorded in the first minute of the protocol. Peak flow velocity was the greatest reading recorded during the first ten images after cuff deflation. The flow stimulus responsible for each FMD response was calculated as the percentage increase that the peak flow velocity was compared to the baseline velocity.

2.12. Forearm IR injury protocol

Transient endothelial dysfunction was produced in the non-dominant forearm by means of a period of IR injury¹⁴⁴. A blood pressure cuff was placed around the upper arm and inflated to 200mmHg using a rapid cuff inflator. The cuff remained inflated for twenty minutes. At this time the cuff was deflated and a twenty minute reperfusion period followed. Quantification of the degree of endothelial dysfunction produced by this stimulus was calculated by repeated ipsilateral FMD analyses, performed both before and after IR injury. The difference between these FMD measurements represented the degree of endothelial injury resulting from exposure to the IR stimulus. Figure 2-11 (page 71) is a schematic diagram of this protocol.

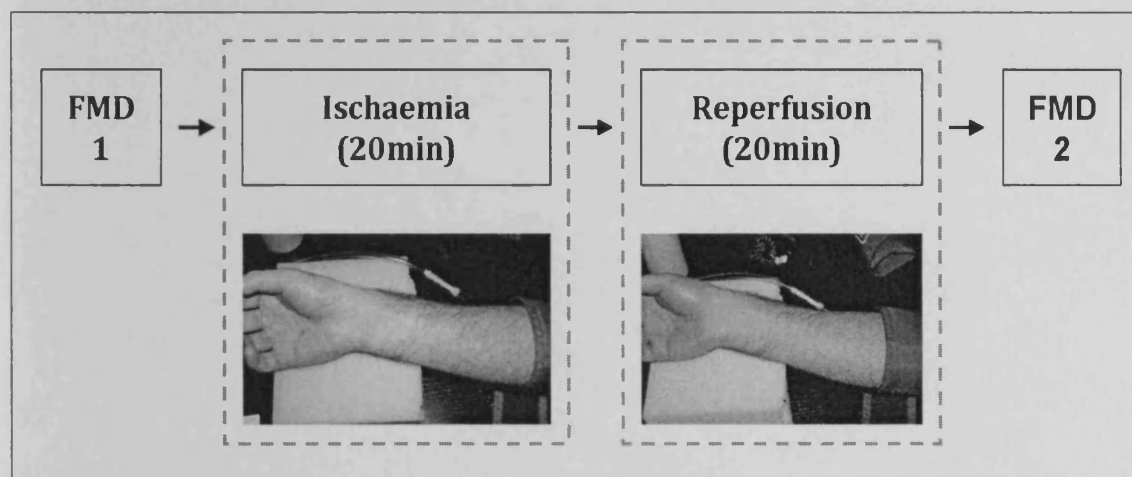


Figure 2-11: Forearm IR injury protocol. The transient endothelial dysfunction that results from twenty minutes of arm ischaemia followed by twenty minutes of reperfusion is quantified by FMD measurements taken at the start and end of the protocol.

2.13. Dobutamine stress echocardiography

A standard dobutamine stress echocardiogram (DSE) protocol combined with myocardial velocity imaging was used to assess functional reserve in subjects with proven ischaemia and CAD¹⁴⁵. Dobutamine was infused into a peripheral arm vein. An escalating dose regime of 0, 5, 10, 20, 30 & 40µg/kg/min was delivered in three minute stages.

Images were obtained by the same method as stated in section 2.4 (page 57); with the exception of the use of a GE System 7 machine. Each subject was rested for thirty minutes prior to the recording of baseline images. At this (and each subsequent) stage the apical 4 chamber, apical 2 chamber and apical long axis windows were recorded together with a PWD trace taken with the cursor placed within the left ventricle at the junction of the mitral inflow and aortic outflow regions (in order that aortic valve closure and mitral valve opening could be timed). Figure 2-12 (page 72) contains examples of the four echo images taken at each stage of the protocol. Three cardiac cycles were recorded for each window. The depth and width of each image was optimised to ensure that the frame rate recorded was >120 frames per second.

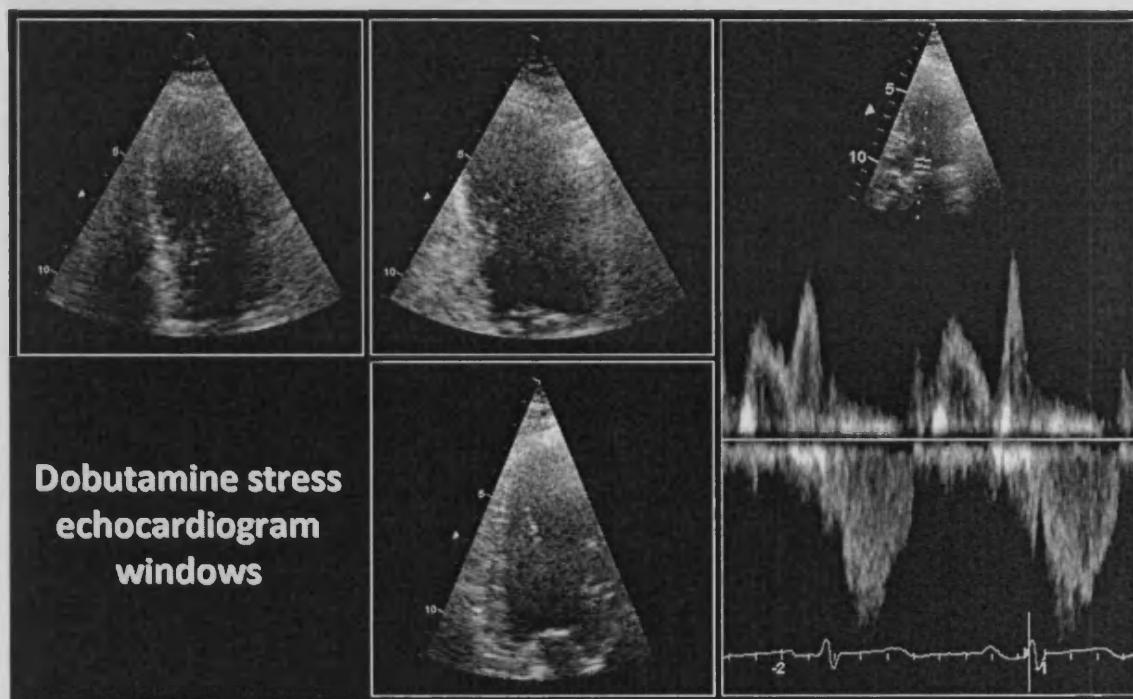


Figure 2-12: Example images taken at each stage of the DSE protocol. Clockwise from top left: 1. Apical 4 chamber window. 2. Apical 2 chamber window. 3. PWD trace taken at the junction between mitral inflow and aortic outflow. 4: Apical long axis window.

2.13.1. Myocardial velocity imaging parameters

A six segment basal wall model was used to assess the longitudinal peak systolic velocity (PSV) of myocardium in all regions of the left ventricle¹⁴⁵. This comprised of the basal septal (BS) and basal lateral (BL) walls in the apical 4 chamber window, the basal anterior (BA) and basal inferior (BI) walls in the apical 2 chamber window and the basal antero-septal (BAS) and basal posterior (BPost) walls in the apical long axis window. The myocardial velocity profile of each basal wall was assessed at a site that was above the mitral annulus throughout the whole cardiac cycle, (see Figure 2-13; below). The PSV was measured as the maximum systolic velocity outside of the left ventricular isovolumic contraction time period. The PSV is always positive when measured in apical windows.

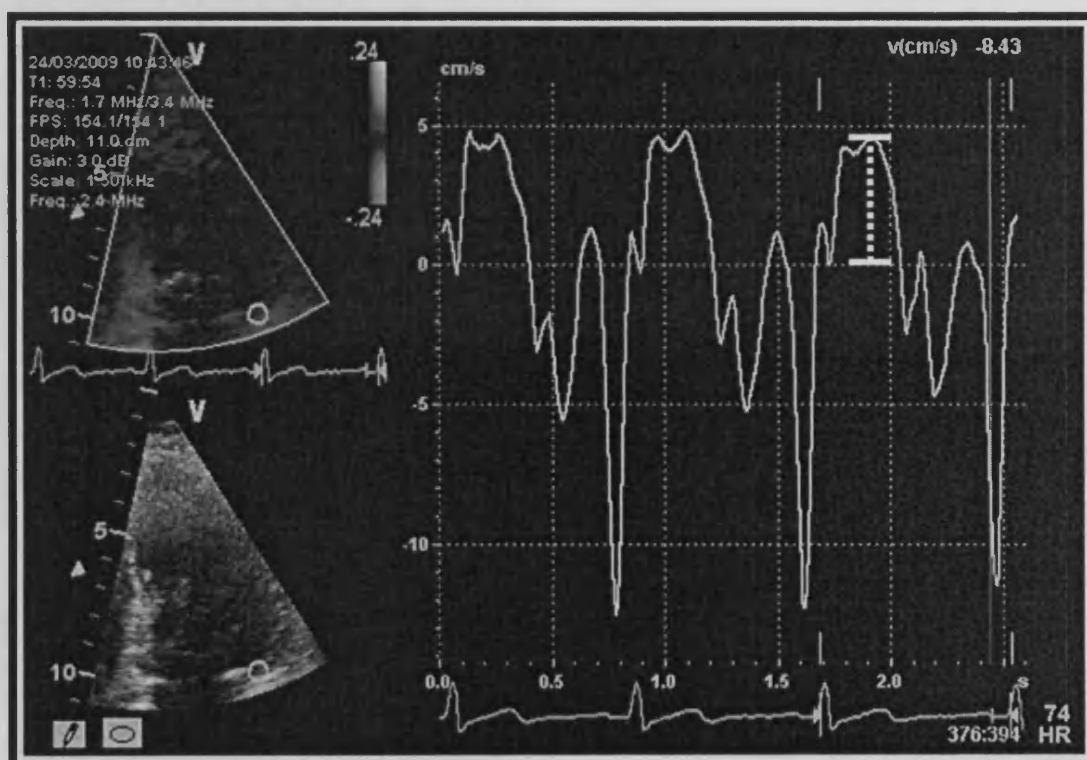


Figure 2-13: Example profile of the velocity of the left ventricular basal lateral wall. The far right cardiac cycle has been annotated to illustrate PSV measurement.

2.14. Isolated vessel preparation

New Zealand White rabbits (male, 2-2.5 kg, 6-8 weeks old) were terminally anaesthetised with intravenous pentobarbitone (150mg/kg). The abdominal aorta and the main pulmonary artery (just proximal to its bifurcation) were dissected and prepared into 2mm wide rings. These were mounted using hooks facing opposing directions and attached to a force transducer. Mounted rings were placed into 8ml individual organ chamber bioactivity assays maintained at 37°C by surrounding warm water, (Figure 2-14, page 75). Each ring was bathed in 5mls of Krebs solution and perfused with 95% O₂. After thirty minutes equilibration time a basal tension of 2g was set. Three successive constriction / relaxation cycles were performed using 1µM phenylephrine (PE) and 10µM ACh. The bath was emptied and washed out four times over a thirty minute period between each cycle.

After the rings had been prepared as outlined above they were again constricted using 1µM PE. NaNO₂ was added to the bath once peak tension had been achieved. Matched control rings did not receiving any additional agents. The resulting relaxed tensions at twenty minutes were measured. Each bath was then washed four times as described earlier.

In order to create hypoxic conditions the perfusing gas was changed from 95% oxygen to a mixture of 95%N₂/5% CO₂. Given that each organ chamber was exposed at its surface to room air this resulted in an effective local tissue environment of 1% O₂. After a 10 minute equilibration period constriction was again performed but this time using 3µM PE. The increased dose was necessary in order to achieve the same quantitative level of constriction as that gained during normoxia⁸⁹. 10µM NaNO₂ was added to each bath and the tension at twenty minutes recorded. This dose of NaNO₂ was

chosen as it has previously been shown in this model to be the lowest dose that results in an appreciable dilator effect⁸⁹.

The relaxation response of each vessel to NaNO_2 was expressed as a percentage of the maximal tension achieved, averaged between each pair of rings and corrected for the corresponding control ring pair.

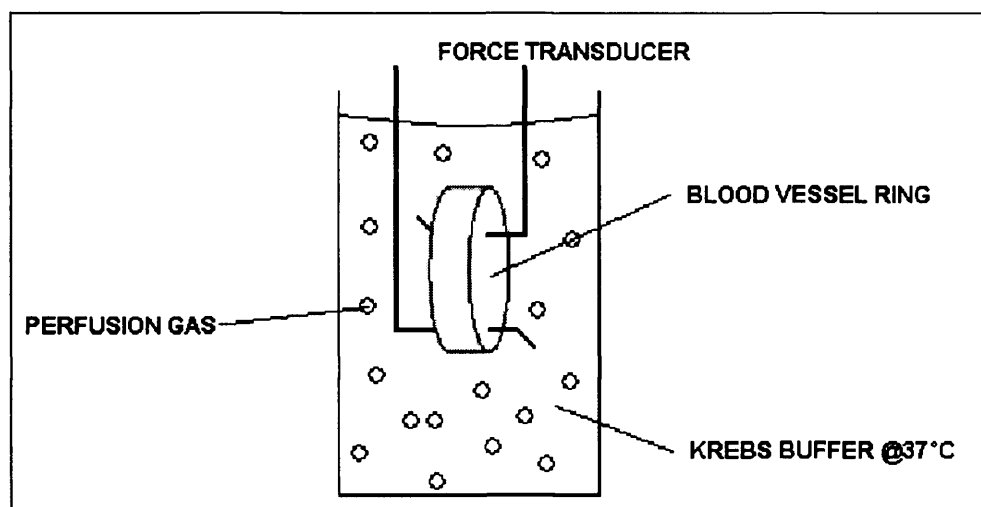


Figure 2-14: *Diagram of the setup of the organ chamber bioassay study.*

Chapter 3: Nitrite and Hypoxia

3.1. Introduction

3.1.1. The physiological effect of hypoxia upon the cardiovascular system

In man, exposure to acute hypoxia results in systemic vasodilation and pulmonary vasoconstriction¹⁴⁶. These physiological changes work in tandem to ensure that O₂ delivery to tissue remains as efficient as possible. An increase in cardiac output and systemic vasodilatation augment the cycling of oxygenated blood around the body. In addition, regions of the pulmonary vasculature will constrict to shunt blood away from hypoventilated lung segments. This is an appropriate response if there is regional hypoxia, for example in the case of a lobar pneumonia. However, when hypoxia is global (e.g. when FiO₂ is decreased) then the entire pulmonary vascular tree will constrict and the workload of the right ventricle will increase.

The above physiological changes occur over a period of hours. Dorrington reported, in six healthy individuals, the pulmonary and systemic cardiovascular responses during eight hours exposure to isocapnic hypoxia (FiO₂ 12%)⁹¹. After two hours of hypoxia more than 70% of the total eight hour reduction in systemic vascular resistance had occurred (see Figure 3-1, Panel B; page 77). Furthermore, the rate of change in systemic vascular resistance decreased markedly after this time-point; a plateau having already been reached. In addition, cardiac output increased as a function of HR alone with stroke volume remaining unchanged. This increase in cardiac output compensated for the decrease in systemic vascular resistance, resulting in systemic blood pressure remaining constant (see Figure 3-1, Panel A; page 77).

Changes in the pulmonary circulation followed a similar profile, with approximately 80% of the total eight hour augmentation of pulmonary vascular resistance having occurred after two hours of exposure to hypoxia (see Figure 3-1, Panel C; below).

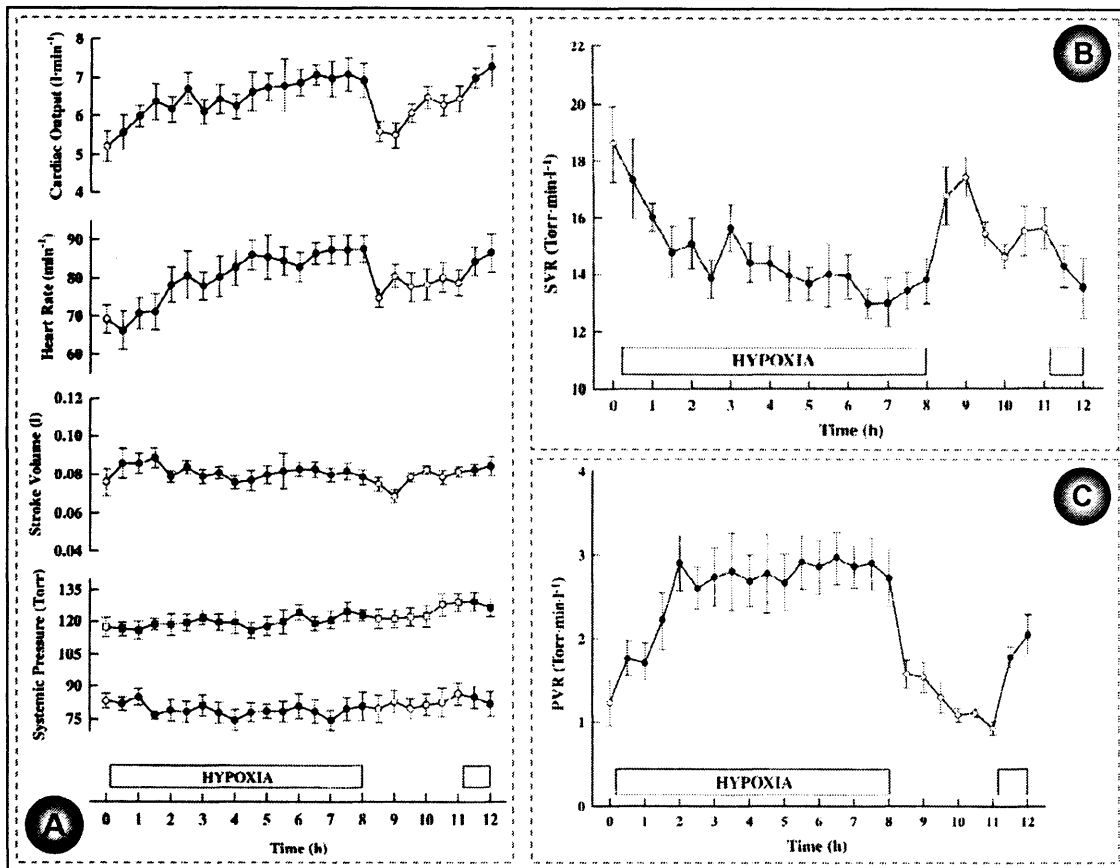


Figure 3-1: The cardiovascular effects of eight hours exposure to hypoxia (FiO_2 12%).

Panel A; systemic blood pressure, cardiac output, HR and left ventricular stroke volume. Panel B; systemic vascular resistance. Panel C; pulmonary vascular resistance

Adapted from Dorrington et al⁹¹.

3.1.2. Aims of this chapter

The present study was designed to test the physiological effects that a modest elevation in plasma $[\text{NO}_2^-]$ would have upon the systemic and pulmonary vasculature when tested in either hypoxia or normoxia. Healthy volunteers were investigated during stable hypoxia in an environmental chamber and during normoxic conditions breathing room air. An iv infusion of a low-dose of NaNO_2 or 0.9% saline was given.

Due to the intensive nature of data collection required during this study it was performed in partnership with another British Heart Foundation PhD Fellow, Andrew Pinder. I acquired and analysed all of the physiological measurements and the plasma NO_x samples. Andrew analysed the erythrocyte component of each blood sample. In addition, Janis Weeks (Medical Microbiology, Cardiff University) performed the analysis of plasma NO_3^- levels.

3.1.3. Original hypotheses

- 1. NaNO_2 will vasodilate the systemic vasculature preferentially in hypoxia compared to normoxia and this effect will be associated with a change in blood NO metabolite levels.**
- 2. NaNO_2 will vasodilate the pulmonary vasculature preferentially in hypoxia compared to normoxia.**

3.2. Study design (specific protocols)

The criteria used to recruit healthy volunteers for the studies performed in this chapter are outlined in section 2.2.1 (page 53). Subjects were asked to refrain from alcohol, caffeine and foods with a high $\text{NO}_2^-/\text{NO}_3^-$ content for twelve hours before each study. Each had a light breakfast before and then fasted for the duration of the study. Three studies were conducted, one as the index intervention (*hypoxia/NO₂⁻*) and two as control studies (*hypoxia/saline*, *normoxia/NO₂⁻*).

3.2.1. Protocol 1: Hypoxia/NO₂⁻

In twelve subjects, “*baseline*” (*i.e. protocol time = 0 min*) investigations were completed during normoxia, and then the FiO_2 in the environmental chamber was reduced from 21% to 12% over a one hour period. It was maintained at 12% for two more hours, so that subjects experienced a total of three hours of hypoxia (known as the hypoxia-equilibration period) before the “*pre-infusion*” (*i.e. protocol time = 180min*) measurements were obtained. An iv infusion of NaNO_2 was then given, into the dominant arm, at 1ml/min (1 $\mu\text{mol/min}$) for thirty minutes before “*peak*” (*i.e. protocol time = 210 min*) measurements were taken. The study infusion was given single-blind so that the study physician was aware of when NaNO_2 was being infused for safety reasons. Subjects remained in the hypoxic chamber for a further one hour after the infusion was completed, before a final “*one hour*” (*i.e. protocol time = 270 min*) set of measurements were made.

In addition to the four key stages outlined above, where all physiological and biochemical measurements were performed, further blood and FBF measures were taken at additional times during the protocol as outlined in Figure 3-2 (page 80); a schematic diagram of both protocols 1 & 2.

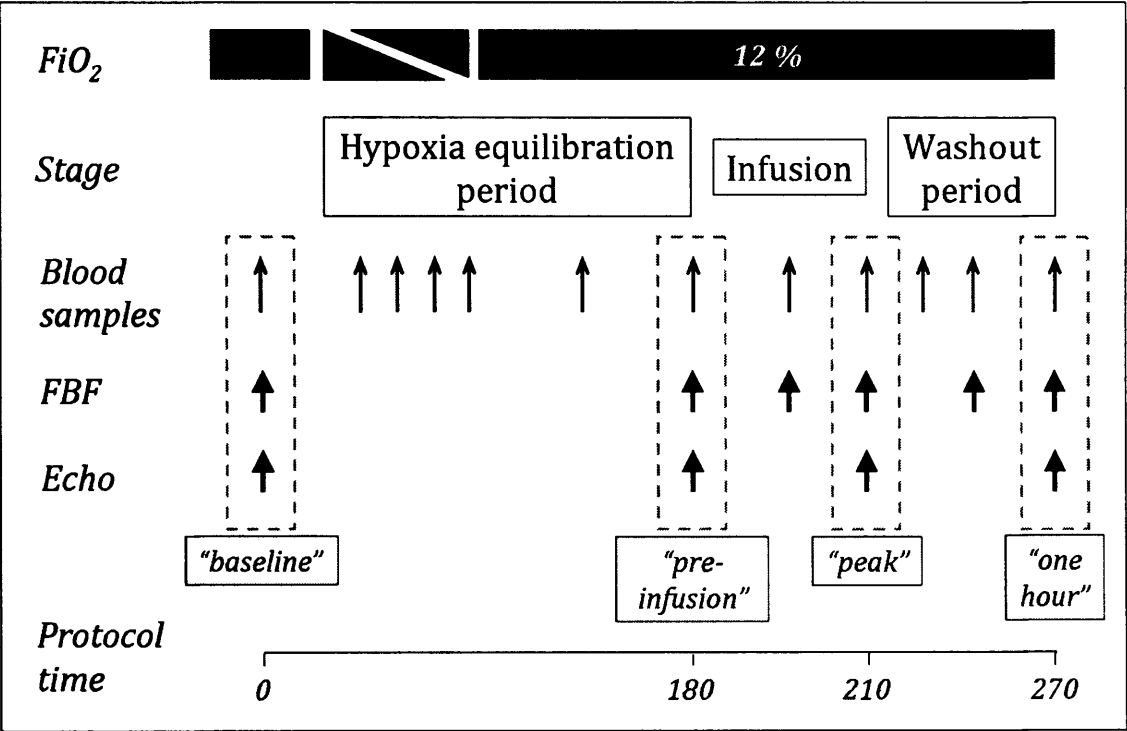


Figure 3-2: Diagram of the experimental design of protocol 1 (hypoxia/NO₂⁻) & protocol 2 (hypoxia/saline).

3.2.2. Protocol 2: Hypoxia/saline

Six different subjects underwent a control study in the hypoxic chamber. This group followed an identical protocol to that outlined previously in section 3.2.1 (page 79), but a single-blinded infusion of 0.9% saline (1ml/min for thirty minutes) was given instead of NaNO₂.

3.2.3. Protocol 3: Normoxia/NO₂⁻

Six of the twelve subjects whom had participated in protocol 1 (*hypoxia/NO₂⁻*) underwent this control study, which was performed in room air (FiO₂ 21%). Consequently no hypoxia-equilibration period was included, and only a short period of rest was required before the “*pre-infusion*” (*protocol time = 0 min*) measures were taken. Thereafter, the study was identical to that of protocol 1; with “*peak*” (*protocol time = 30 min*) and “*one hour*” (*protocol time = 90 min*) measurements being taken. The same infusion regime of NaNO₂ was used as in protocol 1. Figure 3-3 (below) is a diagram of this protocol.

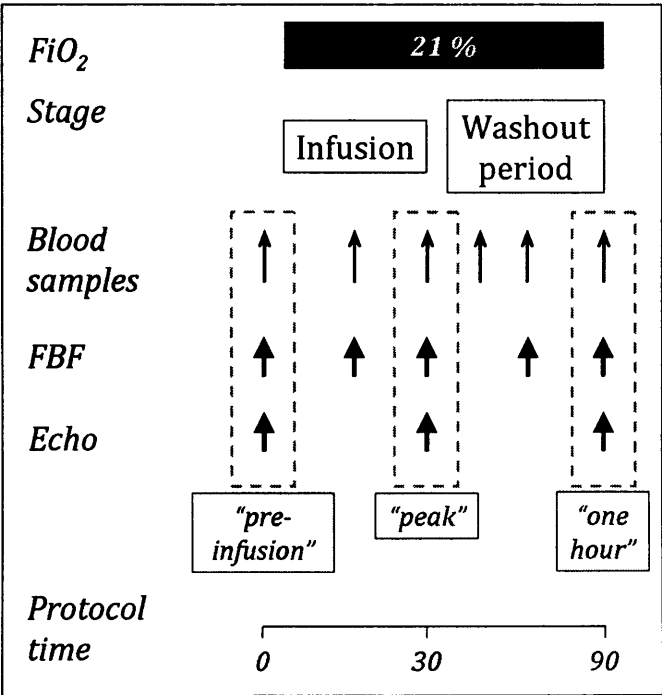


Figure 3-3: Diagram of the experimental design of protocol 3 (normoxia/NO₂⁻).

3.3. Results

The interpretation of the biochemical and physiological variables recorded is concentrated upon certain key time points within each protocol. In protocols 1 & 2 these are: “*baseline*” (0 min), “*pre-infusion*” (180min), “*peak infusion*” (210 min) and “*one hour*” (270min). In protocol 3 these are “*pre-infusion*” (0 min), “*peak*” (30 min) and “*one hour*” (90 min). For each variable, where appropriate, the effects of hypoxia are dealt with separately to the effects of the infusion. All continuous data is reported as mean \pm SEM.

Within group comparisons have been carried out using a repeated-measures ANOVA test with Newman-Keuls post-test. Between-groups comparisons, at the same protocol time-point, have been performed using an unpaired t-test.

3.3.1. Demographics

Summary demographics of the participants in this study are outlined below in Table 3-1. The left ventricular ejection fraction was calculated by the biplane Simpson’s method.

Demographic	
Number	18
Age (years)	24.2 \pm 1.0
Weight (kg)	78.6 \pm 2.2
Body Mass Index	24.3 \pm 0.6
Left Ventricular Ejection Fraction (%)	65.0 \pm 1.0

Table 3-1: Summary demographics of the subjects who participated in the studies reported in Chapter 3.

3.3.2. The environmental chamber & subject oxygenation

Figure 3-4 (page 84) contains four graphs which detail the chamber's ambient environment and the subject's capillary SaO₂ during the two studies where the controlled environmental chamber was used (i.e. *hypoxia/NO₂⁻* and *hypoxia/saline* protocols).

The FiO₂ had reached 12% by one hour into each hypoxia study and remained constant following this. The temperature during the *hypoxia/NO₂⁻* protocol was slightly greater than during the *hypoxia/saline* protocol at each point (e.g. “peak” *hypoxia/NO₂⁻* = 22.3°C ± 0.4 vs. “peak” *hypoxia/saline* = 21.0°C ± 0.3; p = <0.05). However the temperature remained constant within each protocol for their duration.

Capillary SaO₂ decreased by a similar degree during the hypoxia-equilibration period of both hypoxia protocols (i.e. *hypoxia/NO₂⁻*: “baseline” = 97.7 ± 0.2% vs “pre-infusion” = 82.0 ± 2.4 %, p<0.01. *hypoxia/saline*: “baseline” = 97.8 ± 0.4% vs “pre-infusion” = 85.7 ± 1.2 %, p<0.01) and did not change thereafter for the remainder of either protocol. There was no difference in the degree of hypoxia achieved between these two groups.

In summary, by 180 minutes into each study both hypoxia protocols had achieved a steady state in terms of room temperature and subject oxygenation.

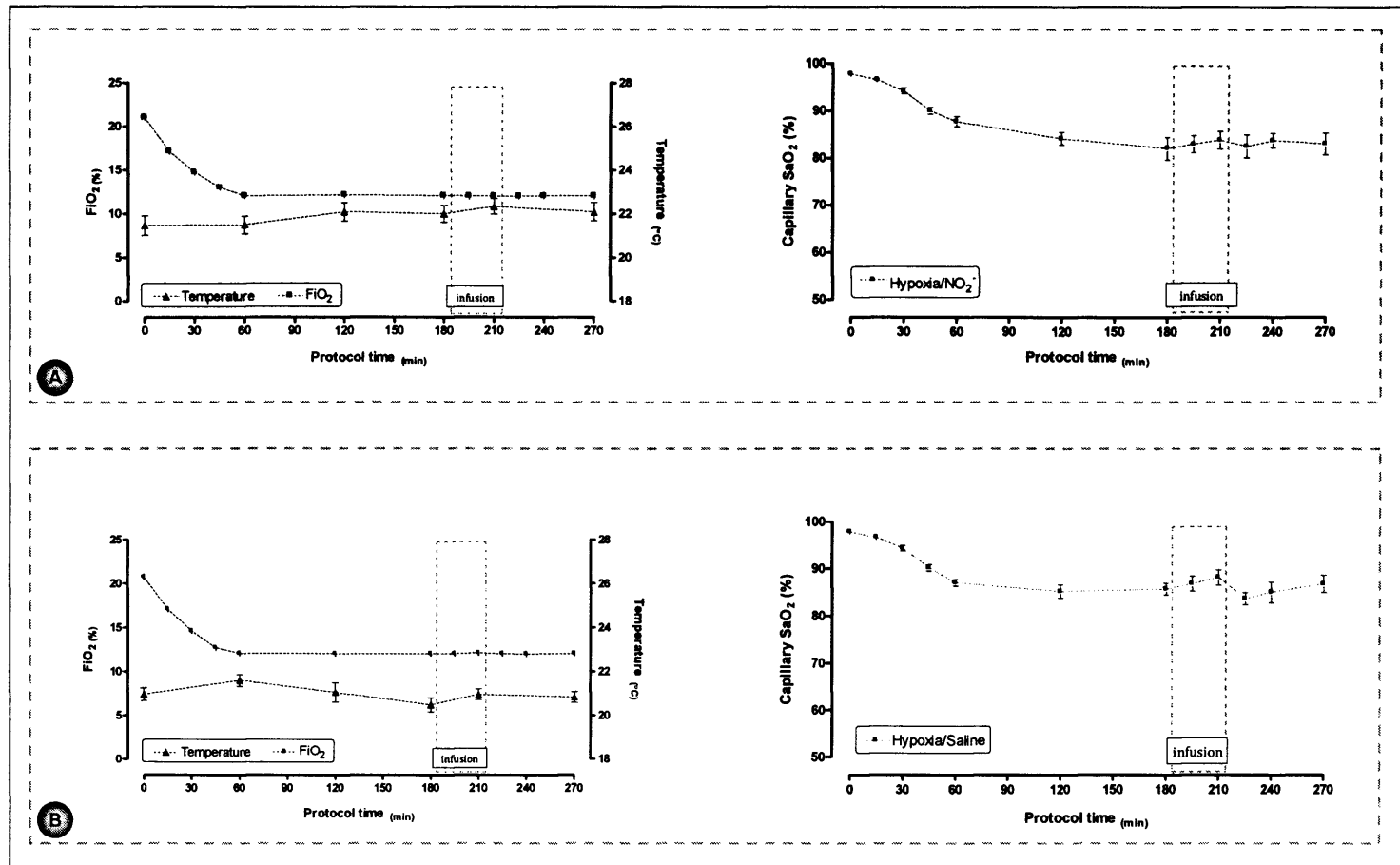


Figure 3-4: The ambient FiO_2 and temperature inside the environmental chamber (left column) and subject SaO_2 (right column) during the hypoxia/ NO_2^- protocol (panel A) and the hypoxia/saline protocol (panel B).

3.3.3. Basic haemodynamic variables

Figure 3-5 (below) shows the HR and BP profiles recorded during each of the three protocols performed.

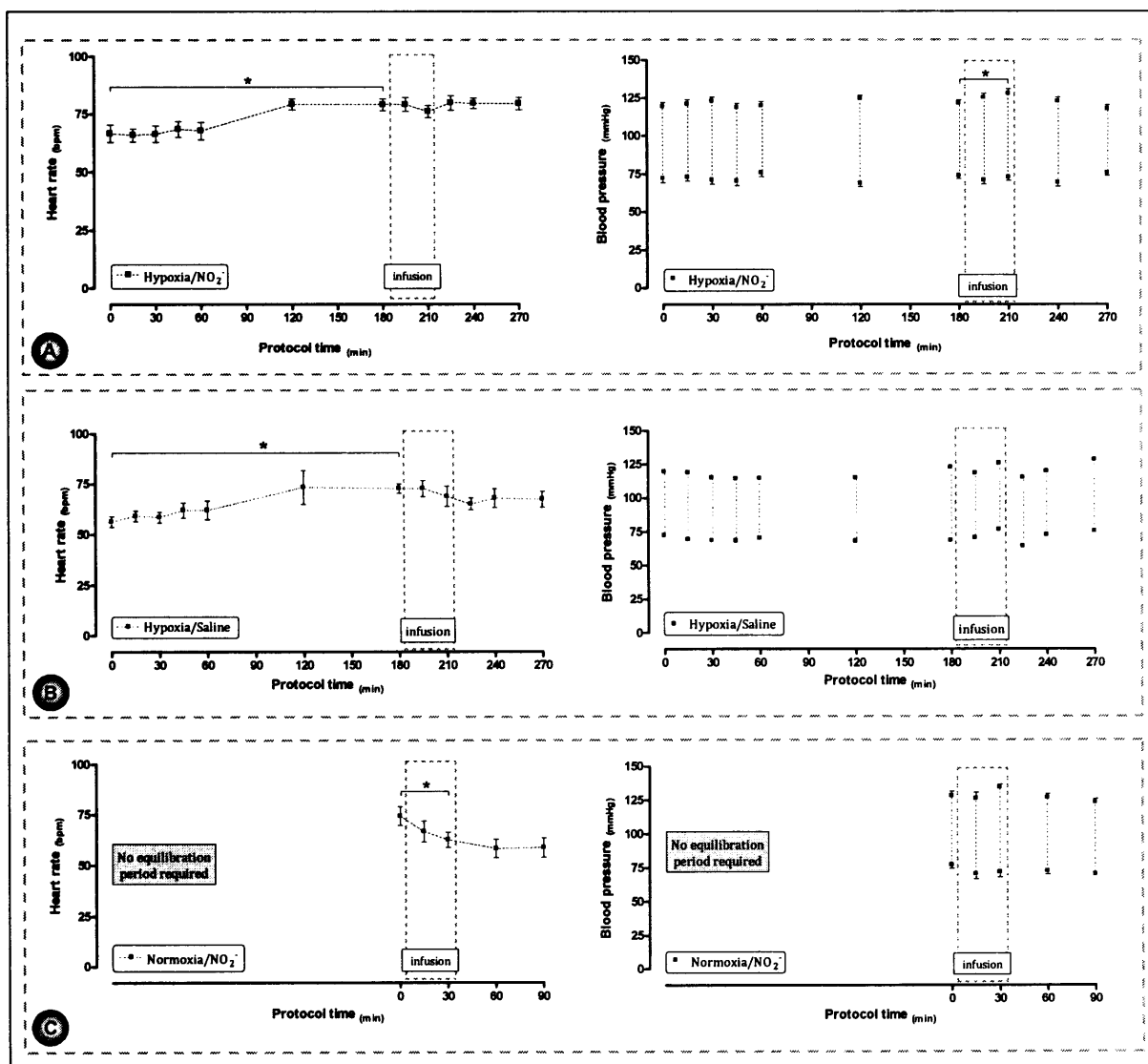


Figure 3-5: HR (left column) and systolic/diastolic BP (right column) during the three protocols: hypoxia/ NO_2^- (panel A), hypoxia/saline (panel B) and normoxia/ NO_2^- (panel C). * $p < 0.05$.

In both hypoxia protocols HR increased as a result of the hypoxia-equilibration period (combined data, “*baseline*” = 63 ± 3 bpm vs “*pre-infusion*” = 77 ± 2 bpm, $p < 0.01$), and thereafter it did not alter significantly during either protocol. This increase in HR resulted in the increase in cardiac output observed during the hypoxia-equilibration period (see section 3.3.7 page 97). HR decreased during the *normoxia/NO₂⁻* protocol, a difference occurring between “*pre-infusion*” = 74.2 ± 4.6 bpm and “*peak*” = 62.5 ± 3.8 bpm ($p < 0.05$).

Blood pressure did not alter as a result of the hypoxia-equilibration period. In addition blood pressure did not change throughout the *hypoxia/saline* or the *normoxia/NO₂⁻* protocol. However, systolic BP did increase in the *hypoxia/NO₂⁻* protocol (“*pre-infusion*” = 122 ± 2 mmHg vs “*peak*” 128 ± 3 mmHg; $p < 0.05$).

In summary the effect of hypoxia upon HR and BP are as would be expected from the literature⁹¹. In particular, a steady state had been achieved by the end of the hypoxia-equilibration period on which the effects of the subsequent infusion could be assessed.

3.3.4. Plasma NO metabolites

Figure 3-6 (page 87) contains summary profiles of the three plasma metabolites of NO recorded during each protocol. No difference was seen across any protocol in [RSNO] or [NO₃⁻] levels. Changes were observed in plasma [NO₂⁻] levels which are expanded on further in the next section.

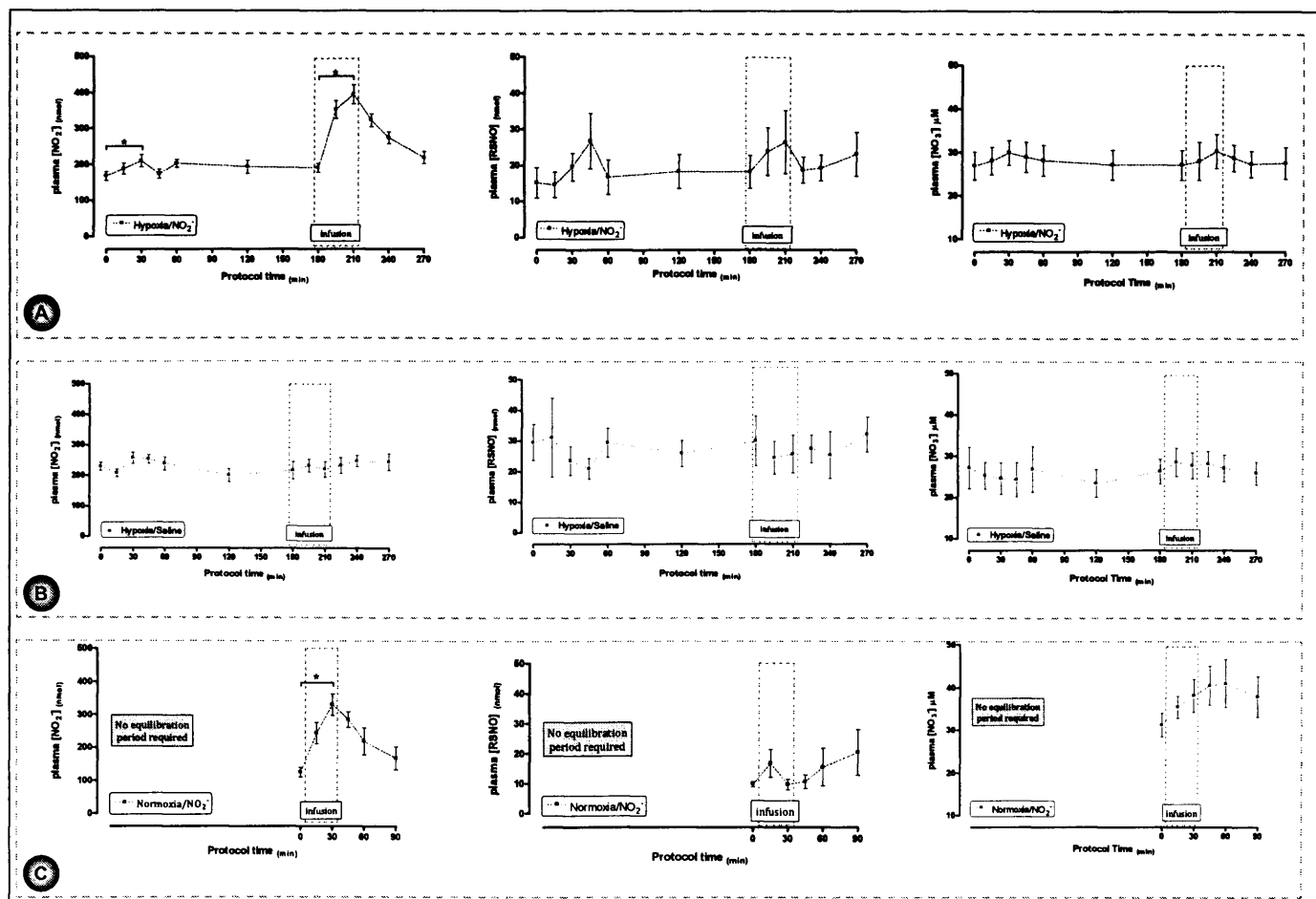


Figure 3-6: Plasma $[\text{NO}_2^-]$ (left column), plasma $[\text{RSNO}]$ (middle column) and plasma $[\text{NO}_3^-]$ (right column) profiles during the: hypoxia/ NO_2^- protocol (panel A), hypoxia/saline protocol (panel B) and normoxia/ NO_2^- protocol (panel C). * $p < 0.05$.

3.3.4.1. The effect of acute hypoxia upon plasma [NO₂⁻]

Plasma [NO₂⁻] increased during the first thirty minutes of the hypoxia-equilibration period in all eighteen subjects whom underwent a hypoxia study (combined data, “*baseline*” = 189.0 ± 11.3 nmol/l vs. “*protocol time 30 min*” = 226.2 ± 13.8 nmol, p<0.05). However, in the same subjects no difference in plasma [NO₂⁻] was present (again compared to “*baseline*”) after the hypoxia-equilibration period had been completed (combined data, “*pre-infusion*” = 199.4 ± 12.4 nmol/l; p>0.05).

“*Pre-infusion*” plasma [NO₂⁻] levels were similar between the two hypoxia groups and both of these concentrations were greater than the “*pre-infusion*” plasma [NO₂⁻] measured in the normoxia group (*hypoxia/NO₂⁻* = 191.0 ± 12.3 nmol/l, *hypoxia/saline* = 216.0 ± 28.6 nmol/l, *normoxia/NO₂⁻* = 125.5 ± 14.8 nmol/l; p<0.05). A difference was also present between the plasma [NO₂⁻] sample taken in room air in the *hypoxia/NO₂⁻* study and the *normoxia/NO₂⁻* study in the six subjects who underwent both of these protocols (i.e. *hypoxia/NO₂⁻* “*baseline*” = 177.0 ± 12.4 nmol/l & *normoxia/NO₂⁻* “*pre-infusion*” = 125.5 ± 14.8 nmol/l; p<0.05).

These combined results demonstrate a difference in plasma [NO₂⁻] when samples were taken in hypoxia compared to normoxia. However, the nature of these results means that it is difficult to ascribe this difference to an isolated effect of hypoxia alone. In particular it should be emphasized that plasma NO metabolites have a large dietary component⁶¹ and therefore significant day to day variability will be present in their levels. This point is illustrated in the previous paragraph by the difference in starting plasma [NO₂⁻] values in the same six subjects who were studied on different days in different protocols.

In addition, it should be acknowledged that although plasma $[\text{NO}_2^-]$ varied from day to day in this study it did not alter over the relatively short investigation period of the, control, *hypoxia/saline* study (i.e. 270 minutes). In particular, it did not alter over the 90 minute infusion-investigation period of the study (*hypoxia/saline* “*pre-infusion*” = 216.0 ± 28.6 nmol/l vs “*one hour*” 244.2 ± 27.1 nmol/l; $p = \text{ns}$).

3.3.4.2. The pharmacokinetics of NaNO_2

The pharmacokinetic profiles of plasma $[\text{NO}_2^-]$ were similar in both the *hypoxia/NO₂⁻* and *normoxia/NO₂⁻* protocols (see Figure 3-7; page 90).

There was no difference in the infusion-associated increase in plasma $[\text{NO}_2^-]$ concentration (“*peak*” minus “*pre-infusion*” concentration) observed in the *hypoxia/NO₂⁻* and *normoxia/NO₂⁻* protocols ($+205.5 \pm 20.9$ nmol/l vs. $+206.3 \pm 36.7$ nmol/l; $p > 0.05$). The half lives for decay of plasma $[\text{NO}_2^-]$ after stopping the infusion were also similar (in hypoxia 21.7 ± 3.0 min, and in normoxia 21.3 ± 3.4 min). In both groups plasma $[\text{NO}_2^-]$ had returned to a level similar to the corresponding pre-infusion concentration by one hour after cessation of the NaNO_2 infusion.

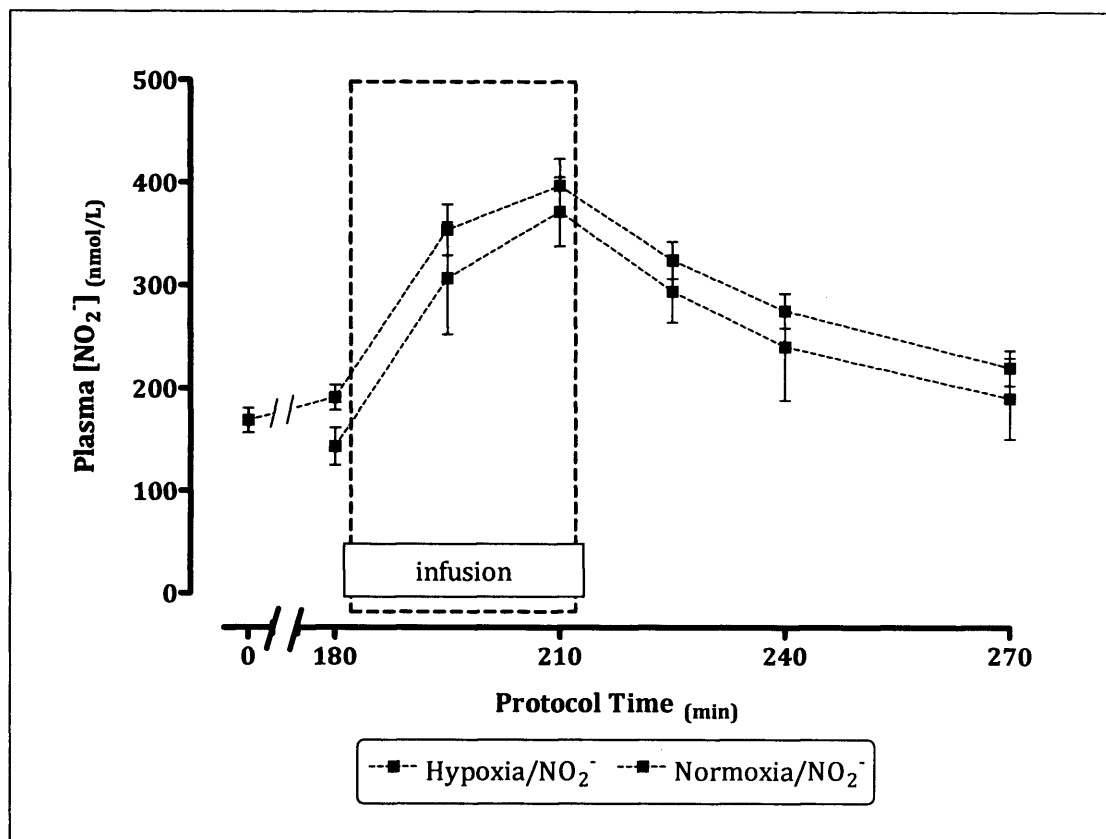


Figure 3-7: The profiles of plasma $[\text{NO}_2^-]$ resulting from an iv infusion of NaNO_2 given in either hypoxia or normoxia.

3.3.5. Erythrocyte NO metabolites

Figure 3-8 (page 93) is a series of graphs detailing the profiles of the three erythrocyte metabolites of NO recorded during each study. No difference was seen across any protocol in erythrocyte-associated $[\text{NO}_2^-]$ and $[\text{HbSNO}]$ levels. Changes were observed in $[\text{HbNO}]$ levels which are expanded on in the next section.

3.3.5.1. The effect of acute hypoxia exposure upon $[\text{HbNO}]$

During the first thirty minutes of the hypoxia-equilibration period $[\text{HbNO}]$ did not alter in either hypoxia protocol (combined data: “*baseline*” = 53.7 ± 7.9 nmol vs “*protocol time 30 min*” = 45.8 ± 6.0 nmol, $p > 0.05$). This finding is dissimilar to plasma $[\text{NO}_2^-]$, which increased over the same time period. However, in the same 18 subjects there was an increase in $[\text{HbNO}]$ as a result of the whole hypoxia-equilibration period (combined data: “*baseline*” = 53.7 ± 7.9 nmol vs “*pre-infusion*” = 98.4 ± 14.8 nmol; $p < 0.05$). Accordingly, a difference in “*pre-infusion*” $[\text{HbNO}]$ levels between the combined hypoxia groups and the normoxia group was also present (normoxia/ NO_2^- “*pre-infusion*” = 28.9 ± 12.4 nmol; $p < 0.05$).

3.3.5.2. The response of [HbNO] to the NaNO₂ infusion

[HbNO] increased as a result of the infusion of NaNO₂ in hypoxia (*hypoxia/NO₂⁻*: “*pre-infusion*” = 106.0 ± 19.1 nmol vs “*peak*” = 237.6 ± 58.4 nmol; p<0.01). However, the increased [HbNO] level had returned to a level similar to “*pre-infusion*” by fifteen minutes after the infusion had finished (“*protocol time 225 min*” = 101.8 ± 12.4 nmol, p>0.05).

During the *normoxia/NO₂⁻* protocol [HbNO] increased as a result of the infusion of NaNO₂ (“*pre-infusion*” = 28.9 ± 12.4 nmol, “*peak*” = 90.9 ± 13.2 nmol; p<0.05). The [HbNO] concentration was then slower to reduce than in the *hypoxia/NO₂⁻* protocol, reaching a level similar to “*pre-infusion*” only one hour after the infusion had stopped (“*one hour*” = 64.1 ± 15.3nmol).

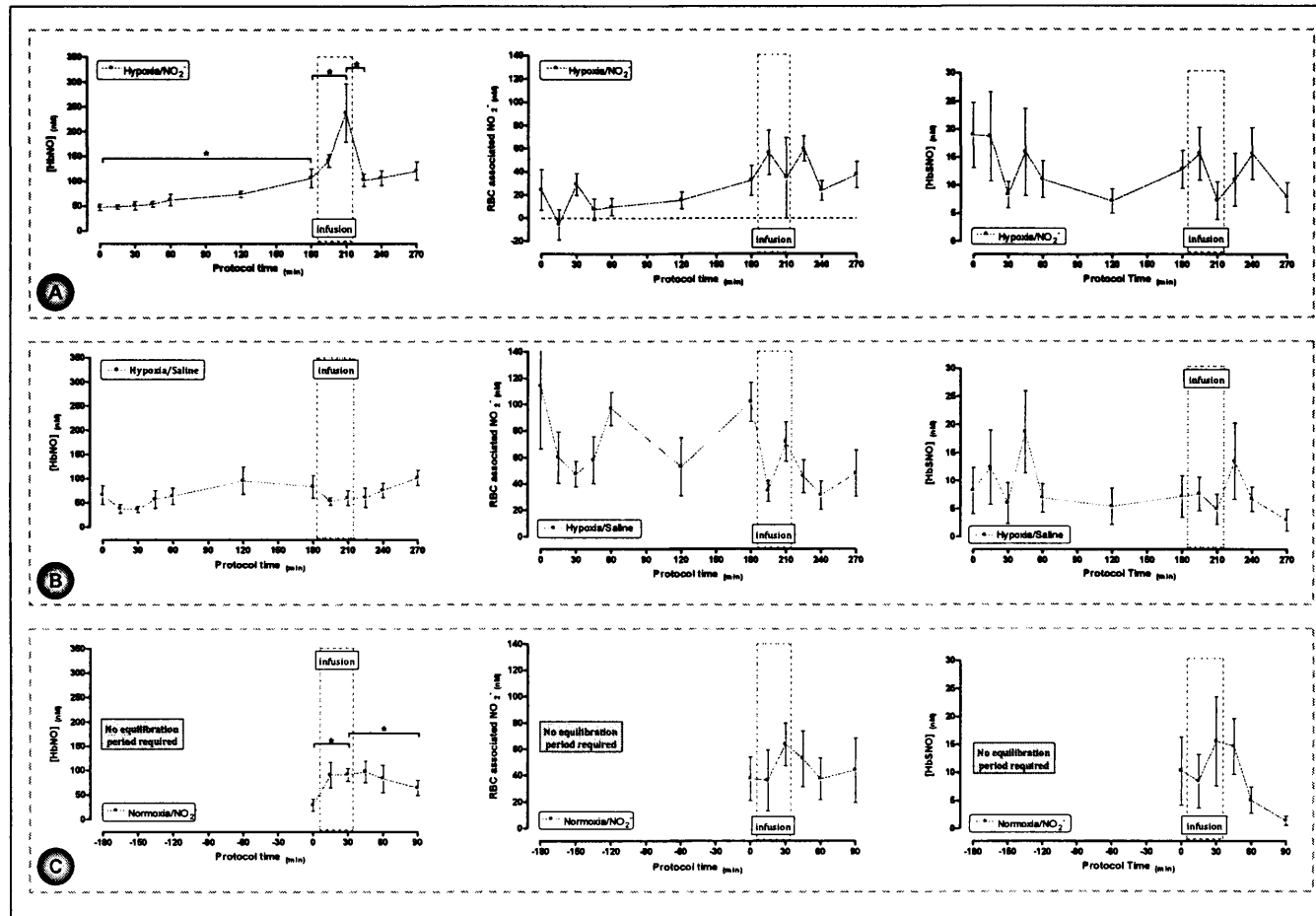


Figure 3-8: $[HbNO]$ (left column), erythrocyte-associated $[NO_2^-]$ (middle column) and $[HbSNO]$ (right column) profiles during the: hypoxia/ NO_2^- protocol (panel A), hypoxia/saline protocol (panel B) and normoxia/ NO_2^- protocol (panel C). * $p < 0.05$.

3.3.6. Forearm blood flow

Figure 3-9 (page 95) contains three graphs detailing the profiles of FBF recorded during each protocol. FBF did not alter as a result of the hypoxia-equilibration period in either of the two hypoxia protocols (combined data: “baseline” = 2.10 ± 0.12 ml/100ml/min vs “pre-infusion” = 2.24 ± 0.10 ml/100ml/min, $p > 0.05$). Indeed, FBF remained unchanged throughout the *hypoxia/saline* protocol; demonstrating that the experimental design provided a steady baseline on which the infusion of NaNO_2 could be assessed.

FBF increase during the NaNO_2 infusion in the *hypoxia/NO₂⁻* group (“pre-infusion” = 2.15 ± 0.13 ml/100ml/min vs “peak” = 2.77 ± 0.17 ml/100ml/min; $p < 0.05$). This increase in FBF had reduced by thirty minutes after the infusion had finished to a value similar to that measured “pre-infusion” (“protocol time 240” = 2.61 ± 0.24 ml/100ml/min; $p > 0.05$). FBF did not change throughout the *normoxia/NO₂⁻* protocol.

3.3.6.1. Changes in FBF compared to key NO metabolites

The profile of change in FBF in the *hypoxia/NO₂⁻* group was of a similar pattern to plasma $[\text{NO}_2^-]$ but not $[\text{HbNO}]$, see Figure 3-10 (page 96). Further analysis of the data, detailed in Figure 3-11 (page 96), demonstrated that a significant correlation between plasma $[\text{NO}_2^-]$ and FBF was present in the *hypoxia/NO₂⁻* group (Pearson $r = 0.31$, $p < 0.01$). No similar correlation was present in the *normoxia/NO₂⁻* group, or between FBF and $[\text{HbNO}]$ in either group (Pearson r values shown for comparison on the relevant graphs within the same figure).

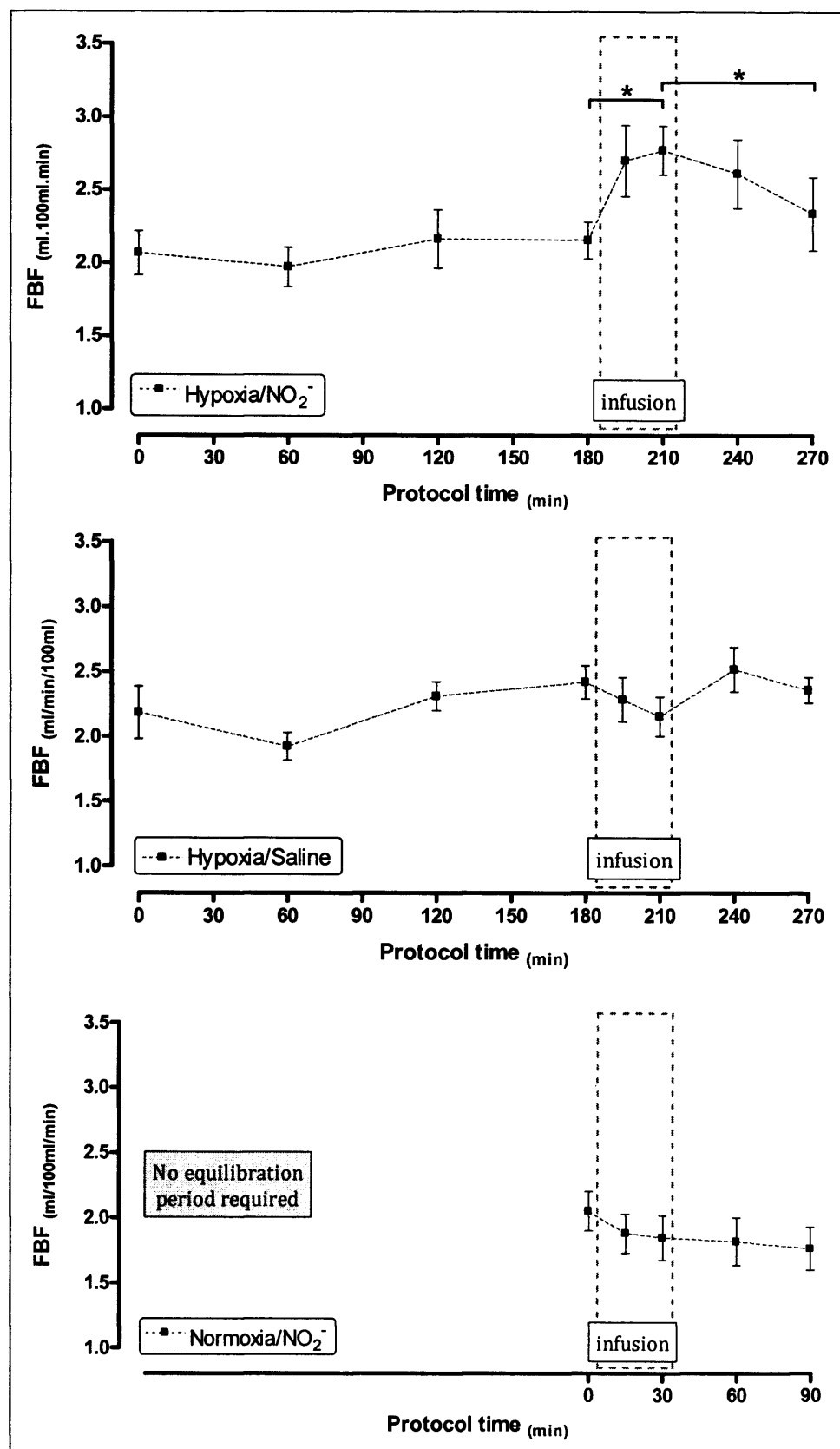


Figure 3-9: FBF profile during the hypoxia/NO₂⁻ protocol (top), hypoxia/saline protocol (middle) and normoxia/NO₂⁻ protocol (bottom). * $p < 0.05$

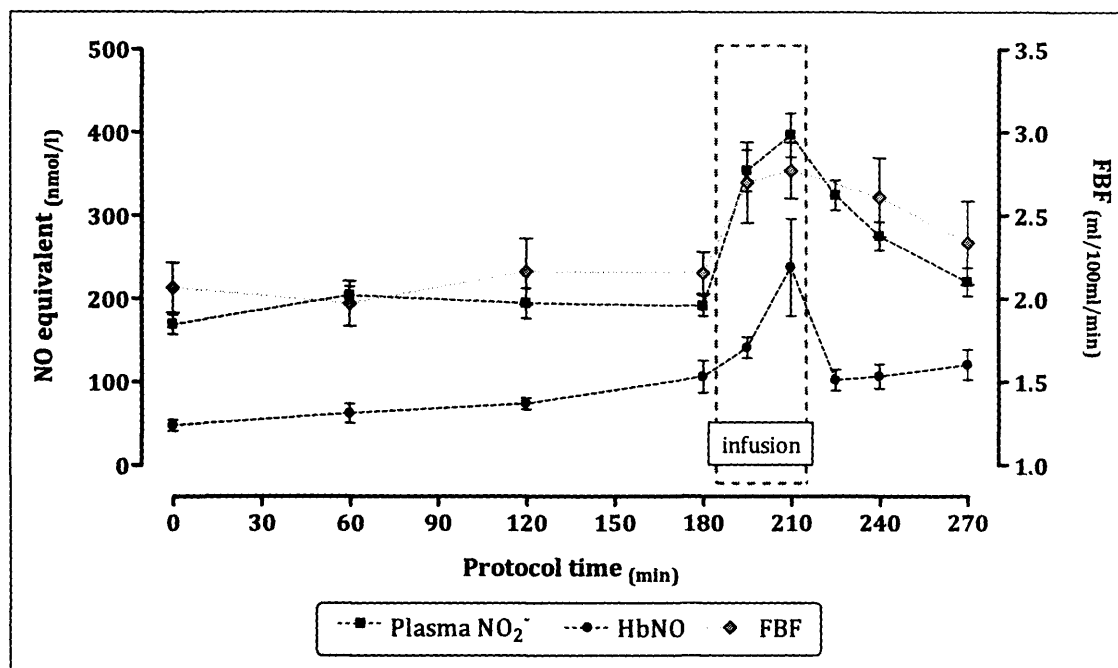


Figure 3-10: The profile of plasma $[\text{NO}_2^-]$, $[\text{HbNO}]$ and FBF during the hypoxia/ NO_2^- protocol.

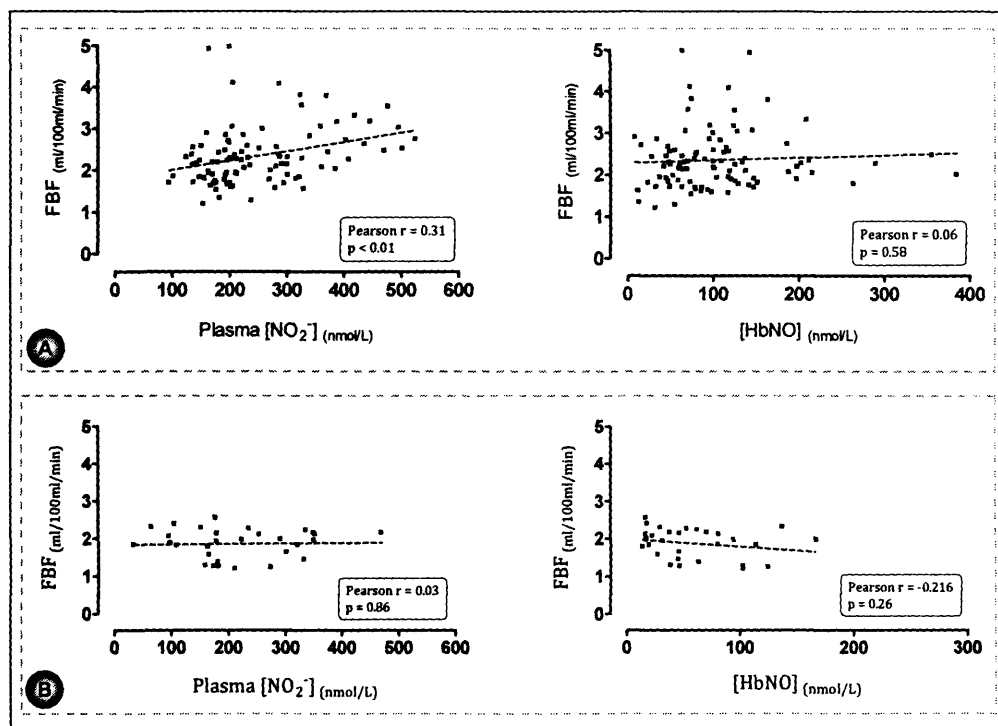


Figure 3-11: Correlation between FBF and plasma $[\text{NO}_2^-]$ (left column) & FBF and $[\text{HbNO}]$ (right column). Panel A = hypoxia/ NO_2^- protocol, panel B = normoxia/ NO_2^- protocol.

3.3.7. Pulmonary arterial pressure (PAP)

The profiles of the echocardiographic surrogate markers of pulmonary arterial pressure (PAP) throughout the three protocols are reported in Table 3-2, (page 100).

3.3.7.1. The effect of acute hypoxia exposure upon PAP

Figure 3-12, (page 98) contains typical examples of the echocardiographic images recorded to measure the three surrogate markers of PAP both before and after the hypoxia-equilibration period. All three markers significantly altered as a result of this three-hour hypoxia exposure.

The estimated PASP almost doubled in response to the hypoxia-equilibration period in the two hypoxia protocols (combined data: “*baseline*” = 20 ± 1 mmHg vs “*pre-infusion*” = 39 ± 2 mmHg, $p < 0.01$). The diameter of the inferior vena cava and its respiratory variation did not change significantly throughout all studies, and so the estimated right atrial pressure was constant at 5 mmHg. A significant shortening of the PAT occurred (combined data: “*baseline*” = 157 ± 4 ms vs “*pre-infusion*” = 113 ± 3 ms, $p < 0.01$) and the IVRT of the right ventricle lengthened (combined data: “*baseline*” = 7 ± 6 ms vs “*pre-infusion*” = 96 ± 8 ms, $p < 0.01$). There were no significant differences between the *hypoxia/NO₂⁻* and *hypoxia/saline* groups in all three indices recorded at either “*baseline*” or “*pre-infusion*”.

Subsequent to the hypoxia-equilibration period both the estimated PASP and the PAT did not alter for the remainder of the *hypoxia/saline* protocol. However, the IVRT did continue to increase at the “*peak*” and “*one hour*” time-points of this control protocol (see Table 3-2; page 100).

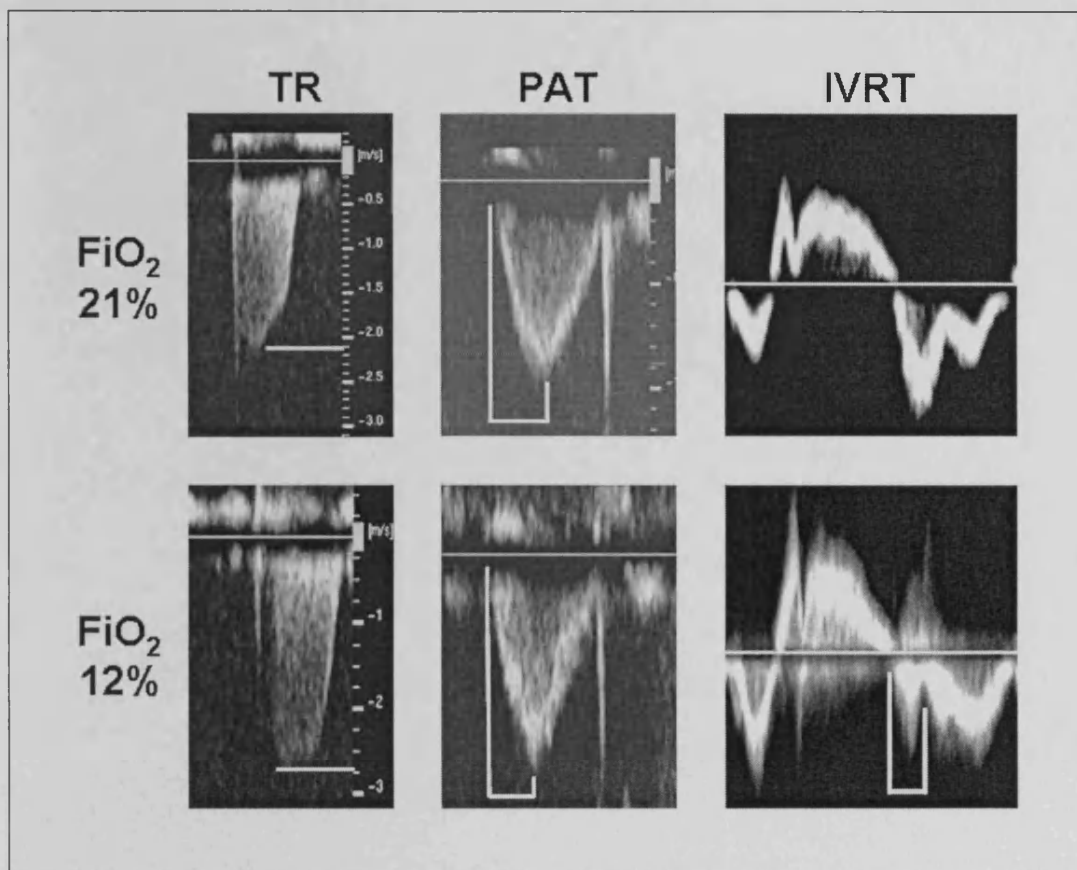


Figure 3-12: Example, annotated, echocardiographic images recorded to measure the three surrogate markers of PAP, acquired at “baseline” (top row) or “pre-infusion” (bottom row).

3.3.7.2. The effects of NaNO_2 upon the hypoxic pulmonary vasculature

In the *hypoxia/NO₂⁻* group the infusion of NaNO_2 reduced the estimated PASP by 16%. Furthermore, although plasma $[\text{NO}_2^-]$ had returned to normal by one hour after the infusion had stopped, estimated PASP remained significantly reduced compared to “pre-infusion”, see Figure 3-13 (page 99).

Similar changes were observed in the two alternative echo indices recorded. The PAT was prolonged at peak infusion by 12% compared to pre-infusion, an effect which was also present one hour later. The duration of the IVRT was attenuated by

NaNO₂ both at the end of the infusion (by 17%) and one hour later. All three echo surrogates of pulmonary arterial pressure were unchanged throughout the *normoxia/NO₂⁻* protocol.

Between group analysis confirmed an effect of NaNO₂ at peak ($p < 0.01$ for all three indices). The persistent vasodilator effect of NaNO₂ at one hour was shown by changes in IVRT ($p < 0.01$); the effect upon PAT tended to significance ($p = 0.07$) while the changes in PASP were not analyzed between groups due to a low prevalence of a TR jet in the *hypoxia/saline* group. See marked comparisons and legend in Table 3-2 (page 100) for details.

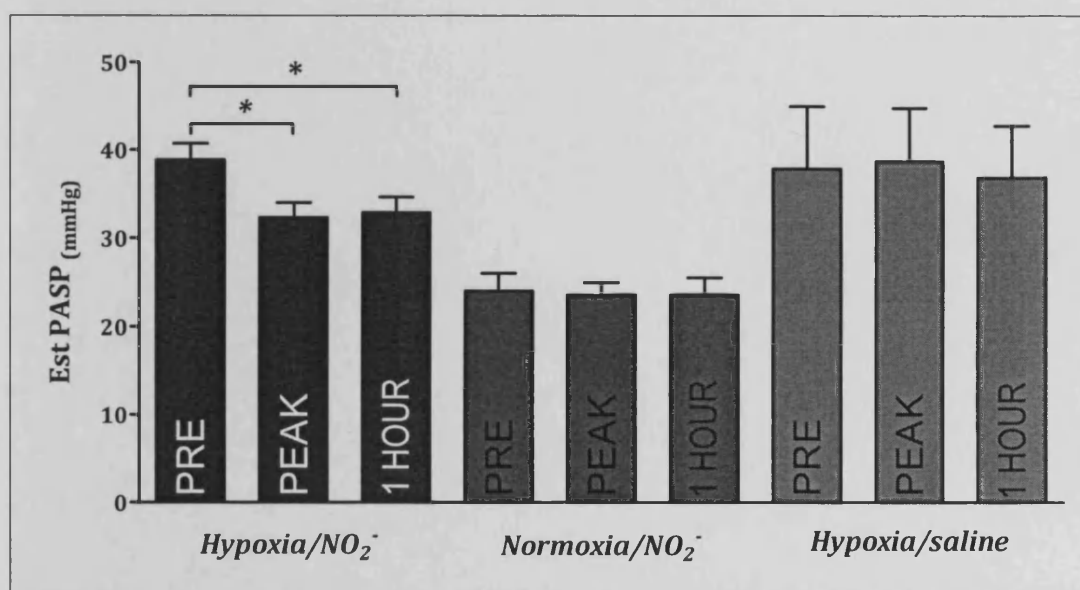


Figure 3-13: Estimated PASP during the infusion of either NaNO₂ or saline in each of the three protocols performed. * $p < 0.01$. Only statistically significant comparisons are shown.

	Baseline	Pre-infusion	Peak	p value vs pre-infusion	One hour	p value vs pre-infusion	N
PASP (mmHg)							
hypoxia/NO ₂ ⁻	20 ± 1	38 ± 2	32 ± 2] * ns ns	33 ± 2	<0.01	7
hypoxia/saline	20 ± 4	38 ± 7	39 ± 6		37 ± 6	ns	3
normoxia/ NO ₂ ⁻	n/a	24 ± 2	24 ± 1		24 ± 1	ns	5
PAT (ms)							
hypoxia/NO ₂ ⁻	153 ± 5	111 ± 3	124 ± 3] * ns ns	121 ± 4] † ns ns	12
hypoxia/saline	164 ± 3	116 ± 6	114 ± 6		113 ± 6		6
normoxia/ NO ₂ ⁻	n/a	166 ± 7	162 ± 8		161 ± 4		6
IVRT (ms)							
hypoxia/NO ₂ ⁻	8 ± 8	105 ± 11	87 ± 9] * ns n/a	95 ± 9] * ns n/a	11
hypoxia/saline	5 ± 5	79 ± 10	91 ± 13		103 ± 12		6
normoxia/ NO ₂ ⁻	n/a	0	0		0		6

Table 3-2: Echo surrogate markers of pulmonary arterial pressure during each protocol. Additional statistical comparisons between the hypoxia/NO₂⁻ and hypoxia/saline groups are marked in the “peak” and “one hour” columns. This analysis compares the delta between “pre-infusion” and “peak” (“pre-infusion” minus “peak”) or “pre-infusion” and “one hour” (“pre-infusion” minus “one hour”).

* $p < 0.01$, † $p = 0.07$. N = number of subjects.

3.3.8. Cardiac output

Table 3-3 (page 102) summarises the profile of cardiac output (together with its constituent components of stroke distance (i.e. $VTI_{(LVOT)}$) and HR) during each protocol. Cardiac output increased by 25% in response to the hypoxia-equilibration period in all subjects whom underwent a hypoxia protocol (combined data: “baseline” = 4.53 ± 0.23 l/min vs “pre-infusion” 5.61 ± 0.26 l/min, $p < 0.01$). This was due to an increase in HR, see Section 3.3.3 (page 85).

In the *hypoxia/NO₂⁻* group cardiac output decreased by an average of 8% when the study-infusion was infused. This was the result of a small reduction in both HR and stroke distance. Of the two variables stroke distance tended towards significance ($p = 0.07$), consistent with reduced preload secondary to NaNO₂ induced venodilation.

The increase in cardiac output related to hypoxia was unaltered by the infusion of saline. When NaNO₂ was infused during normoxia, no changes were observed in HR, $VTI_{(LVOT)}$ or cardiac output.

3.3.9. Analysis of variance of physiological measures

Thirty paired readings, chosen at random, of the five physiological variables used in this chapter were used to determine intra-observer reproducibility. The results of these analyses are shown in Figure 3-14 (page 103) and Table 3-4, (page 104). The coefficient of variation was calculated as the ratio of the standard deviation of the differences (i.e. measurement 1 – measurement 2) divided by the mean, (expressed as a percentage).

	Baseline	Pre-infusion	(<i>p</i> value vs baseline)	Peak	(<i>p</i> value vs pre-infusion)	1 hour after infusion	(<i>p</i> value vs pre-infusion)
Cardiac output (l/min)							
<i>hypoxia/NO₂⁻</i>	4.45 ± 0.27	5.64 ± 0.30	<0.01	5.14 ± 0.28	<0.05	5.09 ± 0.31	ns (*)
<i>hypoxia/saline</i>	4.70 ± 0.48	5.56 ± 0.51	<0.05	5.47 ± 0.51	ns	5.14 ± 0.42	ns
<i>normoxia/ NO₂⁻</i>	n/a	4.43 ± 0.21	n/a	4.15 ± 0.27	ns	4.14 ± 0.30	ns
Heart rate (bpm)							
<i>hypoxia/NO₂⁻</i>	66 ± 4	79 ± 3	<0.01	76 ± 3	ns	80 ± 3	ns
<i>hypoxia/saline</i>	56 ± 3	73 ± 2	<0.01	69 ± 5	ns	67 ± 4	ns
<i>normoxia/ NO₂⁻</i>	n/a	74 ± 5	n/a	63 ± 4	ns	59 ± 5	ns
VTI_(LVOT) (cm/s)							
<i>hypoxia/NO₂⁻</i>	23.3 ± 0.5	23.8 ± 1.0	ns	22.5 ± 0.8	ns (*)	22.8 ± 0.9	ns
<i>hypoxia/saline</i>	22.4 ± 1.3	23.4 ± 1.3	ns	23.2 ± 1.7	ns	22.3 ± 1.6	ns
<i>normoxia/ NO₂⁻</i>	n/a	20.7 ± 1.4	n/a	21.5 ± 2.0	ns	22.5 ± 1.4	ns

Table 3-3: Cardiac output and its constituent components. * *p* = 0.07

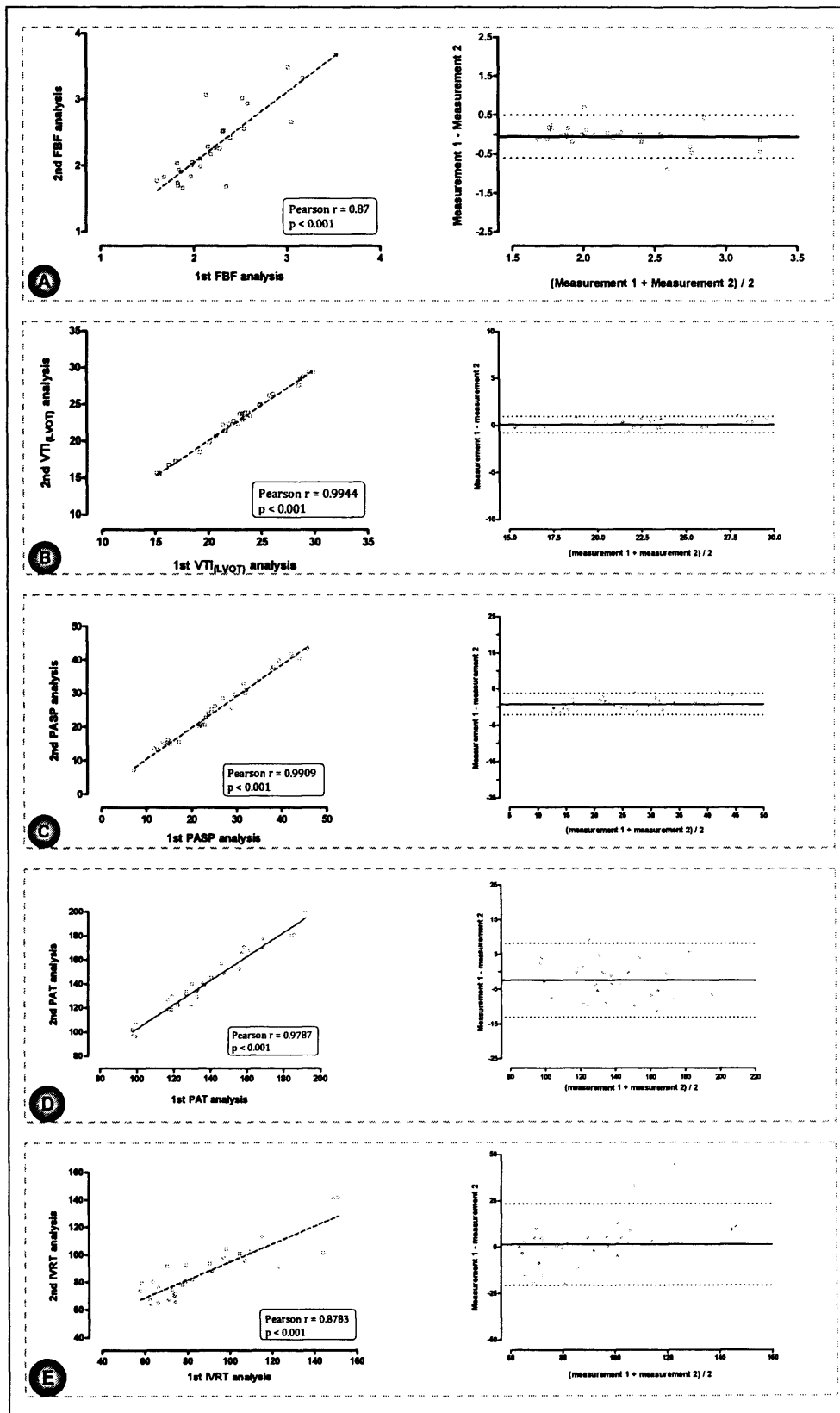


Figure 3-14: Correlation (left column) and Bland-Altman plots (right column) of the intra-observer variability in the five physiological variables recorded (panels from top:

A = FBF, B = VTl_{LVOT} , C = estimated PASP, D = PAT and E = IVRT).

	Feasibility (%)	Mean reading (units)	R ²	Bland-Altman analysis: Bias (95% CI)	Coefficient of Variation (%)
<u>Pulmonary arterial pressure</u>					
TR	62	29.8 (mmHg)	0.98	0.8 (-2.1 to 3.8)	5.8
PAT	100	156.3 (ms)	0.96	-2.5 (-13.2 to 8.2)	3.9
IVRT	96	93.3 (ms)	0.77	1.4 (-20.6 to 23.3)	14.8
<u>Cardiac output</u>					
VTI _(LVOT)	100	4.9 (l/min)	0.99	0.1 (-0.8 to 0.9)	1.9
<u>Systemic vascular resistance</u>					
FBF	100	2.3 (ml/100ml/min)	0.76	-0.1 (-0.6 to 0.5)	12.5

Table 3-4: *Summary table of the intra-observer variability in the physiological measures recorded.*

3.3.10. Organ chamber bioassay

The vasodilator effect of NaNO_2 upon isolated rings of rabbit pulmonary artery (PA) and abdominal aorta (AA) are displayed in Figure 3-15 (below).

The responses of both the PA and the AA to $10\mu\text{M}$ NaNO_2 were potentiated by a hypoxic environment (PA: 95% O_2 $8.3 \pm 1.6\%$ vs 1% O_2 $16.7 \pm 1.2\%$, $p < 0.05$; AA: 95% O_2 $3.0 \pm 1.1\%$ vs 1% O_2 $45.0 \pm 5.7\%$, $p < 0.05$). However, whilst the vasodilator effect of NaNO_2 was more pronounced upon the PA than the AA in an oxygenated environment, this effect was reversed in hypoxia.

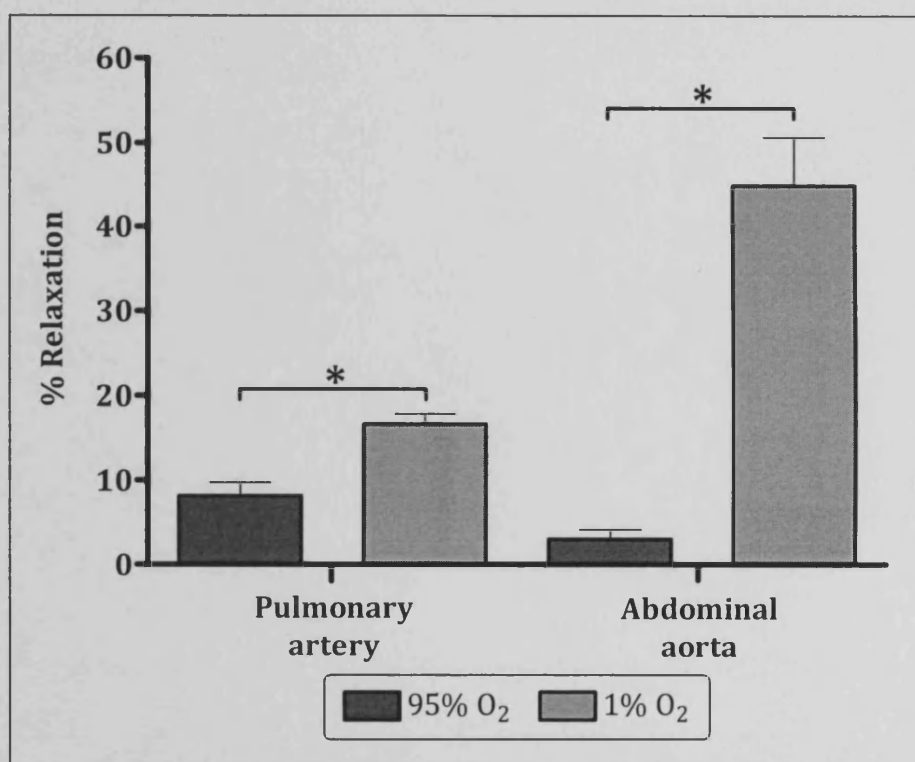


Figure 3-15: Aortic & Pulmonary arterial responses to $10\mu\text{M}$ NaNO_2 . $N=6$. * $p < 0.05$ (paired t -test).

3.4. Discussion

3.4.1. The effective utilisation of hypoxia in a physiological study

The hypoxia protocols were conducted in an environmental chamber that eliminated the difficulties of achieving stable control of hypoxia associated with the use of a face-mask. There are three major problems with studies which utilize a face-mask delivered ventilation system. Firstly, subjects are immediately exposed to the maximal degree of hypoxia being tested, which is associated with an acute and significant cardiovascular stress. For example, the investigators in this study reported pronounced tachycardia and tachypnoea upon entering the chamber before each set of measurements. Secondly, any study performed will be too short to reliably assert that changes observed have not been influenced by the evolving effects of hypoxia itself. Thirdly, subjects may find the wearing of a face-mask claustrophobic¹⁴⁷, compromising their breathing pattern and potentially altering blood pH via a respiratory alkalosis.

In this study one hour was required in order for the chamber to reach a FiO_2 of 12%, therefore subjects were exposed to a gradual decline in FiO_2 rather than a sudden drop. Consequently HR did not increase during this one hour period. In addition the subject was free to move around a large experimental space during each protocol. Partly as a result of the detailed attention afforded to subject wellbeing everybody recruited completed their study, despite a total protocol time of nearly five hours.

The results of the *hypoxia/saline* protocol demonstrate that after the hypoxia-equilibration period a steady baseline had been achieved in virtually all physiological variables; a baseline from which the effects of NaNO_2 could be assessed. The only measurement where this was not the case was the IVRT of the right ventricle. However,

this variable is the least established of the three echo surrogates markers used in this study.

3.4.2. Limitations of the physiological measures employed

Ideally this study would have measured pulmonary vascular resistance directly, for example using a Swan-Ganz thermodilution catheter. However, facilities for this were not available in the environmental chamber and its use in healthy volunteers outside of a hospital environment is ethically questionable. Instead three validated surrogate echocardiographic measurements of pulmonary arterial pressure were used.

It should be acknowledged that without invasive measurements it is not possible to be certain that a change in pulmonary arterial pressure equates to a change in pulmonary vascular resistance. For instance, if vascular resistance is constant but cardiac output falls pressure will also reduce. However, in our study the NO_2^- associated reduction in pulmonary arterial pressure was between 12-17%, which was approximately double the reduction in cardiac output observed. This suggests that a vasodilator effect of NO_2^- upon pulmonary vascular resistance was present, although invasive studies are needed to confirm this finding.

Non-invasive assessment of pulmonary arterial pressure using echocardiography has some limitations. An estimation of PASP from the velocity of TR remains the most widely accepted and reproducible marker, but it is limited by a prevalence of regurgitation of only 30 to 70%¹³². In this study TR was detected in just over half of subjects. However the other two markers used, PAT and the right ventricular IVRT, gave similar results with a detection rate approaching 100% and a robust coefficient of variation. The sensitivity of these two markers to demonstrate a difference in this protocol was reliant upon their use in the same subject, at a consistent location within the RV for each measurement to

minimise variance. They are therefore strong research tools but may be of less use in a clinical environment.

Venous strain gauge forearm occlusion plethysmography is a well established technique for measuring systemic arterial blood flow, but the assumption is made that changes observed in a single vascular bed can be generalised to the whole of the systemic vasculature. The test is also strongly influenced by changes in temperature, which alter the flow of blood to the skin, and therefore assiduous control of the experimental environment is needed, as was present in this study. Invasive monitoring of arterial systemic pressure would have been useful, but facilities to perform this were not available in the environmental chamber and its use in healthy volunteers would again have been ethically questionable.

Lastly, the reduction in HR during the *normoxia/NO₂* protocol may have resulted in an unsteady baseline of FBF on which the effects of NaNO₂ were assessed in normoxia. This could have been limited by incorporating a longer relaxation period for each subject before the start of these protocols.

3.4.3. Limitations of the biochemical measures employed

Tri-iodide reagent OBC has been established through a number of studies to be a sensitive and accurate technique to detect plasma [NO₂⁻] and [HbNO]^{55, 138, 140, 148}. Indeed, in this thesis both plasma [NO₂⁻] and [HbNO] provided values sufficiently robust for successful statistical analysis to be employed. In particular, variability in the baseline values of these two NO metabolites in the *hypoxia/NO₂* protocol (i.e. mean ± SD: plasma [NO₂⁻] = 168.6 ± 40.9 and [HbNO] = 47.5 ± 23.1) indicated that adequate power was present to detect, respectively, a 30% & 25% difference between means with a sample size of six.

In contrast to above, the measurement of both plasma and erythrocyte thiol-groups in this thesis provided disappointing results. This finding is consistent with previous reports criticising the ability of tri-iodide reagent OBC to accurately quantify thiol-group concentrations^{76, 77, 149}. One of the principle concerns expressed is that the labile nature of the S-NO bond results in sample degradation either during initial processing or by the addition of sulphanilamide. The results of this thesis are consistent with these concerns as the quantity of liberated NO measured in baseline thiol-group samples were much lower than those previously reported measured using different analytical techniques^{52, 150}.

Furthermore, the concentrations of thiol-groups measured in this thesis were much lower than those of plasma $[\text{NO}_2^-]$ or $[\text{HbNO}]$. Therefore, the inherent “signal noise”, which forms part of the raw output obtained when measuring NO metabolites using OBC, would have formed a larger proportion of the total signal, see Figure 2-8 (page 66). This factor, known as an adverse “signal to noise ratio”, reduces the sensitivity of the assay to detect a difference between low-concentration samples and has previously been reported by this laboratory⁹⁶.

One alternative method used to measure thiol-group concentration is photolysis-based chemiluminescence, a process whereby light is used to cleave the S-NO bond instead of a chemical reagent. Previous studies using this assay have shown significant differences in thiol-group concentrations during transit across a single vascular bed⁶⁰. However, authors using this methodology tend to report a much greater basal concentrations of thiol-groups than those found in the current study⁷⁷.

In summary, the use of tri-iodide reagent OBC in this thesis to measure blood NO metabolites provided a robust measure of both plasma $[\text{NO}_2^-]$ and $[\text{HbNO}]$. However, in keeping with previous reports in the literature, thiol-groups could not be measured with

the same degree of confidence and therefore their significance in this model could not be commented on further.

3.4.4. The effect of hypoxia upon blood NO metabolites

During the hypoxia-equilibration period [HbNO] increased. This is due to Hb possessing a greater number of free haem-binding sites as SaO₂ decreases⁵⁵. It would also be expected that plasma [NO₂⁻] would decrease in this situation if simple reappportionment of blood NO metabolites was occurring, (see section 1.4.4; page 18). However, plasma [NO₂⁻] did not alter during the hypoxia-equilibration period. Indeed, a transient rise compared to “baseline” was present at “protocol time 30 min”. These findings taken together suggest an additional factor is controlling plasma [NO₂⁻] and [HbNO] levels during acute exposure to hypoxia. It is likely that a balance is present between the increased formation of plasma [NO₂⁻] and [HbNO] as a product of endothelial NO production and the reappportionment of NO metabolites into the erythrocyte as O₂ levels falls.

Other groups have previously reported that plasma [NO₂⁻] does not alter after six hours of exposure to FiO₂ 12%¹⁴². However, one study¹⁵¹ has shown that long term residents at high altitude (Tibetans, 4,200m) have a ten-fold greater plasma [NO₂⁻] than lowland dwellers (USA residents, 200m). The authors of this study propose that this increased plasma [NO₂⁻] is the mechanism by which Tibetans are adapted to life at high-altitude.

3.4.5. The enhanced vasodilator effects of NaNO₂ in hypoxia

A systemic, intravenous, infusion NaNO₂ resulted in a vasodilator effect in hypoxia which was not present when the same infusion regime was given in normoxia. Importantly, only a small rise in plasma [NO₂⁻] occurred as a result of the single low-dose

infusion regime given. The approximate doubling in systemic plasma $[\text{NO}_2^-]$ present in this study is similar to the increase observed in man following maximal stimulation of the endothelium by ACh⁸⁷.

As would be expected, the vasodilator activity of NaNO_2 resulted in an increase in FBF (arteriodilation), a decrease in cardiac output (venodilation causing a decrease in stroke volume) and no change in HR. Unexpectedly, however, an increase in peripheral systolic blood pressure was also present. A possible explanation why systolic blood pressure did not fall would be that there was peripheral pressure amplification present. In healthy young subjects the peripheral blood pressure is greater than the central blood pressure, due to its augmentation by the backward reflections of systolic arterial pulse waves traveling at a relatively slow velocity through a compliant vascular tree¹⁵². This effect is exaggerated by the administration of a vasodilator¹⁵³, which further slows the reflected pulse wave. In this study, brachial sphygmomanometry may have recorded augmented peripheral pressure, when central pressure might have fallen or remained constant.

Despite the observation that NaNO_2 has an enhanced vasodilator effect in hypoxia, three features of this study suggest that the mechanism by which this occurred is not consistent with the deoxy-Hb theory of NO_2^- reduction.

Firstly the most compelling data is that the profiles of plasma $[\text{NO}_2^-]$ following NaNO_2 infusion were similar in both hypoxia and normoxia. According to this theory NO_2^- should enter the deoxygenated erythrocyte preferentially to generate vasodilatory NO and HbNO. It would therefore be expected that plasma $[\text{NO}_2^-]$ would achieve a lower maximum and have a shorter half-life when infused in hypoxia compared to normoxia. However, the similar profiles of plasma $[\text{NO}_2^-]$ reported in this thesis suggest that NO_2^- entry into the erythrocyte and absorption by surrounding tissue is unchanged in hypoxia

compared to normoxia, despite the presence of a vasodilator effect in the former environment.

Secondly the changes in [HbNO] across the *hypoxia/NO₂⁻* protocol were not temporally matched with the vasodilator effects of NO₂⁻ observed. Previously, increases in [HbNO] associated with concomitant physiological changes have been used by proponents of the deoxy-Hb theory of NO₂⁻ reduction as evidence for its validity⁸⁸. However, this thesis demonstrates that [HbNO] is not an appropriate index of NO₂⁻ associated vasodilator activity. This finding does not negate the deoxy-Hb theory of NO₂⁻ reduction, as it is free NO rather than HbNO which is important for biological activity. However it does suggest a limited role of Hb-mediated NO generation in the vasodilator effect of NO₂⁻.

Thirdly, the persistence of a vasodilator effect of NaNO₂ in the pulmonary vascular bed at a time when both [HbNO] and plasma [NO₂⁻] had returned back to pre-infusion levels is again inconsistent with this theory.

Therefore, the results of the present study suggest that alternative mechanisms are responsible for the bioactivity of low-dose NaNO₂ in hypoxia.

3.4.6. Potential mechanisms for the biological activity of NaNO_2

Figure 3-16 (page 115) summarises two potential mechanisms responsible for the enhanced bioactivity of NaNO_2 in hypoxia. It should also be acknowledged that a component of NaNO_2 associated hypoxic-vasodilator activity is both NO-independent and indomethacin-labile⁸⁴, though little is known regarding this potential route of action.

3.4.6.1. Tissue-based reductase activity

One possible mechanism which recent in-vitro work has proposed is that NO_2^- reduction at a tissue level is the major source of bioactive NO resulting from its supplementation^{154, 155}. Several tissue NO_2^- reductases have been suggested, including myoglobin, XO, eNOS and aldehyde dehydrogenase^{93, 156, 157}, all of which exhibit enhanced NO_2^- reducing capacity in hypoxia. This theory is supported by the observation that, as a small anion, NO_2^- is capable of rapidly equilibrating across the entire fluid volume of the body⁴³ (i.e. the intra-vascular, extra-vascular and intra-cellular spaces). Therefore, any NO_2^- entering the circulation will rapidly become available to enzymes within the vessel wall. In contrast, the same cannot be said for the transit of NO_2^- across the erythrocyte membrane, which is slow especially at concentrations of less than 400nM (data from this laboratory, manuscript currently in preparation).

Furthermore, in keeping with a tissue based mechanism of NO_2^- reduction, the prolonged effect of NaNO_2 observed in the pulmonary vasculature may be due to the lower O_2 levels present in the pulmonary arteries compared to the systemic arterial circulation. Therefore, pulmonary tissue enzymes would have been primed by a greater degree of hypoxia than those in the systemic arterial circulation; resulting in an enhanced and potentially prolonged vasodilator effect observed following administration of the same dose of NaNO_2 .

Unfortunately this in-vivo observation was not repeated in the isolated vessel model. This model was designed following previous publications which demonstrate that at high doses of NaNO_2 veins are more responsive than arteries⁸⁹. In the present study, the vasodilator effect of NaNO_2 , whilst being enhanced by hypoxia, was more pronounced in the AA rather than the PA. However a number of differences between these two systems exist. Firstly, the in-vitro model is blood independent. Secondly, it is necessary to use a much larger dose of NaNO_2 in an in-vitro isolated vessel model in order to see a vasodilator effect of NaNO_2 than it is in-vivo. Also, capacitance rather than resistance vessels are used. These vessels are not directly responsible for the control of vascular resistance¹⁴⁶, and correspondingly they may behave in a different manner. Lastly the degree of hypoxia present in the in-vitro model was much greater than that achieved in our subjects in the chamber.

3.4.6.2. An intermediate molecule

A second potential mechanism is that stable, intermediate, metabolites of NO_2^- in blood is responsible for its vascular activity. These include erythrocyte-associated NO_2^- -mediated ATP release¹⁵⁸ and N_2O_3 ¹⁵⁹. SNO groups have also been proposed as this intermediate¹⁶⁰, and it has been shown that a transient increase in plasma $[\text{NO}_2^-]$ increases their population⁹⁵. However, as previously explained, we were unable to detect a change in plasma or erythrocyte SNO levels in this study due to the limitations of the biochemical assay employed.

In summary the data provided in this thesis strongly suggests that a differential metabolism of NO_2^- at a tissue level is the key behind the enhanced vasodilator activity of NaNO_2 in hypoxia.

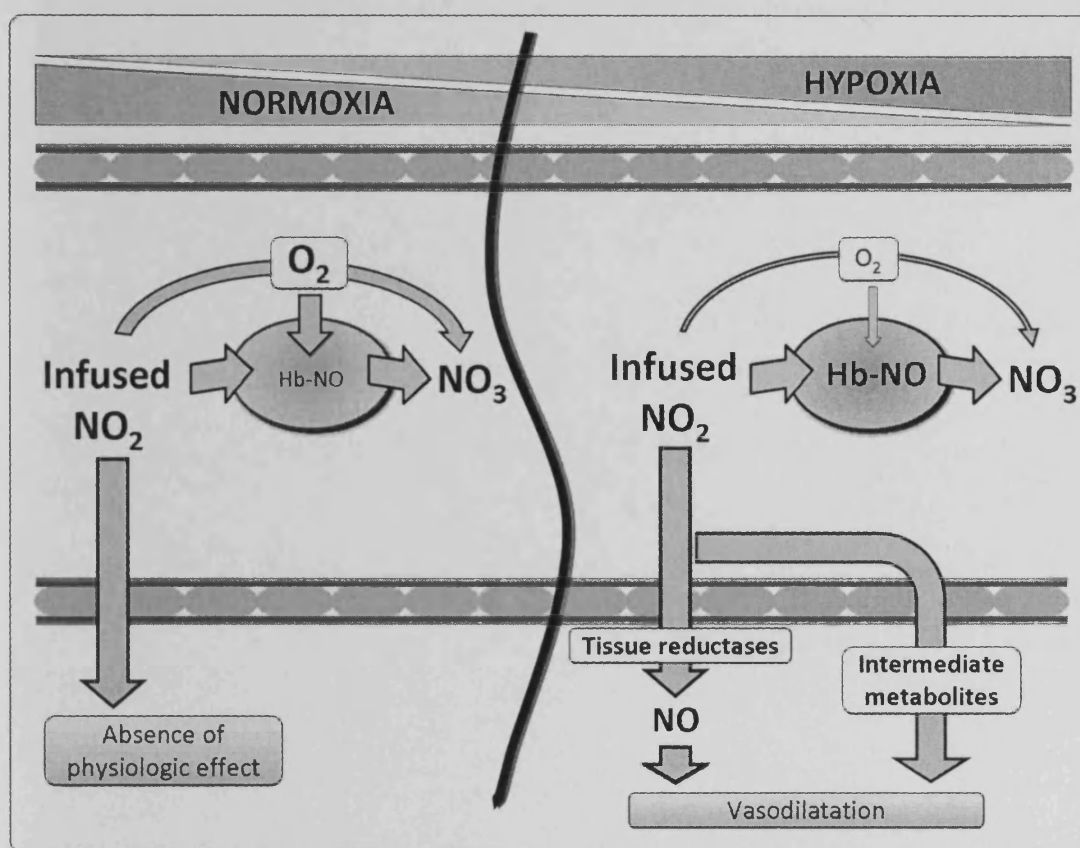


Figure 3-16: Diagram of the potential mechanisms responsible for the metabolism of $NaNO_2$ in normoxia (left) and hypoxia (right). Note that NO_3 levels may be marginally lower in hypoxia compared to normoxia, however the change (nmol) would be outside of the detectable range of plasma NO_3 possible with OBC (mmol).

3.5. Chapter summary

- 1. In man, NaNO_2 has an enhanced vasodilator effect upon both the systemic and pulmonary circulations when given in hypoxia compared to normoxia.**
- 2. The pharmacokinetic profiles of NaNO_2 are the same whether it is given in hypoxia or normoxia.**
- 3. The vasodilator action of NaNO_2 in hypoxia does not have a temporal associated with the concentration of $[\text{HbNO}]$.**
- 4. The vasodilator effect of NaNO_2 in the hypoxic pulmonary vasculature is independent of an elevated plasma $[\text{NO}_2]$ level.**
- 5. Points 2, 3 & 4 are all supportive of an alternative mechanism of hypoxia-associated enhanced NaNO_2 activity than the deoxy-Hb theory of NO_2^- reduction. Possible routes include tissue-based reduction of NO_2^- or the formation of an intermediate molecule.**

Chapter 4: Nitrite and Ischaemia

4.1. Introduction

4.1.1. A historical perspective of NO_2^- as an anti-anginal agent

The earliest account of the use of NO_2^- as an anti-anginal agent is in a Chinese medical manuscript from the 8th Century AD¹⁶¹. This document details the ingestion of potassium NO_3^- , which in itself possesses no vasodilator properties, as a treatment for angina. However, the author specifically requests that the recipient '*hold the medicine under their tongue and swallow the saliva*'; a phenomenon now known to facilitate oral-bacteria mediated reduction of NO_3^- to NO_2^- , (see section 1.4.5; page 20).

More recently, publications from the 19th century demonstrate that NO_2^- had become a popular means of treating angina¹⁶² as its stable chemical structure allowed for cheap preparation and easy storage¹⁶³. However, the effects were slow and unpredictable and so NO_2^- fell out of favour as faster-acting agents such as organic nitrates became available¹⁶⁴.

Common to all of these early accounts was the use of high-doses of NO_2^- , a treatment regime which can result in vascular collapse and syncope in the recipient¹⁶⁵. However, as chapter 3 of this thesis demonstrates, NaNO_2 is a preferential vasodilator in hypoxia. Therefore NaNO_2 could potentially be an anti-ischaemic agent at much lower doses than were used historically. This would be an important finding for two reasons. Firstly, it would prove that NaNO_2 is a targeted vasodilator. Secondly, and of greater practical importance, the administration of NaNO_2 at these doses would be without the side effects of systemic vasodilatation associated with the use of organic nitrates¹⁶⁶.

4.1.2. Quantification of ischaemia by myocardial tissue Doppler imaging

The longitudinal fibres of the myocardium are responsible for long-axis left-ventricular function¹⁶⁷. They are predominantly located in the sub-endocardium and are therefore situated further away from the conduit epicardial coronary arteries than the rest of the myocardium. In addition, the sub-endocardium is under an increased pressure load during systole when compared to the remainder of the myocardial wall, as it lies immediately adjacent to the non-compressible blood volume of the intra-ventricular cavity. Both of these factors serve to create a watershed area for ischaemia in the sub-endocardial region¹⁶⁸, with myocardial long axis function falling progressively from 5 seconds after the onset of ischaemia¹⁶⁹.

Exertional myocardial ischaemia, resulting from an imbalance between myocardial blood supply and cardiac workload, will therefore cause a reduction in myocardial wall systolic velocities¹⁶⁹. Furthermore, the measurement of myocardial wall PSV using tissue Doppler echocardiography can be used to identify patients with significant coronary artery disease during DSE¹⁴⁵.

In summary tissue Doppler imaging of acute changes in systolic myocardial wall velocities (in particular PSV) obtained at the time of DSE is a previously validated means by which cardiac function can be quantified and myocardial ischaemia identified.

4.1.3. Aims of this chapter

The study in this chapter was designed to quantify regional myocardial function during a DSE in subjects with known inducible myocardial ischaemia. Subjects underwent two separate studies, each conducted double-blind. On one occasion a low-dose iv infusion of NaNO_2 was administered, one shown in chapter 3 of this thesis to be physiologically inert when infused in normoxia. On the other visit a matched 0.9% saline (placebo) infusion was given. Regional cardiac function at different HR was quantified during each study, using tissue Doppler imaging of myocardial basal-wall PSV. Then, following unblinding of the study, PSV was compared between treatments and different myocardial basal-wall segments to see if an anti-ischaemic effect of NaNO_2 was evident.

4.1.4. Original Hypothesis

- 1. In subjects with known inducible cardiac ischaemia the administration of iv NaNO_2 * during dobutamine stress echocardiography will allow the heart to perform more work prior to the onset of angina than a matched placebo infusion given in the same environment.**

*** delivered at a dose known not to vasodilate in normoxia**

4.2. Study design

A placebo-controlled double-blinded cross-over DSE study was performed to assess the effects of NaNO₂ upon cardiac function in patients with established coronary ischaemia, as shown in Figure 4-1, (page 121). The recruitment criteria and pre-study requirements are detailed in section 2.2.2 (page 53).

All subjects underwent two separate DSE examinations, separated by at least two days (mean average time between studies = 10 days). The protocol for each visit was the same apart from the double-blind administration of a different study infusion (i.e. an iv infusion of either NaNO₂ or 0.9% saline). The dose of NaNO₂ given was identical to that used in chapter 3, however it was administered at a slightly faster rate to complement the protocols performed in chapter 5. Randomisation was performed by the clinical trials division of the pharmacy department of the University Hospital of Wales, Cardiff.

Prior to each DSE study subjects had an iv cannula placed into both ante-cubital fossae. The study infusion was given into the dominant arm whilst the non-dominant arm received the dobutamine infusion. The study infusion was started ten minutes before the dobutamine infusion protocol and continued for twenty minutes in total. This regime was chosen as it was anticipated that each DSE study would last for at least ten minutes, therefore resulting in subjects achieving peak plasma [NO₂⁻] levels at the same time as peak-dose dobutamine was being administered. Baseline images were obtained immediately prior to the beginning of the study infusion. At this, and each subsequent DSE protocol stage, the myocardial longitudinal velocity profile was recorded in the basal-wall segments of six different LV walls (BL, BS, BA, BI, BAS, BPost); a process detailed further in section 2.13 (page 71). During subsequent off-line analysis, with the interpreter still blinded to the infusion received, the PSV and its associated HR in each myocardial basal-wall segment was measured. The interpreter was then un-blinded.

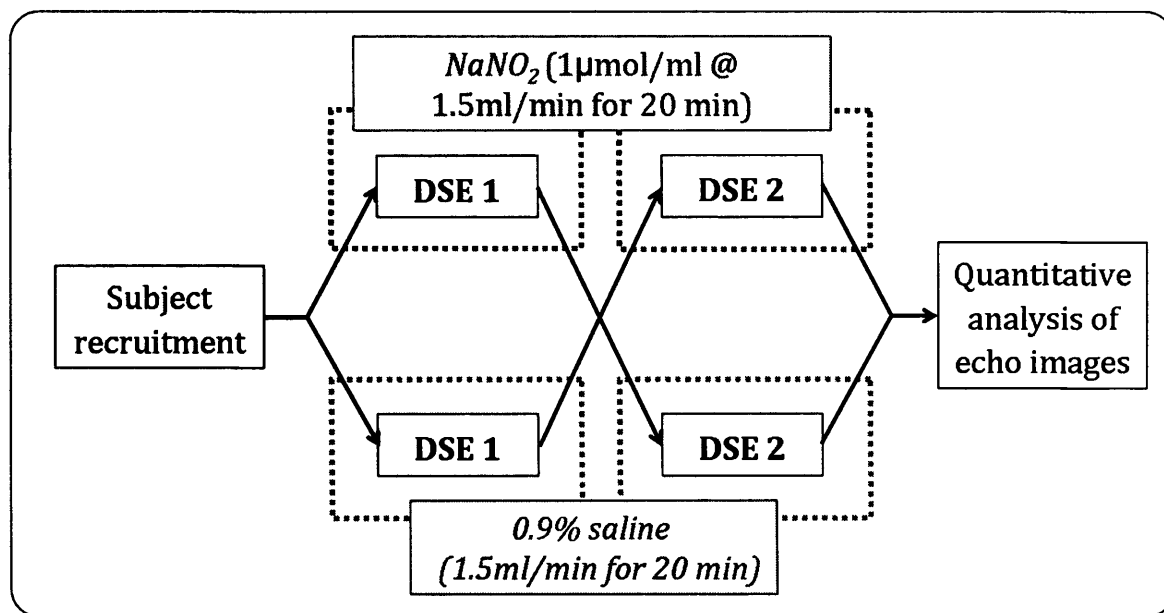


Figure 4-1: Design of the double-blinded placebo-controlled DSE study performed in chapter 4.

4.2.1. Data analysis

Once un-blinded, the two original study data-sets (i.e. *NaNO₂* and *saline*) were divided into different groups in a series of separate analyses. The data was split in order that both *ischaemic* and *control* (non-ischaemic) myocardial walls could be identified; therefore resulting in four key groups of basal-wall segments for comparison: *ischaemia/saline*, *ischaemia/NaNO₂*, *control/saline*, *control/NaNO₂*. Four separate analyses of the overall data-set were undertaken: whole myocardial analysis, angiography-directed analysis, top and bottom halves analysis and upper and lower tertiles analysis. The latter three of these analyses employed different techniques to allocate *ischaemic* and *control* myocardial walls. Figure 4-2 (page 122) is a summary diagram of how the overall data-set was used to perform these different analyses.

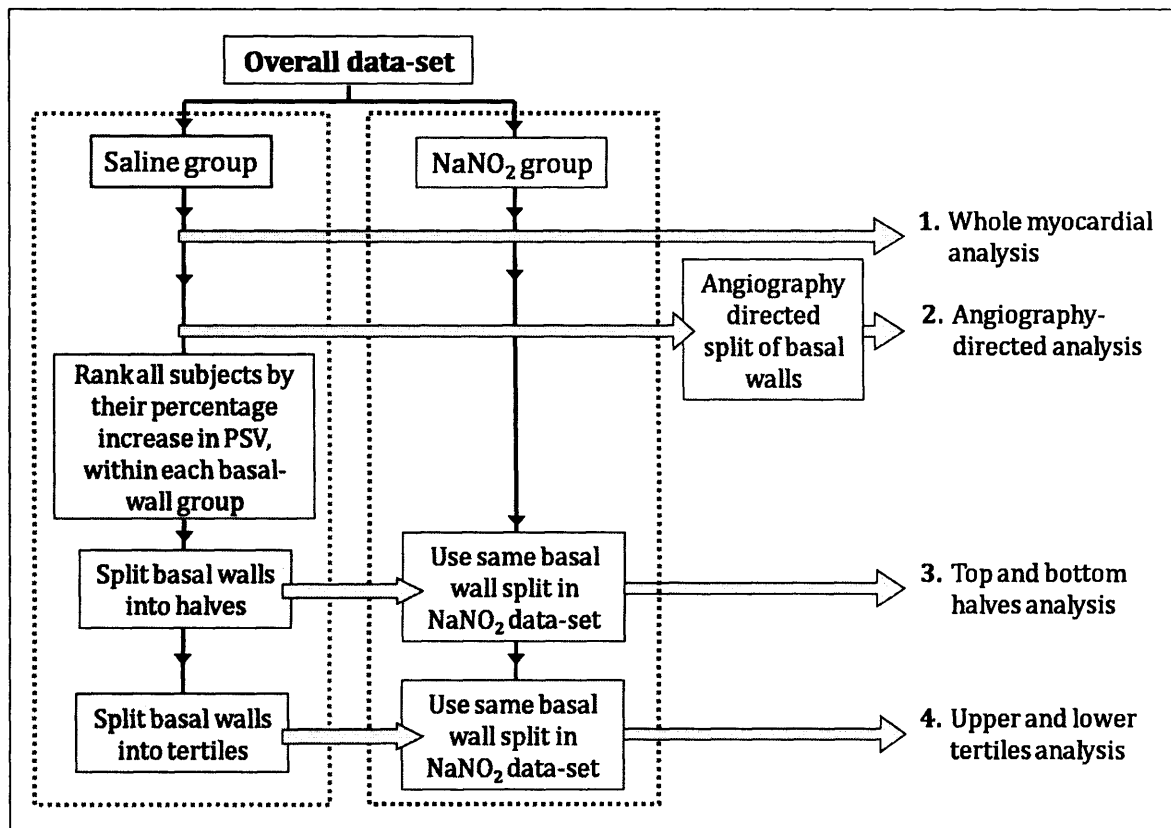


Figure 4-2: Summary flow diagram of the analyses applied to the overall data-set to allow specific interpretation of both ischaemic and control regions of myocardium.

4.2.1.1. Whole myocardial analysis

The first analysis included data from all myocardial basal-wall segments, split only into two groups depending upon the study infusion received (i.e. NaNO₂ or saline). Here the response in both *ischaemic* and *control* myocardial walls was pooled within each group to see if a gross effect of NaNO₂ on whole myocardial function was present.

4.2.1.2. Angiography-directed analysis

Established criteria¹⁴⁵ were used to focus analysis upon the myocardial basal-wall segments most likely to be subtended by the subject's stenosed coronary artery or arteries; which had previously been ascertained by coronary angiography. The BA wall was measured where disease to the left anterior descending (LAD) coronary artery was present, the BI wall with right coronary artery (RCA) disease and the BPost wall with circumflex (Cx) coronary artery disease. A control basal-wall segment was also selected, from a region of myocardium supplied by a non-stenosed coronary artery. Consequently only one *ischaemic* and one *control* myocardial basal-wall segment was identified from each subject.

4.2.1.3. Top and bottom halves analysis

The above analysis, whilst being highly specific to the identification of ischaemic myocardial walls, ignored a large pool of data obtained from other potentially ischaemic basal-wall segments. A third analysis was therefore performed to stratify and assess all of the myocardial basal-wall segments in the overall data-set.

The first stage of this analysis required additional examination of the saline data-set. This data-set represented the results of a standard DSE performed in each subject, i.e. one without an active study intervention. Therefore, in the saline data-set only, the percentage increase of absolute PSV from baseline to peak-dose dobutamine was calculated for each basal-wall segment of each subject. It has previously been reported that the average percentage increase, compared to baseline, in a healthy myocardial basal-wall segment at peak-dose dobutamine is about 100%. This is opposed to the average percentage increase in ischaemic myocardial walls being approximately 50-75%¹⁴⁵. It therefore follows that, in a study population which contains ischaemic myocardial walls,

the range of percentage increases in myocardial basal-wall segment PSV between baseline and peak-dose dobutamine most likely represents a continuum. At one end of this scale will lie the basal-wall segments of the most ischaemic myocardial walls (i.e. those with the lowest percentage increase in PSV) and at the other end of the scale the least ischaemic myocardial walls' basal-wall segments (i.e. those with the greatest percentage increase in PSV).

Therefore, within each of the six myocardial basal-wall segment categories (e.g. BS), subjects were ranked according to their percentage increase in absolute PSV between baseline and peak-dose dobutamine (in the saline study data-set). An example of this process can be seen in Table 4-4 (page 130). Following on from this ranking (within each basal-wall segment category) the data was split into those subjects' myocardial walls which were in the top half of responders (i.e. *control* walls) and those in the bottom half of responders (i.e. *ischaemic* walls). This resulted in four different groups of data: *ischaemia/saline*, *ischaemia/NaNO₂*, *control/saline*, *control/NaNO₂*. Importantly, this process of data analysis ensured that the groups of myocardial basal-wall segments labelled as *ischaemic* was not biased towards the inclusion of a particular category of basal-wall segment.

4.2.1.4. Upper and lower tertile analysis

This analysis employed the same ranking of subjects, within each of the six myocardial basal-wall segment categories, as outlined above. However, this time subjects' myocardial basal-wall segments were split into tertiles within each category of basal-wall segment. The lower tertile represented the *ischaemic* group and the upper tertile the *control* group. The middle tertile was not included in this analysis.

4.3. Results

4.3.1. Demographic data and clinical characteristics

The summary demographics and clinical characteristics of the subjects recruited to participate in chapter 4 are shown in Table 4-1 (below).

Variable	
Number	10
Age (years)	56.2 ± 4.2
Gender (male/female)	5/5
Weight (kg)	89.6 ± 5.3
BMI	30.9 ± 1.3
Cardiac disease profile:	
1 VD	7/10
2 VD	3/10
Left ventricular ejection fraction (%)	55.6 ± 2.0
Cardiovascular risk factors:	
Hypercholesterolaemia	10/10
(total cholesterol (mmol/l))	5.4 ± 0.5
Diabetes mellitus	4/10
Hypertension	6/10
Family history of premature IHD	3/10
Smoker (current or within the last 3 months)	4/10
Medication:	
Aspirin	10/10
Statin	10/10
Beta-blocker	7/10
Long acting nitrate	4/10
Calcium channel blocker	4/10
Clopidogrel	1/10
Nifedipine	1/10

Table 4-1: Demographics and clinical characteristics of the subjects who participated in chapter 4. 1VD = single vessel coronary disease, 2VD = two vessel coronary disease. Left ventricular ejection fraction was measured using the biplane Simpson's method.

4.3.2. Anatomical details of subject coronary vasculature

Digital quantitative coronary angiography was used to assess the coronary anatomy of each subject prior to recruitment. Summary details of the coronary arteries responsible for the inducible myocardial ischaemia present in each subject are shown in Table 4-2 (below).

Diameter stenosis (%)	Area stenosis (%)	MLD (mm)
81.8 ± 4.4	93.9 ± 1.9	0.52 ± 0.16

Table 4-2: Angiographic summary data of the index coronary artery stenoses. Thirteen lesions were present (ten subjects; seven with single vessel disease (1VD) and three with two vessel disease (2VD)). Lesion breakdown by individual coronary artery: LAD = 5, Cx = 3 and RCA = 5. MLD (minimal luminal diameter).

4.3.3. Example individual data-set

Figure 4-3 (page 128) and Table 4-3 (page 129) show a typical data-set obtained from a subject who had a 95% stenosis of the proximal LAD coronary artery. Data is presented as a series of scatter-plot graphs with change in HR (Δ HR) on the x axis and change in PSV (Δ PSV) on the y axis (each value is compared to the baseline reading taken from the same basal-wall segment). Six graphs are shown, each relating to a separate myocardial wall. Both NaNO_2 and saline studies are represented within each graph by a series of points; each an x/y plot of Δ HR and its corresponding Δ PSV at a different DSE protocol stage. The relationship between PSV and dobutamine-dose during a DSE examination in healthy human subjects has previously been stated to be linear¹⁶⁷. Therefore a linear regression analysis of the points within individual DSE studies (i.e. NaNO_2 or saline) is also displayed on each graph. The gradients of these twelve linear regression lines can be found in Table 4-3 (page 129).

The calculations performed in this subject to help identify whether a myocardial wall was *ischaemic* or *control* are also shown in Table 4-3 (page 129). Baseline and peak-dose dobutamine absolute PSV values from each basal-wall segment in the saline data-set are displayed, together with the percentage increase in PSV between these two time-points. The same analysis is performed in all subjects; the results are then pooled and grouped according to basal-wall segment category (e.g. BL). Within these groups subjects are ranked according to the percentage increase in PSV recorded, see Table 4-4 (page 130) for an example of this process performed in the BL wall. According to this ranking each myocardial basal-wall segment group is split into either halves or tertiles for identification of the different *ischaemia* and *control* groups used in analyses 3 and 4 respectively.

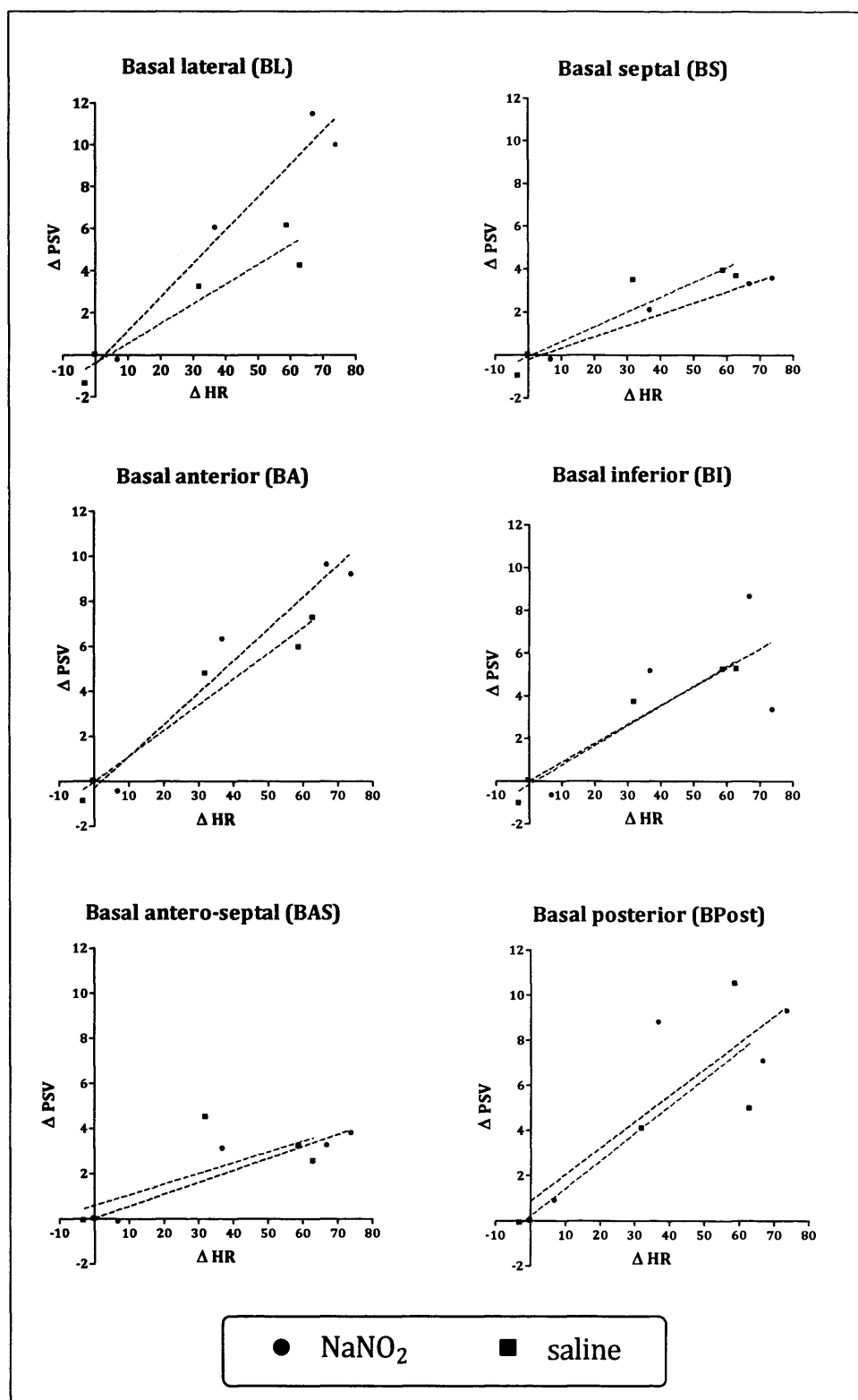


Figure 4-3: An example data-set taken from an individual subject. Each of the six graphs displayed is of a different myocardial wall category. The response of ΔPSV to ΔHR during both of the DSE studies performed (i.e. $NaNO_2$ and saline) are plotted separately on each graph together with their associated mean linear regression analysis lines.

	Saline study				NaNO ₂ study
Myocardial wall segment	Baseline PSV (cm/s)	Peak-dose dobutamine PSV (cm/s)	% Increase in PSV	Linear regression gradient	Linear regression gradient
BL	6.61	10.84	64	0.093	0.159
BS	6.09	10.03	65	0.069	0.052
BA	6.61	13.88	110	0.110	0.142
BI	6.62	11.87	79	0.093	0.089
BAS	4.81	7.33	53	0.048	0.053
BPost	4.84	9.80	103	0.120	0.120
P	P	P	P	P	P

Table 4-3: Analysis of each basal-wall segment of the subject outlined in Figure 4-3 (page 128). The absolute baseline PSV and peak-dose dobutamine PSV are displayed, together with percentage increase in absolute PSV which occurs between these two time-points. This data is used to rank the responses of all subjects within each category of basal-wall segment and then to identify myocardial walls as either ischaemic or control; see Table 4-4 (page 130). The twelve individual linear regression analyses gradients measured in Figure 4-3 are also shown.

Subject number	Percentage increase in PSV from baseline to peak-dose dobutamine in the saline data-set
05	185
10	167
09	167
03	105
06	102
01	95
11	92
08	67
02	64
07	47

Table 4-4: *The ranking of subjects' individual basal-wall segments within the BL basal-wall segment category. Those basal-wall segments which lie in the upper and lower tertiles are shaded and the dotted line delineates the boundary between the top half and the bottom half of results. This same process was performed for all six basal-wall segment categories. Those basal-wall segments identified as belonging to a specific tertile/half within each category were then pooled for use in analyses 3 & 4. The subject presented previously in this section is highlighted (subject number = 02).*

4.3.4. Study haemodynamics

Table 4-5 (below) and Figure 4-4 (page 132) show the summary haemodynamic characteristics of the two sets of DSE studies performed. The majority of DSE studies were stopped due to the onset of typical anginal symptoms and patient request; apart from five studies where the full protocol was completed. No significant adverse events happened during any study. There were two cases of transient bradycardia at peak dose-dobutamine, both occurring in the saline DSE study of subjects with 2VD. It is possible that these two events were due to an increase in vagal tone resulting from ischaemia-derived stimulation of myocardial mechano-receptors.

DSE protocol stage	NaNO ₂ study	N	Saline study	N	p value
Baseline	66 ± 2	10	73 ± 4	10	ns
5 µg/kg/min	66 ± 2	10	72 ± 5	10	ns
10 µg/kg/min	79 ± 5	10	85 ± 7	10	ns
20 µg/kg/min	105 ± 6	10	107 ± 7	10	ns
30 µg/kg/min	117 ± 5	9	120 ± 7	9	ns
40 µg/kg/min	119 ± 12	3	127 ± 2	2	n/a
+ 3 min	102 ± 6	10	101 ± 7	10	ns
+ 15 min	76 ± 2	10	80 ± 4	10	ns

Table 4-5: The HR profile in each group of DSE studies. N = number of subjects who achieved this stage. Between-groups statistical analysis was performed within individual stages using an unpaired t-test.

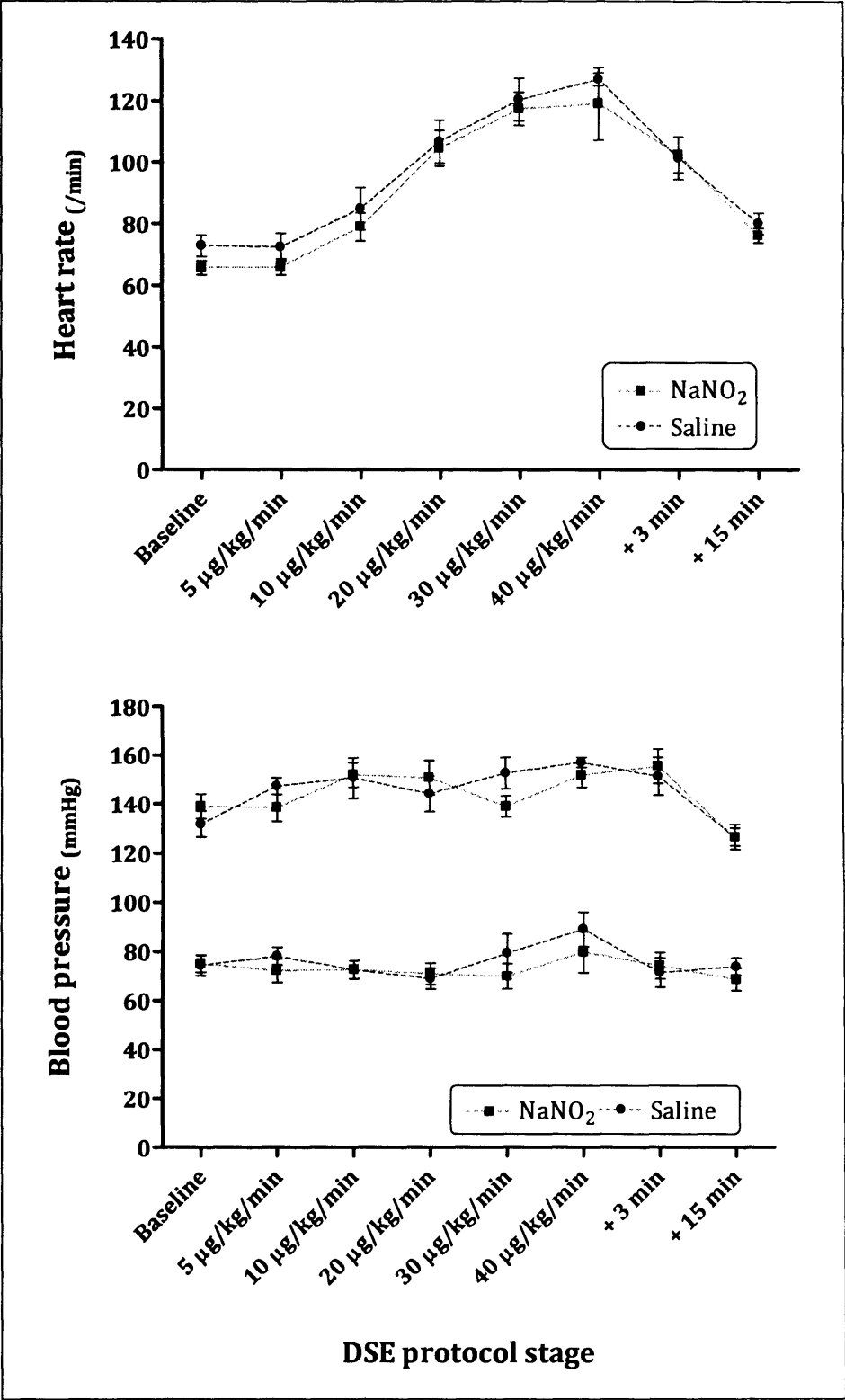


Figure 4-4: HR profile (top) and systolic/diastolic blood pressure profiles (bottom) in both sets of DSE studies. Note that only two subjects (saline group) and three subjects (NaNO₂ group) reached the highest level of dobutamine infusion.

4.3.5. The effect of NaNO_2 upon PSV in ischaemic and control myocardium

Data from 55 of 60 potential (six walls in ten subjects) myocardial walls were of sufficient quality to analyse their basal-wall PSV throughout each DSE study. Four separate analyses of the overall data-set were performed, as outlined previously in section 4.2.1 (page 121). Three of these analyses employed different criteria to separate myocardial basal-wall segments into either *ischaemic* or *control* groups, thus splitting the data into four groups for comparison (i.e. *ischaemia/saline*, *ischaemia/ NaNO_2* , *control/saline* and *control/ NaNO_2*).

Each analysis consists of a scatter-plot graph of the pooled data. The mean linear regression gradient, its associated 95% CI and R^2 value for each group are also shown. Two different sets of variables are used for statistical comparison between groups. Firstly, the *individual linear regression gradients* measured in each myocardial wall (averaged within each grouping) are compared (see example data-set in Table 4-3; page 129). Secondly, the values of $\Delta\text{PSV}/\Delta\text{HR}$ at *peak-dose dobutamine* measured in each myocardial basal-wall segment are also compared. A repeated-measures ANOVA with Newman-Keuls post-test was used to compare the difference in all cases unless only two groups of data were present, when a unpaired t-test was used.

4.3.5.1. Whole myocardial analysis

An x/y scatter-plot of the relationship between ΔHR and ΔPSV in all basal-wall segments of the *saline* and *NaNO₂* data-sets is shown in Figure 4-5 (page 135). Table 4-6 (page 136) summarises the outputs of linear regression analyses of these scatter-plots. Each of the two groups analysed contained data from 55 basal-wall segments.

There was an approximate 10% difference in the mean linear regression gradient between the *saline* (0.091) and *NaNO₂* (0.105) groups, but a large overlap was present between their respective 95% CI.

Between-groups statistical analysis is shown in Figure 4-6 (page 136). Comparison of the *individual linear regression gradient* data demonstrated no difference between the two groups (i.e. *saline* = 0.12 ± 0.01 vs *NaNO₂* = 0.13 ± 0.01 ; $p > 0.05$). In addition, no difference was present with analysis of the $\Delta PSV/\Delta HR$ at *peak-dose dobutamine* data (i.e. *saline* = $7.3 \pm 0.6 \text{ cm/s/s}$ vs *NaNO₂* = $8.1 \pm 0.5 \text{ cm/s/s}$; $p > 0.05$).

In summary, analysis of this data-set provided no clear evidence of an influence of *NaNO₂* upon whole myocardial function. However, linear regression analysis of the data did suggest that a difference between the *NaNO₂* and the *saline* groups may be present.

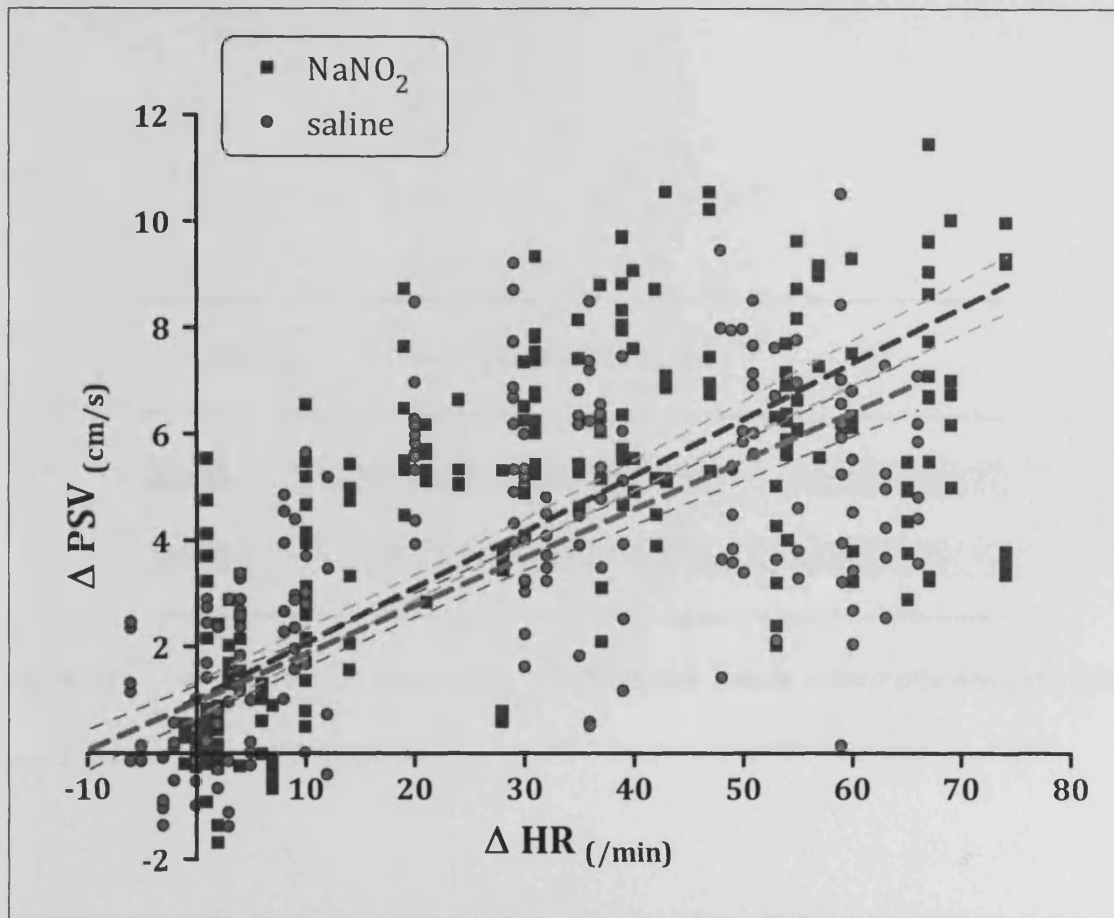


Figure 4-5: A scatter-plot graph of ΔPSV and ΔHR in the 'whole myocardial analysis' data-set. The mean linear regression lines of the two data-sets, together with their respective 95% CI, are also displayed. Each of the two groups plotted contains data from all of the 55 walls contained in the overall data-set.

Group	Mean gradient (95% CI)	R ²
NaNO ₂	0.105 (0.096 – 0.115)	.61
Saline	0.091 (0.081 – 0.101)	.55

Table 4-6: Linear regression analysis outputs from the 'whole myocardial analysis' data-set; shown in Figure 4-5 (page 135).

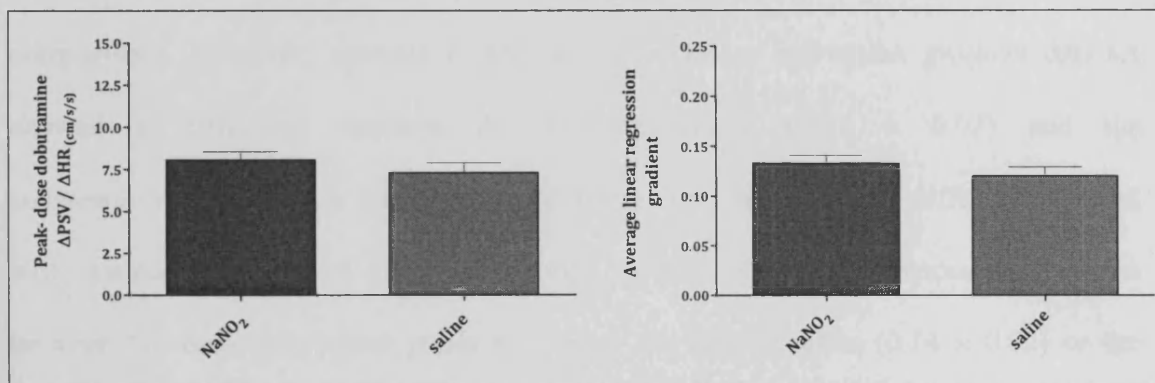


Figure 4-6: Between-group comparison of the 'whole myocardial analysis' data-set. $\Delta\text{PSV}/\Delta\text{HR}$ at peak-dose dobutamine data (left) and averaged individual wall linear regression gradient data (right). No significant results were present.

4.3.5.2. Angiography-directed analysis

Scatter-plot graphical representations of the relationship between Δ PSV and Δ HR in the '*angiography-directed analysis*' data-set are shown in Figure 4-7 (page 138); with the outputs from linear regression analyses of these plots summarised in Table 4-7 (page 139). Ten basal-wall segments were included in each of the four groups analysed.

There was an approximate 25% difference between the mean linear regression gradients of the *ischaemia/NaNO₂* (0.119) and *ischaemia/saline* (0.092) groups; however their respective 95% CI overlapped. The mean linear regression gradients in the control groups were of values between those measured in the two ischaemia groups, (*control/NaNO₂* = 0.103, *control/saline* = 0.112).

Between-groups statistical comparisons of this data-set are shown in Figure 4-8 (page 139). No differences were present within the Δ PSV/ Δ HR at peak-dose dobutamine analysis (i.e. *ischaemia/saline* = 7.0 ± 1.2 cm/s/s vs. *ischaemia/NaNO₂* = 8.6 ± 1.2 cm/s/s, *control/saline* = 9.9 ± 1.5 cm/s/s and *control/NaNO₂* = 7.8 ± 1.0 cm/s/s; $p > 0.05$ for each comparison). However, analysis of the *individual linear regression gradient* data-set showed a difference between the *ischaemia/saline* (0.11 ± 0.02) and the *ischaemia/NaNO₂* (0.15 ± 0.02) groups ($p < 0.05$). This was the only difference present with statistical analysis of these four groups, in particular no differences were shown between the *ischaemia/saline* group and either the *control/saline* (0.14 ± 0.02) or the *control/NaNO₂* (0.13 ± 0.02) groups.

In summary, in this focused data-set of myocardial basal-wall segments which had been selected by coronary angiography to be highly likely to exhibit features of inducible ischaemia, evidence was present that low-dose NaNO₂ was acting as an anti-ischaemic agent.

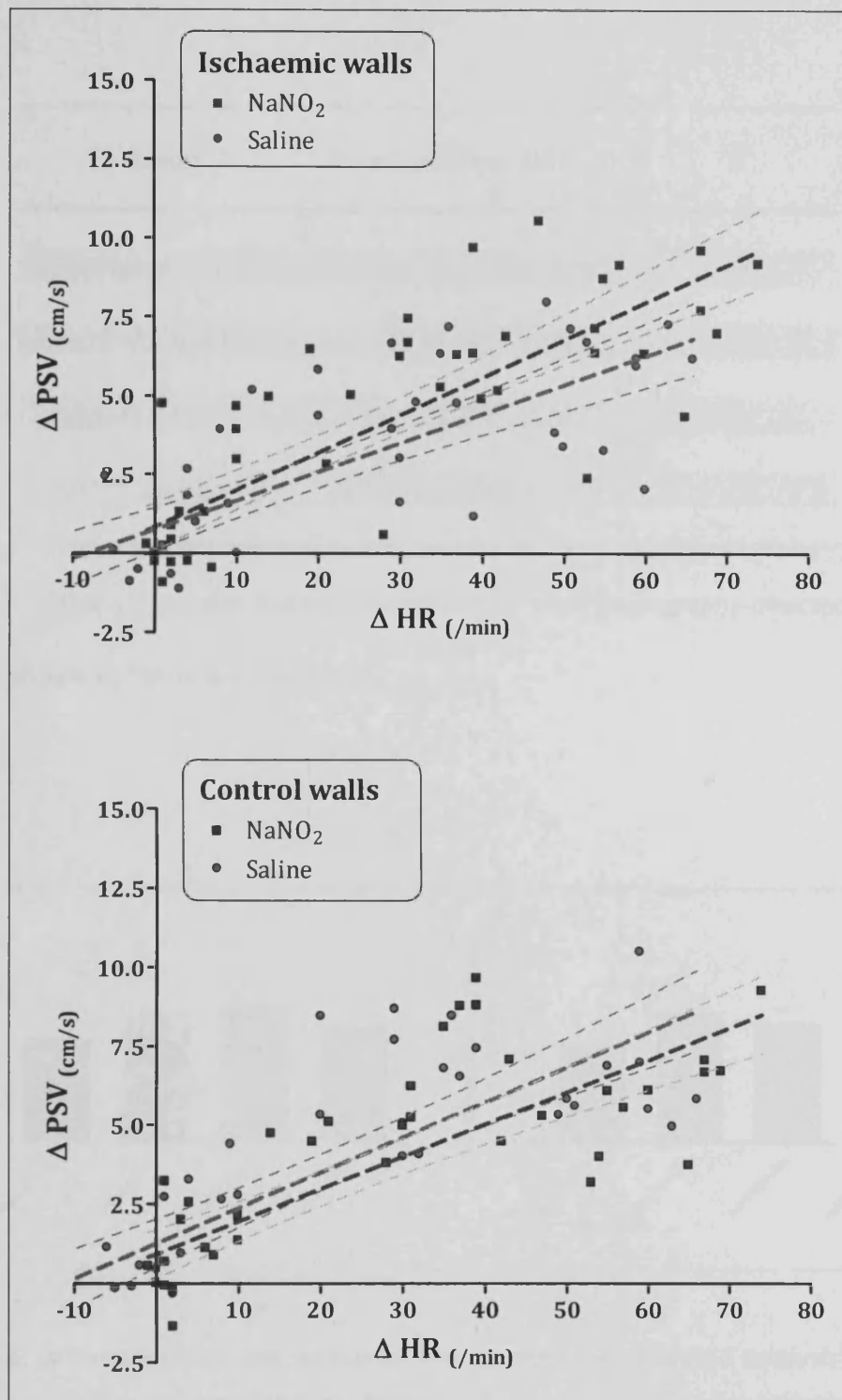


Figure 4-7: Scatter-plot graphs of ΔPSV and ΔHR in the 'angiography-directed analysis' data-set (top graph = ischaemic walls, bottom graph = control walls. The response in 10 different myocardial walls is analysed in each group plotted). Linear regression analyses (mean & 95% CI) of the combined data for each group are also displayed.

Group	Mean gradient (95% CI)	R ²
ischaemia/saline	0.092 (0.070 – 0.114)	.60
ischaemia/NaNO ₂	0.119 (0.097 – 0.141)	.69
control/saline	0.112 (0.087 – 0.137)	.67
control/NaNO ₂	0.103 (0.080 – 0.125)	.66

Table 4-7: Linear regression analysis outputs from the 'angiography-directed analysis' data-set; shown in Figure 4-7 (page 138).

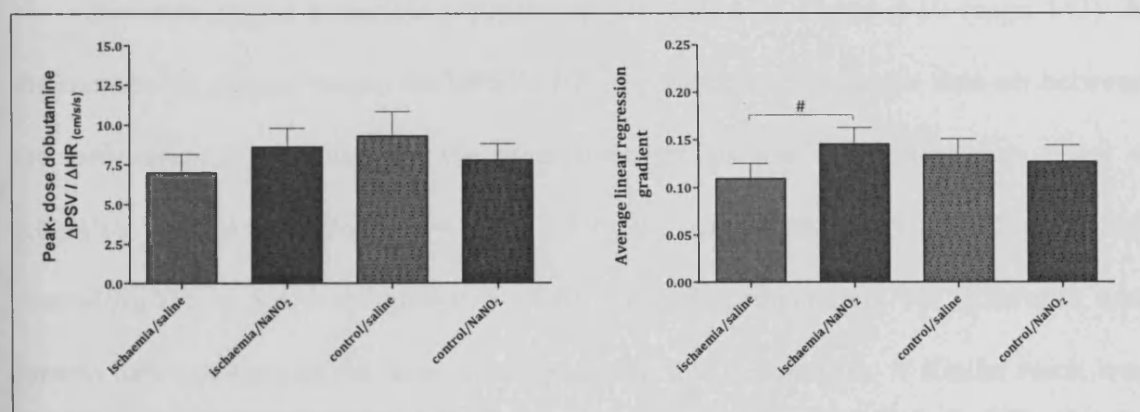


Figure 4-8: Between-group comparison of the 'angiography-directed analysis' data-set. $\Delta PSV / \Delta HR$ at peak-dose dobutamine data (left) and averaged individual wall linear regression gradient data (right). # $p < 0.05$. Only statistically significant comparisons are shown.

4.3.5.3. Top and bottom halves analysis

X/y scatter-plot graphs of the relationship between Δ PSV and Δ HR in the '*top and bottom halves analysis*' data-set are shown in Figure 4-9 (page 141), and the linear regression analyses of these plots are summarised in Table 4-8 (page 142). As the overall data-set contained 55 myocardial walls the split of data for this analysis was not quite even: the ischaemia category contained 28 basal-wall segments and the control category 27 basal-wall segments.

An approximate 25% difference was present in the mean linear regression gradients of the *ischaemia/NaNO₂* (0.100) and *ischaemia/saline* (0.076) groups, with only a small overlap of their respective 95% CI. In addition, there was no appreciable difference between the mean linear regression gradients measured in the two control myocardial wall groups (*control/NaNO₂* = 0.112, *control/saline* = 0.114).

Between-groups statistical comparisons are shown in Figure 4-10 (page 142). A difference was present within the Δ PSV/ Δ HR at peak-dose dobutamine data-set between the *ischaemia/saline* group and the other three groups (i.e. *ischaemia/saline* = 4.9 ± 0.6 cm/s/s vs. *ischaemia/NaNO₂* = 8.0 ± 0.8 cm/s/s, *control/saline* = 9.7 ± 0.8 cm/s/s and *control/NaNO₂* = 8.4 ± 0.7 cm/s/s; $p < 0.01$ for each comparison). No difference was present between each of the three other groups in this comparison. A similar result was present with analysis of the *individual linear regression gradient* data, with a difference demonstrated between the *ischaemia/saline* group and the other three groups (i.e. *ischaemia/saline* = 0.10 ± 0.01 vs. *ischaemia/NaNO₂* = 0.13 ± 0.01 , *control/saline* = 0.15 ± 0.01 and *control/NaNO₂* = 0.14 ± 0.01 ; $p < 0.05$ for each comparison).

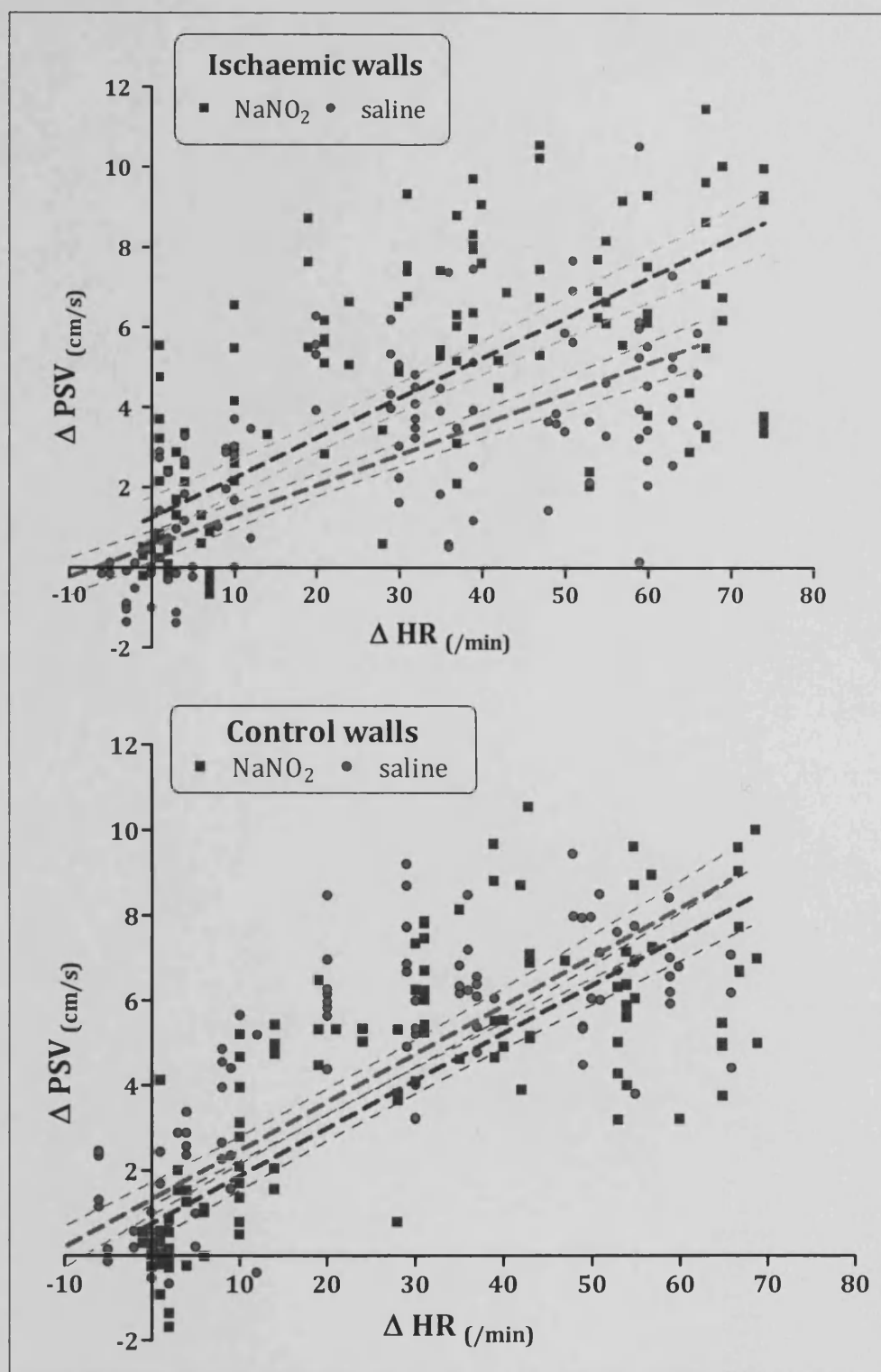


Figure 4-9: Scatter-plot graphs of the relationship between ΔPSV and ΔHR in the 'top and bottom halves analysis' data-set. Top = ischaemic walls (28 basal-wall segments) and bottom = control walls (27 basal-wall segments). Linear regression analyses (mean & 95% CI) of the combined data for each group are also displayed.

Group	Mean gradient (95% CI)	R ²
Saline/ischaemia	0.076 (0.064 – 0.088)	.55
NaNO ₂ /ischaemia	0.100 (0.085 – 0.114)	.56
Saline/control	0.114 (0.101 – 0.127)	.69
NaNO ₂ /control	0.112 (0.100 – 0.125)	.68

Table 4-8: Linear regression analysis outputs from the 'top and bottom halves analysis' data-set; shown in Figure 4-9 (page 141).

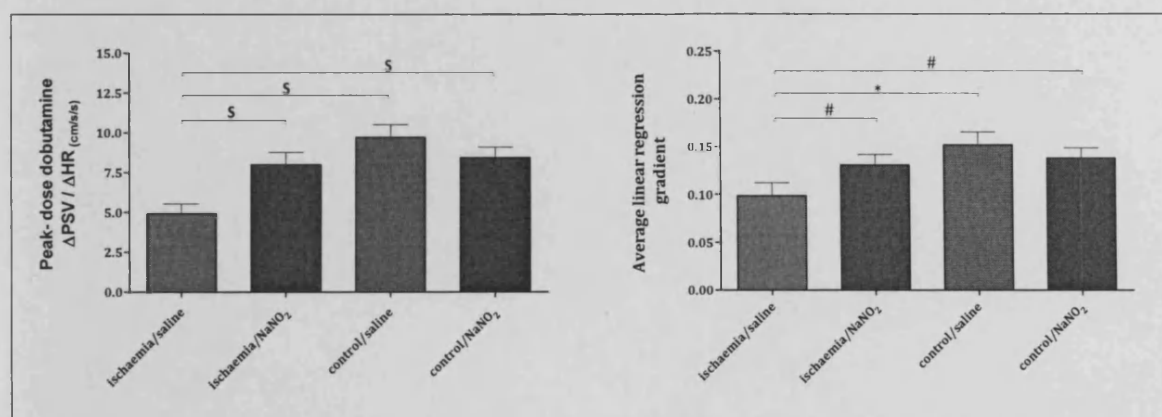


Figure 4-10: Between-group comparison of the 'top and bottom halves analysis' data-set.

$\Delta\text{PSV}/\Delta\text{HR}$ at peak-dose dobutamine data (left) and averaged individual wall linear regression gradient data (right). # $p < 0.05$, * $p < 0.01$. Only statistically significant comparisons are shown.

4.3.5.4. Upper and lower tertiles analysis

The relationship between Δ PSV and Δ HR in the '*upper and lower tertiles analysis*' data-set is shown graphically in Figure 4-11 (page 145), with the linear regression analysis outputs of these plots summarised in Table 4-9 (page 146). 18 basal-wall segments are contained within each group, with the balance of 19 basal-wall segments from the middle tertile not included in this analysis. Of the 18 basal-wall segments in the lower tertile (i.e. *ischaemic* group) only two were from a myocardial region that was not either directly subtended by a stenosed coronary artery, or adjacent to a subtended segment.

An approximate 40% difference was present in the mean linear regression gradients of the *NaNO₂/ischaemia* (0.100) and *saline/ischaemia* (0.063) groups, with no overlap of their respective 95% CI. Furthermore, there was no appreciable difference between the mean linear regression gradients measured in the two *control* myocardial wall groups (*NaNO₂/control* = 0.118, *saline/control* = 0.113).

Between-groups statistical comparisons are shown in Figure 4-12 (page 146). A similar result was seen with both the Δ PSV/ Δ HR at *peak-dose dobutamine* data and the *individual linear regression gradient* data. The Δ PSV/ Δ HR at *peak-dose dobutamine* data demonstrated a lower increase in PSV, adjusted for HR, in the *ischaemia/saline* group compared to the other three groups, (i.e. *ischaemia/saline* = 3.7 ± 0.6 cm/s/s vs. *ischaemia/NaNO₂* = 8.2 ± 1.0 cm/s/s, *control/saline* = 10.5 ± 1.1 cm/s/s and *control/NaNO₂* = 8.4 ± 0.7 cm/s/s; $p < 0.001$ for each comparison). No difference was present between each of the three other groups in this comparison.

Similarly, the *individual linear regression gradient* data demonstrated that the average gradient in the *ischaemia/saline* group was lower than the three other groups, (i.e.

ischaemia/saline = 0.08 ± 0.01 vs. *ischaemia/NaNO₂* = 0.13 ± 0.02 , *control/NaNO₂* = 0.16 ± 0.02 and *control/saline* = 0.14 ± 0.01 ; $p < 0.01$ for each comparison).

In summary, in the previous two sets of analyses where individual myocardial basal-wall segments were ranked according to their PSV response, a difference was clearly demonstrated between the *ischaemia/saline* group and the three other groups categorised within these data-sets. Furthermore, a difference could not be shown statistically between the *ischaemia/NaNO₂* group and the two *control* groups. These combined results demonstrate that low-dose NaNO₂ is capable of improving functional reserve in myocardial walls subtended by a stenosed coronary artery.

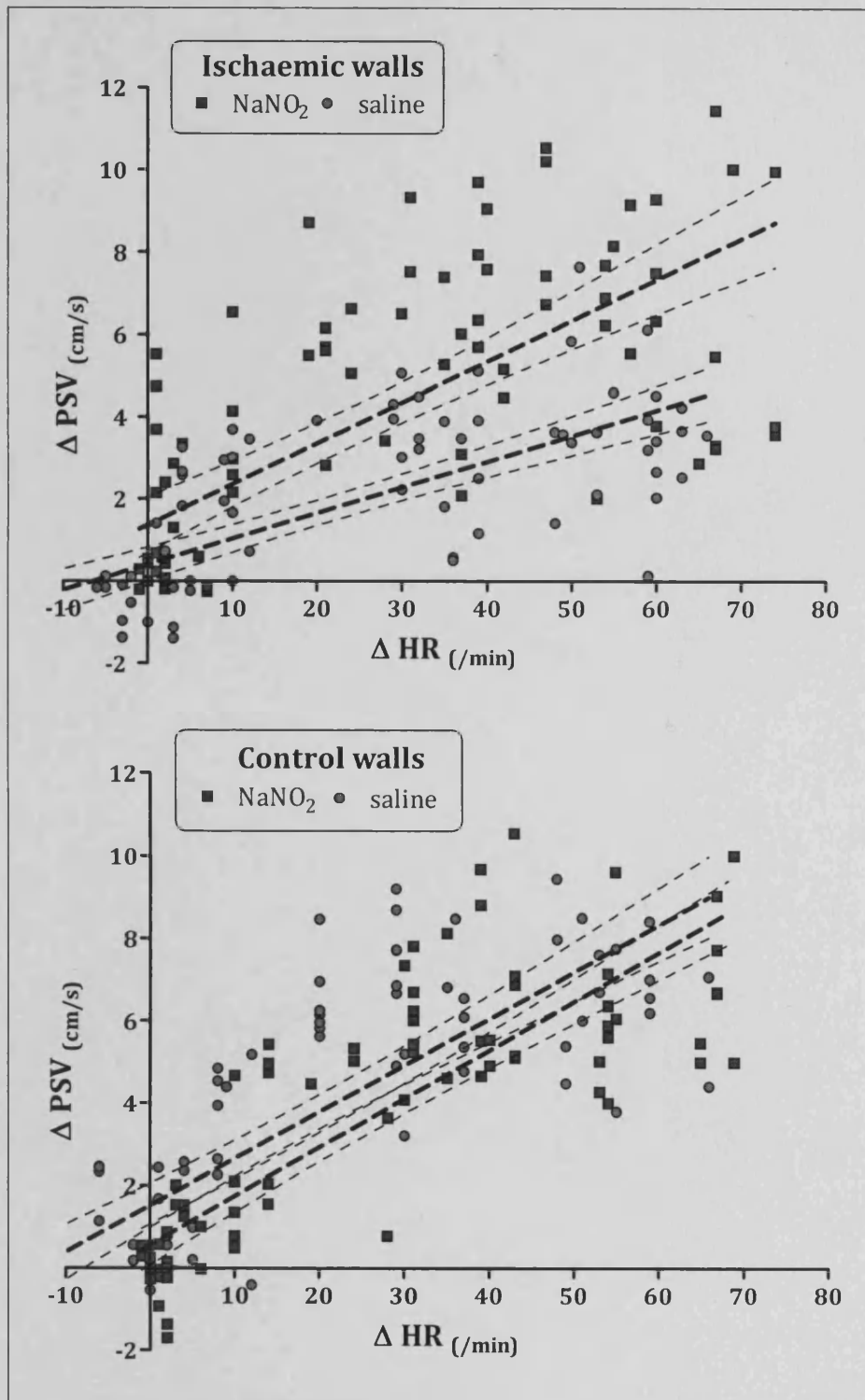


Figure 4-11: Scatter-plot graphs of the relationship between ΔPSV and ΔHR in the 'upper and lower tertiles analysis' data-set. Top graph = ischaemic walls and bottom graph = control walls (18 basal-wall segments in each group). A linear regression analysis (mean & 95% CI) of the combined data for each group is also displayed.

Group	Mean gradient (95% CI)	R ²
ischaemia/saline	0.063 (0.050 – 0.075)	.53
ischaemia/NaNO ₂	0.100 (0.080 – 0.119)	.52
control/saline	0.113 (0.095 – 0.132)	.64
control/NaNO ₂	0.118 (0.103 – 0.133)	.72

Table 4-9: Linear regression analysis outputs from the 'upper and lower tertiles analysis' data-set; shown in Figure 4-11 (page 145).

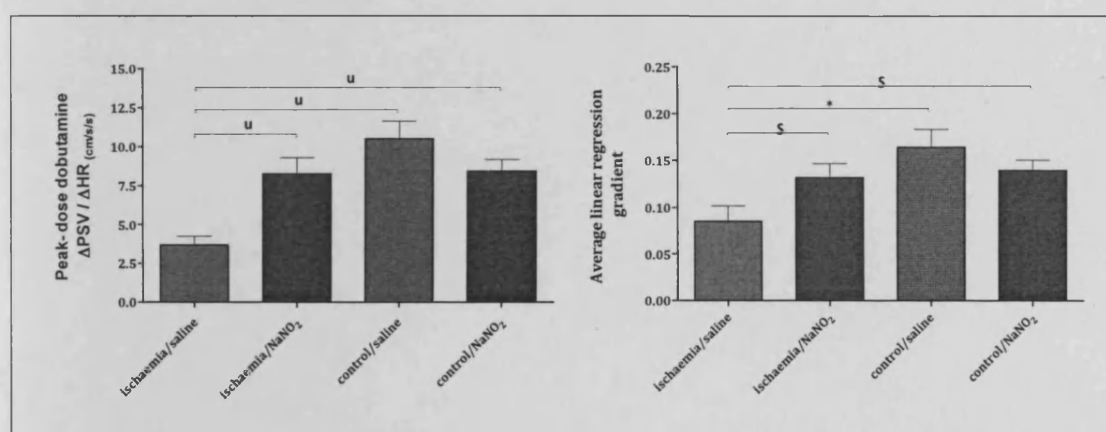


Figure 4-12: Between-group comparison of the 'upper and lower tertiles analysis' data-set. $\Delta\text{PSV}/\Delta\text{HR}$ at peak-dose dobutamine data (left) and individual wall linear regression gradient data (right). * $p < 0.01$. † $p < 0.001$. Only statistically significant comparisons are shown.

4.3.6. Retrospective analysis of the Δ PSV vs Δ HR data

Initial, visual, interpretation of the relationship between Δ PSV and Δ HR in the different analyses performed suggested that this relationship may not be linear, as has previously been stated to be the case in healthy controls¹⁶⁷. Subsequent analysis of the 'upper and lower tertiles analysis' data-set, shown in Figure 4-13 (page 148) demonstrated that the relationship of Δ PSV to Δ HR also fit a non-linear regression analysis with a one-phase exponential-association-curve equation. Indeed, the R^2 values for this fit were greater than those obtained with linear regression analysis in three of the four groups contained within this data-set (i.e. *ischaemia/saline* R^2 : linear regression = 0.53 vs non-linear regression = 0.60; *ischaemia/NaNO₂* R^2 : linear regression = 0.52 vs non-linear regression = 0.65; *control/saline* R^2 : linear regression = 0.64 vs non-linear regression = 0.59 and *control/NaNO₂* R^2 : linear regression = 0.72 vs non-linear regression = 0.80).

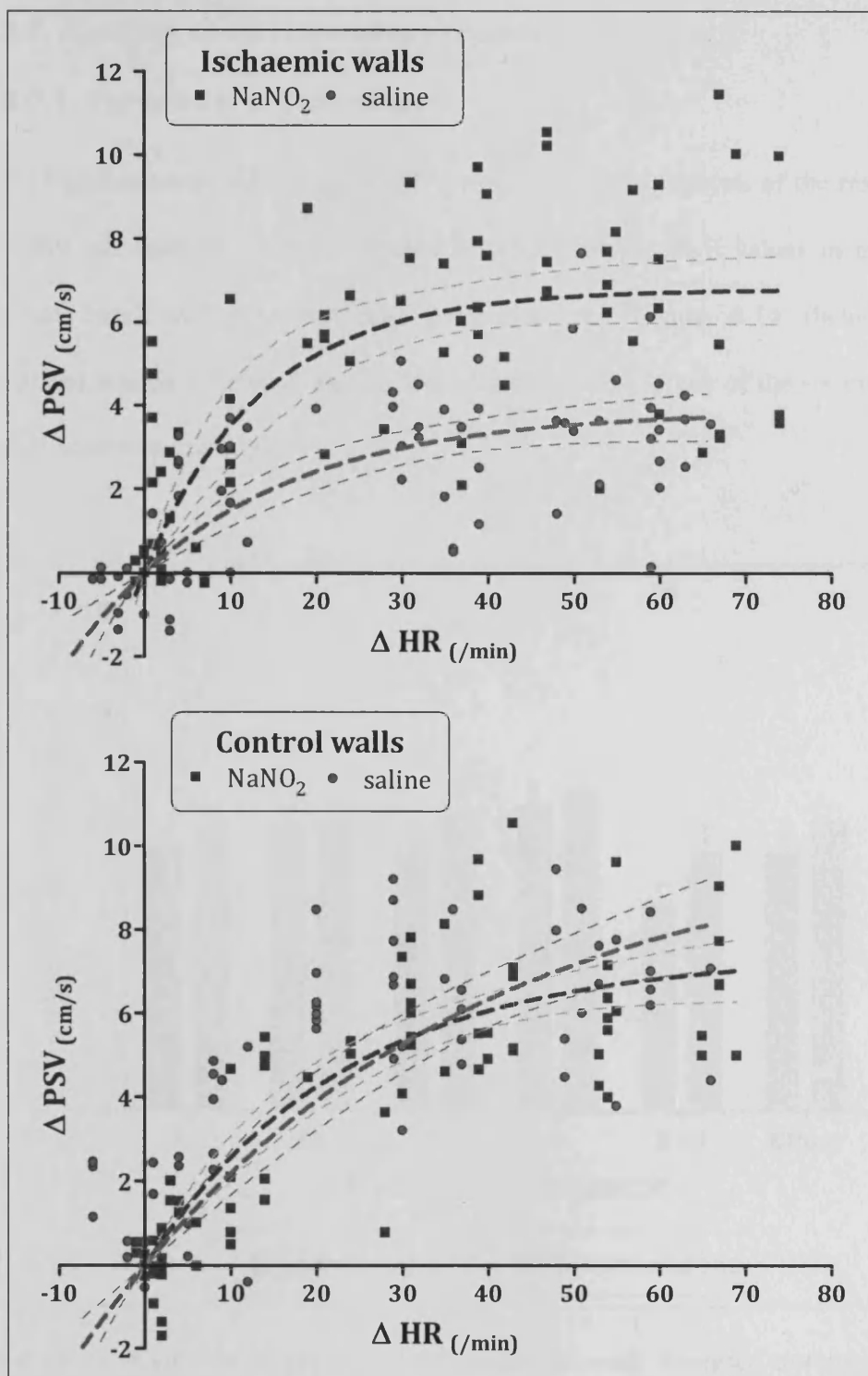


Figure 4-13: Scatter plot graphs of the 'upper and lower tertile analysis' data-set as previously shown in Figure 4-11 (page 145). Mean non-linear regression analyses with a one-phase exponential-association equation (with 95% CI) of the combined data within each group are also displayed.

4.3.7. Analysis of variance of the results

4.3.7.1. Variability between days

As baseline-corrected changes in PSV were used in the analysis of the response of PSV to HR, an analysis of the difference between baseline PSV values in individual myocardial basal wall segments was performed; see Figure 4-14 (below). This demonstrated that no difference was present between studies in any of the six myocardial basal wall segments investigated.

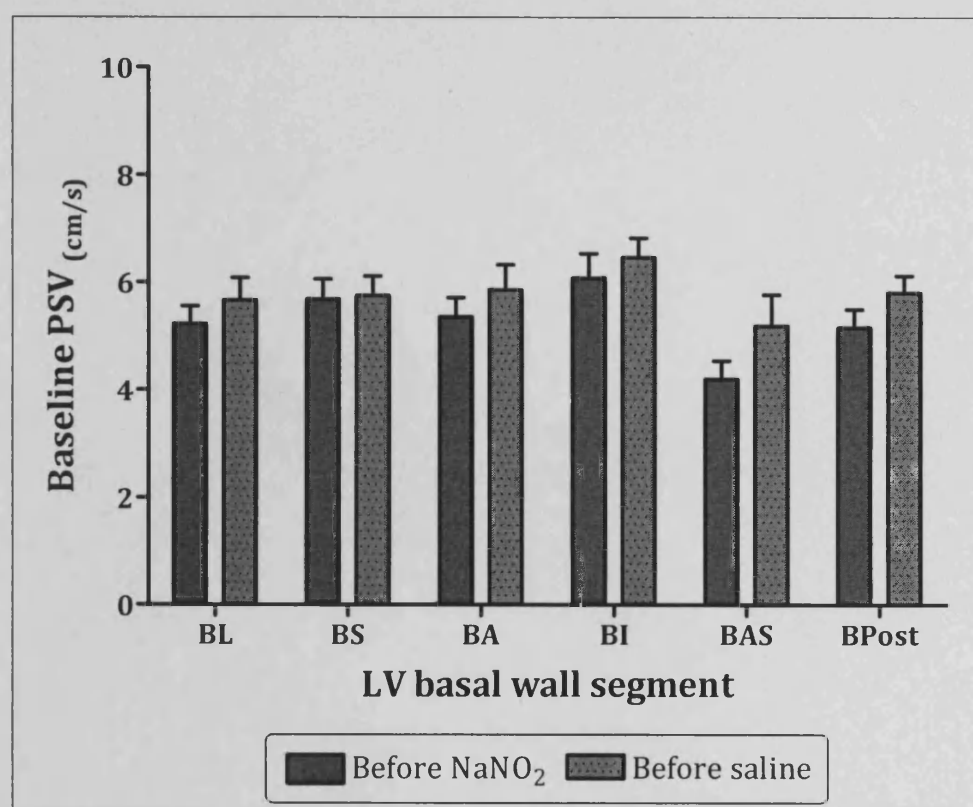


Figure 4-14: Baseline PSV of the six basal myocardial walls analysed during each DSE study. No difference was present between visits in any of the basal wall segments, (repeated measures ANOVA with Newman-Keuls post-test).

4.3.7.2. Intra-observer variability

Thirty paired readings of PSV, chosen from all stages of either DSE study, were used to determine the intra-observer reproducibility of this variable. The results are shown in Figure 4-15 (below). The mean of the explored readings was 8.46cm/s. Linear regression analysis of the correlation between these two readings gave an R^2 of 0.96. Bland-Altman analysis showed no significant paired difference, with a bias of 0.15cm/s (95% CI -1.16 to 1.45). The coefficient of variation was 4.4%, (calculated using the method described in section 3.3.9, page 101).

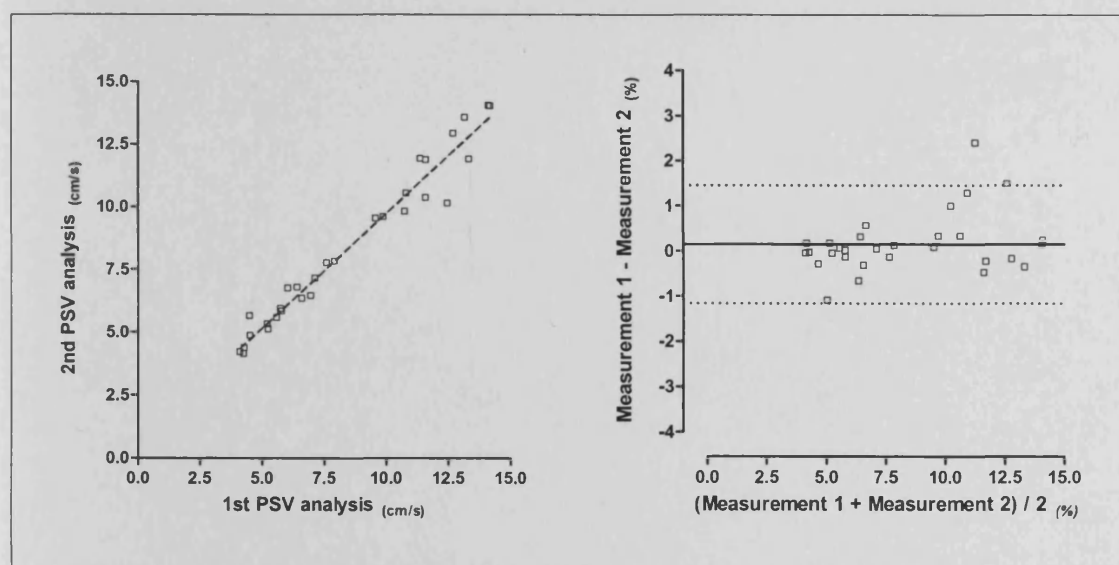


Figure 4-15: Intra-observer variability in PSV measurement. Correlation (left) and Bland-Altman plot (right) are shown.

4.4. Discussion

The key finding of this chapter is that in human subjects with inducible myocardial ischaemia, due to a flow limiting coronary artery stenosis, an infusion of a low-dose of NaNO_2 is capable of alleviating objective measures of ischaemia when administered during quantitative tissue Doppler DSE. Furthermore the dose of NaNO_2 used is one established in chapter 3 of this thesis to approximately double plasma $[\text{NO}_2^-]$ and be physiologically inert in normoxia.

4.4.1. Limitations of this study

The use of a double-blinded placebo-controlled cross-over study in this chapter was one of the strongest possible study designs available to detect a treatment difference between NaNO_2 and placebo in subjects with inducible myocardial ischaemia. The number of subjects recruited into this study was small, but appropriate to the original aims of this chapter, i.e. an initial exploratory investigation of a biochemical hypothesis in a clinical model.

A potential criticism of this study is the limitation of myocardial imaging to the measurement of a single variable: basal-wall PSV. From the tissue Doppler images obtained it would have been possible to analyse a number of different indices of myocardial function. PSV was chosen as it has previously been validated in a large multi-centre study to be a sensitive means of identifying ischaemic myocardium during DSE¹⁴⁵. However, it is less specific to the identification of individual ischaemic territories than other deformation parameters such as strain and strain rate imaging¹⁷⁰. This is for two reasons.

Firstly, PSV is a composite measure of myocardial function in all three segments of the myocardial wall being measured (i.e. the apical, mid and basal wall segments). The heterogeneity of coronary blood supply to different myocardial walls means that an

individual coronary artery may perfuse a number of different segments across a number of adjacent myocardial walls. For example, all six basal-wall PSV measurements may be reduced by a stenosis to a coronary artery which supplies the entire apical region. The tethering of adjacent segments with different coronary blood supplies enhances the sensitivity of basal-wall PSV to detect ischaemia but reduces the specificity it has to identify which coronary artery is subtending an ischaemic region of myocardium.

A second caveat to the interpretation of PSV is that it is reduced, both at baseline and during stress, by the presence of diseases which are cardiovascular risk factors (e.g. hypercholesterolaemia¹⁷¹ and DM¹⁷²). Subjects who participated in this study had multiple cardiovascular risk factors (see Table 4-1; page 125). Therefore the response of PSV to HR in each myocardial basal-wall segment will have been influenced by a composite of both ischaemia-associated myocardial dysfunction and the underlying cardiovascular risk factor burden. However, whilst it should be acknowledged that in the early stages of these diseases myocardial functional deterioration may be regional¹⁷³, the subjects in this study all had long-standing, established, adverse cardiovascular risk factor profiles. Therefore, in this study, the deterioration in myocardial function that resulted from the associated co-morbidities present will have been predominantly global rather than segmental^{174, 175}. In addition, when identifying *ischaemic* myocardial walls, specific criteria were used to ensure that an equal number of basal-wall segments from within each basal-wall segment category were included. This process limited the bias towards the inclusion of any particular basal-wall segment category in the *ischaemia* group.

It follows that the difference in myocardial function observed in this study between the *ischaemia/saline* groups and the *control/saline* groups is most likely attributable to myocardial ischaemia alone. Therefore, this second criticism does not detract from the overall result of this chapter. It does, however, provide a potential explanation for the

better fit than non-linear regression analysis with a one-phase exponential association curve equation had to the data presented compared to linear regression analysis, (i.e. a reduction in subjects' myocardial functional reserve resulted in Δ PSV reaching a plateau within the range of Δ HR included in this analysis).

In summary, it was never within the scope of this thesis to perform an exhaustive analysis of the effect of NaNO_2 upon ischaemic myocardial tissue; in fact such an analysis could form the basis of a whole different thesis. In particular, in this chapter it was not my intention to include all of the many different methods by which myocardial ischaemia can be quantified. Indeed other, more specific, deformation-imaging markers could have been used (e.g. post-systolic strain index¹⁷⁶, peak-systolic strain rate¹⁷⁷ or strain imaging diastolic index¹⁷⁸). Consequently, there are significant caveats to the interpretation of the results presented; specifically whether the segments identified as *ischaemic* were actually ischaemic. However, the overall design of this study and its subsequent analysis incorporated several careful features to try and limit the influence of these caveats. Lastly, it should be emphasized that each of the four analyses performed were in agreement, with more than one of them demonstrating a clear beneficial effect of low-dose NaNO_2 upon the function of ischaemic myocardium.

4.4.2. Targeted therapeutic delivery by NaNO_2

NaNO_2 is a slow vasodilator in normoxia when compared to other more efficient NO-donors³⁸ (e.g. GTN). As the historical context of NaNO_2 therapeutics outlined in the introduction to this chapter demonstrates, this biological feature led in the past to large doses being prescribed (in order to achieve a quick response). This provided an erratic, profound and sustained systemic vasodilator effect in patients which was neither conducive to compliance nor effective pharmacotherapy. However, the results of this chapter demonstrate that administration of low-dose NaNO_2 , at a level which does not

influence normoxic vasculature, can prevent exertional myocardial ischaemia in patients with stable angina. Thus NaNO_2 is a targeted vasodilator, capable of providing an NO-type effect (though not necessarily acting exclusively via this mechanism of action⁸⁴) to tissues in need without the systemic side effects associated with other, less discriminate, NO-donors.

Chronic low-dose NO_2^- supplementation may therefore be an effective alternative treatment for angina. Whilst organic nitrates will remain the primary pharmacological means of administering an NO-type effect in clinical practice there are two key benefits which NO_2^- therapy may have over these agents. Firstly, it may avoid tolerance since primates that received a continuous iv NO_2^- infusion over a 14 day period did not exhibit features of tachyphylaxis in their blood pressure responses to additional intermittent high-dose NO_2^- bolus administration⁸⁸; a problem intricately associated with the chronic use of organic nitrates. Secondly, there is no mortality benefit to the long-term administration of organic nitrates post-MI¹⁷⁹; indeed their use in this clinical setting may be harmful¹⁸⁰. In contrast, there is a growing body of literature from animal studies which proposes that chronic oral NO_2^- supplementation protects against damage resulting from a subsequent MI^{181, 182}, an idea expanded on in chapter 5. The proposal that long term NO_2^- supplementation has a beneficial influence upon the cardiovascular system is also supported by the observations that a 'healthy' Mediterranean diet is one high in both NO_2^- and NO_3^- ¹⁸³, as are certain Chinese medicines which pertain to be beneficial to the cardiovascular system¹⁸⁴.

4.5. Chapter summary

- 1. In human subjects with inducible myocardial ischaemia due to obstructive coronary artery disease a low-dose NaNO_2 infusion reduces objective markers of myocardial ischaemia measured during DSE.**
- 2. The dose of NaNO_2 administered suggests that its mechanism of action is one of targeted therapeutic delivery to tissue in need only.**

Chapter 5: Nitrite and Ischaemia/Reperfusion Injury

5.1. Introduction

The stimulus of remote ischaemic pre-conditioning (RIPC) protects tissue from injury during IR. Kharbanda used a regime of RIPC whereby a cuff attached to the contralateral arm to that being studied was inflated to 200mmHg for five minutes, a process repeated three times with a five minutes gap between inflations. This procedure mitigated against the endothelial dysfunction produced immediately afterwards by twenty minutes of forearm ischaemia and subsequent reperfusion¹²². The protective effects of IPC are therefore systemic. As outlined in section 1.6.4 (page 47), IPC acts through a series of complex molecular cascades, of which NO is a key component. Furthermore, the administration of either a low-dose of sublingual GTN¹⁸⁵ (25µg; dose used clinically to treat angina = 400µg¹⁶⁶) or oral NO₃⁻ supplementation¹⁸⁶ both offered similar protection to that achieved by RIPC when applied to the same model as Kharbanda. In the study where oral NO₃⁻ was given an approximate two-fold increase in plasma [NO₂⁻] was observed.

This in-vivo data, together with a substantial body of in-vitro and animal work (see section 1.6.5, page 49) strongly suggests that the administration of a low-dose of NaNO₂ should offer protection against IR injury. However, this has not explicitly been shown in man. Also, it has not been shown whether the process of RIPC is associated with an alteration in plasma [NO₂⁻] levels.

More importantly, the in-vivo studies outlined above have been limited to exploring the pre-conditioning benefits of NO₂⁻. Of greater clinical relevance would be whether NaNO₂ is an effective post-conditioning agent. The animal study performed by Gonzalez suggests that this would be the case¹⁸⁷, but this result has yet to be translated into man. If NaNO₂ were capable of post-conditioning then it could offer a valuable new means of

limiting the damage of an acute MI, if administered at the time of reperfusion during primary percutaneous coronary intervention.

5.1.1. Aims of this chapter

The first study in this chapter was designed to assess whether plasma NO metabolite levels alter as a result of RIPC. The remaining series of studies were formulated to test whether NaNO_2 is a pre-conditioning or a post-conditioning agent. The same model of forearm IR injury was used as that employed by the studies outlined in the previous section. NaNO_2 was given either before (IPC model) or after (IPostC model) simulated IR. FMD measurement was used to assess endothelial function before and after forearm IR injury, the difference between these two values indicating the degree of endothelial damage which had occurred and thus whether any protection had been afforded by NaNO_2 .

5.1.2. Original Hypotheses

- 1. RIPC will be associated with an increase in plasma $[\text{NO}_2^-]$ and/or RSNO levels.**
- 2. Low-dose iv NaNO_2 will mitigate against IR injury in an in-vivo forearm model when given either as a pre-conditioning or a post-conditioning agent.**

5.2. Study protocols

Each subject recruited in this chapter was asked to prepare for their study in the same manner as outlined in section 3.23 (page 79). Studies were performed in a temperature controlled room in the Wales Heart Research Institute. All forearm IR studies were powered as is appropriate for a similarly designed FMD crossover study¹⁸⁸. For statistical analysis either a repeated measures ANOVA test with Newman-Keuls post test (for analysis of more than two variables) or a paired t-test was used.

5.2.1. RIPC protocol

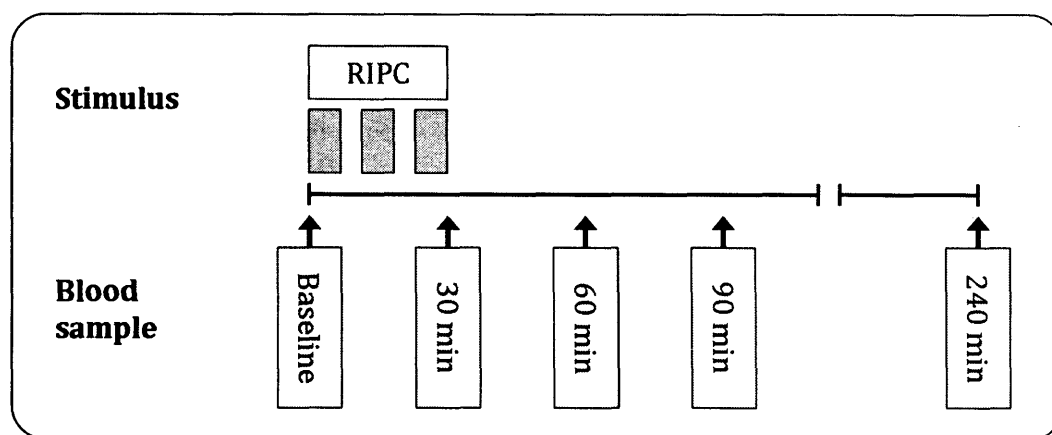


Figure 5-1: Diagram of the RIPC protocol; designed to assess the systemic plasma NO metabolite profile during the four hours following the stimulus of RIPC.

The plasma NO metabolite profile during the four hours following RIPC was assessed in six healthy volunteers; see Figure 5-1 (above). An iv cannula was placed in the dominant arm from which venous blood samples were taken. “Baseline” blood was sampled, followed by three five minutes cycles of contralateral upper arm cuff inflation to 200mmHg, each separated by a five minute rest period. Blood sampling was repeated at “30 min”, “60 min”, “90 min” and “240 min”.

5.2.2. Stage of damage protocol

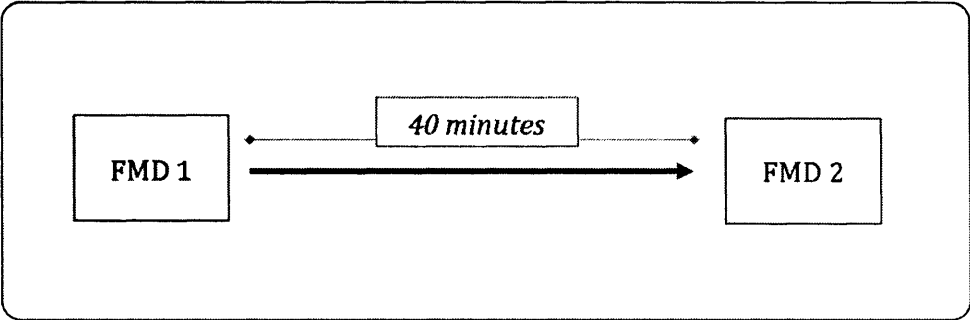


Figure 5-2: Diagram of the stage of damage protocol.

To assess whether any transient damage to endothelial function occurred as a result of a single FMD measurement the protocol outlined in Figure 5-2 (above) was performed. The purpose of this study was to identify the most appropriate timing of NaNO₂ administration when used as a pre-conditioning agent (i.e. before or after the first FMD reading). Two FMD measurements were performed with a forty minute rest period inbetween.

5.2.3. NaNO₂ pre-conditioning protocol

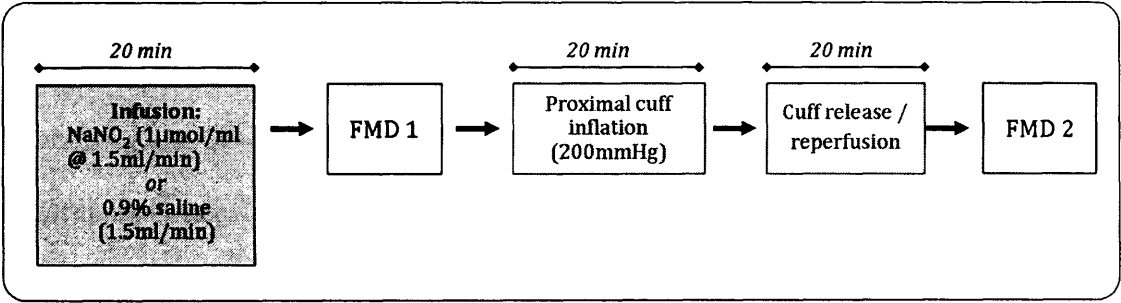


Figure 5-3: Diagram of the NaNO₂ pre-conditioning protocol.

To investigate whether NaNO₂ is a pre-conditioning agent the protocol outlined in Figure 5-3 (above) was performed. The tissue being studied was exposed to an increased level of plasma [NO₂⁻] prior to IR injury. An iv cannula was placed in the contralateral arm to that being studied. An infusion of either NaNO₂ or 0.9% saline was then given.

The infusion dose was identical to that used in chapter 3, however it was given slightly faster to complement the *NaNO₂ post-conditioning protocol* (see section 5.2.4, below). Each individual returned on a separate occasion at least 72 hours later to repeat the study, this time receiving the alternative infusion to that given during the first visit. Subjects were blinded as to which infusion they received at each visit.

5.2.4. NaNO₂ post-conditioning protocol

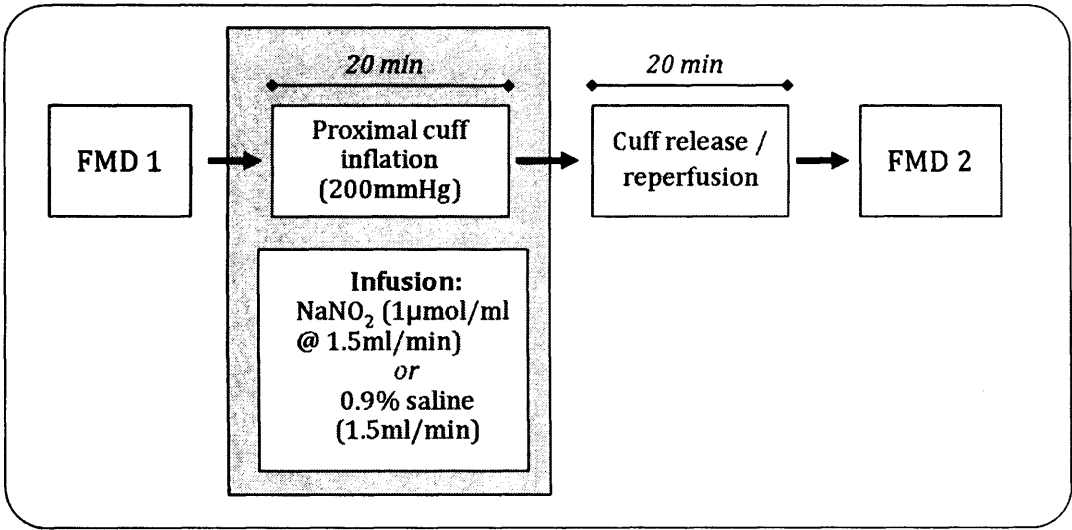


Figure 5-4: Diagram of the *NaNO₂ post-conditioning protocol*.

To investigate whether *NaNO₂* is a post-conditioning agent the protocol outlined in Figure 5-4 (above) was performed. This study was identical in design to the *NaNO₂ pre-conditioning protocol*, apart from the timing of the study infusion being altered so that it was received exclusively during the ischaemic phase. Consequently the forearm tissue bed under investigation was only exposed to an increase in plasma [*NO₂⁻*] at the point of reperfusion.

5.2.5. Analysis of pH/SaO₂ peri-ischaemia

On a separate day, in six of the participants whom had volunteered for an IR protocol, venous samples were taken for analysis of the pH and SaO₂ during forearm IR. A cuff was placed around the upper arm and a venous cannula was sited in the ipsilateral antecubital fossa. A '*baseline*' blood sample was taken and the cuff inflated to 200mmHg. Immediately prior to cuff release at twenty minutes a second sample was taken ('*20 minutes*'). One minute into reperfusion a third sample was taken ('*+1 minute*') and a final sample was also taken after twenty minutes of reperfusion ('*+20 minutes*').

5.3. Results

All data was analysed by a single individual who was blinded to the original infusion (NaNO₂ or 0.9% saline). All continuous data is presented as mean ± SEM.

5.3.1. RIPC protocol

5.3.1.1. Subject demographics

The summary demographics of the healthy volunteers recruited to participate in the *RIPC protocol* are displayed in Table 5-1 (below).

Demographic	
Number	6
Age (years)	29.3 ± 2.7
Male / Female	5 / 1
Weight (kg)	78.5 ± 6.6
BMI	25.4 ± 1.7

Table 5-1: *RIPC protocol summary demographics.*

5.3.1.2. Plasma NO metabolite profile following RIPC

Table 5-2 (below) and Figure 5-5 (page 164) are a summary of the results of this protocol. Plasma $[\text{NO}_2^-]$ increased in response to RIPC, being greater than “baseline” at all subsequent time points. The increase in plasma $[\text{NO}_2^-]$ at “30 min” compared to “baseline” was $+134.8 \pm 28.5$ nmol/l, a rise of a similar magnitude to that reported after the infusion of NaNO_2 given in chapter 3 (i.e. $+205.5 \pm 20.9$ nmol/l, see page 89). Plasma [RSNO] levels were much lower than plasma $[\text{NO}_2^-]$ and did not change throughout the study.

Protocol stage	Plasma $[\text{NO}_2^-]$ (nmol/l)	P value (vs baseline)	Plasma [RSNO] (nmol/l)	P value (vs baseline)
Baseline	112.4 ± 10.5	n/a	11.1 ± 1.3	n/a
30 minutes	247.2 ± 26.3	<0.01	10.1 ± 2.9	ns
60 minutes	235.4 ± 22.1	<0.01	10.4 ± 1.7	ns
90 minutes	203.7 ± 15.8	<0.05	18.7 ± 3.5	ns
240 minutes	180.8 ± 29.4	<0.05	8.4 ± 2.1	ns

Table 5-2: The four hour plasma NO metabolite profile following RIPC.

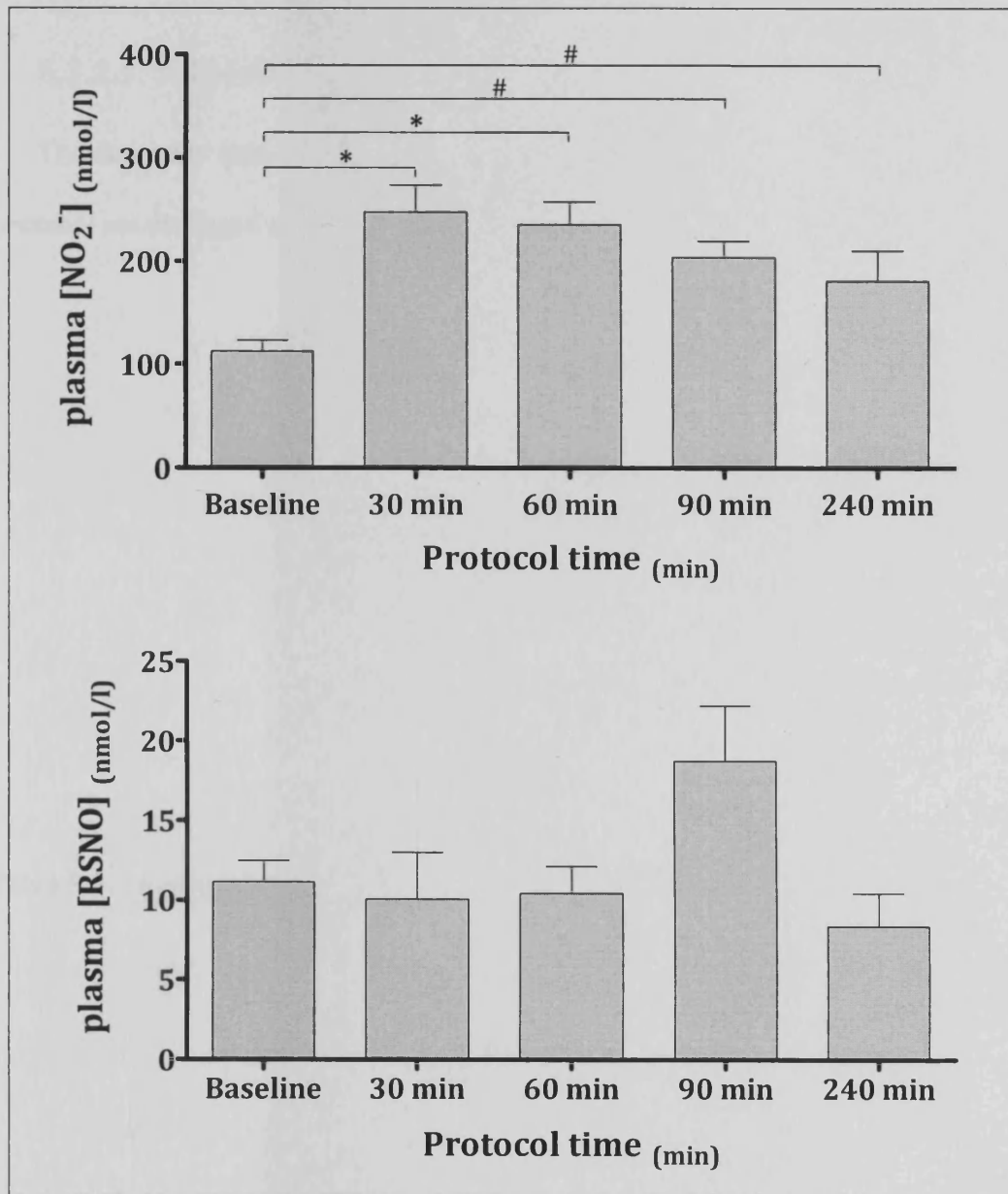


Figure 5-5: The profile of systemic venous plasma $[NO_2^-]$ (top) and $[RSNO]$ (bottom) during the four hours following RIPIC. * $p < 0.01$, # $p < 0.05$.

5.3.2. Stage of damage protocol

5.3.2.1. Subject demographics

The summary demographics of the participants who performed the *stage of damage protocol* are displayed in Table 5-3 (below).

Demographic	
Number	9
Age (years)	27.7 ± 2.0
Male / Female	5 / 4
Weight (kg)	71.9 ± 5.6
BMI	24.3 ± 1.3

Table 5-3: *Stage of damage protocol subject demographics.*

5.3.2.2. FMD measurement variability

In order to ensure that the same stimulus was being delivered into a matched environment for both FMD measurements certain key variables were recorded; summarised in Table 5-4 (below).

A difference in skin temperature was present between the two FMD measurements. However, this change was not associated with a difference in any of the other key variables. In particular the baseline brachial arterial diameter and flow stimulus responsible for each FMD response was similar between each reading.

Variable	FMD 1	FMD 2	P value
Room Temperature (°C)	23.5 ± 0.3	23.8 ± 0.5	<i>ns</i>
Skin Temperature (°C)	30.7 ± 1.1	27.1 ± 1.3	<0.05
Baseline arterial diameter (mm)	3.5 ± 0.2	3.5 ± 0.2	<i>ns</i>
Baseline arterial VTI (cm/s)	0.053 ± 0.005	0.050 ± 0.005	<i>ns</i>
Flow stimulus (%)	691 ± 61	717 ± 57	<i>ns</i>
Heart rate (/min)	66 ± 4	66 ± 4	<i>ns</i>
Blood pressure (mmHg)	123/72 ± 4/4	119/73 ± 5/4	<i>ns</i>

Table 5-4: Summary of the key stimulus and environment variables recorded at each FMD measurement. Statistical comparisons performed by paired t-test.

5.3.2.3. Endothelial function

The peak FMD measurements taken during this protocol are shown in Figure 5-6 (below). The second peak FMD was reduced by approx 30% as compared to the first FMD (FMD 1 = $7.1 \pm 1.0\%$ vs FMD 2 = $4.8 \pm 0.8\%$; $p < 0.01$). This difference may have been influenced by the small change in environmental conditions present between the two protocols (i.e. a reduction in skin temperature). However, for the purposes of this study it was assumed that a degree of damage to endothelial function was present over the forty minutes following the performance of a FMD reading. In the *NaNO₂ pre-conditioning protocol* it was therefore decided that the study infusion should be given prior to the first FMD measurement.

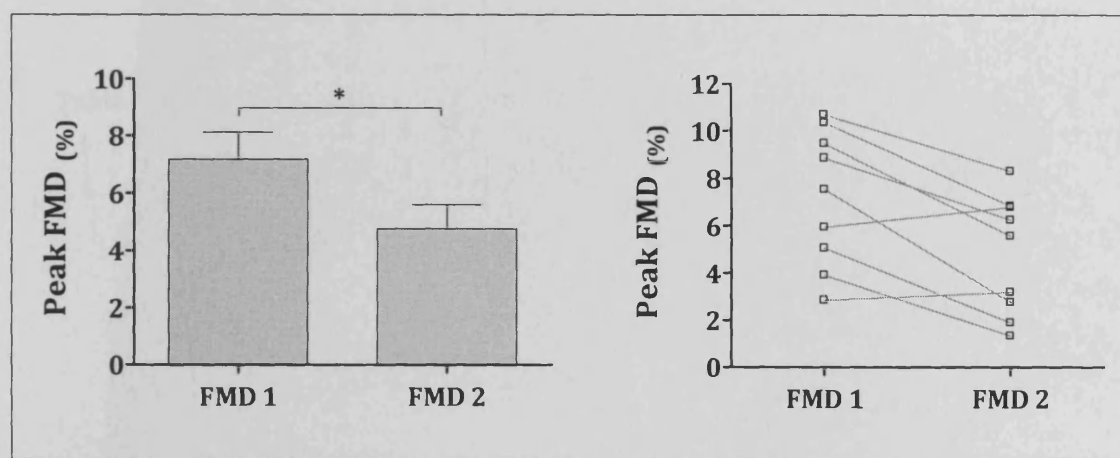


Figure 5-6: Peak FMD measured in the stage of damage protocol, mean data (left) and individual data (right). * $p < 0.01$.

5.3.3. NaNO_2 pre-conditioning protocol

5.3.3.1. Subject demographics

The demographic data of the subjects who took part in the *NaNO_2 pre-conditioning protocol* is contained in Table 5-5 (below).

Demographic	
Number	10
Age (years)	24.6 ± 1.4
Male / Female	6 / 4
Weight (kg)	70.2 ± 4.1
BMI	23.7 ± 0.9

Table 5-5: Subject demographics for the *NaNO_2 pre-conditioning protocol*.

5.3.3.2. FMD measurement variability

Table 5-6 (page 169) contains details of the environmental conditions and flow stimulus delivered during each FMD study. Comparison between the two FMD studies performed within each visit showed that no differences were present with any of these variables.

Variable	<u>Control</u>			<u>NaNO₂</u>		
	FMD 1	FMD 2	P value	FMD 1	FMD 2	P value
Room Temperature (°C)	24.0 ± 0.4	25.0 ± 0.4	<i>ns</i>	24.6 ± 0.9	25.2 ± 0.9	<i>ns</i>
Skin Temperature (°C)	29.8 ± 0.9	29.1 ± 1.2	<i>ns</i>	29.0 ± 1.3	29.6 ± 1.2	<i>ns</i>
Baseline arterial diameter (mm)	3.7 ± 0.2	3.8 ± 0.2	<i>ns</i>	3.8 ± 0.2	3.8 ± 0.2	<i>ns</i>
Baseline arterial VTI (cm/s)	0.051 ± 0.003	0.051 ± 0.004	<i>ns</i>	0.051 ± 0.004	0.048 ± 0.004	<i>ns</i>
Flow stimulus (%)	719 ± 65	728 ± 62	<i>ns</i>	761 ± 70	837 ± 60	<i>ns</i>
Heart rate (/min)	61 ± 2	58 ± 1	<i>ns</i>	59 ± 2	56 ± 2	<i>ns</i>
Blood pressure (mmHg)	119/72 ± 4/3	116/72 ± 4/3	<i>ns</i>	116/68 ± 3/1	113/68 ± 2/1	<i>ns</i>

Table 5-6: Summary of the key stimulus and environment variables within each visit of the NaNO₂ pre-conditioning protocol. Statistical comparisons are made between the two FMD measurements performed during each visit using a paired t-test.

5.3.3.3. IR injury

Peak FMD was reduced by approximately 40% in the control group (FMD 1 = $6.8 \pm 0.7\%$ vs FMD 2 = $3.9 \pm 0.7\%$; $p < 0.01$), confirming that the stimulus for forearm IR injury used in this study causes damage to endothelial function. This damage did not occur during the visit when NaNO_2 was infused (FMD 1 = $5.9 \pm 0.7\%$ vs FMD 2 = $5.2 \pm 0.5\%$; $p = ns$). There was no difference between FMD 1 taken at each of the two visits. Figure 5-7 (below) is a graphical display of this data.

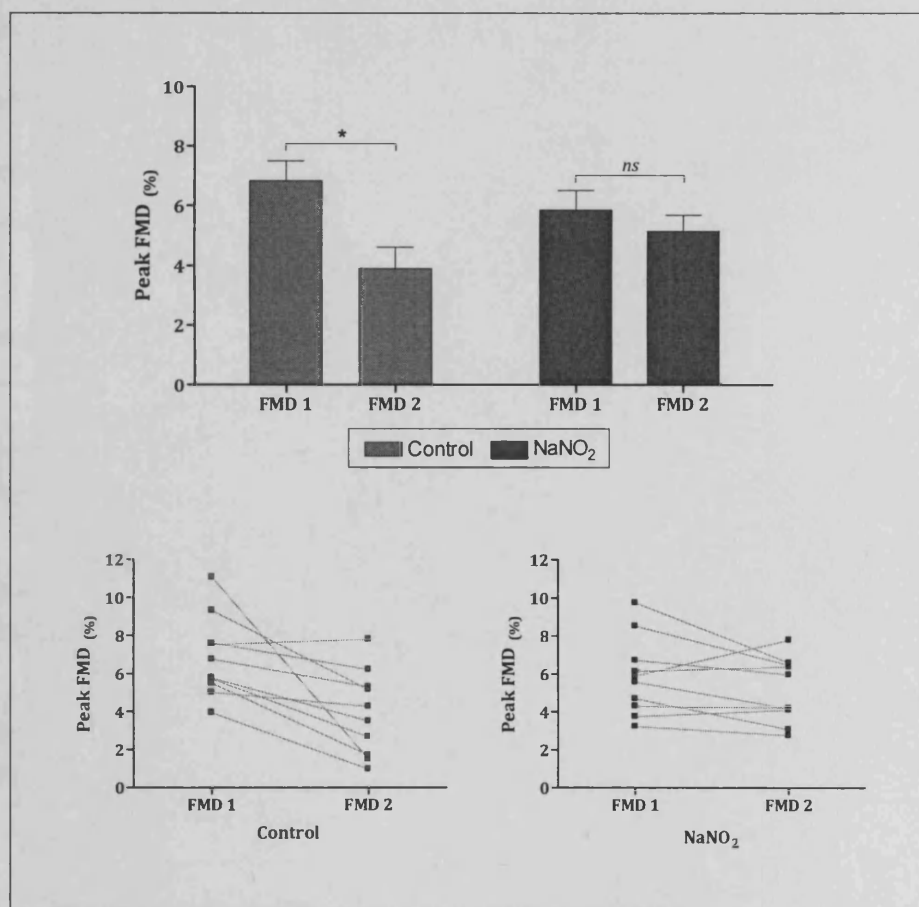


Figure 5-7: Peak FMD results from the NaNO_2 pre-conditioning protocol. Mean data (top graph) and individual data (bottom graphs) is presented. * $p < 0.01$.

5.3.3.4. The haemodynamic response to the study infusion

In section 3.3.6 (page 94) it was demonstrated that the same dose of NaNO_2 as used in this chapter had no effect upon FBF when delivered intravenously in a normoxic environment. To confirm this finding brachial arterial diameter, HR and blood pressure were recorded at the start and end of the twenty minute study-infusion period in the *NaNO₂ pre-conditioning protocol*; the results of which are reported in Table 5-7 (below).

No change was observed with any of these variables as a result of the infusion of either 0.9% saline or NaNO_2 . This result reiterates the fact that the infusion regime of NaNO_2 used in the current study does not have an appreciable dilator effect upon normoxic vasculature.

Variable	<u>Control</u>			<u>NaNO₂</u>		
	Start	End	P value	Start	End	P value
Arterial diameter (mm)	3.8 ± 0.3	3.8 ± 0.3	ns	3.9 ± 0.3	3.9 ± 0.3	ns
Heart rate (/min)	63 ± 2	61 ± 2	ns	62 ± 3	59 ± 2	ns
Blood pressure (mmHg)	118/72 ± 3/4	118/72 ± 6/4	ns	113/69 ± 2/2	114/69 ± 3/1	ns

Table 5-7: Arterial diameter, HR and peripheral blood pressure at the start and end of the twenty minute study-infusion period during both visits of the *NaNO₂ pre-conditioning protocol*. (n=7). Statistical comparisons are made by paired t-test.

5.3.4. NaNO₂ post-conditioning protocol

5.3.4.1. Subject demographics

Table 5-8 (below) is a summary of the demographic data of the subjects who participated in the *NaNO₂ post-conditioning protocol*.

Demographic	
Number	9
Age (years)	26.1 ± 1.8
Male / Female	5 / 4
Weight (kg)	71.3 ± 5.0
BMI	24.1 ± 1.3

Table 5-8: *Summary demographics for participants in the NaNO₂ post-conditioning protocol.*

5.3.4.2. FMD measurement variability

Table 5-9 (page 173) is a summary of the variables measured during each FMD recording at each visit of the *NaNO₂ post-conditioning protocol*. All variables remained constant within each visit, apart from systolic blood pressure which fell by approximately 6% at both visits. Importantly, there was no difference in baseline arterial diameter or flow stimulus during each FMD measurement within each visit.

Variable	<u>Control</u>			<u>NaNO₂</u>		
	FMD 1	FMD 2	P value	FMD 1	FMD 2	P value
Room Temperature (°C)	23.7 ± 0.2	Not recorded	n/a	23.8 ± 0.2	Not recorded	n/a
Skin Temperature (°C)	28.9 ± 1.0	Not recorded	n/a	28.2 ± 1.2	Not recorded	n/a
Baseline diameter (mm)	3.4 ± 0.2	3.5 ± 0.2	ns	3.4 ± 0.2	3.5 ± 0.2	ns
Baseline VTI (cm/s)	0.046 ± 0.005	0.044 ± 0.005	ns	0.042 ± 0.002	0.039 ± 0.003	ns
Flow stimulus (%)	764 ± 55	768 ± 41	ns	829 ± 59	868 ± 47	ns
Baseline heart rate (/min)	63 ± 2	61 ± 2	ns	61 ± 2	59 ± 2	ns
Baseline blood pressure (mmHg)	121/74 ± 3/3	114/73 ± 5/3	<0.05 *	118/75 ± 4/3	112/74 ± 4/2	<0.05 *

Table 5-9: Summary of the key stimulus and environment variables within each visit of the NaNO₂ post-conditioning protocol. Comparisons are made between the two FMD measurements performed during each visit using paired t-test. * Difference in systolic BP only.

5.3.4.3. IR injury

Similar to the *NaNO₂ pre-conditioning protocol*, the percentage FMD was reduced by approximately 40% as a result of IR exposure during the control visit (FMD 1 = $8.6 \pm 0.6\%$ vs FMD 2 = $5.6 \pm 1.0\%$; $p < 0.05$). However, unlike with the previous study, the same difference was observed at the NaNO₂ visit (FMD 1 = $7.5 \pm 0.5\%$ vs FMD 2 = $4.4 \pm 0.5\%$; $p < 0.05$). These results are displayed in Figure 5-8 (below).

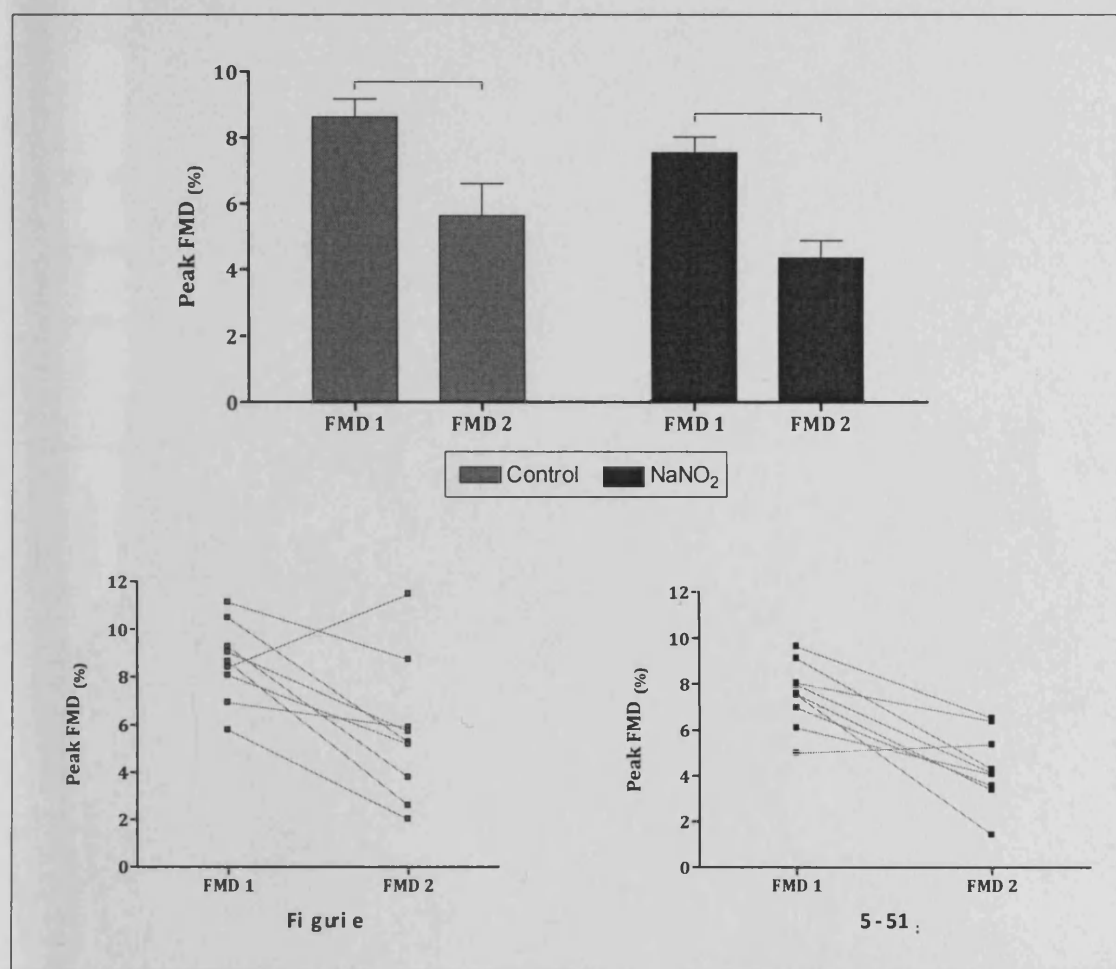


Figure 5-8: Peak FMD results for the NaNO₂ post-conditioning protocol. Mean data (top graph) and individual data (bottom graph) is shown. * $p < 0.05$.

5.3.5. Summary of the ischaemic conditioning effects of NaNO_2

Figure 5-9 (below) is a summary graph of the two IR protocols performed in this chapter. The degree of endothelial dysfunction caused by the IR stimulus is displayed on the y axis (i.e. $\text{FMD } 2 - \text{FMD } 1$). A similar amount of damage was produced in the two control groups and the *IPostC*/ NaNO_2 group (i.e. $\text{IPC/saline} = 2.9 \pm 0.9\%$, $\text{IPostC/saline} = 3.0 \pm 0.9\%$ and $\text{IPostC/NaNO}_2 = 3.2 \pm 0.6\%$; $p > 0.05$ for all comparisons). However, the degree of damage present in all three of these groups was greater than that found in the *IPC/NaNO}_2 protocol ($0.7 \pm 0.5\%$; $p < 0.01$ for all comparisons).*

Taken together these results suggest that a low-dose iv infusion of NaNO_2 can act as an ischaemic pre-conditioning agent, as would be expected from the literature^{125, 186}. However the same regime of NaNO_2 does not appear capable of acting as an ischaemic post-conditioning agent.

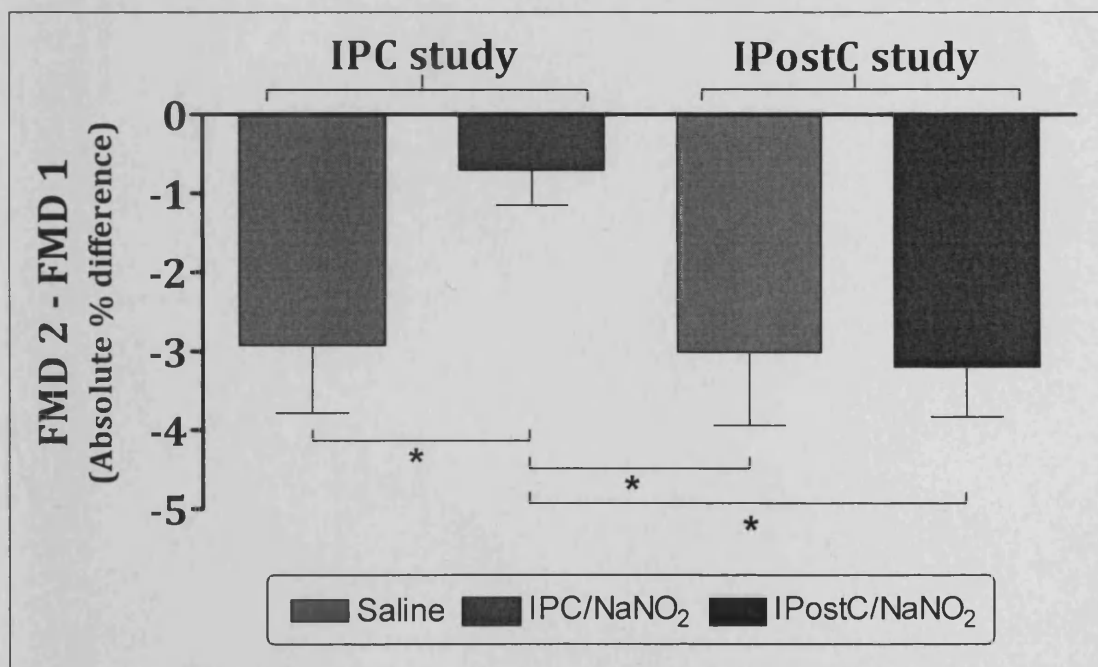


Figure 5-9: Summary graph detailing the degree of endothelial dysfunction produced as a result of the two IR protocols performed in this chapter. * $p < 0.01$.

5.3.5.1. Analysis of pH / SaO₂ peri-ischaemia

The peri-ischaemia profiles of forearm venous blood pH and SaO₂ are reported in *Table 5-10* (below). Venous SaO₂ reduced as a result of twenty minutes exposure to ischaemia. At one minute into reperfusion it was increased compared to baseline, typical of the reduced O₂ extraction per cardiac cycle which results from reactive hyperaemia¹⁴⁶. After twenty minutes reperfusion venous SaO₂ had returned to a value not different to that recorded at baseline. Venous blood pH did not alter at any point during the protocol.

Protocol stage	SaO ₂	P value (vs baseline)	pH	P value (vs baseline)
Baseline	71.5 ± 7.2	<i>n/a</i>	7.34 ± 0.02	<i>n/a</i>
20 minutes	50.9 ± 5.8	<0.05	7.34 ± 0.02	<i>ns</i>
+ 1 minute	87.1 ± 2.8	<0.05	7.34 ± 0.02	<i>ns</i>
+ 20 minute	65.0 ± 8.2	<i>ns</i>	7.37 ± 0.03	<i>ns</i>

Table 5-10: Venous pH and SaO₂ of the ischaemic forearm during the IR protocol.

5.3.6. Subsequent analysis: Does NaNO_2 vasodilate during early reperfusion?

Motivated by the previous results in this chapter further analysis was performed to investigate whether the regime of NaNO_2 given exhibited any vasodilator activity immediately upon entry into a recently ischaemic vascular bed. The brachial arterial diameter, recorded every three seconds during the first five minutes of the reperfusion phase of the *NaNO_2 post-conditioning protocol*, was analysed. If the effects of NaNO_2 were being potentiated by the ischaemic vascular bed (e.g. via conversion to NO) then it would be expected that the brachial arterial diameter would be greater in the early reperfusion phase during the active (NaNO_2) visit compared to the control (0.9% saline) visit. Figure 5-10 (below) details the three variables of arterial diameter measured from the profile obtained.

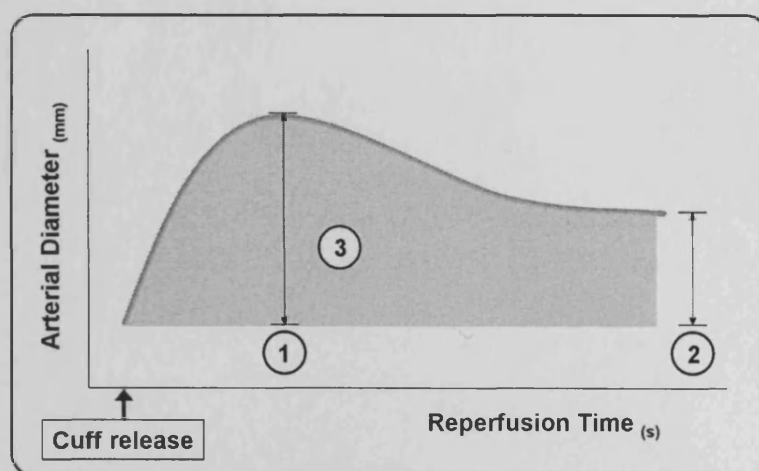


Figure 5-10: Brachial arterial diameter profile during the first five minutes of the reperfusion phase. Three different parameters were measured: 1. Peak increase in diameter. 2. Increase in diameter at five minutes. 3. Area under curve of the increase in arterial diameter over the initial five minutes. The first two values are expressed as a percentage increase in size relative to the baseline diameter reading taken immediately before the twenty minute ischaemic period.

5.3.6.1. Results

Figure 5-11 and Table 5-11 (both on page 179) demonstrate that no difference was present in the arterial diameter profile recorded during the reperfusion phase of each visit of the *NaNO₂ post-conditioning protocol*. This data suggests that NaNO₂ was not being converted to NO in this model; evidence that may explain why NaNO₂ was not an effective post-conditioning agent when used in this chapter.

It is possible that the brachial artery was maximally dilated as a result of the large flow stimulus created by the preceding twenty minutes of arm ischaemia. However, although this argument may compromise the validity of the peak diameter measurement it should be noted that no difference was present between the other two parameters measured. Furthermore, comparison between the FMD 1 peak increases in arterial diameter in the two branches of the *NaNO₂ pre-conditioning study* showed a similar result (control = $6.8 \pm 0.7\%$ vs NaNO₂ = $5.9 \pm 0.7\%$; $p=ns$). This final comparison is between five minutes of forearm ischaemia with or without an infusion of NaNO₂ immediately preceding.

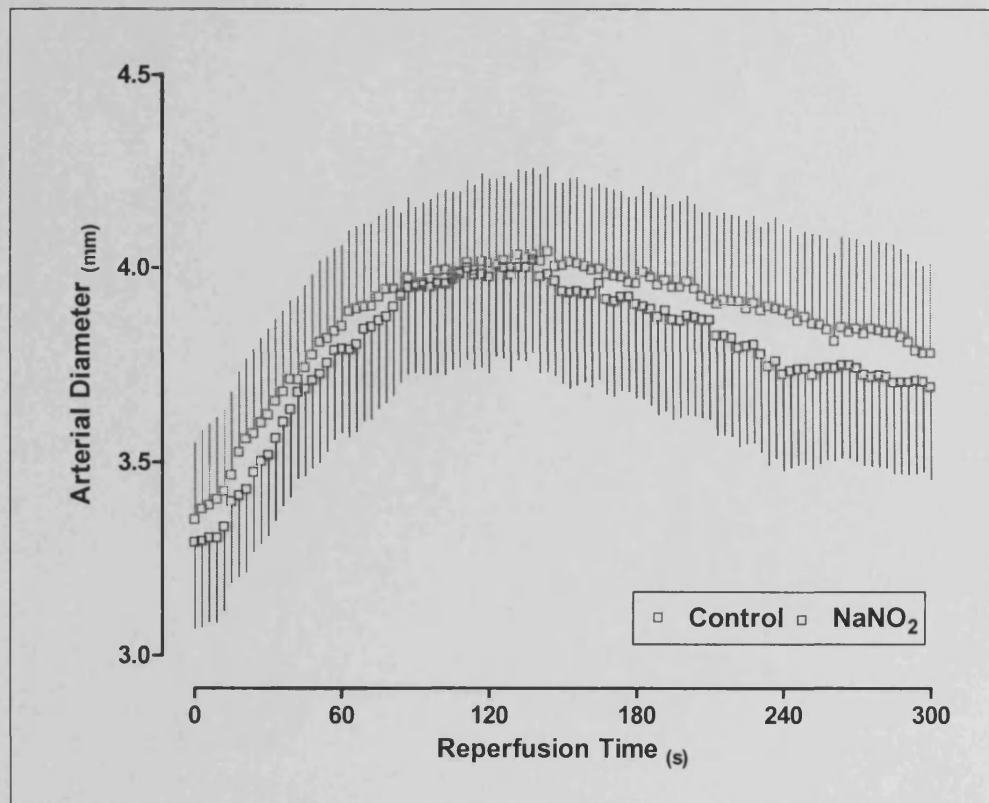


Figure 5-11: Profile of the brachial arterial diameter during the first five minutes of reperfusion in the NaNO_2 post-conditioning protocol.

Variable	Control	NaNO_2	P value
1. % Δ peak	20.7 ± 1.4	21.9 ± 1.6	ns
2. % Δ 5min	13.4 ± 1.0	12.8 ± 1.5	ns
3. 5min AUC (mm.s)	93.7 ± 5.0	92.1 ± 5.2	ns

Table 5-11: Summary measurements of the arterial diameter profile in the early reperfusion phase of the NaNO_2 post-conditioning protocol. Statistical comparisons are made using paired t-test.

5.3.7. Variability of measures employed

Thirty paired readings, chosen at random, of the four key measures employed in this chapter were used to determine their intra-observer reproducibility. The results of these analyses are reported in Table 5-12 (below) and Figure 5-12 (page 181). The coefficient of variation was calculated using the method described in section 3.3.9 (page 101).

Measure	Mean value explored	r^2	Bland-Altman analysis: Bias (95% CI)	Coefficient of Variation (%)
Baseline diameter (mm)	3.81	0.98	-0.001 (-0.17 to 0.17)	1.6
Baseline flow VTI (cm/s)	0.050	0.89	-0.0002 (-0.011 to 0.010)	7.5
Flow stimulus (%)	710	0.82	-24 (-224 to 178)	10.0
FMD (%)	5.61	0.86	-0.11 (-2.02 to 1.79)	12.2

Table 5-12: Summary of the intra-observer variability of the four key indices reported in chapter 5.

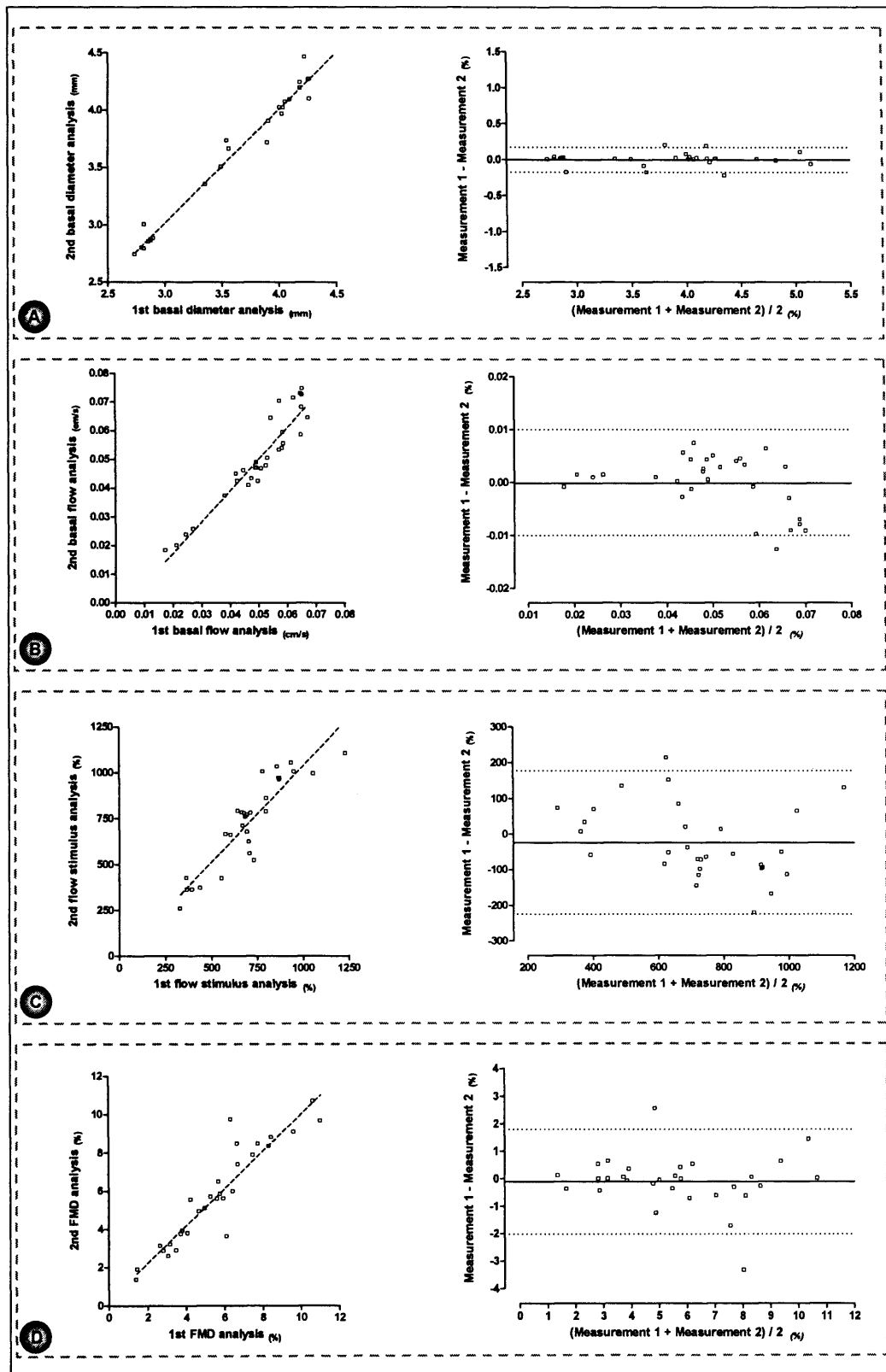


Figure 5-12: Correlation and Bland-Altman intra-observer analyses of the four key indices reported in chapter 5. Panels: A – basal diameter, B – basal flow, C – flow stimulus, D – FMD.

5.4. Discussion

5.4.1. Plasma $[\text{NO}_2^-]$ increases in response to RIPC

The stimulus of RIPC caused venous plasma $[\text{NO}_2^-]$ to increase over a four hour time period. An increase in venous plasma $[\text{NO}_2^-]$ has previously been proposed to be a marker of enhanced eNOS activity⁸⁷. The potential implications of this finding are two-fold: firstly as an insight into the process of IPC and secondly as a simple test of endothelial functional reserve.

The profile of plasma $[\text{NO}_2^-]$ after RIPC appears similar in temporal nature to the early window of tissue protection from IR injury which this stimulus also affords¹⁸⁵. However, in itself this is a simple observation of an association and not a proof of mechanism. It is therefore not possible to state from the data in this chapter that an increase in plasma $[\text{NO}_2^-]$ is an essential part of the IPC process. Indeed, the more likely conclusion is that an increase in plasma $[\text{NO}_2^-]$ is a shadow of an increase in NO production, which as previously stated in section 1.6.4 (page 47), is known to be an important component of the IPC cascade.

Venous plasma $[\text{NO}_2^-]$ has been reported by Rassaf to increase acutely (i.e. within 30 seconds) after cuff deflation during an FMD measurement¹⁸⁹. This study also noted a close relationship between the profile of brachial arterial diameter and plasma $[\text{NO}_2^-]$ during FMD measurement. This similarity extended across patient groups, with the brachial arterial diameter and plasma $[\text{NO}_2^-]$ response to FMD measurement being blunted in subjects with multiple cardiac risk factors. The authors proposed that the profile of plasma $[\text{NO}_2^-]$ produced during FMD measurement is a marker of eNOS activity and endothelial function. However, although a correlation is clearly present in this study it is not certain that the difference in plasma $[\text{NO}_2^-]$ across patients groups is directly caused by a decrease in eNOS activity. It is also possible that the change in

plasma $[\text{NO}_2^-]$ observed is due to a reapportionment of NO metabolites as the blood oxygenation state alters; a principle explained in section 1.4.4 (page 18). Specifically, immediately upon cuff deflation the forearm experiences a hyperaemic state. This will result in a decrease in O_2 extraction per cardiac cycle and an increase in venous SaO_2 ¹⁴⁶, as demonstrated in this chapter. Correspondingly, plasma $[\text{NO}_2^-]$ levels will increase in proportion to the degree of reactive hyperaemia present. It therefore follows that a subject with an attenuated FMD response will experience less forearm hyperaemia and correspondingly a blunted increase in plasma $[\text{NO}_2^-]$ levels. These acute changes in plasma $[\text{NO}_2^-]$ are therefore independent of eNOS production of NO.

The present study is of a different design to that of Rassaf in several important ways. Firstly, a five minute reperfusion period is present prior to the first plasma $[\text{NO}_2^-]$ measure. Secondly, a longer time period is profiled following cuff deflation, one remote from the effects of reactive hyperaemia. Consequently the increase in plasma $[\text{NO}_2^-]$ observed is more in keeping with enhanced eNOS-associated NO-production, as the shear stress of RIPC was the only stimulus placed upon plasma $[\text{NO}_2^-]$ levels in this fasted model. However, in order to confirm that the source of raised plasma $[\text{NO}_2^-]$ is eNOS derived this study would have to be repeated in the presence of L-NMMA.

The *RIPC protocol* is therefore a potential '*endothelial stress test*'; a means of assessing endothelial function which could require substantially less technical expertise than FMD measurement. Furthermore, although it has previously been proposed that an isolated measure of venous plasma $[\text{NO}_2^-]$ reflects an adverse cardiovascular risk profile¹⁹⁰, it is uncertain as to whether a raised¹⁸⁹ or lowered¹⁹¹ level is abnormal. This conflicting data in the literature probably reflects the measurement of plasma $[\text{NO}_2^-]$ in both compensated and decompensated disease states. However, this problem could be

avoided if instead of looking at the absolute level of plasma $[\text{NO}_2^-]$, the delta increase after a fixed physiological stimulation is analysed.

5.4.2. Limitations of the forearm model of IR injury

Tight control of forearm physiology was achieved within each visit in the two protocols in this chapter where transient forearm IR injury was created. In particular, both the baseline arterial diameter and percentage flow stimulus were similar for each FMD reading. It was also shown that the infusion regime of NaNO_2 administered had no effect upon systemic haemodynamics or brachial arterial diameter. Taken together, these observations confirm that the only stimulus responsible for any difference present between the two FMD measures performed at each visit was the intervening IR period.

Surprisingly, in the *stage of damage protocol* a decrease in FMD was noted simply upon its repetition forty minutes after being initially performed. One previous study has reported that FMD does not alter when repeated in the same subject after intervals of 30, 60 and 120 minutes¹⁹². It is uncertain why the data reported in this chapter is different to this study. It is possible that the difference presently observed was related to different environmental conditions (i.e. skin temperature) between the two FMD measures performed in that specific protocol.

However, it is important to state that the results of the *stage of damage protocol* do not interfere with the original aims of this chapter. In particular a reproducible model of IR injury was created and systemic iv NaNO_2 was administered into this model at a stage before any injury had occurred; in order to assess whether a pre-conditioning effect could be produced. Also, even if performing a single FMD measurement caused a degree of endothelial dysfunction (stage of damage protocol: $\text{FMD 1} - \text{FMD 2} = \text{approx. } 2\%$), additional damage was produced in the IR control protocols ($\text{FMD 1} - \text{FMD 2} =$

approx. 3%). This latter value was not affected by the addition of NaNO₂ as a post-conditioning agent.

5.4.3. NaNO₂ is a pre-conditioning but not a post-conditioning agent

In this chapter iv NaNO₂ delivered at a low-dose, one which approximately doubles plasma [NO₂⁻] to a level similar to that achieved with RIPC, had a pre-conditioning effect upon ischaemic tissue. However, the same regime of NaNO₂ when delivered as a post-conditioning agent did not confer a similar benefit. This result is different to that previously reported by Gonzalez¹⁸⁷, who showed that NaNO₂ could act as a post-conditioning agent in a canine model of acute MI. However, it is a result in keeping with those reported in chapter 3 of this thesis. In particular this finding confirms that favourable environmental conditions are required for bioactivity of low-dose NO₂⁻ to be observed (i.e. hypoxia or ischaemia).

Gonzalez reported that NaNO₂, given systemically during the final five minutes of a sixty minute coronary artery ligation protocol, reduced myocardial IR injury. A high-dose of NaNO₂ was used; one associated with a thirty-fold increase of plasma [NO₂⁻] to 6μmol/l. It is therefore possible that the dose of NaNO₂ used in the current study was too low. However, this is unlikely for two reasons. Firstly, it has previously been reported that doses of NaNO₂ similar to those used in this chapter are effective pre-conditioning agents¹²⁶; and secondly it is known that a timely administered post-conditioning stimulus confers a similar degree of tissue protection to that observed after an IPC stimulus¹⁰⁶.

An alternative explanation for the success of NaNO₂ as a post-conditioning agent in the Gonzalez model could be that systemically administered NaNO₂ was absorbed, before the reperfusion phase, from within the left ventricular cavity into the ischaemic portion of myocardium. An increased level of myocardial tissue NO₂⁻ would have therefore been present peri-ischaemia. Consequently, this tissue-located NO₂⁻ would have been exposed

to an ischaemic environment; thus favouring its bioconversion to NO. It follows that NaNO₂ was not tested as a pure post-conditioning agent in the Gonzalez study. Contrastingly, the model of IR injury used in this thesis was able to avoid this problem and assess NaNO₂ as a pure post-conditioning agent.

In summary, in order for NaNO₂ to produce an ischaemic-conditioning effect it most likely first requires reduction to NO¹²⁵. This is in contrast to the hypoxic-vasodilator effects of NaNO₂ which are still present (though reduced) in the presence of the NO scavenger CPTIO⁸⁴. Reduction of NO₂⁻ to NO is favoured in ischaemic tissue¹⁹³, and if NaNO₂ is present within tissue at this time then a beneficial effect can be observed (i.e. a pre-conditioning effect). However, upon reperfusion the favourable substrates for NO₂⁻ reduction associated with an ischaemic environment will rapidly reduce. It follows that conversion will not be favoured at that time and NaNO₂ will not be effective as a post-conditioning agent. This theory is supported by a recent study which demonstrates the critical role of the tissue-based enzyme myoglobin in NO₂⁻-associated protection from IR injury¹²⁴. Figure 5-13 (page 187) is a summary diagram of this potential mechanism of action.

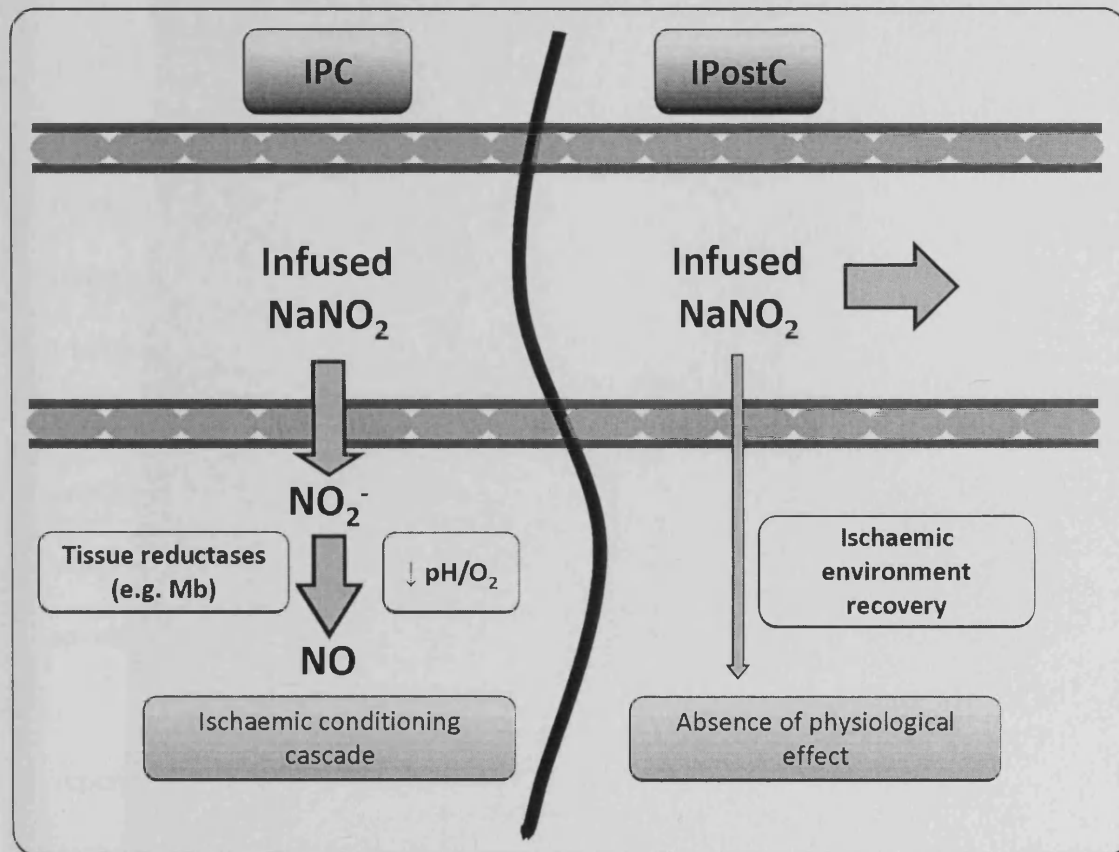


Figure 5-13: The potential mechanism behind the presence of a pre-conditioning but lack of a post-conditioning effect of NaNO₂. When given prior to an ischaemic insult NO₂⁻ has time to equilibrate with the surrounding tissue, from where it is reduced to NO by the favourable environment of ischaemia. This increase in NO in turn promotes the ischaemic conditioning cascade. However, when NaNO₂ administration is delayed until the reperfusion phase the associated hyperaemia present discourages its transit to the surrounding tissue. In addition, the recovery of the ischaemic environment reduces the substrate available to reduce NO₂⁻ to NO. As a result of these two hostile factors a beneficial effect of NaNO₂ administration is not observed in the post-conditioning setting.

5.4.4. A clinical appreciation of the results

Both the model of forearm IR injury used in this chapter and the animal model of myocardial IR injury used by Gonzalez¹¹⁰ have design limitations which restrict the interpretation of their results. Each is inferior to a well conducted randomised controlled trial performed in patients. However, it is important not to discount the potential insights which can be gained from these studies. In particular, the results of this chapter raise concerns regarding the efficiency of NaNO₂ as a post-conditioning agent. This observation is pertinent as a large scale clinical trial is currently underway, designed to investigate the post-conditioning role of NaNO₂ in acute myocardial infarction¹⁹⁴.

A proportion of patients undergoing acute primary PCI to treat a MI will have reperfused their coronary vasculature at the time of initial imaging. This is a result of early antiplatelet treatment¹⁹⁵ and the endogenous production of the lytic agent tPA¹⁹⁶. Furthermore the effect of a post-conditioning stimulus is lost if it is not administered within 10 min of reperfusion¹¹⁴. Whilst these caveats are applicable to any post-conditioning agent they assume a greater importance when considering NaNO₂, as this agent appears to require an initial ischaemic environment to exhibit an effect, possible via bioconversion to NO.

Therefore, it can be predicted that NaNO₂ should be a clinically effective IPC agent. However, its translation into an ischaemic post-conditioning agent is less certain. Several other promising ischaemic-conditioning agents investigated in the past have failed to translate sound laboratory findings into a measurable clinical benefit¹⁹⁷. These previous disappointing results are due to a number of reasons. Firstly, the process of post-conditioning is only capable of limiting infarct size when the occlusion time has been less than 45 minutes¹⁹⁸. Secondly, only large MI provide enough tissue at risk to demonstrate a convincing mortality/morbidity benefit with the use of post-conditioning agents¹⁹⁹.

Therefore surrogate end-points are often reported (e.g. AUC of a 48-hour plasma creatinine kinase profile²⁰⁰) in order to observe a statistically significant benefit; but obfuscating the advantages gained by performing a RCT in patients. Thirdly, the process of ischaemic-conditioning becomes less effective with increasing age²⁰¹ or in diseased states such as DM or heart failure²⁰². Unfortunately, patients who fulfil these criteria are at an increased risk of a MI and are therefore well represented in clinical trials. Lastly, conventional pharmacological treatment of a MI (e.g. morphine, aspirin and GTN) may itself inadvertently trigger a conditioning response¹⁹⁷. It follows that any available benefit to patients in the form of ischaemic-conditioning may already be conferred through best current medical practice.

In summary the data presented in this thesis would suggest that, despite the previous publication of promising laboratory studies, low-dose NaNO₂ may not be an effective post-conditioning agent when utilized in a clinically relevant model (e.g. peri-MI).

5.5. Chapter summary

- 1. Plasma $[\text{NO}_2^-]$ increases over a four-hour period following RIPC, probably as a result of enhanced eNOS activity.**
- 2. A low-dose iv infusion of NaNO_2 protects against forearm IR injury when administered as a pre-conditioning but not a post-conditioning agent.**
- 3. The exposure of an ischaemic vascular bed to a modest increase in plasma $[\text{NO}_2^-]$ at the point of reperfusion does not result in conduit vessel vasodilatation.**

Chapter 6: Pilot study

6.1. NO₂⁻ associated myocardial protection in CABG patients

Chapter 5 of this thesis demonstrated that NaNO₂ is an IPC agent. Patients undergoing on-pump coronary artery bypass grafting (CABG) would be ideal recipients of such a protective mechanism, as this surgical procedure is associated with a significant reperfusion injury to myocardial tissue²⁰³. This insult occurs as a result of cardioplegia associated cardiac arrest; a process whereby the heart is stopped by perfusion of a cardioplegia solution (e.g. St. Thomas's solution) and the patient's circulation is switched to an external cardio-pulmonary bypass machine (i.e. on-pump)²⁰⁴. This is a necessary stage of the operation as it enables the surgeon to create anastomoses between the diseased coronary arteries and the bypass grafts. Pre-treatment of cardiac tissue with NaNO₂ (i.e. by supplementation of the cardioplegia solution) could potentially reduce the degree of myocardial injury that occurs during on-pump CABG surgery.

6.1.1. Study design

To investigate this potential therapeutic use of NaNO₂ a pilot study to ascertain plasma [NO₂⁻] levels peri-CABG surgery was undertaken in six patients undergoing on-pump CABG surgery for the treatment of significant coronary arterial atherosclerotic disease at the University Hospital of Wales. All patients received a cardioplegia solution consisting of a 4:1 mix of blood:crystalloid-cardioplegia; a treatment known to be superior to the use of crystalloid-cardioplegia alone²⁰⁵. The crystalloid-cardioplegia solution used was a diluted mixture (i.e. 30ml in 500ml of 0.9% saline) of *sterile concentrate for cardioplegia* (also known as St. Thomas's solution), from Martindale pharmaceuticals, Essex, UK. Two samples were obtained from each subject: one of

arterial blood and the other of the blood/crystalloid cardioplegia solution. Both were taken simultaneously, immediately prior to the administration of cardioplegia to the heart.

6.1.2. Results

The individual levels of plasma $[\text{NO}_2^-]$ measured in each subject are shown in Table 6-1 (below). The results of this pilot study were surprising, as they demonstrated that the addition of dilute *sterile concentrate for cardioplegia* to whole blood increased plasma $[\text{NO}_2^-]$ in the resulting mixture (i.e. *untreated blood* = $180.7 \pm 50.2\text{nmol/l}$ vs. *blood/crystalloid cardioplegia* = $338.3 \pm 75.3\text{nmol/l}$; $p < 0.05$, paired t-test). This increase (approximately $+160\text{nmol/l}$) occurred despite the concentration of $[\text{NO}_2^-]$ in dilute *sterile concentrate for cardioplegia* being only 56nmol/l ; suggesting that simple NO_2^- donation from crystalloid-cardioplegia was not the mechanism responsible for the observed difference.

Patient number	Untreated blood (nmol/l)	Blood + crystalloid-cardioplegia (nmol/l)
1.	113	151
2.	182	309
3.	129	540
4.	321	540
5.	325	378
6.	14	112

Table 6-1: The individual levels of plasma $[\text{NO}_2^-]$ present in the two samples taken from each of the six subjects analysed in this pilot study.

6.2. Additional laboratory based pilot work

To investigate the results of the previous pilot study further an additional laboratory-based pilot study was performed. The aim of this experiment was to create in-vitro the same two samples obtained in the patient pilot study and analyse their plasma $[\text{NO}_2^-]$ and total-erythrocyte $[\text{NOx}]$ levels. Total-erythrocyte $[\text{NOx}]$ was measured as it is a marker of all NO metabolites present within the erythrocyte¹⁴⁰ (i.e. erythrocyte-associated NO_2^- and Hb-bound NO). This was chosen over the measurement of erythrocyte $[\text{NO}_2^-]$ because the latter was insensitive to detecting changes following NaNO_2 infusion in chapter 3 of this thesis. Venous blood samples from ten healthy individuals were mixed 4:1 with the same dilute *sterile concentrate for cardioplegia* solution as used in the previous section. Plasma $[\text{NO}_2^-]$ and total-erythrocyte $[\text{NOx}]$ of both the venous blood and the laboratory-prepared blood/cardioplegia solution were measured.

6.2.1. Results

The results of this experiment are shown in Figure 6-1, (below). This data replicated the findings of the first study, demonstrating that plasma $[\text{NO}_2^-]$ increases with the addition of a crystalloid-cardioplegia solution (*untreated blood* = $79.3 \pm 17.7\text{nmol/l}$ vs. *blood/crystalloid cardioplegia* = $123.2 \pm 14.9\text{nmol/l}$; $p < 0.05$, paired t-test). In addition, total-erythrocyte $[\text{NOx}]$ was lower in the blood/cardioplegia sample than the untreated blood sample (*untreated blood* = $134.8 \pm 17.9\text{nmol/l}$ vs *blood/crystalloid cardioplegia* = $105.2 \pm 13.4\text{nmol/l}$; $p < 0.05$, paired t-test).

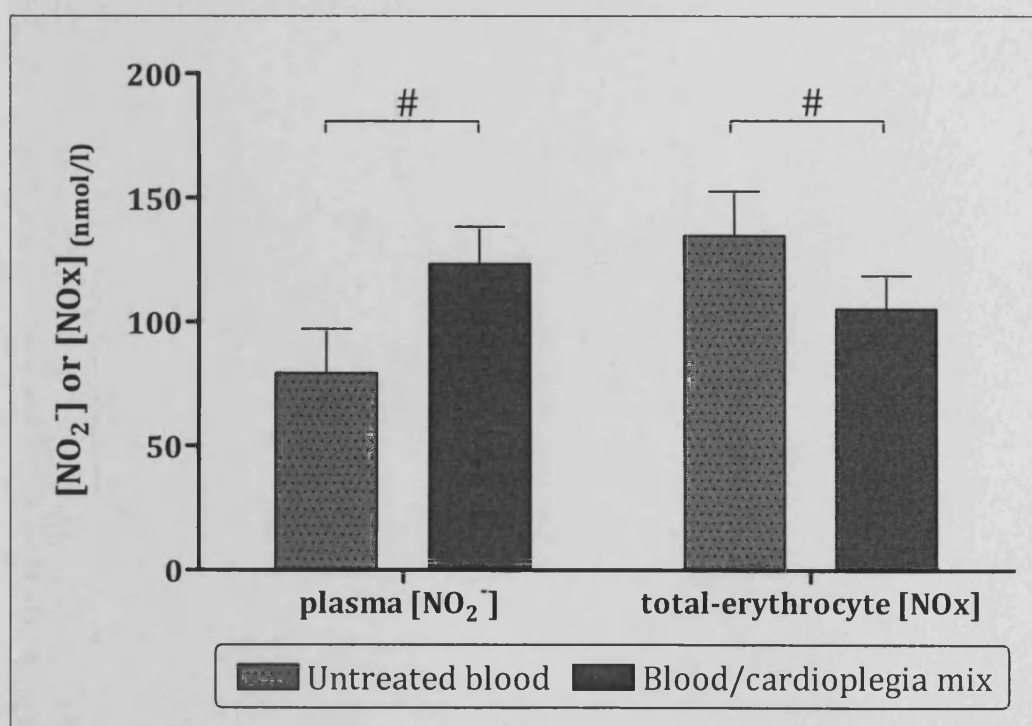


Figure 6-1: The relationship of plasma $[\text{NO}_2^-]$ and total-erythrocyte $[\text{NOx}]$ in the laboratory pilot study. $N=10$. # $p < 0.05$.

6.3. Discussion

The pilot data presented in this chapter demonstrates that the addition of crystalloid-cardioplegia to whole blood results in a partial redistribution of NO metabolites from within the erythrocyte into plasma.

6.3.1. The redistribution of NO metabolites

One possible explanation behind the redistribution of NO_2^- observed in this pilot study, from the intra- to the extra-erythrocyte compartment, could lie in the composition of the dilute *sterile concentrate for cardioplegia* solution. This preparation contains a high concentration of anions, in particular Cl^- ions (see Table 6-2, page 196). The normal plasma level of $[\text{Cl}^-]$ is approximately 70mmol/l and the normal intra-erythrocyte concentration approximately 100mmol/l²⁰⁶. Therefore, the addition of approximately 60mmol/l of Cl^- to the system (i.e. blood mixed 4:1 with dilute *sterile concentrate for cardioplegia* (total concentration $\text{Cl}^- = 305\text{mM}$)) will disrupt this equilibrium and osmosis will prompt the redistribution of Cl^- ions from plasma to inside the erythrocyte. Transit of Cl^- ions across the erythrocyte membrane will occur via AE1 with the concomitant exchange of both HCO_3^- and NO_2^- into plasma, (see section 1.4.1.2.1, page 11). This exchange will result in an increase in plasma $[\text{NO}_2^-]$ levels in the blood/cardioplegia solution.

In addition, cardioplegia also contains the local anaesthetic agent procaine hydrochloride. This is a sodium channel inhibitor¹⁶⁶, but it also stimulates the release of K^+ from within the erythrocyte²⁰⁷. It is possible that this release of cations by the erythrocyte is associated with a concomitant loss of anions; perhaps intra-erythrocytic NO_2^- . The precise mechanism of the observed NO_2^- release from erythrocytes demonstrated in this chapter is unknown, but certainly warrants further investigation.

Content	Concentration in diluted solution (30ml neat solution in 500ml 0.9% saline)
MgCl ₂	130 mmol/l
KCl	45 mmol/l

Table 6-2: Composition of the 'sterile concentration for cardioplegia' diluted solution. In addition this product also contains: procaine hydrochloride, disodium edetate, sodium hydroxide and water.

6.3.2. The beneficial effects of blood/crystalloid cardioplegia

In summary, the beneficial effects observed in CABG patients treated with a blood/crystalloid cardioplegia solution²⁰⁵ may be due to an increase in the level of plasma [NO₂⁻] present in the blood/crystalloid-cardioplegia solution compared to arterial blood or crystalloid-cardioplegia alone. This effective NO₂⁻ supplementation of the cardioplegia solution would result in an increase in myocardial tissue [NO₂⁻] levels immediately prior to the onset of ischaemia; a process which could potentially act as an IPC stimulus. Whether further supplementation of NO₂⁻ levels above those achieved by this process would confer an additional benefit to patients is unknown. Recent literature would suggest that this was possible. It has been shown that RIPC, administered after anaesthesia and in addition to blood/crystalloid cardioplegia, has a beneficial effect upon patients in terms of their serum troponin-t AUC profile in the first 72 hours after surgery²⁰⁸. Chapter 5 of this thesis demonstrated that the process of RIPC is associated with an increase in plasma [NO₂⁻] levels. Interestingly, the increase in plasma [NO₂⁻] observed in patients in this pilot study with the addition of cardioplegia solution to blood (i.e. +160nmol/l) is similar in magnitude to that recorded after RIPC in chapter 5 (i.e. +135nmol/l) and following low-dose iv NaNO₂ infusion in chapter 3 (i.e. +200nmol/l).

Chapter 7: General Discussion and Future Directions

The *BHF Clinical Research Training Fellowship* which formed the foundation of this thesis was conceived to investigate the effect of NO_2^- supplementation in man in different environments; created by either deliberate modification in healthy subjects (i.e. hypoxia or simulated forearm ischaemia) or the presence of underlying pathology (i.e. inducible myocardial ischaemia). The work was motivated by experimental literature suggesting that NO_2^- has enhanced biological activity in altered environments which promote its reduction to NO (i.e. hypoxia or ischaemia)^{80, 82, 83}. The overall focus of this thesis was therefore to translate the results of these promising laboratory and early human studies into models of greater physiological and clinical relevance.

This thesis had two aims. The first was to examine whether the theory of deoxy-Hb mediated NO_2^- reduction was consistent with analysis of the biochemical and physiological changes which occur following iv NaNO_2 infusion in both hypoxia and normoxia to healthy human subjects. The second was to ascertain whether NaNO_2 is capable of targeted therapeutic delivery in human pathological models of inducible ischaemia and IR injury.

To achieve these goals a low-dose of NaNO_2 was used throughout this thesis. This dose was chosen on the back of pilot studies performed by other groups at much higher doses; with the driving rationale being that a minimally effective dose should be aimed for. In chapter 3 of this thesis this dose is shown to only increase plasma $[\text{NO}_2^-]$ approximately two-fold. It is interesting to note that this degree of increase in plasma $[\text{NO}_2^-]$ is similar in magnitude to that observed after maximal stimulation of the endothelium by ACh⁸⁷. A low-dose infusion regime was important for two scientific reasons. Firstly, previous studies in man of NO_2^- supplementation have almost exclusively

employed much higher doses of NaNO_2 ; resulting in a ten-fold or greater increase in plasma $[\text{NO}_2^-]$ ^{80, 87, 88}. Such high doses were chosen so that convincing physiological changes could be demonstrated in normoxia. However, as a result subtle biochemical changes with important mechanistic insights have been missed; as outlined in Chapter 3. Secondly, in order to demonstrate that NaNO_2 is capable of targeted therapeutic delivery it was important to administer a dose of NaNO_2 that did not display vasodilator activity in normoxic tissue. Therefore, any observed effects were a result of environmental modification (i.e. hypoxia or ischaemia) enhancing the bioactivity of NaNO_2 .

7.1. The key findings of this thesis

In summary the key findings of this thesis are:

- A low-dose infusion of NaNO_2 has an enhanced vasodilator effect upon the systemic and pulmonary circulations in man when given in hypoxia compared to normoxia. In addition, the mechanism of this finding is more in keeping with enhanced tissue-based NO_2^- bioactivity (via tissue reductase enzymes, e.g. XO) than deoxy-Hb mediated reduction of NO_2^- to NO. This mechanism is supported by the observations that (i) deoxy-Hb levels do not correlate with the pattern of induced vasodilation observed and (ii) a prolonged vasodilator effect was present in the pulmonary vasculature even after plasma $[\text{NO}_2^-]$ levels had returned back to baseline.
- The same low-dose of NaNO_2 is capable of reducing exertion-induced myocardial ischaemia in patients with known stable angina. This beneficial effect occurs despite no vasodilator activity being present in normoxic tissue; suggesting that low-dose NaNO_2 delivers a targeted therapeutic effect.

- Low-dose NaNO_2 is an IPC but not an IPostC agent when given in a forearm model of IR injury. These results imply that the presence of NO_2^- in blood at reperfusion alone is not sufficient for an ischaemic conditioning effect to be observed. This discrepancy is due to the need for an augmented level of NO_2^- to be present within tissue prior to the onset of ischaemia. Consequently, the altered environmental conditions which follow potentially allow bioconversion of NO_2^- to NO, which in turn will initiate the molecular cascades of pre-conditioning.

Two individual themes contained within these key findings warrant further discussion. Firstly the importance of tissue NO_2^- levels when considering the biochemical and physiological effects of NO_2^- supplementation and secondly the potential role of NaNO_2 as a therapeutic agent in different pathological situations.

7.2. The pharmacokinetics of NaNO_2 – the forgotten element

One of the principle results of this thesis is the important role that NO_2^- has outside of the intravascular compartment (i.e. the intracellular or interstitial spaces). Chapter 3 demonstrated that, following an iv infusion of NaNO_2 , a similar profile of plasma $[\text{NO}_2^-]$ was present in both normoxia and hypoxia but only the latter environment was associated with a measurable vasodilator effect. Furthermore, vasodilation persisted in the hypoxic pulmonary circulation at a time when plasma $[\text{NO}_2^-]$ levels had returned to a level similar to baseline. Chapter 5 also showed that in order for low-dose NaNO_2 to exhibit an ischaemic conditioning effect it needs to be delivered prior to the onset of IR injury; again stressing the importance of tissue $[\text{NO}_2^-]$ levels. These observations are supported by a study which shows that NO_2^- rapidly equilibrates across all fluid spaces of the body within 5 minutes of its infusion⁴³, with the exception of transit into the erythrocyte which is slower⁴².

Previous publications have reported gradients of plasma $[\text{NO}_2^-]$ across a single vascular bed from artery to vein, either at rest⁷⁴ or following NaNO_2 infusion⁸⁰. These gradients, combined with physiological changes also present in these models, have been used as evidence in support of the deoxy-Hb mediated NO_2^- reduction theory of enhanced NO_2^- activity in hypoxia. However, consumption of NO_2^- is only one of three potential routes by which plasma $[\text{NO}_2^-]$ can be removed from the intravascular space. These three potential routes are:

1. Redistribution of NO_2^- within the vasculature to other, inert, products (e.g. HbNO or NO_3^-), with no overall change in total NO metabolite levels.
2. Redistribution of NO_2^- by diffusion to the intracellular and interstitial spaces.
3. Conversion of NO_2^- to NO, or another compound within the vasculature, resulting in a measurable NO-type effect.

This thesis illustrates the importance of the second route of NO_2^- loss from the intravascular compartment. Specifically, during both hypoxia and normoxia tissue uptake of infused NO_2^- is likely to be the same (hence the similar profiles of plasma $[\text{NO}_2^-]$ in both hypoxia and normoxia shown in chapter 3). However, hypoxic tissue will utilise this NO_2^- differently. Therefore, the results of this thesis do not detract from the observation that NO_2^- is a vasodilator whose effects are potentiated by hypoxia; however they do raise concerns that this process is not due to deoxy-Hb mediated reduction of NO_2^- to NO. It is therefore likely that, when one considers the bioactivity of NO_2^- , tissue $[\text{NO}_2^-]$ levels are more important than plasma $[\text{NO}_2^-]$ levels. This point is illustrated by comparison of the results of this thesis to two human studies where oral NO_3^- has been used as a means to increase plasma $[\text{NO}_2^-]$ levels.

Dietary supplementation with NO_3^- for three days reduced diastolic blood pressure by 3.7 mmHg⁴⁰, with a comparable increase in plasma $[\text{NO}_2^-]$ levels to that achieved in

this thesis. In addition, a second study reported a similar reduction in both systolic and diastolic blood pressure three hours after a thirty minute period of oral ingestion of foods rich in NO_3^- ¹⁸⁶. Here, again, a comparable plasma $[\text{NO}_2^-]$ level was reached to that reported in this thesis. In both of these studies a large (mmol) dose of NO_3^- was given which was gradually absorbed from the recipient's stomach. This led to a sustained elevation of plasma $[\text{NO}_2^-]$ levels over a longer period than that used in this thesis. Consequently a large proportion of NO_2^- would have been absorbed into the surrounding tissue in these studies, probably achieving sufficient tissue NO_2^- levels to exert a vasodilator effect despite the normoxic environment. This explanation is supported by a different in-vivo study where an intra-arterial NaNO_2 infusion was given; here no vasodilator effect of NaNO_2 was present in normoxia at doses greater than those used in this thesis⁸⁹.

In summary, the measurement of plasma $[\text{NO}_2^-]$ alone is not a true marker of total body $[\text{NO}_2^-]$ as it disregards the presence of NO_2^- in the body's other fluid compartments. In addition, the observation that changes in plasma $[\text{NO}_2^-]$ levels do not always concur with physiological changes suggests that extravascular NO_2^- is an important source of NO_2^- associated bioactivity. Importantly, this conclusion does not detract from the prospect that administration of NaNO_2 to patients, to boost their tissue levels of NO_2^- , will be of benefit in situation where the tissue-environment has been modified by either hypoxia or ischaemia.

7.3. The clinical implications of NaNO₂

This thesis has demonstrated that low-dose NaNO₂ is capable of exerting a therapeutic effect in human models of: hypoxia, hypoxic pulmonary vasoconstriction, myocardial ischaemia and forearm IR injury. However an appreciation of the biochemistry of NaNO₂ activity is essential if its use as a therapeutic agent is to be matched with those pathologies where it is most likely to be of benefit.

7.3.1. Pulmonary hypertension

In light of the prolonged effect on the pulmonary circulation shown in chapter 3, NaNO₂ may be particularly effective in the treatment of pulmonary hypertension. One limitation to this could be that the aetiology of pulmonary hypertension is often structural, rather than functional, and therefore some patients may not respond to the selective pulmonary vasodilator effect of NaNO₂. However, current therapies for pulmonary hypertension include vasodilators (such as nifedipine) which are known to help only a minority of patients²⁰⁹. Nonetheless, it is standard practice to test whether patients respond to vasodilators²¹⁰ and future studies would allow NaNO₂ to find its position alongside established therapies. Interestingly, the enhanced vasoconstriction specific to high altitude pulmonary oedema might also respond very well to NaNO₂.

7.3.2. The modulation of ischaemic environments

It appears essential that NaNO₂ be present within tissue before the onset of an ischaemic event for the maximum beneficial effect to be achieved. This makes NaNO₂ more suited to use as a prophylactic agent for the treatment of stable ischaemic symptoms (i.e. stable angina) or the prevention of damage due to a predictable acute ischaemic event (i.e. as an IPC stimulus before elective surgery). However, the slow onset of action of NaNO₂ means that other NO-donor agents (e.g. organic nitrates) have a distinct

therapeutic advantage when administered for the relief of symptoms which are already present.

Little work has been performed on the in-vivo effects of organic nitrates in hypoxia. One study has shown that their vasodilator effects are prolonged²¹¹. This would suggest that NaNO₂ could merely be the vehicle by which NO is provided to tissue and that any NO-donor drug would be equally effective. However, it must be recognized that in many of the pathologies where an increase in regional NO concentration would be desirable (such as MI, stroke or solid organ transplantation), the highly effective nature of even a low-dose of organic nitrate could cause variability in blood pressure that would be undesirable. Consequently, the regime for the acute administration of NaNO₂ suggested by this thesis could offer the therapeutic benefits of local vasoactivity delivered to hypoxic tissue without systemic vascular collapse. In addition, the venoselective nature of NO₂⁻ makes it especially suited to the treatment of acute heart failure⁸⁹; as the use of iv organic nitrates in this setting, to reduce cardiac preload, is often limited by disabling systemic arterial vasodilation¹⁶⁶.

Lastly, it should be acknowledged that despite suggestions in the past that NO₂⁻ is a potential carcinogen²¹², more recent literature has not upheld this concern²¹³. Also, previous studies have demonstrated that doses in excess of those used in this thesis resulted in only a minor increase in met-Hb levels, which were not clinically significant⁹⁰.

7.3.3. Dietary supplementation of NO₂⁻

Several studies have been published during the course of this thesis on the subject of dietary NO₂⁻ therapy. Supplementation of NO₂⁻, delivered via oral NO₃⁻, has been shown in man to reduce diastolic blood pressure⁴⁰, protect against endothelial dysfunction resulting from forearm IR injury¹⁸⁶, have an antiplatelet effect¹⁸⁶ and reduce the O₂ cost of exercise in healthy individuals²¹⁴. In addition oral NO₂⁻ reduces myocardial IR injury in

mice¹⁸¹. It should also be noted that the total NO_2^- donation which results from oral NO_2^- administration is the same, though spread over a longer time period, than with iv NaNO_2 use²¹⁵.

Taking the above results together with the findings of this thesis one can conclude that low-dose NaNO_2 is most suited to use as a long term oral supplementation agent. This mode of therapeutic delivery capitalises on the relatively inert nature of NO_2^- in normoxia; augmenting the body's pool of NO_2^- as a potential reserve of NO-type effect, to be tapped into in the appropriate tissue compartment during times of need.

On a cautionary note long term augmentation of the eNOS-NO axis with l-arginine has been shown not to be beneficial, and perhaps harmful, to patients with peripheral vascular disease²¹⁶ and post MI patients²¹⁷. These results are complemented by studies detailed in section 4.4.2 (page 153) which show a similar lack of beneficial effect observed in post MI patients given long term NO supplementation via organic nitrates therapy^{179, 180}. However, there are important differences between these two drugs and low-dose NaNO_2 . Firstly, the effects of l-arginine will have been partly endothelial function dependent; a capacity which deteriorates with age and chronic disease²¹⁸. Secondly, long term NO donation will result in an increase in a number of different NO metabolites, including the potentially damaging molecule ONOO^- (see section 1.4.1.3.2; page 14). By contrast, chronic NO donation should not be a feature of oral NO_2^- therapy and neither should its effect be dependent upon intact endothelial function. Instead low-dose NaNO_2 only provides an NO-type effect in times of need. Therefore what historically has been considered to be the weakest feature of NO_2^- pharmacology could in fact be its greatest asset.

Publications related to this thesis

Published scientific abstracts:

- **Ingram TE**, Pinder AG, Bailey DM, Fraser AG, James PE. *Low dose IV nitrite dilates both peripheral and central vessels in hypoxia – a potential new therapy for ischaemia*. Heart 2008;94(S2):A45-6.
- **Ingram TE**, Pinder AG, Milsom AB, Rogers SC, Thomas DE, James PE. *Blood vessel specific vasoactivity to nitrite under normoxic and hypoxic conditions*. The 35th meeting of the International Society of Oxygen Transport to Tissue. August 26-30. 2007. Uppsala, Sweden.
- **Ingram TE**, Pinder AG, Pittaway E, Fraser AG, James PE. *Nitrite-associated hypoxic vasodilatation in man: The pulmonary circulation is more susceptible to the vasodilator effects of nitrite than the systemic circulation*. Nitric oxide 2008;19(S1);S38.
- Pinder AG, **Ingram TE**, Bailey DM, Fraser AG, James PE. *Low dose systemic nitrite infusion to healthy human subjects in a hypoxic environmental chamber*. Nitric Oxide 2008;19(S1);S55.

Peer reviewed publications

- **Ingram TE**, Pinder AG, Milsom AB, Rogers SC, Thomas DE, James PE. *Blood vessel specific vasoactivity to nitrite under normoxic and hypoxic conditions*. Advances in Experimental Medicine & Biology 2009;645: 21-5.
- **Ingram TE**, Pinder AG, Bailey DM, Fraser AG, James PE. *Low-dose sodium nitrite vasodilates hypoxic human pulmonary vasculature by a means which is not dependent upon a simultaneous elevation in plasma nitrite*. American Journal of Physiology 2010; 298:H331-9.

- Pinder AG, **Ingram TE**, Bailey DM, Morris K, James PE. *Nitrite – Induced Nitrosyl Haemoglobin within Erythrocytes over the Near Physiological Concentration Range – Relevance to Blood Vessel Dilatation During Hypoxia in Humans*. Submitted to Blood.

Textbook chapters

- Pinder AG, Rogers SC, Khalatbari A, **Ingram TE**, James PE. *The measurement of nitric oxide and its metabolites in biological samples by ozone-based chemiluminescence*. In: Redox-Medicated Signal Transduction, Humana press, 2008.
- Ellins EA, **Ingram TE**, Halcox JPJ. *Clinical Assessment of Endothelial Dysfunction*. In: Silent vasculopathy in childhood: Should the clinicians care? Research Signpost press, 2009.

References

1. **Furchgott RF, Zawadzki JV.** The obligatory role of endothelial cells on the relaxation of arterial muscle by acetylcholine. *Nature* 1980;288(5789):373-6.
2. **Palmer RMJ, Ferrige AG, Moncada S.** Nitric oxide release accounts for the biological activity of endothelium-derived relaxing factor. *Nature* 1987;327(6122):524-6.
3. **Ignarro LJ, Buga GM, Byrns RE, Wood KS, Chaudhuri G.** Endothelium-derived relaxing factor and nitric oxide possess identical pharmacologic properties as relaxants of bovine arterial and venous smooth muscle. *J Pharmacol Exp Ther* 1988;246(1):218-26.
4. **Moncada S, Higgs A.** The L-arginine-nitric oxide pathway. *N Engl J Med* 1993;329(27):2002-12.
5. **Zieve L.** Conditional deficiencies of ornithine or arginine. *J Am Coll Nutr* 1986;5(2):167-76.
6. **Panza JA, Casino PR, Kilcoyne CM, Quyyumi AA.** Role of endothelium-derived nitric oxide in the abnormal endothelium-dependent vascular relaxation of patients with essential hypertension. *Circulation* 1993;87(5):1468-74.
7. **Moncada S, Gryglewski R, Bunting S, Vane JR.** An enzyme isolated from arteries transforms prostaglandin endoperoxides to an unstable substance that inhibits platelet aggregation. *Nature* 1976;263(5579):663-5.
8. **Chen G, Suzuki H, Weston AH.** Acetylcholine releases endothelium-derived hyperpolarizing factor and EDRF from rat blood vessels. *Br J Pharmacol* 1988;95(4):1165-74.
9. **Azuma H, Ishikawa M, Sekizaki S.** Endothelium-dependent inhibition of platelet aggregation. *Br J Pharmacol* 1986;88(2):411-5.
10. **Brown GC.** Regulation of mitochondrial respiration by nitric oxide inhibition of cytochrome c oxidase. *Biochimica et Biophysica Acta (BBA) - Bioenergetics* 2001;1504(1):46-57.
11. **Malmström BG.** Cytochrome c oxidase: some current biochemical and biophysical problems. *Q Rev Biophys* 1973;6(04):389-431.
12. **Victor VM, Nunez C, D'Ocon P, Taylor CT, Esplugues JV, Moncada S.** Regulation of oxygen distribution in tissues by endothelial nitric oxide. *Circ Res* 2009;104(10):1178-83.

References

13. **Bloch KD, Ichinose F, Roberts JD, Jr., Zapol WM.** Inhaled NO as a therapeutic agent. *Cardiovasc Res* 2007;75(2):339-48.
14. **Baraldi E, Filippone M.** Chronic lung disease after premature birth. *N Engl J Med* 2007;357(19):1946-55.
15. **Gillespie JS, Liu XR, Martin W.** The effects of L-arginine and NG-monomethyl L-arginine on the response of the rat anococcygeus muscle to NANC nerve stimulation. *Br J Pharmacol* 1989;98(4):1080-2.
16. **Bredt DS, Hwang PM, Snyder SH.** Localization of nitric oxide synthase indicating a neural role for nitric oxide. *Nature* 1990;347(6295):768-70.
17. **Jaffrey SR, Snyder SH.** Nitric oxide: a neural messenger. *Annu Rev Cell Dev Biol* 1995;11(1):417-40.
18. **Toda N, Ayajiki K, Okamura T.** Cerebral blood flow regulation by nitric oxide: recent advances. *Pharmacol Rev* 2009;61(1):62-97.
19. **Prendergast MA, Terry JRAV, Jackson WJ, Buccafusco JJ.** Nitric oxide synthase inhibition impairs delayed recall in mature monkeys. *Pharmacology Biochemistry and Behavior* 1997;56(1):81-7.
20. **Boulton CL, Southam E, Garthwaite J.** Nitric oxide-dependent long-term potentiation is blocked by a specific inhibitor of soluble guanylyl cyclase. *Neuroscience* 1995;69(3):699-703.
21. **Sanchez-Andrade G, Kendrick KM.** The main olfactory system and social learning in mammals. *Behav Brain Res* 2009;200(2):323-35.
22. **Seddon MD, Chowienzyk PJ, Brett SE, Casadei B, Shah AM.** Neuronal nitric oxide synthase regulates basal microvascular tone in humans in-vivo. *Circulation* 2008;117(15):1991-6.
23. **Nathan C, Xie Q-w.** Nitric oxide synthases: roles, tolls, and controls. *Cell* 1994;78(6):915-8.
24. **Stuehr DJ, Marletta MA.** Mammalian nitrate biosynthesis: mouse macrophages produce nitrite and nitrate in response to Escherichia coli lipopolysaccharide. *Proc Natl Acad Sci U S A* 1985;82(22):7738-42.
25. **Hibbs JB, Jr., Taintor RR, Vavrin Z.** Macrophage cytotoxicity: role for L-arginine deiminase and imino nitrogen oxidation to nitrite. *Science* 1987;235(4787):473-6.
26. **Nathan CF, Hibbs JB, Jr.** Role of nitric oxide synthesis in macrophage antimicrobial activity. *Curr Opin Immunol* 1991;3(1):65-70.

References

27. **Castro L, Rodriguez M, Radi R.** Aconitase is readily inactivated by peroxynitrite, but not by its precursor, nitric oxide. *J Biol Chem* 1994;269(47):29409-15.
28. **Reddy D, Lancaster JR, Jr., Cornforth DP.** Nitrite inhibition of Clostridium botulinum: electron spin resonance detection of iron-nitric oxide complexes. *Science* 1983;221(4612):769-70.
29. **Thiemermann C.** Nitric oxide and septic shock. *General Pharmacology: The Vascular System* 1997;29(2):159-66.
30. **Lopez A, Lorente JA, Steingrub J, et al.** Multiple-center, randomized, placebo-controlled, double-blind study of the nitric oxide synthase inhibitor 546C88: effect on survival in patients with septic shock. *Crit Care Med* 2004;32(1):21-30.
31. **Cauwels A.** Nitric oxide in shock. *Kidney Int* 2007;72(5):557-65.
32. **Lange M, Enkhbaatar P, Nakano Y, Traber DL.** Role of nitric oxide in shock: the large animal perspective. *Front Biosci* 2009;14:1979-89.
33. **Annane D, Bellissant E, Bollaert PE, et al.** Corticosteroids in the treatment of severe sepsis and septic shock in adults: a systematic review. *JAMA* 2009;301(22):2362-75.
34. **Radomski MW, Palmer RM, Moncada S.** Glucocorticoids inhibit the expression of an inducible, but not the constitutive, nitric oxide synthase in vascular endothelial cells. *Proc Natl Acad Sci U S A* 1990;87(24):10043-7.
35. **Mitchell HH, Shonle HA, Grindley HS.** The origin of the nitrates in the urine. *J Biol Chem* 1916;24(4):461-90.
36. **Wennmalm A, Benthin G, Petersson AS.** Dependence of the metabolism of nitric oxide (NO) in healthy human whole blood on the oxygenation of its red cell haemoglobin. *Br J Pharmacol* 1992;106(3):507-8.
37. **Furchgott RF, Bhadrakom S.** Reactions of strips of rabbit aorta to epinephrine, isopropylarterenol, sodium nitrite and other drugs. *J Pharmacol Exp Ther* 1953;108(2):129-43.
38. **Ignarro LJ, Lippton H, Edwards JC, et al.** Mechanism of vascular smooth muscle relaxation by organic nitrates, nitrites, nitroprusside and nitric oxide: evidence for the involvement of S-nitrosothiols as active intermediates. *J Pharmacol Exp Ther* 1981;218(3):739-49.
39. **Wennmalm A, Benthin G, Edlund A, et al.** Metabolism and excretion of nitric oxide in humans. An experimental and clinical study. *Circ Res* 1993;73(6):1121-7.

References

40. **Larsen FJ, Ekblom B, Sahlin K, Lundberg JO, Weitzberg E.** Effects of dietary nitrate on blood pressure in healthy volunteers. *N Engl J Med* 2006;355(26):2792-3.
41. **Liao JC, W. Hein T, Vaughn MW, Huang K-T, Kuo L.** Intravascular flow decreases erythrocyte consumption of nitric oxide. *Proc Natl Acad Sci U S A* 1999;96(15):8757-61.
42. **Shingles R, Roh MH, McCarty RE.** Direct Measurement of Nitrite Transport Across Erythrocyte Membrane Vesicles Using the Fluorescent Probe, 6-Methoxy-N-(3-sulfopropyl) quinolinium. *J Bioenerg Biomembr* 1997;29(6):611-6.
43. **Bryan NS, Fernandez BO, Bauer SM, et al.** Nitrite is a signaling molecule and regulator of gene expression in mammalian tissues. *Nat Chem Biol* 2005;1(5):290-7.
44. **Yeagle PL.** Cholesterol and the cell membrane. *Biochim Biophys Acta* 1985;822(3-4):267-87.
45. **Huie RE, Padmaja S.** The reaction of NO with superoxide. *Free Radic Res Commun* 1993;18(4):195-9.
46. **Alp NJ, Channon KM.** Regulation of endothelial nitric oxide synthase by tetrahydrobiopterin in vascular disease. *Arterioscler Thromb Vasc Biol* 2004;24(3):413-20.
47. **Pacher P, Beckman JS, Liaudet L.** Nitric oxide and peroxynitrite in health and disease. *Physiol Rev* 2007;87(1):315-424.
48. **Beckman JS.** Oxidative damage and tyrosine nitration from peroxynitrite. *Chem Res Toxicol* 1996;9(5):836-44.
49. **Cai H, Harrison DG.** Endothelial dysfunction in cardiovascular diseases: the role of oxidant stress. *Circ Res* 2000;87(10):840-4.
50. **Halcox JPJ, Schenke WH, Zalos G, et al.** Prognostic value of coronary vascular endothelial dysfunction. *Circulation* 2002;106(6):653-8.
51. **Peter K, Santiago L.** Regulation of protein function by S-glutathiolation in response to oxidative and nitrosative stress. *Eur J Biochem* 2000;267(16):4928-44.
52. **Stamler JS, Jaraki O, Osborne J, et al.** Nitric oxide circulates in mammalian plasma primarily as an S-nitroso adduct of serum albumin. *Proc Natl Acad Sci U S A* 1992;89(16):7674-7.
53. **Stamler JS, Simon DI, Osborne JA, et al.** S-nitrosylation of proteins with nitric oxide: synthesis and characterization of biologically active compounds. *Proc Natl Acad Sci U S A* 1992;89(1):444-8.

References

54. **Dejam A, Hunter CJ, Pelletier MM, et al.** Erythrocytes are the major intravascular storage sites of nitrite in human blood. *Blood* 2005;106(2):734-9.
55. **Rogers SC, Khalatbari A, Datta BN, et al.** NO metabolite flux across the human coronary circulation. *Cardiovasc Res* 2007;75(2):434-41.
56. **Berg JM, Tymoczko JL, Stryer L.** In: *Biochemistry (Mosc)*. 6th ed: WH Freeman; 2006.
57. **Tomoda A, Yubisui T, Tsuji A, Yoneyama Y.** Kinetic studies on methemoglobin reduction by human red cell NADH cytochrome b5 reductase. *J Biol Chem* 1979;254(8):3119-23.
58. **Doyle M, Pickering R, Pater D.** Kinetics and mechanism of the oxidation of human deoxyhemoglobin by nitrites. *J Biol Chem* 1981;256(23):12393-98.
59. **Antonini E, Ioppolo C, Giardina B, Brunori M.** Chemical modifications of SH groups of intraerythrocytic hemoglobin. *Biochem Biophys Res Commun* 1977;74(4):1647-55.
60. **Jia L, Bonaventura C, Bonaventura J, Stamler JS.** S-nitrosohaemoglobin: a dynamic activity of blood involved in vascular control. *Nature* 1996;380(6571):221-6.
61. **Kleinbongard P, Dejam A, Lauer T, et al.** Plasma nitrite reflects constitutive nitric oxide synthase activity in mammals. *Free Radic Biol Med* 2003;35(7):790-6.
62. **Lundberg JO, Weitzberg E.** The biological role of nitrate and nitrite: The times they are a-changin'. *Nitric Oxide* 2010;22(2):61-3.
63. **Lundberg JO, Govoni M.** Inorganic nitrate is a possible source for systemic generation of nitric oxide. *Free Radic Biol Med* 2004;37(3):395-400.
64. **Moore EG, Gibson QH.** Cooperativity in the dissociation of nitric oxide from hemoglobin. *J Biol Chem* 1976;251(9):2788-94.
65. **Kelm M, Schrader J.** Control of coronary vascular tone by nitric oxide. *Circ Res* 1990;66(6):1561-75.
66. **Liu X, Srinivasan P, Collard E, et al.** Oxygen regulates the effective diffusion distance of nitric oxide in the aortic wall. *Free Radic Biol Med* 2010;48(4):554-9.
67. **Lancaster JR.** Simulation of the diffusion and reaction of endogenously produced nitric oxide. *Proc Natl Acad Sci U S A* 1994;91(17):8137-41.
68. **Cannon ROI, Schechter AN, Gladwin MT.** Effects of inhaled nitric oxide on regional blood flow are consistent with intravascular nitric oxide delivery. *J Clin Invest* 2001;108(2):279-87.

References

69. **McMahon TJ, Moon RE, Luschinger BP, et al.** Nitric oxide in the human respiratory cycle. *Nat Med* 2002;8(7):711-7.
70. **Allen BW, Piantadosi CA.** How do red blood cells cause hypoxic vasodilation? The SNO-hemoglobin paradigm. *Am J Physiol Heart Circ Physiol* 2006;291(4):H1507-12.
71. **Joshi MS, Ferguson TB, Han TH, et al.** Nitric oxide is consumed, rather than conserved, by reaction with oxyhemoglobin under physiological conditions. *Proc Natl Acad Sci U S A* 2002;99(16):10341-6.
72. **Gow AJ, Luchsinger BP, Pawloski JR, Singel DJ, Stamler JS.** The oxyhemoglobin reaction of nitric oxide. *Proc Natl Acad Sci U S A* 1999;96(16):9027-32.
73. **Gladwin MT, Wang X, Reiter CD, et al.** S-nitrosohemoglobin Is unstable in the reductive erythrocyte environment and lacks O₂/NO-linked allosteric function. *J Biol Chem* 2002;277(31):27818-28.
74. **Gladwin MT, Shelhamer JH, III RC.** Role of circulating nitrite and S-nitrosohemoglobin in the regulation of regional blood flow in humans *Proc Natl Acad Sci U S A* 2000;97(21):11482-7.
75. **Schechter AN, Gladwin MT.** Hemoglobin and the paracrine and endocrine functions of nitric oxide. *N Engl J Med* 2003;348(15):1483-5.
76. **Hausladen A, Rafikov R, Angelo M, Singel DJ, Nudler E, Stamler JS.** Assessment of nitric oxide signals by triiodide chemiluminescence. *Proceedings of the National Academy of Sciences* 2007;104(7):2157-62.
77. **Stamler JS, Gaston BM, Hare JM, et al.** Hemoglobin and nitric oxide. *N Engl J Med* 2003;349(4):402-5.
78. **Isbell TS, Sun C-W, Wu L-C, et al.** SNO-hemoglobin is not essential for red blood cell-dependent hypoxic vasodilation. *Nat Med* 2008;14(7):773-7.
79. **Huang KT, Keszler A, Patel N, et al.** The reaction between nitrite and deoxyhemoglobin: reassessment of reaction kinetics and stoichiometry. *J Biol Chem* 2005;280(35):31126-31.
80. **Cosby K PK, Crawford JH, Patel RP, Reiter CD, Martyr S, Yang BK, Wacławski MA, Zalos G, Xu X, Huang KT, Shields H, Kim-Shapiro DB, Schechter AN, Cannon RO 3rd, Gladwin MT.** Nitrite reduction to nitric oxide by deoxyhemoglobin vasodilates the human circulation. *Nat Med* 2003;9(12):1498-505.

References

81. **Dalsgaard T, Simonsen U, Fago A.** Nitrite-dependent vasodilation is facilitated by hypoxia and is independent of known NO-generating nitrite reductase activities. *Am J Physiol* 2007;292(6):H3072-H8.
82. **Huang Z, Shiva S, Kim-Shapiro DBA, et al.** Enzymatic function of hemoglobin as a nitrite reductase that produces NO under allosteric control. *The Journal of Clinical Investigation* 2005;115(8):2099-107.
83. **Gladwin MT RN, Shiva S, Dezfulian C, Hogg N, Kim-Shapiro DB, Patel RP.** Nitrite as a vascular endocrine nitric oxide reservoir that contributes to hypoxic signaling, cytoprotection, and vasodilation. *Am J Physiol* 2006;291(5):H2026-H35.
84. **Pinder AG, Pittaway E, Morris K, James PE.** Nitrite directly vasodilates hypoxic vasculature via nitric oxide-dependent and -independent pathways. *Br J Pharmacol* 2009;157(8):1523-30.
85. **Li H, Samouilov A, Liu X, Zweier JL.** Characterization of the magnitude and kinetics of xanthine oxidase-catalyzed nitrite reduction. Evaluation of its role in nitric oxide generation in anoxic tissues. *J Biol Chem* 2001;276(27):24482-9.
86. **Johnson Gr, Tsao PS, Mulloy D, Lefer AM.** Cardioprotective effects of acidified sodium nitrite in myocardial ischemia with reperfusion. *J Pharmacol Exp Ther* 1990;252(1):35-41.
87. **Lauer T, Preik M, Rassaf T, et al.** Plasma nitrite rather than nitrate reflects regional endothelial nitric oxide synthase activity but lacks intrinsic vasodilator action. *Proc Natl Acad Sci U S A* 2001;98(22):12814-9.
88. **Dejam A, Hunter CJ, Tremonti C, et al.** Nitrite infusion in humans and nonhuman primates. Endocrine effects, pharmacokinetics, and tolerance formation. *Circulation* 2007;116(16):1821-31.
89. **Maher AR, Milsom AB, Gunaruwan P, et al.** Hypoxic modulation of exogenous nitrite-induced vasodilation in humans. *Circulation* 2008;117(5):670-7.
90. **Mack AK, McGowan VR, Carole II, et al.** Sodium nitrite promotes regional blood flow in patients with sickle cell disease: a phase I/II study. *Br J Haematol* 2008;142(6):971-8.
91. **Dorrington KL, Clar C, Young JD, Jonas M, Tansley JG, Robbins PA.** Time course of the human pulmonary vascular response to 8 hours of isocapnic hypoxia. *Am J Physiol* 1997;273(3):H1126-34.
92. **Hunter CJ, Dejam A, Gladwin MT.** Inhaled nebulized nitrite is a hypoxia-sensitive NO-dependent selective pulmonary vasodilator. *Nat Med* 2004;10(10):1122-7.

References

93. **Casey DB, Badejo AM, Jr., Dhaliwal JS, et al.** Pulmonary vasodilator responses to sodium nitrite are mediated by an allopurinol-sensitive mechanism in the rat. *Am J Physiol Heart Circ Physiol* 2009;296(2):H524-33.
94. **Dias-Junior CAC, Gladwin MT, Tanus-Santosa JE.** Low-dose intravenous nitrite improves hemodynamics in a canine model of acute pulmonary thromboembolism. *Free Radic Biol Med* 2006;41(12):1764-70.
95. **Angelo M, Singel DJ, Stamler JS.** An S-nitrosothiol (SNO) synthase function of hemoglobin that utilizes nitrite as a substrate. *Proc Natl Acad Sci U S A* 2006;103(22):8366-71.
96. **Pinder AG, Rogers SC, Khalatbari A, Ingram TE, James PE.** The measurement of nitric oxide and its metabolites in biological samples by ozone-based chemiluminescence. In: Hancock JT, ed. *Redox-Mediated Signal Transduction Methods and Protocols*: Humana; 2009.
97. **Calvert JW, Lefer DJ.** Clinical translation of nitrite therapy for cardiovascular diseases. *Nitric Oxide* 2010;22(2):91-7.
98. **Alberts B, Johnson A, Lewis J, Raff M, Roberts K, Walter P.** *Molecular biology of the cell*. 4th ed. New York: Garland Science; 2002.
99. **Ginks WR, Sybers HD, Maroko PR, Covell JW, Sobel BE, Ross J, Jr.** Coronary artery reperfusion. II. Reduction of myocardial infarct size at 1 week after the coronary occlusion. *J Clin Invest* 1972;51(10):2717-23.
100. **Braunwald E, Kloner RA.** Myocardial reperfusion: a double-edged sword? *J Clin Invest* 1985;76(5):1713-9.
101. **Steenbergen C, Murphy E, Levy L, London RE.** Elevation in cytosolic free calcium concentration early in myocardial ischemia in perfused rat heart. *Circ Res* 1987;60(5):700-7.
102. **Yellon DM, Hausenloy DJ.** Myocardial reperfusion injury. *N Engl J Med* 2007;357(11):1121-35.
103. **Murphy E, Steenbergen C.** Mechanisms underlying acute protection from cardiac ischemia-reperfusion injury. *Physiol Rev* 2008;88(2):581-609.
104. **Murry CE, Jennings RB, Reimer KA.** Preconditioning with ischemia: a delay of lethal cell injury in ischemic myocardium. *Circulation* 1986;74(5):1124-36.
105. **Bolli R.** Cardioprotective function of inducible nitric oxide synthase and role of nitric oxide in myocardial ischemia and preconditioning: an overview of a decade of research. *J Mol Cell Cardiol* 2001;33(11):1897-918.

References

106. **Zhao Z-Q, Corvera JS, Halkos ME, et al.** Inhibition of myocardial injury by ischemic postconditioning during reperfusion: comparison with ischemic preconditioning. *Am J Physiol Heart Circ Physiol* 2003;285(2):H579-88.
107. **Halestrap AP, Clarke SJ, Javadov SA.** Mitochondrial permeability transition pore opening during myocardial reperfusion--a target for cardioprotection. *Cardiovasc Res* 2004;61(3):372-85.
108. **Hausenloy DJ, Yellon DM.** New directions for protecting the heart against ischaemia-reperfusion injury: targeting the Reperfusion Injury Salvage Kinase (RISK)-pathway. *Cardiovasc Res* 2004;61(3):448-60.
109. **Heusch G, Boengler K, Schulz R.** Cardioprotection: nitric oxide, protein kinases, and mitochondria. *Circulation* 2008;118(19):1915-9.
110. **Sack MN, Yellon DM.** Insulin therapy as an adjunct to reperfusion after acute coronary ischemia: A proposed direct myocardial cell survival effect independent of metabolic modulation. *J Am Coll Cardiol* 2003;41(8):1404-7.
111. **Bell RM, Yellon DM.** Atorvastatin, administered at the onset of reperfusion, and independent of lipid lowering, protects the myocardium by up-regulating a pro-survival pathway. *J Am Coll Cardiol* 2003;41(3):508-15.
112. **Klein HH, Pich S, Lindert S, Nebendahl K, Warneke G, Kreuzer H.** Treatment of reperfusion injury with intra-coronary calcium channel antagonists and reduced coronary free calcium concentration in regionally ischemic, reperfused porcine hearts. *J Am Coll Cardiol* 1989;13(6):1395-401.
113. **Gumina RJ, Buerger E, Eickmeier C, Moore J, Daemmgen J, Gross GJ.** Inhibition of the Na⁺/H⁺ exchanger confers greater cardioprotection against 90 minutes of myocardial ischemia than ischemic preconditioning in dogs. *Circulation* 1999;100(25):2519-26.
114. **Yang X-M, Proctor JB, Cui L, Krieg T, Downey JM, Cohen MV.** Multiple, brief coronary occlusions during early reperfusion protect rabbit hearts by targeting cell signaling pathways. *J Am Coll Cardiol* 2004;44(5):1103-10.
115. **Yang X-M, Philipp S, Downey JM, Cohen MV.** Postconditioning's protection is not dependent on circulating blood factors or cells but involves adenosine receptors and requires PI3-kinase and guanylyl cyclase activation. *Basic Res Cardiol* 2005;100(1):57-63.
116. **Konorev EA, Tarpey MM, Joseph J, Baker JE, Kalyanaraman B.** S-nitrosoglutathione improves functional recovery in the isolated rat heart after cardioplegic

References

ischemic arrest-evidence for a cardioprotective effect of nitric oxide. *J Pharmacol Exp Ther* 1995;274(1):200-6.

117. **Eugene FT, Joy M, Jody M, Lionel HO, Friedrich B.** Effect of nitrovasodilators and inhibitors of nitric oxide synthase on ischaemic and reperfusion function of rat isolated hearts. *Br J Pharmacol* 1998;123(6):1159-67.

118. **Bell RM, Yellon DM.** Bradykinin limits infarction when administered as an adjunct to reperfusion in mouse heart: the role of PI3K, Akt and eNOS. *J Mol Cell Cardiol* 2003;35(2):185-93.

119. **Sun J, Morgan M, Shen R-F, Steenbergen C, Murphy E.** Preconditioning results in S-nitrosylation of proteins involved in regulation of mitochondrial energetics and calcium transport. *Circ Res* 2007;101(11):1155-63.

120. **Burwell LS, Nadtochiy SM, Tompkins AJ, Young S, Brookes PS.** Direct evidence for S-nitrosation of mitochondrial complex I. *Biochem J* 2006;394(3):627-34.

121. **Brown GC, Borutaite V.** Nitric oxide and mitochondrial respiration in the heart. *Cardiovasc Res* 2007;75(2):283-90.

122. **Kharbanda RK, Mortensen UM, White PA, et al.** Transient limb ischemia induces remote ischemic preconditioning in-vivo. *Circulation* 2002;106(23):2881-3.

123. **Zweier JL, Samouilov A, Kuppusamy P.** Non-enzymatic nitric oxide synthesis in biological systems. *Biochimica et Biophysica Acta (BBA) - Bioenergetics* 1999;1411(2-3):250-62.

124. **Hendgen-Cotta UB, Merx MW, Shiva S, et al.** Nitrite reductase activity of myoglobin regulates respiration and cellular viability in myocardial ischemia-reperfusion injury. *Proceedings of the National Academy of Sciences* 2008;105(29):10256-61.

125. **Webb A, Bond R, McLean P, Uppal R, Benjamin N, Ahluwalia A.** Reduction of nitrite to nitric oxide during ischemia protects against myocardial ischemia-reperfusion damage. *Proc Natl Acad Sci U S A* 2004;101(37):13683-8.

126. **Duranski MR.** Cytoprotective effects of nitrite during in vivo ischemia-reperfusion of the heart and liver. *The Journal of Clinical Investigation* 2005;115(5):1232-40.

127. **Mendelsohn ME, Karas RH.** The protective effects of estrogen on the cardiovascular system. *N Engl J Med* 1999;340(23):1801-11.

128. **Lahm T, Patel KM, Crisostomo PR, et al.** Endogenous estrogen attenuates pulmonary artery vasoreactivity and acute hypoxic pulmonary vasoconstriction: the effects of sex and menstrual cycle. *Am J Physiol* 2007;293(3):E865-71.

References

129. **Soul JS, du Plessis AJ.** Near-infrared spectroscopy. *Semin Pediatr Neurol* 1999;6(2):101-10.
130. **Livera LN, Spencer SA, Thorniley MS, Wickramasinghe YA, Rolfe P.** Effects of hypoxaemia and bradycardia on neonatal cerebral haemodynamics. *Arch Dis Child* 1991;66(4):376-80.
131. **Whitney R.** The measurement of volume changes in human limbs. *J Physiol (Lond)* 1953;121:1-27.
132. **Naeije R, Torbicki A.** More on the noninvasive diagnosis of pulmonary hypertension: Doppler echocardiography revisited. *Eur Respir J* 1995;8(9):1445-9.
133. **Chan KL, Currie PJ, Seward JB, Hagler DJ, Mair DD, Tajik AJ.** Comparison of three Doppler ultrasound methods in the prediction of pulmonary artery pressure. *J Am Coll Cardiol* 1987;9(3):549-54.
134. **Brechot N, Gambotti L, Lafitte S, Roudaut R.** Usefulness of right ventricular isovolumic relaxation time in predicting systolic pulmonary artery pressure. *Eur J Echocardiogr* 2008;9(4):547-54.
135. **Yock P, Popp R.** Noninvasive estimation of right ventricular systolic pressure by Doppler ultrasound in patients with tricuspid regurgitation. *Circulation* 1984;70(4):657-62.
136. **Kircher BJ, Himelman RB, Schiller NB.** Noninvasive estimation of right atrial pressure from the inspiratory collapse of the inferior vena cava. *The American Journal of Cardiology* 1990;66(4):493-6.
137. **McLennan FM, Haites NE, Mackenzie JD, Daniel MK, Rawles JM.** Reproducibility of linear cardiac output measurement by Doppler ultrasound alone. *Br Heart J* 1986;55(1):25-31.
138. **Rassaf T, Feelisch M, Kelm M.** Circulating no pool: assessment of nitrite and nitroso species in blood and tissues. *Free Radic Biol Med* 2004;36(4):413-22.
139. **Yang BK, Vivas EX, Reiter CD, Gladwin MT.** Methodologies for the sensitive and specific measurement of S-nitrosothiols, iron-nitrosyls, and nitrite in biological samples. *Free Radic Res* 2003;37(1):1-10.
140. **Rogers SC, Khalatbari A, Gapper PW, Frenneaux MP, James PE.** Detection of human red blood cell-bound nitric oxide. *J Biol Chem* 2005;280(29):26720-8.
141. **Braman RS, Hendrix SA.** Nanogram nitrite and nitrate determination in environmental and biological materials by vanadium (III) reduction with chemiluminescence detection. *Anal Chem* 1989;61(24):2715-8.

References

142. **Bailey DM, Evans KA, James PE, et al.** Altered free radical metabolism in acute mountain sickness: implications for dynamic cerebral autoregulation and blood-brain barrier function. *The Journal of Physiology* 2009;587(1):73-85.
143. **Celermajer DS, Sorensen KE, Gooch VM, et al.** Non-invasive detection of endothelial dysfunction in children and adults at risk of atherosclerosis. *The Lancet* 1992;340(8828):1111-5.
144. **Kharbanda RK, Peters M, Walton B, et al.** Ischemic preconditioning prevents endothelial injury and systemic neutrophil activation during ischemia-reperfusion in humans in-vivo. *Circulation* 2001;103(12):1624-30.
145. **Madler CF, Payne N, Wilkeshoff U, et al.** Non-invasive diagnosis of coronary artery disease by quantitative stress echocardiography: optimal diagnostic models using off-line tissue Doppler in the MYDISE study. *Eur Heart J* 2003;24(17):1584-94.
146. **Levick J.** Cardiovascular responses in pathological situations. In: *An Introduction to Cardiovascular Physiology*. 4th ed: Hodder Education; 2003.
147. **Holanda MA, Reis RC, Winkeler GF, Fortaleza SC, Lima JW, Pereira ED.** Influence of total face, facial and nasal masks on short-term adverse effects during noninvasive ventilation. *J Bras Pneumol* 2009;35(2):164-73.
148. **Bryan NS, Rassaf T, Rodriguez J, Feelisch M.** Bound NO in human red blood cells: fact or artifact? *Nitric Oxide* 2004;10(4):221-8.
149. **Stamler JS.** S-nitrosothiols in the blood: roles, amounts, and methods of analysis. *Circ Res* 2004;94(4):414-7.
150. **Tyurin VA, Liu S-X, Tyurina YY, et al.** Elevated levels of S-nitrosoalbumin in pre-eclampsia plasma. *Circ Res* 2001;88(11):1210-5.
151. **Erzurum SC, Ghosh S, Janocha AJ, et al.** Higher blood flow and circulating NO products offset high-altitude hypoxia among Tibetans. *Proc Natl Acad Sci U S A* 2007;104(45):17593-8.
152. **Wilkinson IB, Franklin SS, Hall IR, Tyrrell S, Cockcroft JR.** Pressure amplification explains why pulse pressure is unrelated to risk in young subjects. *Hypertension* 2001;38(6):1461-6.
153. **Carter SA.** Effect of age, cardiovascular disease, and vasomotor changes on transmission of arterial pressure waves through the lower extremities. *Angiology* 1978;29(8):601-16.
154. **Zweier JL, Li H, Samouilov A, Liu X.** Mechanisms of nitrite reduction to nitric oxide in the heart and vessel wall. *Nitric Oxide* 2010;22(2):83-90.

References

155. **Li H, Cui H, Kundu TK, Alzawahra W, Zweier JL.** Nitric oxide production from nitrite occurs primarily in tissues not in the blood: critical role of xanthine oxidase and aldehyde oxidase. *J Biol Chem* 2008;283(26):17855 - 63.
156. **Alzawahra WF, Talukder MAH, Liu X, Samouilov A, Zweier JL.** Heme proteins mediate the conversion of nitrite to nitric oxide in the vascular wall. *Am J Physiol Heart Circ Physiol* 2008;295(2):H499-508.
157. **Zuckerbraun BS, Shiva S, Ifedigbo E, et al.** Nitrite potently inhibits hypoxic and inflammatory pulmonary arterial hypertension and smooth muscle proliferation via xanthine oxidoreductase-dependent nitric oxide generation. *Circulation* 2010;121(1):98-109.
158. **Cao Z, Bell JB, Mohanty JG, Nagababu E, Rifkind JM.** Nitrite enhances RBC hypoxic ATP synthesis and the release of ATP into the vasculature: a new mechanism for nitrite-induced vasodilation. *Am J Physiol Heart Circ Physiol* 2009;297(4):H1494-503.
159. **Gladwin MT, Kim-Shapiro DB.** The functional nitrite reductase activity of the heme-globins. *Blood* 2008;112(7):2636-47.
160. **Rassaf T, Preik M, Kleinbongard P, et al.** Evidence for in vivo transport of bioactive nitric oxide in human plasma. *J Clin Invest* 2002;109(9):1241-8.
161. **Butler A.** 'The heart less bounding': treating angina pectoris. *J R Coll Physicians Edinb* 2006;36(2):185-9.
162. **Reichart E, Mitchell S.** On the physiological action of potassium nitrite. *Am J Med Sci* 1880;154:158-80.
163. **Collier W.** A case of angina pectoris treated with nitrite of sodium; remarks. *The Lancet* 1883;122(3143):901-.
164. **Murrell W.** Nitro-glycerine as a remedy for angina pectoris. *The Lancet* 1879;113(2890):80-1.
165. **Weiss S, Wilkins RW, Haynes FW.** The nature of circulatory collapse induced by sodium nitrite. *J Clin Invest* 1937;16(1):73-84.
166. **British National Formulary.** 54 ed. London: BMJ Publishing Group Ltd; 2007.
167. **Sutherland G, Hatle L, Claus P, D'hooge J, Bijnens B.** *Doppler myocardial imaging: a textbook.* Hasselt, Belgium: BSWK bvba; 2006.
168. **Marwick TH.** Assessment of subendocardial function with myocardial contrast echocardiography. *JACC Cardiovasc Imaging* 2008;1(3):279-81.

References

169. **Derumeaux G, Ovize M, Loufoua J, et al.** Doppler tissue imaging quantitates regional wall motion during myocardial ischemia and reperfusion. *Circulation* 1998;97(19):1970-7.
170. **Voigt J-U, Nixdorff U, Bogdan R, et al.** Comparison of deformation imaging and velocity imaging for detecting regional inducible ischaemia during dobutamine stress echocardiography. *Eur Heart J* 2004;25(17):1517-25.
171. **Rietzschel ER, Langlois M, De Buyzere ML, et al.** Oxidized low-density lipoprotein cholesterol is associated with decreases in cardiac function independent of vascular alterations. *Hypertension* 2008;52(3):535-41.
172. **Vinereanu D, Nicolaidis E, Tweddel AC, et al.** Sub-clinical left ventricular dysfunction in asymptomatic patients with type II diabetes mellitus, related to serum lipids and glycated haemoglobin. *Clin Sci* 2003;105(5):591-9.
173. **Baltabaeva A, Marciniak M, Bijmens B, et al.** Regional left ventricular deformation and geometry analysis provides insights in myocardial remodelling in mild to moderate hypertension. *Eur J Echocardiogr* 2008;9(4):501-8.
174. **Yu C-M, Sanderson JE, Marwick TH, Oh JK.** Tissue Doppler Imaging: A New Prognosticator for Cardiovascular Diseases. *J Am Coll Cardiol* 2007;49(19):1903-14.
175. **Fang ZY, Yuda S, Anderson V, Short L, Case C, Marwick TH.** Echocardiographic detection of early diabetic myocardial disease. *J Am Coll Cardiol* 2003;41(4):611-7.
176. **Voigt J-U, Exner B, Schmiedehausen K, et al.** Strain-rate imaging during dobutamine stress echocardiography provides objective evidence of inducible ischemia. *Circulation* 2003;107(16):2120-6.
177. **Ingul CB, Rozis E, Marwick TH.** Incremental value of strain rate imaging to wall motion analysis for prediction of outcome in patients undergoing dobutamine stress echocardiography. *Circulation* 2007;115(10):1252-9.
178. **Ishii K, Imai M, Suyama T, et al.** Exercise-induced post-ischemic left ventricular delayed relaxation or diastolic stunning: is it a reliable marker in detecting coronary artery disease? *J Am Coll Cardiol* 2009;53(8):698-705.
179. **ISIS-4.** ISIS-4: a randomised factorial trial assessing early oral captopril, oral mononitrate, and intravenous magnesium sulphate in 58,050 patients with suspected acute myocardial infarction. ISIS-4 (Fourth International Study of Infarct Survival) Collaborative Group. *Lancet* 1995;345(8951):669-85.

References

180. **Ishikawa K, Kanamasa K, Ogawa I, et al.** Long-term nitrate treatment increases cardiac events in patients with healed myocardial infarction. Secondary Prevention Group. *Jpn Circ J* 1996;60:779-88.
181. **Bryan NS, Calvert JW, Elrod JW, Gundewar S, Ji SY, Lefer DJ.** Dietary nitrite supplementation protects against myocardial ischemia-reperfusion injury. *Proc Natl Acad Sci U S A* 2007;104(48):19144-9.
182. **Bryan NS, Calvert JW, Gundewar S, Lefer DJ.** Dietary nitrite restores NO homeostasis and is cardioprotective in endothelial nitric oxide synthase-deficient mice. *Free Radic Biol Med* 2008;45(4):468-74.
183. **Raat NJH, Noguchi AC, Liu VB, et al.** Dietary nitrate and nitrite modulate blood and organ nitrite and the cellular ischemic stress response. *Free Radic Biol Med* 2009;47(5):510-7.
184. **Tang Y, Garg H, Geng Y-J, Bryan NS.** Nitric oxide bioactivity of traditional Chinese medicines used for cardiovascular indications. *Free Radic Biol Med* 2009;47(6):835-40.
185. **Loukogeorgakis SP, Panagiotidou AT, Broadhead MW, Donald A, Deanfield JE, MacAllister RJ.** Remote ischemic preconditioning provides early and late protection against endothelial ischemia-reperfusion injury in humans: role of the autonomic nervous system. *J Am Coll Cardiol* 2005;46(3):450-6.
186. **Webb AJ, Patel N, Loukogeorgakis S, et al.** Acute blood pressure lowering, vasoprotective, and antiplatelet properties of dietary nitrate via bioconversion to nitrite. *Hypertension* 2008;51(3):784-90.
187. **Gonzalez FM, Shiva S, Vincent PS, et al.** Nitrite anion provides potent cytoprotective and anti-apoptotic effects as adjunctive therapy to reperfusion for acute myocardial infarction. *Circulation* 2008;117(23):2986-94.
188. **Donald AE, Halcox JP, Charakida M, et al.** Methodological approaches to optimize reproducibility and power in clinical studies of flow-mediated dilation. *J Am Coll Cardiol* 2008;51(20):1959-64.
189. **Rassaf T, Heiss C, Hendgen-Cotta U, et al.** Plasma nitrite reserve and endothelial function in the human forearm circulation. *Free Radic Biol Med* 2006;41(2):295-301.
190. **Calvert JW, Lefer DJ.** Myocardial protection by nitrite. *Cardiovasc Res* 2009;83(2):195-203.

References

191. **Kleinbongard P, Dejam A, Lauer T, et al.** Plasma nitrite concentrations reflect the degree of endothelial dysfunction in humans. *Free Radic Biol Med* 2006;40(2):295-302.
192. **Harris RA, Padilla J, Rink LD, Wallace JP.** Variability of flow-mediated dilation measurements with repetitive reactive hyperemia. *Vasc Med* 2006;11(1):1-6.
193. **Zweier JL, Wang P, Samouilov A, Kuppusamy P.** Enzyme-independent formation of nitric oxide in biological tissues. *Nat Med* 1995;1(8):804 - 9.
194. **Sodium nitrite in acute myocardial infarction (NCT00924118).** 2010. (Accessed 24-02-2010, at www.clinicaltrials.gov/ct2/show/NCT00924118.)
195. **Sabatine MS, Cannon CP, Gibson CM, et al.** Addition of clopidogrel to aspirin and fibrinolytic therapy for myocardial infarction with ST-segment elevation. *N Engl J Med* 2005;352(12):1179-89.
196. **Newby DE, Wright RA, Labinjoh C, et al.** Endothelial dysfunction, impaired endogenous fibrinolysis, and cigarette smoking : a mechanism for arterial thrombosis and myocardial infarction. *Circulation* 1999;99(11):1411-5.
197. **Peart JN, Headrick JP.** Clinical cardioprotection and the value of conditioning responses. *Am J Physiol Heart Circ Physiol* 2009;296(6):H1705-20.
198. **Tang X-L, Sato H, Tiwari S, et al.** Cardioprotection by postconditioning in conscious rats is limited to coronary occlusions <45 min. *Am J Physiol Heart Circ Physiol* 2006;291(5):H2308-17.
199. **Miura T, Miki T.** Limitation of myocardial infarct size in the clinical setting: current status and challenges in translating animal experiments into clinical therapy. *Basic Res Cardiol* 2008;103(6):501-13.
200. **Piot C, Croisille P, Staat P, et al.** Effect of cyclosporine on reperfusion injury in acute myocardial infarction. *N Engl J Med* 2008;359(5):473-81.
201. **Abete P, Ferrara N, Cacciatore F, et al.** Angina-induced protection against myocardial infarction in adult and elderly patients: a loss of preconditioning mechanism in the aging heart? *J Am Coll Cardiol* 1997;30(4):947-54.
202. **Ghosh S, Standen NB, Galinanes M.** Failure to precondition pathological human myocardium. *J Am Coll Cardiol* 2001;37(3):711-8.
203. **Roe BB, Hutchinson JC, Fishman NH, Ulliyot DJ, Smith DL.** Myocardial protection with cold, ischemic, potassium-induced cardioplegia. *J Thorac Cardiovasc Surg* 1977;73(3):366-74.

References

204. **Chikwe J.** *Cardiothoracic Surgery (Oxford Specialist Handbooks in Surgery)*. 1st ed. Oxford: Oxford University Press; 2006.
205. **Guru V, Omura J, Alghamdi AA, Weisel R, Fremes SE.** Is blood superior to crystalloid cardioplegia?: a meta-analysis of randomized clinical trials. *Circulation* 2006;114(1_suppl):I-331-8.
206. **Russell N.** *Blood Biochemistry*. Beckenham: Croom Helm Ltd; 1982.
207. **Abu-Salah KM, Gambo A-HA.** An explanation for the efficacy of procaine in the treatment of sickle cell anaemia. *The International Journal of Biochemistry & Cell Biology* 2005;37(4):835-41.
208. **Venugopal V, Hausenloy DJ, Ludman A, et al.** Remote ischaemic preconditioning reduces myocardial injury in patients undergoing cardiac surgery with cold-blood cardioplegia: a randomised controlled trial. *Heart* 2009;95(19):1567-71.
209. **Ghofrani HA, Wilkins MW, Rich S.** Uncertainties in the diagnosis and treatment of pulmonary arterial hypertension. *Circulation* 2008;118(11):1195-201.
210. **Task Force members, Galie N, Torbicki A, et al.** Guidelines on diagnosis and treatment of pulmonary arterial hypertension: the task force on diagnosis and treatment of pulmonary arterial hypertension of the European Society of Cardiology. *Eur Heart J* 2004;25(24):2243-78.
211. **Bekuzarova SA, Khromov AS, Doloman LB, Beslaneev IA, Kurdanov Kh A.** Effect of nitroglycerin on vasodilation at high altitude. *Fiziol Zh* 2003;49(3):118-25.
212. **Magee PN, Barnes JM.** The production of malignant primary hepatic tumours in the rat by feeding dimethylnitrosamine. *Br J Cancer* 1956;10(1):114-22.
213. **Lundberg JO, Weitzberg E, Cole JA, Benjamin N.** Nitrate, bacteria and human health. *Nat Rev Microbiol* 2004;2(7):593-602.
214. **Bailey SJ, Winyard P, Vanhatalo A, et al.** Dietary nitrate supplementation reduces the O₂ cost of low-intensity exercise and enhances tolerance to high-intensity exercise in humans. *J Appl Physiol* 2009.
215. **Hunault CC, van Velzen AG, Sips AJAM, Schothorst RC, Meulenbelt J.** Bioavailability of sodium nitrite from an aqueous solution in healthy adults. *Toxicol Lett* 2009;190(1):48-53.
216. **Wilson AM, Harada R, Nair N, Balasubramanian N, Cooke JP.** L-arginine supplementation in peripheral arterial disease: no benefit and possible harm. *Circulation* 2007;116(2):188-95.

References

217. **Schulman SP, Becker LC, Kass DA, et al.** L-arginine therapy in acute myocardial infarction: the vascular interaction with age in myocardial infarction (VINTAGE MI) randomized clinical trial. *JAMA* 2006;295(1):58-64.
218. **Vane JR, Anggard EE, Botting RM.** Regulatory functions of the vascular endothelium. *N Engl J Med* 1990;323(1):27-35.